博士論文

Development of
Rapid Measurement Methods of
Micro Biological Particles in
Sphere of Human Habitation

生活圏内の生物由来粒子群
迅速計測技術に関する研究

竹 中 啓

広島大学大学院先端物質科学研究科

2018 年 3 月

目次

１．主論文

Development of Rapid Measurement Methods of Micro Biological Particles in Sphere of Human Habitation
（生活圏内の生物由来粒子群迅速計測技術に関する研究）
竹中　啓

２．公表論文

(1) Rapid Live Bacteria Counter Using Cassette-type Flow Cytometry
K. Takenaka, Y. Sasaki, H. Inami, H. Nakamoto, Y. Watanabe, M. Kurihara, K. Takei, J. Ishikawa and R. Miyake
Transactions of the Japan society of Mechanical Engineers Series C, 77, 401-410, (2011),
No.2010-JCR-0124.
(2) Airborne Virus Detection by a Sensing System Using a Disposable Integrated Impaction Device
K. Takenaka, S. Togashi, R. Miyake, T. Sakaguchi and M. Hide
Journal of Breath Research, 10, 036009 (11 pages), (2016),
DOI: 10.1088/1752-7155/10/3/036009.
(3) Analysis of Particle in Liquid using Excitation-Fluorescence Spectral Flow Cytometer
K. Takenaka and S. Togashi
Japanese Journal of Applied Physics, 57 (1), 017001 (7 pages), (2018),
DOI: 10.7567/JJAP.57.017001

３．参考論文

(1) Rapid Live Bacteria Counter with Disposable Flow Cytometry Cassette
K. Takenaka, Y. Sasaki, H. Inami, H. Nakamoto, Y. Watanabe, M. Kurihara, K. Takei, J. Ishikawa and R. Miyake
Chemical and Biological Microsystems Society, 13th International Conference on Miniaturized Systems for Chemistry and Life Sciences

(µTAS2009), Jeju, South Korea, 484-486, (2009),
ISBN: 978-0-9798064-2-1

(2) Integrated Cassette for Counting Low-concentration Live Bacteria in Foods Using 3D Staining Technology
K. Takenaka, Y. Sasaki, H. Inami, H. Nakamoto, Y. Watanabe, M. Kurihara, K. Takei, J. Ishikawa and R. Miyake
Chemical and Biological Microsystems Society, 14th International Conference on Miniaturized Systems for Chemistry and Life Sciences (µTAS2010), Groningen, Netherlands, 1043-1045, (2010),
ISBN: 978-0-9798064-3-8

(3) Rapid Airborne Virus Detection Using Mist-Labeling Based on Micro Reaction Effect,
K. Takenaka, S. Togashi and R. Miyake
Chemical and Biological Microsystems Society, 16th International Conference on Miniaturized Systems for Chemistry and Life Sciences (µTAS2012), Okinawa, Japan, 1885-1887, (2012),
ISBN: 978-0-9798064-5-2

(4) Rapid Airborne Pathogens Detection System Using Disposable Impaction Cartridge,
K. Takenaka, S. Togashi and R. Miyake,
Chemical and Biological Microsystems Society, 17th International Conference on Miniaturized Systems for Chemistry and Life Sciences (µTAS2013), Freiburg, Germany, 877-879, (2013),
ISBN: 978-0-9798064-6-9

(5) Integrated Micro-Impaction Cartridge Covered With Microporus Light-blocking Film for Low-Concentration Airborne Virus Detection
K. Takenaka, S. Togashi, R. Miyake, T. Sakaguchi and M. Hide
Chemical and Biological Microsystems Society, 18th International Conference on Miniaturized Systems for Chemistry and Life Sciences (µTAS2014), San Antonio, Texas, USA, 2041-2043, (2014),
ISBN: 978-0-9798064-7-6

(6) Excitation-Fluorescent 3D Spectral Flow Cytometer for Single-Cell Analysis,
K. Takenaka and S. Togashi
Chemical and Biological Microsystems Society, 19th International Conference on Miniaturized Systems for Chemistry and Life Sciences

(μTAS2015), Gyeongju, South Korea, 1813-1815, (2015),
ISBN: 978-0-9798064-8-3

(7) Analyses of Particle Composition in Vegetables Suspension Using Excitation-Fluorescent Spectral Flow Cytometer
K. Takenaka and S. Togashi
Chemical and Biological Microsystems Society, 20th International Conference on Miniaturized Systems for Chemistry and Life Sciences (μTAS2016), Dublin, Ireland, 1360-1361 (2015),
ISBN: 978-0-9798064-9-0

主論文

To Yumi and Haruka

The Contents summary

This thesis is consisted of six chapters. Brief summaries of each chapter are shown in the following. There is a wide variety of biological particles such as bacteria, viruses etc. on the Earth. These biological particles have effects on human activities, more or less. It is essential for a comfort and healthy life to understand characters and dynamics of biological particles in sphere of human habitation such as foods, water and air we ingest, objects we contact directly. We predict that discoveries of a new kind of biological particles and basic knowledge of phenomenon caused by the biological particles increase at an accelerated pace. Thereby we have to provide rapid measurement methods of biological particles timely to understand character and dynamics of target biological particles.

For this reason, information about biological particles' character and dynamics, and rapid measurement method for these particles are organized from a statistical perspective. Then, we advance a methodology to bring a rapid measurement method and a system configuration using the method for purposes. Finally, we attempted to apply the methodology to three kind of system development.

In chapter 1, first, we investigated biological particles in sphere of human habitation from the perspective of particle type, particle size and phenomenon caused by these particles. Next, we investigated and classified existing measurement methods for these particles and preparations for improving the precision of measurements.

In chapter 2, we organized and discussed measurement methods for biological particles in sphere of human habitation based on the above survey results from a perspective of statistic. The result of discussion shows it necessary to measure a lot of biological particles in practical time for understanding character and dynamics of these particles.

Additionally, we thought that measurement methods of particles in sphere of human habitation can be divided to following three methods from considering relative position between a space where sample containing target biological particles (called as target sample space in the following) and a space to measure target biological particles (called as probe space in the following).

First method is to measure every particles directly in the target sample space by scanning through the target sample space with the probe space at high speed (called as scanning method). Second method is to measure every particles one by one serially in the target sample space by transmitting the target sample space into the probe space (called as flowing method). Third method is to measure target biological particles collected in the probe space at one time by concentrating the target sample space to the approximately

same volume of the probe space (called as concentrating method). Scanning method and flowing method are effective to measure one by one detectable biological particles which is relatively large or bright particles, etc. Additionally, concentrating method is effective to measure one by one non-detectable particles which are very small particles such as virus particles.

Furthermore, number distribution of biological particles in the space follows the Poisson distribution on the premise that biological particles in the space have no mutual interference and keep independence. Thereby, by determining specifics of a dispersion of measurement result or acceptable range of counting loss from the statistic theory based on Poisson's distribution, we developed important specifics of measurement units such as volume of a target sample space and dimension of a probe space (a field of view of a measurement instrument) in a unified concept. Then, we applied these methodologies to developments of a rapid counting system for live bacteria in foods, an excitation-fluorescent spectral flow cytometer for particles in liquid and a sensing system for biological airborne particles. Each research content and achievement are shown in from chapter 3 to chapter 5.

We showed the development of the counting system for live bacteria in foods in chapter 3. The cultural method, which is an accurate method, is used popularly for exhaustive measurements of live bacterial numbers in foods. However, this method is difficult to measure live bacterial numbers simply and rapidly.

Thereby, in this thesis, we applied the flowing method in the above measurement methods to the measurement of live bacterial numbers. Additionally, we developed the rapid counting system for live bacteria in foods. This system proceeds live bacteria counting processes in a disposable cartridge which are consisted of removing process of food debris, labeling process of live bacteria with fluorescent dyes and measurement process of live bacterial numbers by flow cytometry.

We evaluated the performance of this system by measuring numbers of live bacteria in sample solutions. Consequently, the following conclusions based on our work are drawn.

(a) By the decision methodology based on the statistic theory, we designed the flow cell (20×40 μm^2) for the fluorescence flow cytometry which suitable for the conditions that the counting loss is less than 0.05 and the pressure loss is less than 1.0×10^5 Pa. Additionally, we calculated the needed volume of sample solution (number concentration of live bacteria: 10^3 particles/mL) as the target sample space on the basis of the condition that measured sample solution contains more than 50 live bacteria with 99.9 % possibility. As a result, we decide that the volume of

sample solution was 100 μL.

(b) To improve the sensitivity of the system, we developed a new discrimination method for live bacteria in homogenized food suspension using three kinds of fluorescent dyes. SYTO®41 (450-nm fluorescent peak) and LDS751 (720-nm fluorescent peak) were selected as the fluorescent dyes for live/dead bacteria, and SYTOX® ORANGE (570-nm fluorescent peak) was selected as the fluorescent dyes for dead bacteria. Live bacteria can be distinguished from other fluorescent particles because only live bacteria emit fluorescence of SYTO®41 and LDS751

(c) For evaluations of the measuring performance of the system, live bacteria in an emulsion of Escherichia Coli (E Coli) were counted by the system and a cultural method. The measuring performance of the system and the cultural method were judged to be equal because both methods had high correlation, namely, a correlation coefficient of 0.97 in the range of live bacteria concentration of 10^3 to 10^6 cell/ml. This result shows that the decision methodology based on the statistic theory is effective for the design of this system.

(d) For evaluations of the measuring performance of the system, live bacterial numbers in homogenized vegetable suspensions were measured by the system and the culture method. The measuring performance of the system and the cultural method are equal because both methods have high correlation; namely, correlation coefficient is 0.96 in spinach, 0.91 in carrot, 0.90 in red cabbage and 0.93 in potato in the range of live bacteria concentration of 10^2 to 10^6 cell/ml. These results shows the new discrimination method using three kind of fluorescent dyes is effective for the sensitivity improvement of the system.

We showed the development of the system for detailed measurements of particles in liquids by developing the flowing method further in chapter 4.

The fluorescence spectroscope is enable us to understand broadly amounts and types of particles in a liquid by measuring excitation-fluorescence spectra (fluorescence fingerprint) of a liquid containing particles. However, it is hard to measures particles in small amounts because it is impossible to analyze an individual targeted particle. Therefore, we developed an excitation-fluorescent spectral flow cytometer (EFSFCM) using excitation light of dispersed white light which can measure a fluorescence fingerprint of a particle. Additionally, we determined types of particles from fluorescence fingerprint of a particle by the EFSFCM. Consequently, the following conclusions based on our work are drawn.

(a) We designed an optical unit of the EFSFCM by the decision methodology based on the statistic theory. The optical unit irradiates a designed measurement area

(probe space, 200 μm × 350 μm) with dispersed white light and measures a fluorescence fingerprint of a particle (excitation wavelength band, 400 - 650 nm; fluorescence wavelength band: 400 - 700 nm).

(b) Fluorescent particles (particle size: 2 μm, maximum wavelength of excitation light: 441 nm, maximum wavelength of fluorescence: 486 nm) in the range of number concentration ($\leq 1.0 \times 10^4$ particle/mL) fixed from the statistic theory are measured by the EFSFCM. A fluorescence fingerprint of the fluorescent particle was measured in the case that more than one fluorescent particle are measured rarely at the same time. Thereby the decision methodology based on the statistic theory is shown to be of benefit.

(c) Particles in homogenized tomato suspensions and spinach suspensions were measured by the EFSFCM. Homogenized tomato suspension contains many particles emitting blue-green fluorescence whose wavelengths are under 490 nm. Besides, a homogenized spinach suspension contains two kinds of particles that emit blue-green fluorescence and emit near-infrared fluorescence at 695 nm. These results agree with features of components of tomato and spinach.

We showed the development of the system for measurements of biological airborne particles such as virus particles in chapter 5.

Detecting biological airborne particles such as virus particles in bless can enable people to do self-diagnoses of respiratory infections such as influenza. However, it is difficult to detect biological airborne particles one by one because these particles are small (minimum sizes: 0.3 μm). Thereby, we applied the concentrating method to measurements of biological airborne particles in this work. In particular, we designed, manufactured and evaluated the sensing system of biological aerosolized particles (SSBAP) which can collect biological aerosolized particles and detect fluorescence of these particles using a sampling bag with bless and a disposable cartridge. Consequently, the following conclusions based on our work are drawn

(a) We selected an impaction method as one of concentrating methods to collect biological airborne particles on a surface of a collection plate. Additionally, we invented a combined method of the impaction method and the fluorescence detection to detect biological airborne particles.

(b) We designed the disposable cartridge for an impaction use. The cartridge with 109 nozzles (ϕ 70 μm) are designed from theoretical consideration with combination of the Stokes number and the Reynolds number of the air flowing through a nozzle, and particle track analyses of particles flowing through a nozzle in addition to the decision methodology based on the statistic theory. A designed cartridge with the

impaction function could collect more than 97% of the ϕ 0.3 μm aerosolized particles in the sampling bag.

(c) In the range of number concentration of E. Coli (less than 1.0×10^5 particles/L) decided by the statistic theory, we measured aerosolized E. Coli by the system. Measurement results show that there is a high correlation between outputs of the system and number concentration of E. Coli. Thereby the decision methodology based on the statistic theory is shown to be of benefit.

(d) We measured aerosolized influenza virus particles (number concentration: 8.3×10^3 - 1.0×10^4 particles/L) by the system. Measurement results show that there is a high correlation between outputs of the system and number concentration of aerosolized influenza virus particles. Thereby, it is possible to measure small influenza particles by the SSBAP.

We summarized results of these works and an effectivity of proposed decision methodology in chapter 6.

(1) We designed and manufactured the rapid counting system for measurements of number of live bacteria in foods. There are high correlation (R^2 is from 0.91 to 0.97) in measurements of live bacteria (number concentration: 10^3-10^6 cell/ml) in homogenized vegetable suspensions. Therefore, these results shows that the system can measure number of live bacteria in foods.

(2) We designed and manufactured an excitation-fluorescence spectral flow cytometer (EFSFCM) for measurements of excitation-fluorescence spectra (fluorescence fingerprints) of particles in liquids. Additionally, we measured fluorescence fingerprints of a particle in the designed range of number concentration (less than 1.0×10^4 particles/mL) by the EFSFCM.

(3) We designed and manufactured the sensing system for biological aerosol particles (SSBAP). The SSBAP collected biological particles in a disposable cartridge by impaction method and detect them by fluorescence method. Measurement results of biological particles (aerosolized E. Coli and influenza virus particles) shows that there are high correlation between outputs of the SSBAP and number of particles in designed range of number concentration (less than 1.0×10^5 particles/L). Therefore, these results shows that the system can measure airborne virus particles.

For all of these reasons, the decision methodology based on the statistic theory is benefit for designs of measurement systems of biological particles in sphere of human habitation.

Contents

Chapter 1. Introduction

1.1 Motivation: Influence of particles in the sphere of human habitation

There are many microparticles which are invisible to the human eyes on the Earth. These particles exert more or less influence on human activities. For example, a large amount of cedar pollen, which is in the air in spring in Japan, causes a large number of hay fever sufferers to have allergy symptoms [1][2]. The occurrence frequency of photochemical smog increases as temperature increases in summer [3]. Additionally, airborne particles including influenza viruses exhaled with coughs and sneezes by influenza patients cause an influenza outbreak from autumn to winter [4].

Furthermore, there are not only particles in the air but also particles in the water, which exert more or less influence on human activities too. For example, a water-bloom, which occurs in a eutrophied lake or a pond is a phenomenon caused by an outbreak of microalgae such as phytoplankton [5]. Additionally, fungi and bacteria in beverage which cause food poisoning are tested rigorously in hygiene inspections [6].

Table 1-1 shows types of particles in the air and liquids, and phenomena caused by these particles. Fig. 1-1 shows the sizes and types of these particles.

Table1-1 Particles in the air or liquid

Particles	Space containing particles	Examinations of phenomenon caused by particle
Cedar pollens	Air	Pollen disease
PM2.5	Air	Smog, Respiratory disease
Influenza virus particles	Air (Breath of infected patients)	Respiratory disease, Outbreak of the flu
Spores of fungi	Air, water,	Food poisoning
Bacteria	Air, water,	Food poisoning
Planktons	Water (Pond, lake)	Blue-green algae

Particles other than those shown in Table 1-1 exert influence on human activities. Thereby, it is important to examine particles in the environment for a comfortable and healthy life because our appetites for better lives increase.
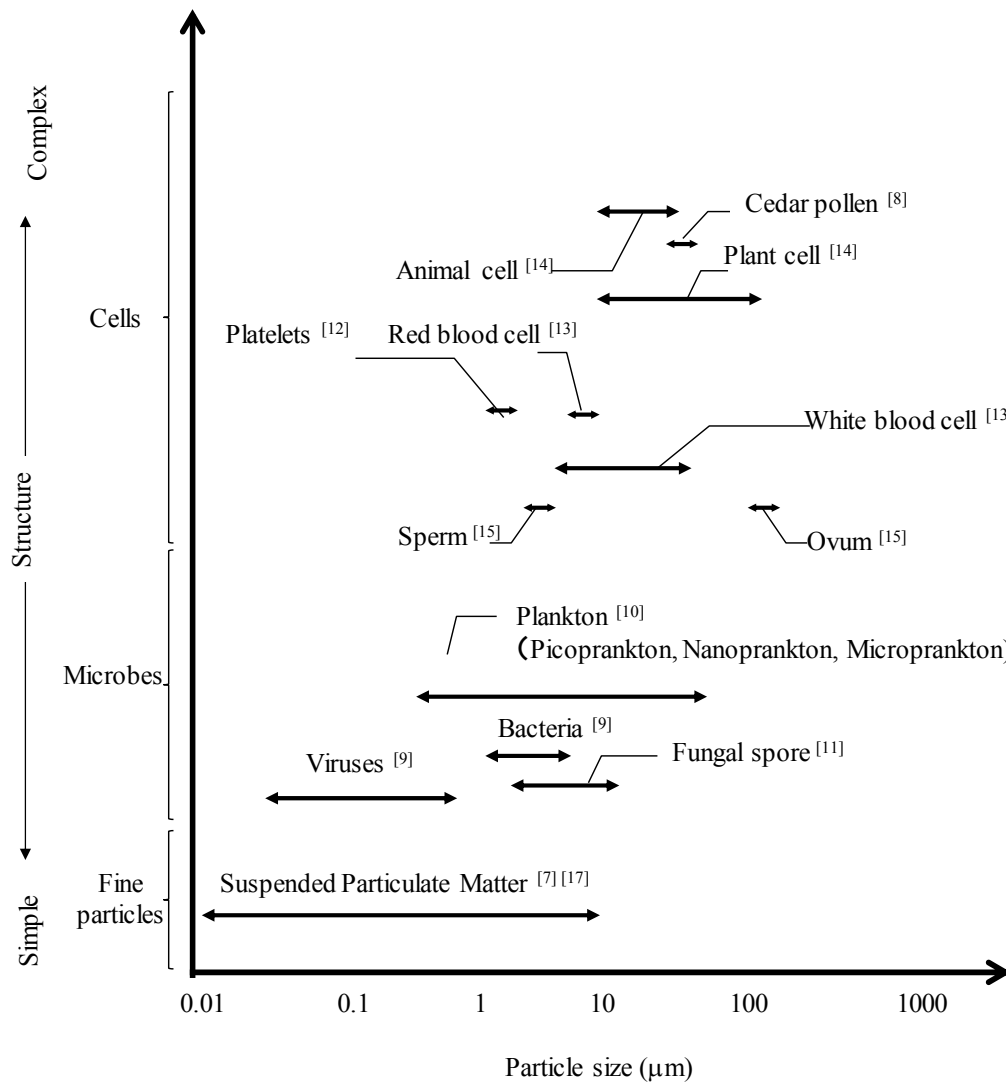
Fig. 1-1 Type and size of particle in the air or liquid

1.2 Classification of measurement methods of particles in environment

There are many types of particles in the air and liquids. These particles exert influence on human activities. Thereby, it is important to understand the types and number of particles in the environment, and to take action such as the elimination of particles in case that there are many harmful particles. Many measurement methods have been developed and used for different types of particles or for different measurement purposes. Table 1-2 shows typical measurement methods for particles.

2

Table 1-2 Measurement methods for particles in the air and liquids

Particle	Sample	Measurement methods				
		Indirect	Direct			
			Weight	Shape, size	Optical properties	Electrical properties
PM 2.5	Air	-	FRM[17], TEOM[17],	Microscopy [18]	PC[19]	Impactor[20]
Cedar pollens	Air	-	-	Microscopy (Durham Method)[21]	PC[22]	-
Plankton	Water	-	-	Microscopy [23]	IFCM[24]	-
Bacteria	Water	CM[25], Immno[25], GA[25]	-	Microscopy [25]	FCM[26], SCM[27]	CC[38]
	Air	Impactor and CM[28], GA[28]	-	Impaction and Microscopy	FCM[29]	-
Viruses	Water	PT[30], Immno[31], GA[31]	-	-	-	-
	Air	Impactor and PT[32]	-	-	-	-
Cell, Blood cell	Water	GA[33]	-	Microscopy [34]	FCM[35], SCM[36], IFCM[37]	CC[38]

FRM: Federal Reference Method, TEOM: Tapered Element Oscillating Microbalance, CM: Cultural method, PT: Plaque technique, Immno: Immuno-chromatography, PC: Particle counter, FCM: Flow cytometer, SCM: Scanning cytometer, IFCM: Imaging flow cytometer, CC: Coulter counter, GA: Gene amplification

Yellow cell: Objects of research in this thesis

(1) PM2.5 (Particle matter 2.5)

The Federal Reference Method (FRM) is the standard and most reliable measurement method for PM 2.5. This is a method to measure a mass concentration using a filter [17]. In this method, PM 2.5 particles are collected on a filter for a set time period by aspirating the air for sampling in a constant flow from an inlet. Next, a mass concentration of PM 2.5 is calculated from a weight difference of the filter between before and after use.

On the other hand, Tapered Element Oscillating Microbalance (TEOM) is a typical measurement method for PM 2.5 using an automatic measurement system [17]. The TEOM system is equipped with an oscillator with a filter tip. The oscillator with the filter is vibrated at its natural frequency. In this system, the natural frequency decreases as the weight of the filter increases when PM 2.5 particles are collected on the filter. Next, the weight of the collected particles is calculated from the change of the natural frequency. The mass concentration of PM 2.5 is calculated by the quotient of the weight of collected particles divided by the volume of aspirated air [17].

As other methods of measuring PM 2.5 particles, manual measurements using an optical microscope [18], and automatic measurements using a particle counter [19] or an impactor [20] are practiced.

(2) Cedar pollen

The Durham method, which was devised by Durham in 1946, is used most commonly for the measurement of cedar pollen [21]. The Durham sampler, which is used most commonly worldwide as a standard pollen sampler, consists of a mount for positioning a slide glass holder between two horizontal circular metallic disks. Cedar pollen collected on the slide glass for 24 hours are counted using a microscope. Additionally, a particle counter is used to automatically measure cedar pollen [22].

(3) Plankton

Plankton in ballast water is commonly counted and judged by differences in its size and shape in the following manner. After ballast water containing plankton is concentrated, the concentrated ballast water is laid on a slide glass. The slide glass is observed using a microscope to count the plankton [23]. Additionally, the Flow CAM®, which is a type of imaging flow cytometer, is commercially supplied by Fluid Imaging Technologies, Inc. [24]. The measurement principle is shown in the appendix at the end of this thesis.

(4) Bacteria in liquid

The culture method is used most commonly to count bacteria in liquids [25]. In the culture method, a sample containing bacteria is suspended in an agar medium. Colonies of bacteria are formed on the agar medium plate after 24-48 hours of cultivation. It is possible to count bacteria in the sample by counting the colonies. Details of the culture method are shown in chapter 3. Other methods include the immunography method for the detection of bacteria antigens and gene amplification for bacteria genes [25].

Additionally, a flow cytometer shown in chapter 3 [26] and a scanning cytometer [27] are commercially supplied. The details of the flow cytometer and the scanning cytometer are shown in the appendix at the end of this thesis.

(5) Bacteria in the air

A combined method of an impaction method and a culture method is used commonly to count airborne bacteria [28]. The impaction method is a method for collecting airborne bacteria on a plate by the inertial force of an air stream. Airborne bacteria are collected on an agar medium plate using the impaction method. After collected bacteria are cultivated for 24-48 hours, colonies of bacteria formed on the agar medium plate are counted.

Additionally, the IMD-ATM, which is an automatic system to count airborne bacteria using the same principle as the particle counter, is commercially supplied by Azbil corp. [29].

(6) Viruses in liquid

In the plaque assay, a sample containing host cells is suspended in an agar medium [30]. The virus-infected cells lyse and spread the infection to adjacent cells, and thereby viral plaques are formed on the agar medium plate after cultivation. It is possible to count the virus titer in the sample by counting plaques.

Additionally, the immunochromatography method for detection of viral antigens and the gene amplification method for viral genes are used [31].

(7) Viruses in the air

A combined method of an impaction method and a viral plaque assay was reported as a method to count aerosolized bacteriophages [32]. On the other hand, no automatic system for measurement of viruses in the air is being commercially supplied at this time. In this thesis, a sensing system of airborne biological particles which can measure airborne viruses will be shown in Chapter 5.

(8) Cells, such as blood cells

Many kinds of methods are used to count cells. For example, a fluorescent flow cytometer is used commonly to measure a large amount of cells in a short time [35]. On the other hand, a microscope is used commonly to examine cells closely [34].

Some of the particles in Table 1-1 and some of the measurement methods in Table 1-2 have become hot topics due to changes in social trends such as social modernization, changes in lifestyles, and the establishment of laws or treaties. PM 2.5 is a social issue in China in the rapid progress of industrialization [39]. Additionally, monitoring plankton in ballast water has become of high importance because the Ballast Water Management Convention was concluded in 2004 [40].

We predict that discoveries of new kinds of biological particles and additions to our basic knowledge of phenomena caused by biological particles will increase at an

accelerated pace.

Thereby we have to provide rapid measurement methods of biological particles timely to understand character and dynamics of target biological particles.

However, it is clearly difficult to develop measurement methods and systems haphazardly from scratch. Thereby, we have to provide rapid measurement methods of biological particles in a timely manner so we can understand the character and dynamics of the target biological particles.

Appendix : Measurement principles of cytometer

In this appendix, measurement principles of cytometers mentioned earlier are shown: particle counter, flow cytometer, imaging flow cytometer and imaging cytometer.

(i) Paricle counter

This is a measurement system to count particles in the air or liquid. This system flows a sample containing particle across a laser, and counts particles in a sample stream according to size by measuring scattering light from a particle passing across the laser.

(ii) Flow cytometer

As with the particle counter, this system can count particles by measuring fluorescence from a particle passing across the laser. The above-mentioned IMD-A^{TM} is a type of flow cytometer using properties that fungus and bacteria irradiated with an ultraviolet lay emit fluorescence [29].

(iii) Imaging flow cytometer

This system sends a sample containing target particles across an imaging area of a camera, and takes pictures of particles passing through the area. A type of a particle can be distinguished by analyzing a shape and a size of the particle from pictures.

(iv) Imaging cytometer

This system can get detailed image data of a cell by moving an area irradiated by an excitation light. First, a surface of a cell fixed on a slide glass is scanned with an excitation light such as a laser. Second, image data of a cell is converted from optical information about scattering light, transmitted light and fluorescence from areas irradiated by the excitation light.

A flow cytometer can get limited information of a cell such as intensities of fluorescence and scattering light, however an imaging cytometer, which needs longer time per particle than a flow cytometer, can measure a single particle particularly.

6

1.3 Preparation of particle measurement

To improve the accuracy of the measurement of target particles, processes to emphasize particles such as purification and so on are often worked out before the measurement. These processes are presented as preparation processes in this thesis. Additionally, processes to measure target particles after a preparation process are presented as measurement processes.

Table 1-3 Preparation for particle measurement

	Preparation	Particle's factor for preparation	Example
Collecting intended particle or removing unintended particle	Filtration	Size	Collecting plankton from sea [23]
	Centrifugal separation	Mass	Separation of plasma and blood cell from whole blood [49]
	Separation by inertial force	Mass	Impaction method [42] Separation of CTC from whole blood [43]
	Separation using difference in degree of adsorption	Adsorption	Chromatography [44], Immunomagnetic separation [45]
	Electrophoresis	Charge and size	Gel electrophoresis [46] Capillary electrophoresis [47]
	Dielectrophoresis	Dielectric constant	
Emphasizing intended particle	Fluorescent modification	Specific binding	Fluorescent flow cytometer [50]
	Large particle modification	Specific binding	Flow cytometer [50]

Preparation processes are roughly divided into two types. The first preparation processes are processes that target particles are collected but other particles are eliminated. The second preparation processes are processes that target particles are marked with characteristic marks. These preparation processes use differences in physical features

between target particles and other particles. Table 1-3 shows the types of preparation processes and the physical features of target particles used for each preparation process by dividing preparation processes into two groups.

(1) Collection of target particles and elimination of other particles
    (a) Separation using differences of particle size (Filtration)

        This is a method to separate target particles from other particles using difference of particle size. A filtration method is shown in the following because this is the most popular method among them. Filtration is a method in which particles larger than a pore size of a filter are collected by flowing air or liquid containing target particles through a filter.

        The purposes of filtration before measurement processes are roughly divided into two types. The first purpose is to measure collected target particles on a filter. The second is to increase the abundance ratio of target particles in a sample solution by removing other larger particles from the sample solution [41].

    (b) Separation using centrifugal force

        This is a method to separate target particles from other particles using differences of particle mass. In this method, target particles are separated from other particles by making target particles sink or float with centrifugal force. Especially in density-gradient centrifugation, it is possible to separate multiple particles at each layer using a concentration gradient liquid [41].

    (c) Separation using inertial force

        This is a method to separate target particles from other particles using differences of particle mass. In this method, target particles are removed from an air or liquid stream by inertial force generated at a sharp bend of the stream [42]. An impaction method is known as a method to separate airborne particles. Additionally, there is a report that tumor cells were separated from blood flowing in a microchannel using inertial force [43].

    (d) Separation using adsorptive property of particle

        This is a method to separate target particles from other particles using differences of adsorption force [41]. In this method, target particles are removed from other particles in the following manner. First, target particles are adsorbed on a surface of an adsorptive material. Second, target particles are separated from other particles by pulling out the adsorptive material. Adsorption forces include an electrostatic force, a hydrophobic force, and a biochemical binding force such as an antigen-antibody reaction. Typical separation methods using the adsorption force are

8

chromatography [44] and a method using magnetic particles with antibodies on the surface [45].

(e) Electrophoresis

   This is a method to separate target particles from other particles using differences of electric charge and size. In this method, target particles are moved in a positive or negative direction of an electric field by generating an electric field on a liquid containing particles. In electrophoresis using a carrier such as paper or a gel, it is possible to finely separate particles using differences of particle size because a reticulate structure of the carrier works as a filter [46]. Electrophoresis in a capillary without a carrier is used to separate DNA using differences of base sequence [47].

(f) Dielectrophoresis

   This is a method to separate target particles from other particles using difference of dielectric constant. In this method, target particles are moved by the force which a nonuniform electric field generates [48]

(2) Labeling target particles with marks

This is a method to detect target particles by improving visualization of particles labeled with fluorescent dyes or large size particle. Specific binding force to labeling target particles with marks includes a biochemical binding force such as an antigen-antibody reaction, an affinity force between DNA and fluorescent dye, and a hydrophobic force [41].

As mentioned above, preparation processes shown in Table 1-3 are roughly divided into two types. The first types are processes that target particles are collected but other particles are eliminated. The second types are processes that target particles are marked.

Preparation processes have to be changed depending on the types of target biological particles. Additionally, as with measurements of target biological particles, it is important to understand the characteristics and dynamics of target biological particles.

1.4 Conclusion

With the increase in the types of biological particles to be measured, measurement methods for these particles are needed more and more. As mentioned in earlier in this chapter, many kinds of preparation processes and measurement processes exist and are used practically. Thereby, it is important in the development of measurements for new target particles to decide a general course of the development by selecting a most suitable method from many existing methods or combining these methods, and to decide the specifications of the measurement method. Additionally, it is important to focus on

solving the particular problems in measurement of the new particles after decisions of the course of the development and specifications of the measurement method.

Veteran developers can decide the most suitable course of the development of the measurement methods for target biological particles depending on their experience. However, inexperienced developers will have great difficulty to develop a measurement method. Additionally, their haphazard developments have the potential to spend a lot of money and time. Thereby, they require a methodology to decide the most suitable course of the development of the measurement methods for target biological particles and decide the specifications of the measurement method.

Therefore, we propose a methodology to develop a rapid measurement method in this thesis. This thesis consists of 6 chapters. First, an overview of measurements of particles in the sphere of human habitation is shown in this chapter. Second, methodologies to develop measurement methods for particles in the sphere of human habitation using statistical theories are shown in chapter 2. Moreover, based on these methodologies, a development of a measurement method of live bacteria numbers in food suspensions is shown in chapter 3, a development of a particle analysis method using an excitation-fluorescent spectrum of a particle is shown in chapter 4, and a development of a measurement method of airborne biological particles is shown in chapter 5. Finally, a general overview and our vision for the future of measurements of particles in the sphere of human habitation are shown in chapter 6.

Reference

[1] Horiguchi, S., and Saitoh, Y. "Japanese Cedar Pollinosis in Nikko, Japan (In Japanese)," *The Japanese Society of Allergology*, Vol. 13(1,2), (1964), pp. 16-18.

[2] Yamada, T., Saito, H., and Fujieda, S. "Present state of Japanese cedar pollinosis: The national affliction," *J. Allergy Clin. Immunol.*, Vol. 133(3), (2014), pp. 632–639.e5.

[3] Colbeck, I and MacKenzie, A. R. *Air pollution by photochemical oxidants*, (1996), Elsevier, ISBN: 978-0-444-88542-5.

[4] Center for Disease Control and Prevention Homepage, Influenza (Flu), https://www.cdc.gov/flu/about/season/flu-season.htm [Accessed 1 April 2017].

[5] United States Environmental Protection Agency Homepage, Harmful Algal Blooms, https://www.epa.gov/nutrientpollution/harmful-algal-blooms
[Accessed 1 April 2017].

[6] NHS choices Homepage, Food poisoning, http://www.nhs.uk/conditions/Food-poisoning/Pages/Introduction.aspx
[Accessed 1 April 2017].

[7] Hays, M. D., Beck, L., Berfield, P., Willis, R. D., Landis, M. S., and Stevens, R. K. "Physical and Chemical Characterization of Residual Oil-Fired Power Plant Emissions," *Energy Fuels*, Vol. 23(5), (2009), pp. 2544–2551.

[8] Morita, J., Wang, Q., Gong, X., Nakamura, S., Suzuki, M., Nakajima, T., Sekiguchi, K., Nakajima, T., and Miwa, M. "Basic Study on Chemical Modification of Japanese Cedar Pollen Allergen (Cry j 1) by Air Pollutants and Apoptosis Inducibility of 3-Nitrotyrosine for Hela Cell," *Earozoru Kenkyu*, Vol. 27(1), (2011), pp. 71-77 (In Japanese).

[9] Baron, S. ed. *Medical Microbiology, 4th Edition* (1996), University of Texas Medical Branch at Galveston, ISBN: 978-0-963-11721-2.

[10] Omori, M., and Ikeda, T. *Methods in marine zooplankton ecology*, (1984), Krieger, ISBN: 978-0-894-64653-9.

[11] Reponen, T., Grinshpun, S. A., Conwell, K. L., Wiest, J., and Anderson, M. "Aerodynamic versus physical size of spores: Measurement and implication for respiratory deposition," *Grana*, Vol. 40(3), (2001), pp. 19-125.

[12] Paulus, J. M. "Platelet size in man," *Blood*, Vol. 46(3), (1975), pp. 321-336.

[13] Ogawa, T., Oshima, T., and Asano, S. *Textbook of Hematology*, Chugai-igakusha, ISBN: 978-4-498-02544-8.

[14] Bolsover, S. R., Shephard, E. A., White, H. A., and Hyams, J. S. *Cell Biology A Short Course 3rd edition*, Wiley, ISBN: 978-0-470-52699-6.

[15] Alberts, B., Johnson, A., Lewis, J., Raff, M., Roberts, K., and Walter, P. *Molecular Biology of the Cell 5th edition,* Garland Science, ISBN: 978-0-815-34105-5.

[16] Acton, Q. A. ed. *Issues in Environmental Research and Application: 2013 Edition,* ScholarlyEditions, ISBN: 978-1-490-10935-0.

[17] Ministry of Environment Homepage., Measurement methods about Particulate Matter 2.5 (PM2.5) (In Japanese).
https://www.env.go.jp/council/former2013/07air/y070-25/mat04-2.pdf
[Accessed 1 April 2017].

[18] Kogakuin univ. homepage,
https://www.u-presscenter.jp/modules/bulletin/index.php?page=article&storyid=6302
[Accessed 1 April 2017].

[19] TSI homepage,
http://www.tsi.com/airassure-pm2-5-indoor-air-quality-monitor-en/
[Accessed 1 April 2017].

[20] Demokritou, P., Kavouras, I. G., Harrison, D., and Koutrakis, P. "Development and evaluation of an impactor for a PM2.5 speciation sampler," *J. Air Waste Manaq. Assoc.*, Vol. 51(4), (2001), pp. 514-523.

[21] Kishikawa, R., Sahashi, N., Saitoh, A., Kotoh, E., Shimoda, T., Shoji, S., Akiyama, K., and Nishima, S. "Japanese Cedar Airborne Pollen Monitoring by Durham's and Burkard Samplers in Japan ―Estimation of the Usefulness of Durham's Sampler on Japanese Cedar Pollinosis―," *AIRIES*, Vol. 13, (2009), pp. 55-62.

[22] Suzuki, M. "Measurement and prediction of cedar and Japanese cypress," *Journal of Japan Society for Atmospheric Environment*, Vol. 42(4), (2007), pp. 34-49.

[23] The Plankton Society of Japan Homepage, Symposium of the plankton society of Japan 2006, Expansion of plankton and ballast water (In Japanese)
http://www.plankton.jp/sub08_15.html [Accessed 1 April 2017].

[24] Fluid Imaging Technologies, Inc. Hmepage, FlowCam® 8000 Series,
http://www.fluidimaging.com/products/flowcam-8000 [Accessed 1 April 2017].

[25] Mise, K. and Inoue, F. ed. *Practical guide of Bacteriological testing of food*, (1996), pp.52-53, Kodansha scientific (in Japanese), ISBN: 978-4-06-153712-5.

[26] Takenaka, K., Sasaki, Y., Inami, H., Nakamoto, H., Watanabe, Y., Kurihara, M., Takei, K., Ishikawa, J. and Miyake, R. "Rapid Live Bacteria Counter Using Cassette-Type Flow Cytometry," *Trans. Jpn. Soc. Mech. Eng. Series C*, Vol. 77, (2011), pp. 401-410 (in Japanese).

[27] Shimakita, T., Tashiro, Y., Katsuya, A., Saito, M., and Matsuoka, H. "Rapid

Separation and Counting of Viable Microbial Cells in Food by Nonculture Method with Bioplorer, a Focusing-Free Microscopic Apparatus with a Novel Cell Separation Unit," *J. Food Prot.*, Vol. 69(1), (2006), pp. 170-176.

[28] Yang, C. S. and Heinsohn, A. ed. *Sampling and Analysis of Indoor Microorganisms*, (2007), p.65, Wiley, ISBN: 978-0-470-11242-7.

[29] Hasegawa, N. "Quantitative Comparison of the Autofluorescence of Bacteria and Polystyrene Microspheres under Violet Wavelength Excitation for Verification of Fluorescencebased Bioaerosol Detector Results," *Biocontrol Science*, Vol. 18(4), (2013), pp. 211-215.

[30] VIRAPUR homepage
http://www.virapur.com/protocols/Phage%20Plaque%20Assay%20Protocol.pdf
[Accessed 1 April 2017].

[31] World health organization. ed, WHO recommendations on the use of rapid testing for influenza diagnosis,
http://www.who.int/influenza/resources/documents/RapidTestInfluenza_WebVersion.pdf [Accessed 1 April 2017].

[32] Jensen, M. M. "Bacteriophage Aerosol Challenge of Installed Air Contamination Control Systems," *Applied Microbiology*, Vol. 15(6), (1967), pp. 1447-1449.

[33] New England biolabs.Inc. home page, Whole-Cell PCR Protocol,
https://www.neb.com/protocols/2012/05/24/whole-cell-pcr-protocol
[Accessed 1 April 2017].

[34] Celeromics homepage, Technical Note - Neubauer Chamber Cell Counting,
http://celeromics.com/en/resources/docs/Articles/Cell-counting-Neubauer-chamber.pdf [Accessed 1 April 2017].

[35] Ibrahim, S. F., and Van den Engh, G. "Flow cytometry and cell sorting," *Adv. Biochem. Eng. Biotechnol.*, Vol. 106, (2007), pp. 19-39.

[36] Han, J. W., Breckon, J. W., Randell, D, A., and Landini, G. "The application of support vector machine classification to detect cell nuclei for automated microscopy," *Machine Vision and Applications*, Vol. 23(1), (2012), pp. 15-24.

[37] George, T. C., Basiji, D. A., Hall, B. E., Lynch, D. H., Ortyn, W. E., Perry, D. J., Seo, M. J., Zimmerman, C. A., and Morrissey, P. J. "Distinguishing Modes of Cell Death Using the ImageStream Multispectral Imaging Flow Cytometer," *Cytometry Part A*, Vol. 59A, (2004), pp. 237–245.

[38] Beckman coulter Homepage, https://beckman.jp/products/cell-counting/
[Accessed 1 April 2017].

[39] Sekine, Y. "Human health effect of Pariculate Matter 2.5 (PM2.5) (In Japanese),"

Indoor Environment, Vol. 17(1), (2014), pp. 19-35.

[40] International Maritime Organization Homepage, International Convention for the Control and Management of Ships' Ballast Water and Sediments (BWM), http://www.imo.org/en/About/conventions/listofconventions/pages/international-convention-for-the-control-and-management-of-ships'-ballast-water-and-sediments-(bwm).aspx [Accessed 1 April 2017].

[41] Stryer, L. *Biochemistry (4th edition)*, (1998), W. H. Freeman, ISBN: 978-0-716-72009-6.

[42] Hind, W. C. ed. *Aerosol Technology: Properties, Behavior, and Measurement of Airborne Particles, 2nd Edition*, (1999), Wiley, ISBN: 978-0-471-19410-1.

[43] Yang, D. K., Leong, S., Sohn, L.L. "High-Throughput Microfluidic Device for Circulating Tumor Cell Isolation from Whole Blood," *Proceedings of the 17th International conference on Miniaturized Systems for Chemistry and Life Sciences (Micro TAS 2013)*, (2010), pp. 413-415, ISBN: 978-0-9798064-3-8.

[44] Hostettmann, K., Marston, A., and Hostettmann, M. *Preparative Chromatography Techniques Applications in Natural Product Isolation Second ed.*, Springer Berlin Heidelberg, (1998), ISBN: 978-3-662-03631-0.

[45] Engstrand, L., and Enroth, H. "Immunomagnetic Separation and PCR for Detection of Helicobacter pylori in Water and Stool Specimens," *Journal of Clinical microbiology*, Vol. 33(8), (1995), pp. 2162-2165.

[46] Robyt, J. F., and White, B. J. *Biochemical Techniques Theory and Practice*, (1990), Waveland Press, ISBN: 978-0-88133-556-9.

[47] Skoog, D.A., Holler, F.J., and Crouch, S.R. *Principles of Instrumental Analysis 6th ed.*, (2007), Thomson Brooks/Cole Publishing Belmont, CA, ISBN: 978-0-495-01201-6.

[48] Gascoyne, P. R. C., Wang, X-B., Huang, Y., and Becker, F. F. "Dielectrophoretic Separation of Cancer Cells from Blood," *IEEE Trans. Ind. Appl.*, Vol. 33(3), (1997), pp. 670-678.

[49] Lorenzo, M. S. D., and Strasinger, S. K. *Blood Collection A SHORT COURSE edition 2*, (2010), F. A Davis company, US, ISBN: 978-0-803-61699-8.

[50] Shapiro, H. M. *Practical Flow Cytometry*, (2003), pp. 1-6, John Wiley & Sons, Inc., ISBN: 978-0-471-62228-4.

Chapter 2. Theoretical conditions of particle measurements

2.1 Categorization of measurement of particles

Measurement methods to measure particles in the sphere of human habitation one by one are categorized as the following two types in terms of a position relation of target particles within a space to measure target biological particles. The first types shown in Fig. 2-1 are measurement methods to measure particles in a space where there is a sample containing target biological particles (called a target sample space in the following (V_t (m^3)) by moving the space to measure target biological particles (called a probe space in the following (v_p (m^3)) like scanning. These methods are called scan methods. The second types shown in Fig. 2-2 are measurement methods to measure particles in a target sample space (V_t (m^3)) by making particles pass through a probe space (v_p (m^3)) with a certain drive force. These methods are called flow methods.

Target particles

probe space (v_p)

target sample space (Vt)
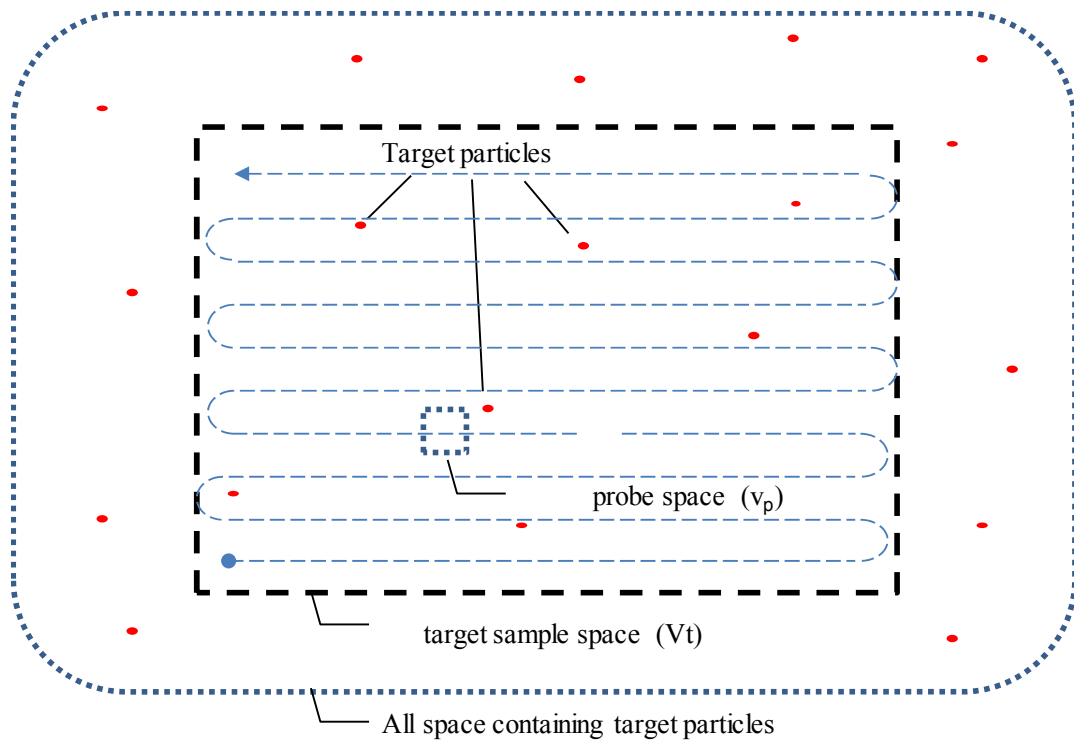
All space containing target particles

Fig. 2-1 Measurement of particles in a target sample space
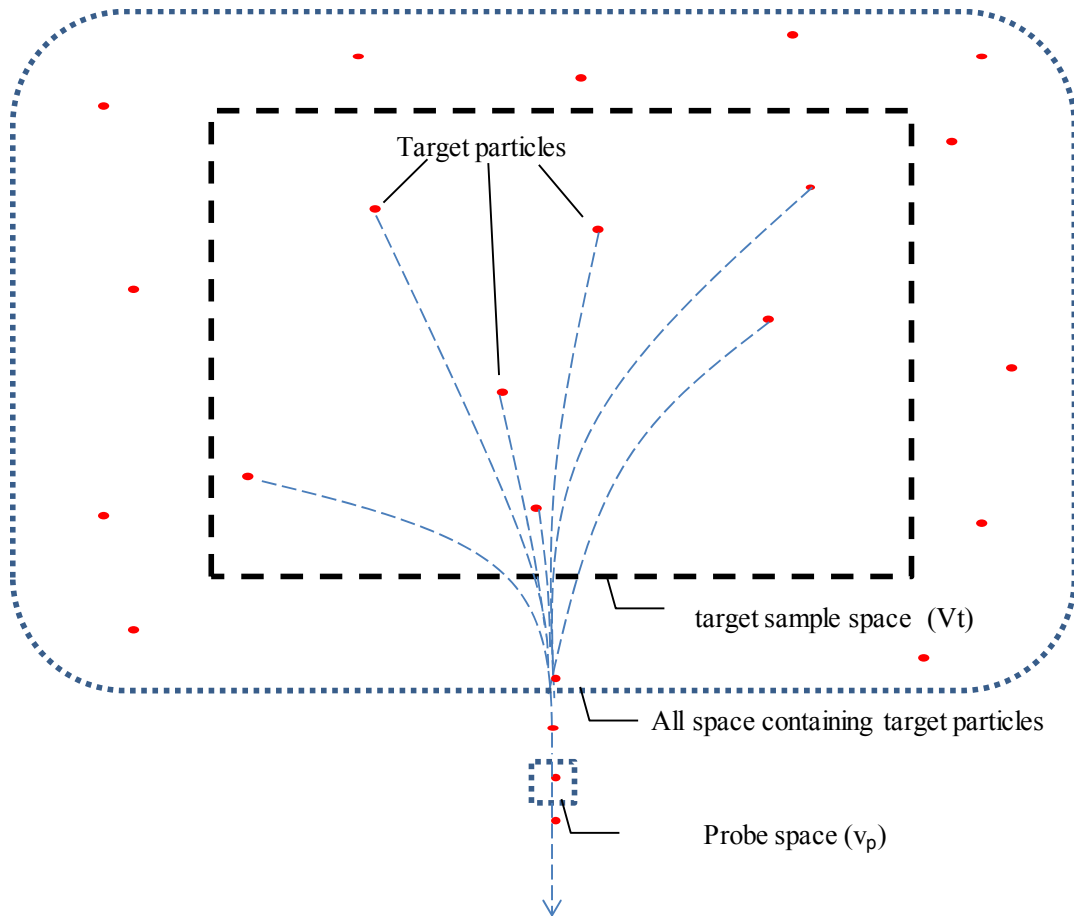by moving a probe space

Fig. 2-2 Measurement of particles in a target sample space by having target particles pass through a probe space

A typical scan method is a measurement of particles with a microscope [1], while a typical flow method is a measurement of particles with a particle counter [2]. The scan method is available for particles that are immobile during a measurement. Additionally, this method can measure target particles more precisely than the flow method by getting and analyzing image data of target particles. On the other hand, the flow method is more suitable than the scan method for measuring mobile particles during a measurement. Additionally, this method can measure a larger count of target particles per unit time than the scan method [3].

In measuring target particles in the sphere of human habitation, it is important to determine a suitable volume for a target sample space (V_t (m^3)) and a probe space (v_p (m^3)) for reliable measurement results. The volume of a target sample space (V_t (m^3)) is

considered in section 3 and the volume of a probe space (v_p (m^3)) is considered in section 4.

2.2 Measurement of particles by concentration

In this section, we consider a method of measuring numbers of particles in the sphere of human habitation other than the scan method and the flow method. The scan method and the flow method need a detector which can detect a single target particle because a single target particle entering the probe space has to be detected absolutely.

Fig. 2-3 shows an example of output of a detector detecting a target particle by the flow method. The X-axis is time and the Y-axis is the output of a detector. The detector outputs strong signals in the case of a particle entering the probe space; by contrast, it outputs weak signals due to background noise otherwise.
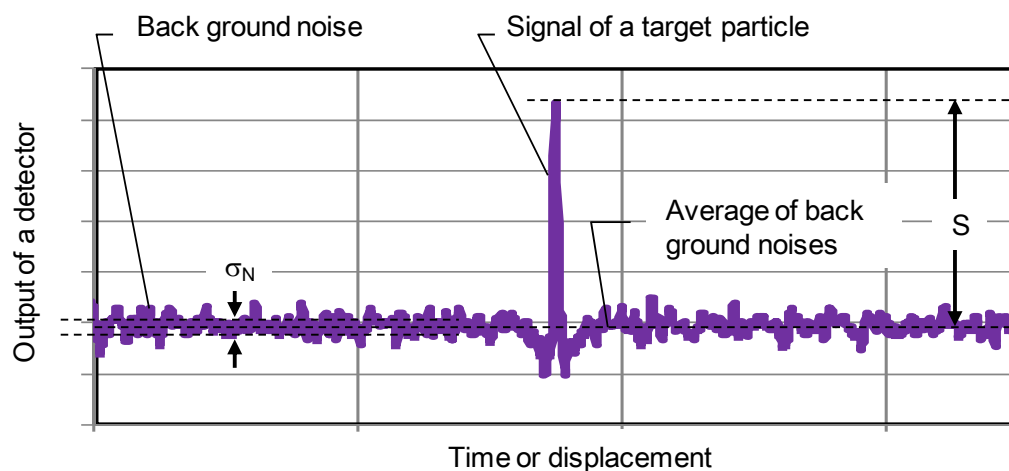
Fig. 2-3 Signal and noise in the case of counting a particle

An S/N ratio of the detector provides an indication in evaluations of a detector performance. S shows output of the detector. Additionally, N shows the standard deviation of background noise (σ_N) [4]. Therefore, we consider a condition to distinguish signals from detected target particles and signals from background noise by output values. In this case, background noise of a detector follows a Gaussian distribution. The standard normal distribution shows that background noise more than $2.81\sigma_N$ is less than 0.5% of the total. Thereby, values of signals more than $2.81\sigma_N$ are considered with high probability as signals from target particles. On the other hand, it is difficult to distinguish

17

signals from background noise signals and signals from detected target particles in the case that values of signals are less than $2.81\sigma_N$. Thereby, highly sensitive detectors which can detect target particles one by one are needed for the scan method or the flow method.

It is difficult to measure the number of target particles by the scan method or the flow method when a value of a signal from a target particle is smaller than $2.81\sigma_N$. In such cases, measurement methods that collect target particles on a probe space (shown in Fig. 2-4) are used because attaining a value of a signal that has become larger than $2.81\sigma_N$ from collected particles on a probe space makes it possible to distinguish signals coming from target particles easily. This method is called a concentration method in this thesis.
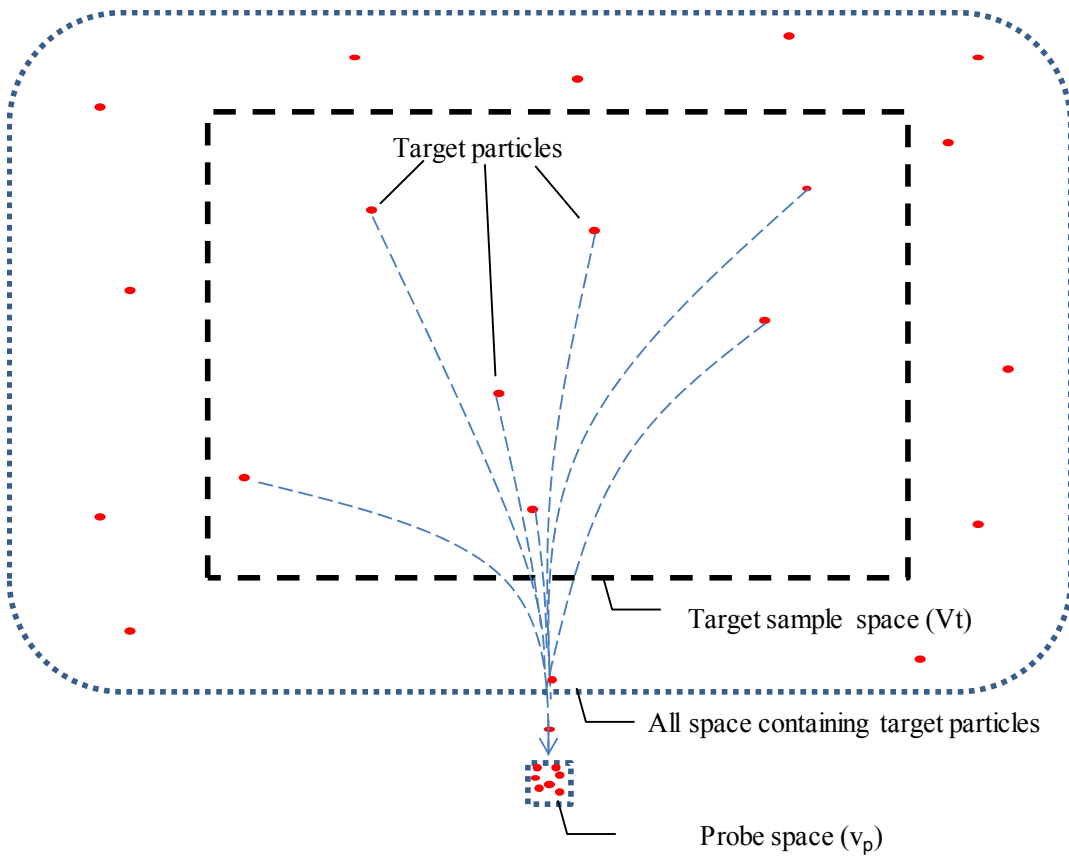

Fig. 2-4 Measurement of particles in a target sample space
by collecting target particles in a probe space

Table 2-1 shows measurement methods for particles mentioned in the previous chapter classified into three groups: (i) Scan method, (ii) Flow method, and (iii) Concentration method

Table2-1 Classification of measurement method for particles in fluid

Measurement method	Particle	Classification (i)Scan, (ii)Flow, (iii)Collection
FRM	PM2.5	(iii) Collection
TEOM	PM2.5	(iii) Collection
Microscopy	PM2.5, Cedar pollen, Plankton, Bacteria, Virus, Cell, Blood cell	(i)Scan
Particle counter	PM2.5, Cedar pollen	(ii)Flow
Impactor	PM2.5	(iii) Collection
Flow cytometer (FCM)	Bacteria, Cell, Blood cell	(ii)Flow
Imaging FCM	Plankton, Cell, Blood cell	(ii)Flow
Scanning cytometer (SCM)	Bacteria, Cell, Blood cell	(i)Scan
Coulter counter	Bacteria, Virus, Cell, Blood cell	(ii)Flow

2.3 Selection of measurement method

We discussed the methodology for selecting a suitable measurement method for target particles from three methods, the scan method, the flow method, and the concentration method. Fig. 2-5 shows an invented methodology.

(1) Selection of concentration method or other methods

The concentration method is different from the other two methods, which are methods to measure target particles one by one, because the concentration method is a method to measure concentrated target particles in the probe space all at once. Thereby, first, we decide whether to use the concentration method. The condition for selecting the concentration method is the case that target particles cannot be measured one by one. As mentioned in Chapter 2, section 2, a criterion for the selection of the

concentration method is that a value of a signal of a target particle be lower than $2.81\sigma_N$. σ_N is the standard deviation of background noise.

(2) Selection of scan method or flow method

Second, we select the scan method or the flow method according to the following three conditions.

(2-1) Target particles cannot move in the target sample space

As mentioned in Chapter 2, section 1, one of the advantages of the scan method is that it is possible to measure the shapes of target particles. On the other hand, one of the disadvantages of this method is that it is difficult to measure moving target particles in the target sample. Thereby, it is better to select the scan method in the case that target particles cannot move in the target sample space.

(2-2) Information on the shape of target particles is needed

In the case that data of shapes of moving target particles are needed, it is better to measure target particles by the scan method after immobilizing particles some way or by a flow method which can get images of target particles such as imaging flow cytometry [5]. While flow methods other than imaging flow cytometry are suitable in the case that neither data of shapes of target particles nor immobilization of particles is needed.

(2-3) Number concentration of target particles is low

The flow method can measure a greater number of target particles per unit time than the scan method [3]. Thereby, in the case that number concentration of target particles is low, it is better to select the flow method because it takes up much time to measure the required number of target particles by the scan method.

(3) Improvement of measurement accuracy of target particles

Finally, improvement of measurement accuracy of target particles is discussed. As described in Chapter 2, section 5, the main causes of difficulty in measuring target particles are the following 3 items: (i) difficulty in detecting target particles, (ii) difficulty in distinguishing target particles from other particles, and (iii) difficulty in distinguishing signals of target particles from other signals. It is necessary to remove these difficulties so that measurement accuracy can be improved. We have to select methods for improvement of measurement accuracy depending on types or conditions of target particles.
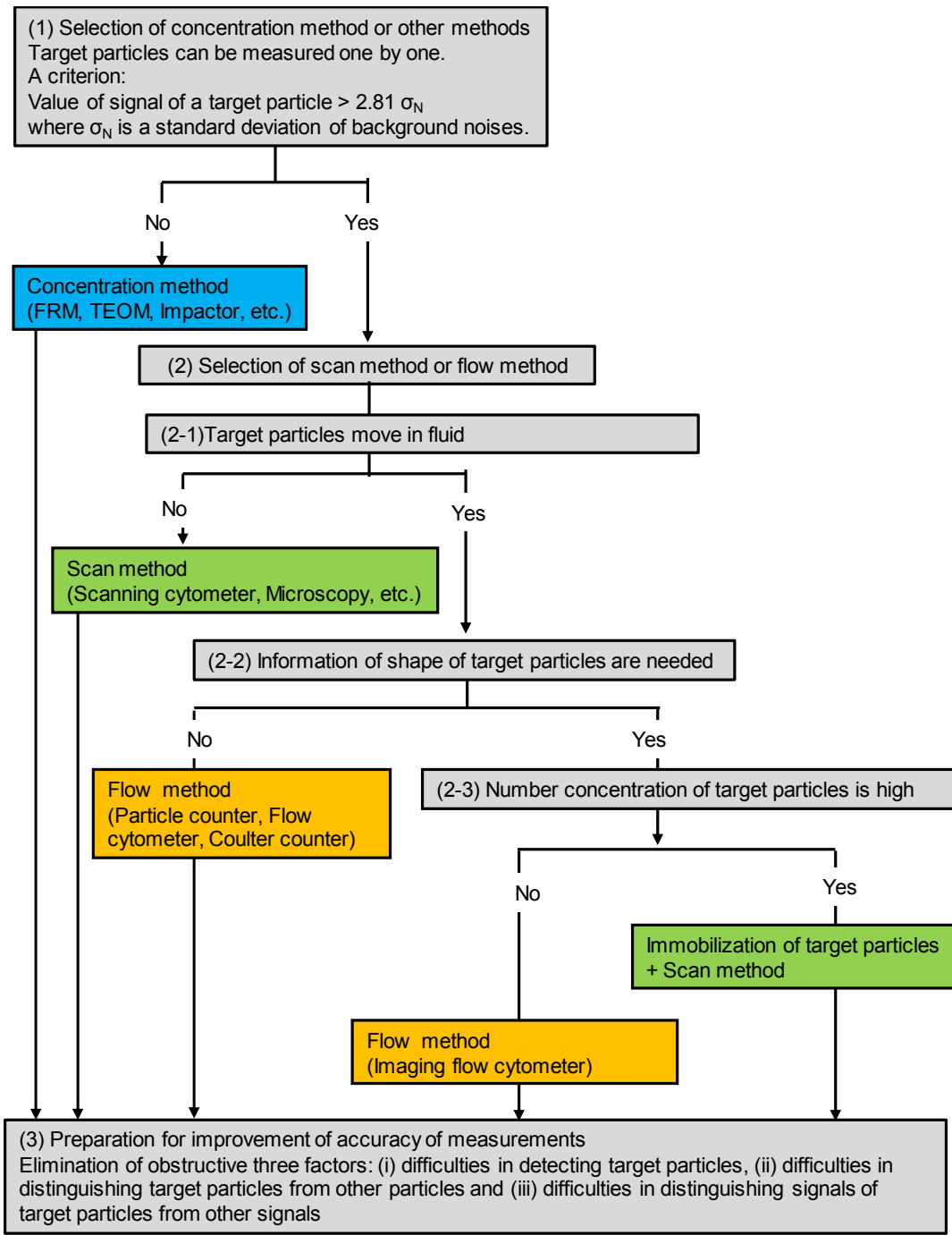
Fig. 2-5 Methodology to select a measurement method of target particles

Table 2-2 Advantage and disadvantage of measurement methods

Measurement methods	Scan method	Flow method		Concentration method
Examples of a system	Microscope, Imaging cytometer	Particle counter, flow cytometer, Coulter counter	Imaging flow cytometer	FRM, TEOM, Impactor
Measuring a particle one by one	S	S	S	U
Measuring a moving particle in sample	U in case of no immobilization of particles	S	S	S
Measuring a fixed particle in sample	S	U	U	U
Getting information of a shape of a particle	S	U	S	U
Measuring low number concentration of particles	U	S	S	S

S: suitable, U: unsuitable

2.4 Volume of target sample space for particle measurement

The volume of the target sample space (V_t (m^3)) is considered in this section. If we measure all the space containing target particles, we can get highly accurate measurement results. However, we have to spend a huge amount of time to finish the measurement. Thereby, we measure the number of particles in a part of the space containing target particles by considering that number concentration of particles in the part of space is equal to number concentration of particles in all the space. Namely, the part of the space can be regarded as the target particle space.

However, a smaller volume for the target particle space increases the variation in the number of particles in each target particle space. Moreover, the increase of the variation increases the difference between the apparent number of particles and the true number of particles. Therefore, it needs to decide the volume of a target sample space (V_t (m^3)) with consideration of the validity of measurement time and accuracy.

It is possible to apply a statistical theory to a decision of the volume of a target sample space (V_t (m^3)). In particular, it is possible to apply a Poisson distribution law to a decision of the volume of a target sample space (V_t (m^3)) if particles are distributed in the target particle space discretely.

The Poisson distribution law, which was presented in 1836 by Poisson, is a discrete probability distribution that expresses the probability of a given number of events occurring in a fixed interval of time and/or space if these events occur with a known average rate and independently of the time since the last event [6]. The probability that events occurring on average λ times will occur k times in an interval of time and/or space is given by

$$p(k) = \frac{\lambda^k e^{-\lambda}}{k!} \qquad \text{2-1.}$$

Next, the Poisson distribution law is applied to a measurement of target particles in a space as below.

In the case that there are particles whose number concentration in the space is ρ (particles/m^3), the probability of counting x particles in the target sample space V_t (m^3) is equal to equation 2-1, whose k and λ are changed into x and ν.

Thereby, this is given by

$$p(x) = \frac{\nu^x e^{-\nu}}{x!} \qquad \text{2-2}$$

23

where v, which is the average number of target particles in the target sample space V_t (m3), is given by

$$v = \rho V_t \qquad\qquad 2\text{-}3.$$

Next, a condition on the smallest volume of the target sample space (v_{tmin} (m^3)) is considered by using equations 2-2 and 2-3. One of the conditions for measurement of target particles in a space is that there be more than a minimally required number of target particles for a measurement in the target sample space. This number is stated as the minimum number of particles (n_{min} (particles)). Thereby, the probability ($P(x \geq n_{min})$) that there are more than a minimally required number of target particles in the target sample space is given from equations 2-2 and 2-3 by

$$P(x \geq n_{min}) = \sum_{i=n_{min}}^{\infty} \frac{(\rho V_{tmin})^i e^{-\rho V_{tmin}}}{i!} \qquad 2\text{-}4$$

Thereby, the smallest volume of the target sample space (v_{tmin} (m^3)) needed in a measurement for certain particles changes depending on number concentration in the space (ρ (particles/m^3)) and minimum required number of target particles (n_{min} (m^3)).

In the following, minimum volume of a target sample space (v_{tmin} (m^3)) under the condition that $P(x \geq n_{min}) \geq 0.999$, $\rho = 10^3$ (particles/m^3), and n_{min}(particles)=1, and under the condition that $P(x \geq n_{min}) \geq 0.999$, $\rho = 10^3$ (particles /m^3), and n_{min}(particles)=100 are calculated as examples.

(1) n_{min}(particles)=1

    Equation 2-4 gives

$$P(x \geq 1) = \sum_{k=1}^{\infty} p(k)$$
$$= 1 - p(0)$$
$$= 1 - e^{-\rho V} \qquad 2\text{-}5$$

Additionally, under the condition that $P(x \geq 1) \geq 0.999$ and $\rho = 10^3$, equation 2-5 gives

$$e^{-10^3 v_{min}} \leq 0.0001 = 10^{-4} \qquad \text{2-6}$$

Finally, equation 2-6 gives

$$10^3 v_{min} \geq 4 \ln 10$$

$$v_{min} \geq \frac{4 \ln 10}{10^3} \cong \frac{1}{10^2} \ (m^3) \qquad \text{2-7}$$

(2) n_{min}(particles)=100

As with the case of (i), equation 2-4 gives

$$P(x \geq 100) = \sum_{k=100}^{\infty} p(k)$$

$$= 1 - \sum_{k=1}^{100} p(k) \qquad \text{2-8}$$

A calculation of equation 2-8 under the condition that $P(x \geq 100) \geq 0.999$ using Excel gives

$$v_{min} \geq 0.135 \ (m^3) \qquad \text{2-9}$$

2.5 Probe space of system

A probe space of a system is considered in this section. A situation that there are a huge amount of particles in a probe space brings a problem of a counting loss. The counting loss occurs when more than one particle enters into the probe space at the same time [7].

Fig. 2-6 is an example to show a counting loss. The situation in Fig. 2-6 is that seven particles in a target sample are measured by dividing the target sample space into five probe spaces.

If a detector used in the measurement counts greater than or equal to one particle in the target space as one, a measurement result output by the detector, which shows five particles, differs from the true number of particles (seven particles). As just described, a counting loss is a difference between measured number of particles and true number of particles. Moreover, the allowable range of a counting loss has an effect on the decision of the maximum size of a target space.

25

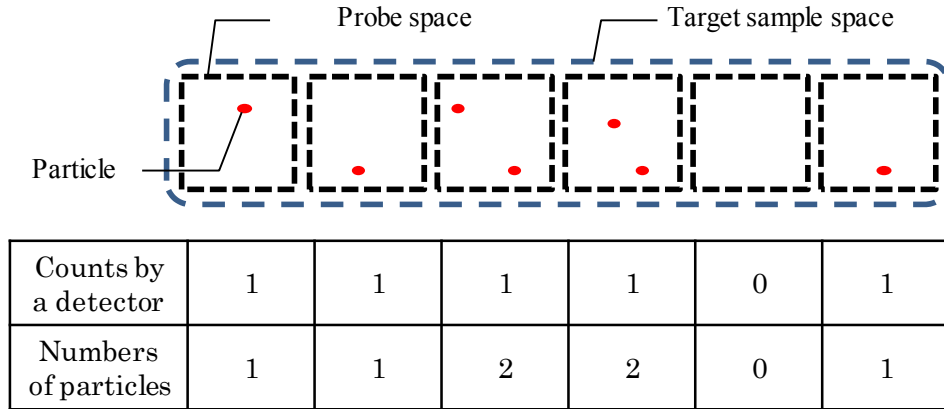|	Probe space		Target sample space		
Counts by a detector	1	1	1	1	0	1
Numbers of particles	1	1	2	2	0	1

Fig. 2-6 example of counting loss

As mentioned in section 1, methods to measure the number of particles in a target sample space are divided into the following three types: (1) measurement methods to measure particles by moving the probe space (scan method), (2) measurement methods to measure particles by making particles pass through the probe space with a certain drive force (flow method), and (3) measurement methods to measure particles by concentrating particles in the probe space. Thereby, we consider the counting loss and the maximum size of the probe space in the scan method, the flow method, and the concentration method.

(1) Scan method

We calculate the counting loss with a statistical theory as in the previous section. In the case that target particles are distributed in the target sample space under the Poisson distribution, the probability of observing x target particles in the probe space is given by

$$p_m(x) = \frac{(\rho v_m)^x e^{-\rho v_m}}{x!} \qquad 2\text{-}9$$

where ρ is the number concentration of target particles in the target sample space and v_p is the volume of the probe space.

Thereby, the probability of observing no target particles in the probe space is given by

$$p_m(0) = e^{-\rho v_m} \qquad 2\text{-}10$$

Additionally, the counting loss (P), which is the probability of observing greater than or equal to one particle, is given by

$$P = \sum_{i=1}^{\infty} p_m(i) = 1 - p_m(0) = 1 - e^{-\rho v_m} \qquad \text{2-11}$$

For example, the volume of the probe space (v_p) is calculated in the case that $\rho = 10^{10}$ (particles/m³) and $P < 0.05$.

Equation 2-11 gives

$$e^{-\rho v_m} \leq 0.05$$

$$\rho v_m \leq -\log 0.95 = 0.0512$$

$$v_m \leq 5.1 \times 10^{-12} \ m^3 \qquad \text{2-12}$$

(2) Flow method

Next, we calculate the counting loss in flow methods. In the flow methods, target particles enter the probe space under the Poisson process. This is the stochastic process where events occur continuously and independently of one another [7].

Thereby, the probability of observing x target particles in the probe space in t_p (s) where a target particle passes through the probe space is given by

$$p_p(x) = \frac{(\rho Q t_p)^x e^{-\rho Q t_p}}{x!} \qquad \text{2-13}$$

in which Q is the volume of flow of fluid containing target particles and ρ is the number concentration of target particles in the fluid. Additionally, equation 2-13 is equal to equation 2-1 whose k and λ are changed into x and $\rho Q t_p$. $Q t_p$, which is the volume of the fluid flowing in t_m (s), is equal to the volume of the probe space in flow methods.

Thereby, the probability of observing no target particles passing through the probe space is given by

$$p_p(0) = e^{-\rho Q t_p} \qquad \text{2-14}$$

Finally, the counting loss P is given by

$$P = 1 - p(0) = 1 - e^{(-\rho Q t_p)} \qquad \text{2-15}$$

27

It is possible to decide the maximum size of the probe space from equation 2-15 and parameters: P, ρ, Q, and t_p.

(3) Concentration method

Finally, we consider the counting loss in the concentration method. It isn't possible to apply a theory of the counting loss in the previous methods to the concentration method just as it is because numbers of collected target particles in the concentration method aren't measured one by one but are converted from strength of a signal of collected target particles.

For example, the situation that target particles are concentrated on a probe space from the target sample space is considered. When target particles in the target sample space are concentrated on the probe space, a distance between particles becomes shorter. Moreover, by concentrating target sample space moreover, target particles which get close to each other appear to overlap from an observational direction. Larger overlaps of target particles prevent signals from target particles from arriving at a detector. Therefore, it is difficult to convert strength of signal to number of target particles because a correlation between number of particles and strength of signal decreases.

Fig. 2-7 shows images on an x-y plane where target particles in the probe space are projected. Additionally, Fig. 2-7 shows changes of appearance numbers of target particles and true numbers of particles in counting overlapping particles as one.
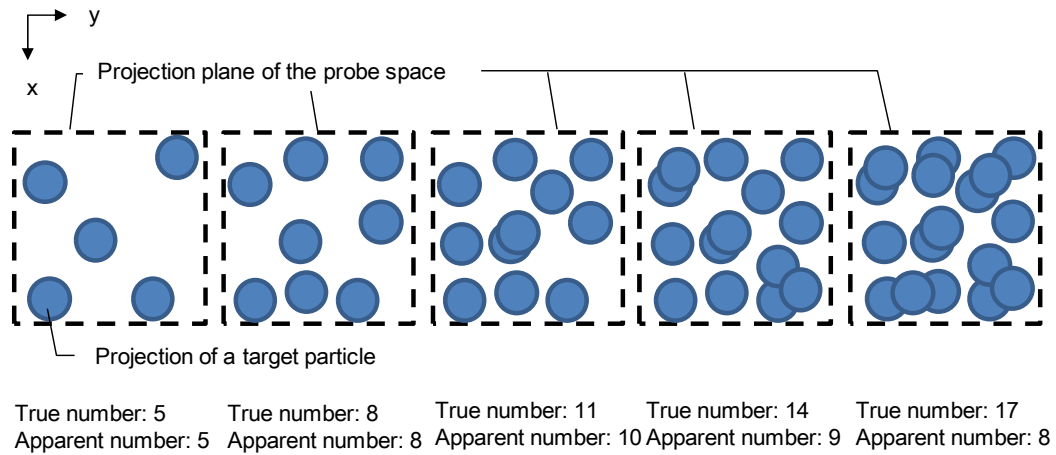

Fig. 2-7 Projections of target particles on an x-y plane

Next, we consider a condition that projections of target particles don't overlap. Unless

target projections of target particles overlap, projecting target particles on an x-y plane is equal to collecting target particles in a space whose height in a z-axis direction is the diameter of a target particle. This space is called a compressed space. For this reason, when the compressed space is divided into spaces whose volume is equal to a target particle, the probability that more than one target particle will enter the divided compressed space is equal to the probability that projections of target particles will overlap on the x-y plane.

Thereby, the probability that projections of target particles don't overlap is given from equations 2-2 and 2-3 by

$$P = \sum_{i=1}^{\infty} p(i) = 1 - p(0) = 1 - e^{-\rho_{tp} v_{tp}} \qquad \text{2-16}$$

where ρ_{tp} is number concentration of target particles in the compressed space and v_{tp} is volume of a target particle.

Additionally, ρ_{tp} is given by

$$\rho_{tp} = N_{tp}/V_c \qquad \text{2-17}$$

where N_{tp} is number of target particles and V_c is volume of the compressed space.

From the above discussion, a statistical theory of the counting loss can be applied to the concentration method when measuring particles indirectly in addition to the scan method and flow method when measuring particles directly.

In this thesis, the theory of counting loss in the concentration method is applied in chapter 5.

2.6 Methods to improve accuracy of measurement

In the previous section, the counting loss was considered on the assumption that all target particles are measured. However, it is difficult to measure all target particles in real measurements because there are obstructive factors of the measurement of target particles. Thereby, it is important to know obstructive factors and take the most effective step for removing these factors for high-accuracy particle measurements.

In this section, we consider obstructive factors in the measurement of target particles and methods to remove these factors. Table 2-2 shows obstructive factors and methods to remove these factors.

Table 2-3 Methods to remove obstructive factors of particle measurements

	factors to obstruct a measurement of target particles		Method to remove the obstructive factor
Difficulties of detecting target particles	Too discreet target particles		Emphasizing target particles
			Increasing sensitivity of detector
	Too blight back-ground		Emphasizing target particles
			Weakening back ground light
Difficulties of distinguishing target particles from other particles	Similar parameter of particle	Size	(1) Distinguishing target particles using other parameter (2) Removing other particles using dissimilar parameter
		Shape	
		Color	
		Consistency	
		Charge	
Difficulties of distinguishing signals of target particles from other signals	Electric noises of detector		Using electromagnetic shield or band-pass filter

(1) Situations of identifying other than target particles as target particles

These are situations that other than target particles are measured as target particles. To avoid misidentifying other than target particles, it is necessary to identify target particles with only features of target particles such as diameter and shape of a target particle. Additionally, it is necessary before measurements to remove other than target particles from target particles with preparation such as filtration.

In other cases of misidentifying other than target particles, noises of detectors are

identified as signals from target particles. It is necessary to improve a sensitivity of a detector in this case.

(2) Situations of not identifying target particles

These are situations that target particles cannot be identified from other that target particles. In these cases, to improve to identify target particles clearly, it is necessary to add specific features to only target particles, to decrease background light and to improve sensitivity for target particles.

2.7 Conclusion

In this chapter, we considered measurements of target particles in the sphere in human habitation.

First, we classified measurements of particle in the sphere in human habitation to the following three cases: (1) measurement methods to measure particles by moving the probe space (scan method), (2) measurement methods to measure particles by making particles pass through the probe space with a certain drive force (flow method), and (3) measurement methods by collecting target particles on the probe space (concentration method).

Second, in each above three cases, we considered that Poisson distribution law is applied to (1) the volume of the target sample space to keep variation of measurement results low and (2) the volume of the probe space to keep the counting loss low.

Third, we classified obstructive factors in measurements of target particles to the following three cases: (1) difficulties of detecting target particles, (2) difficulties of distinguishing target particles from other particles, and (3) difficulties of distinguishing signals of target particles from other signals. Additionally, we consider causes of these factors and methods to remove these factors.

Fourth, we discussed the methodology to select a measurement method of target particles from three methods: scan method, flow method and concentration method. Order of the selection: (1) selection of concentration method or other methods, (2) selection of scan method or flow method, and (3) Improvement of measurement accuracy of target particles.

In the following, we considered the methodology in this chapter for adoptions of developments of measurements of target particles in the sphere in human habitation: (1) measurement of bacteria in food suspensions in chapter 3, (2) measurement of excitation-fluorescence spectra of a particle in liquid in chapter 4, and (3) measurement of airborne biological particles in chapter 5.

Reference

[1] *How to use a microscope – from a first observation to applications (Bio technical series) 3rd edition*, (2011), Yodosha co., ltd. (In Japanese), ISBN: 978-4-89706-930-2.

[2] ISO21501-1:2009 Determination of Particle Size Distribution – Single Particle Light Interaction Methods- Part 1: Light-scattering Aerosol Spectrometer.

[3] Beckman Coulter Homepage, https://www.bc-cytometry.com/FCM/whats_cytometry-6.html (In Japanese).
  [Accessed 1 April 2017].

[4] Wells, G., Prest, H., and Russ IV, C. W. "Why use Signal-To-Nise as a Measure of MS Performance When it is Often Meaningless?," *Agilent Technology Technical Overview*, http://www.agilent.com/cs/library/technicaloverviews/public/5990-8341EN.pdf
  [Accessed 1 April 2017].

[5] George, T.C., Basiji, D. A., Hall, B. E., Lynch, D. H., Ortyn, W. E., Perry, D. J., Seo, M. J., Zimmerman, C. A., and Morrissey, P. J. "Distinguishing Modes of Cell Death Using the ImageStream Multispectral Imaging Flow Cytometer," *Cytometry Part A*, Vol. 59A, (2004), pp. 237–245.

[6] Haight, F. A. *Handbook of the Poisson Distribution*, (1967), John Wiley & Sons, New York, ISBN: 978-0-471-33932-8.

[7] The University of Toronto Homepage, http://individual.utoronto.ca/zheli/poisson.pdf
  [Accessed 1 April 2017].

Chapter 3. Rapid live bacteria counter for food suspension

3.1 Background and purpose

3.1.1 Background

Complying with the food hygiene for preventing from food poisonings is one of the most important duties for people related to food manufacturing because one food poisoning accident can endanger their business. They observes the food safety inspection guidelines under the supervision of Ministry of Health [1] to manage the food hygiene in Japan. Foods, which are listed in the food safety inspection guidelines under the supervision of Ministry of Health, Labour and Welfare, can be considered as hygienic if live bacterial numbers in it are less than reference numbers specified by the standard of the Food Sanitation Act. Additionally, a food not listed in the list can be considered as hygienic if live bacterial numbers in this are less than reference numbers.

Thereby, it is a fundamental condition for the food hygiene to ensure that live bacterial numbers is less than the reference numbers by measuring live bacterial numbers in foods [2].

Live bacteria here refers to mesophilic aerobic bacteria. The basic method to measure live bacterial numbers is the culture method invented by Robert Koch, who is considered the founder of modern bacteriology. The culture method is a method to measure number of colonies formed on an agar medium by the growth of bacteria in cultivation [2].

Fig. 3-1 shows a procedure of the culture method. Details of the procedure of the culture method in Fig. 3-1 are shown below.
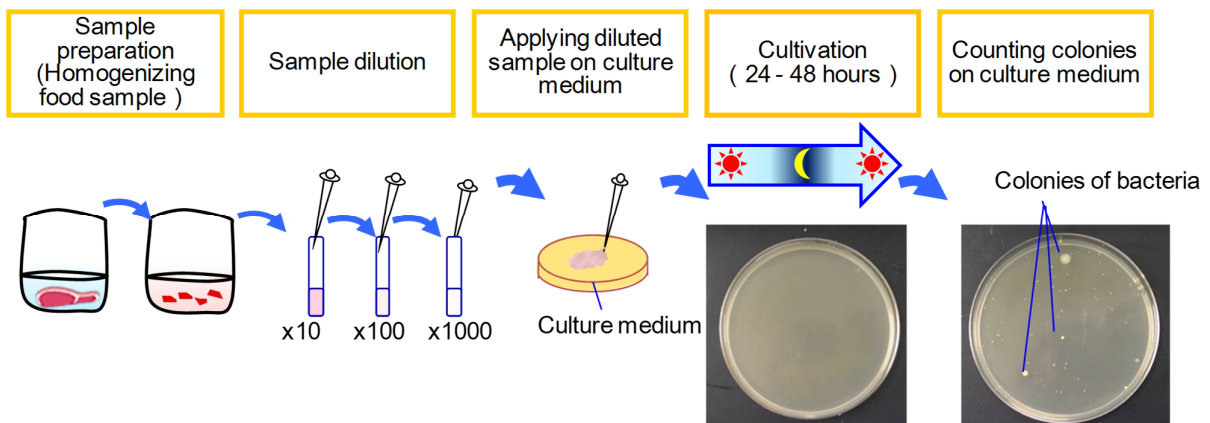
Fig. 3-1 Process of cultivation method

(1) Preparing undiluted sample solution:

     10 g food sample for a measurement is mixed with 10 times its volume of distilled water in a bag. Next, the food sample in the distilled water is homogenized for 10 min using a stomacher®. The stomacher® crushes the food and drives bacteria in suspension.

(2) Diluting sample solution

     Undiluted sample solution made by the stomacher is diluted with distilled water. In this case, a dilution magnification is often 10^x such as 10^1, 10^2, and 10^3.

(3) Mixing sample solution with agar medium

     1 mL diluted sample solution and agar medium just before solidification are poured on Petri dishes. Next, the sample solution and agar medium are mixed well and left until solidification.

(4) Incubating live bacteria on agar plates

     Petri dishes filled with solidified agar mediums are left in an incubator at constant temperature for 24 – 48 hours.

(5) Counting colonies formed by growth of bacteria

     Colonies are formed on an agar plate containing one or more bacteria by growth of bacteria. A colony is formed from a live bacterium, thereby, it is possible to measure live bacterial numbers in agar plate from number of colony. For example, it can be determined that there are 53,000 live bacteria in 1mL sample solution if 53 colonies are formed on agar plate containing 10^3 times diluted sample solution.

   The cultural method is a useful method to measure accurately live bacterial numbers in a sample solution. However, this method has two problems bellow for people related to food manufacturing. First, this method needs more than 48 hours to get results. Second, this method, which is burdensome, needs testers with specialized knowledge and technique.

   Thereby, this method can measure live bacterial numbers accurately but this does not fully meet needs of people related to food manufacturing.

3.1.2 Purpose

   Methods to measure live bacterial numbers in sample solution simply, rapidly and high-accurately (stated as Simple rapid measurements), which are ATP (Adenosine TriPhosphate) method [3], the impedance method [4], fluorescent image cytometry [5] and fluorescent flow cytometry [6][7][8], has been developed recently and used in food manufacturing scenes.

   Live bacteria identified by each previous method are strictly different from live

bacteria identified by the culture method. However, the number of live bacteria identified by each method is correlated with one by the culture method. Thereby, both are equated in this thesis.

Table 3-1 shows (a) Principle of measurement, (b) Method to measure particles, (c) Preparation, (d) Performances and (e) Remarks.

(1) ATP method

ATP (**A**denosine **t**ri**p**hosphate) is contained in a live cell, also in a live prokaryote such as a bacterium. ATP changes into AMP in a chemical reaction of oxygen and luciferin catalyzed by luciferase. In the reaction called luciferin luciferase reaction, luminescence is produced [9].

An ATP method is a method to detect live bacteria by measuring amount of ATP eluted from live bacteria using this chemical reaction. Amount of luminescence is proportional to amount of ATP. Thereby, it is possible to measure amount of ATP in live bacteria by measuring amount of luminescence. In the ATP method, removing big food debris with a filter and eliminating ATP from food debris with an ATP eliminant are conducted as preparation. The ATP method is high sensitive method to detect amount of ATP corresponding to a bacterium. However, Amount of ATP changes depending on types or states of bacteria. Additionally, ATP in unremoved food debris has an effect of measurement results.

(2) Impedance method

This is a method to measure a change of impedance of a liquid culture medium mixed with a sample [4]. It is possible to measure vital activity of live bacteria using a change of an electrical property of the liquid culture medium by vital activity of live bacteria.

This is a so useful that it is possible to measure vital activity of live bacteria by doing nothing other than pouring a liquid culture medium mixed with a sample to a dedicated case. However, this method, which requires long time incubation, is insufficient of immediacy. Additionally, this is insufficient of quantitative capability because impedance of liquid culture medium is affected easily by types or states of bacteria.

(3) Fluorescent image cytometry

This is a method to measure numbers of live bacteria on filter in the following procedure [5]. First, bacteria in a sample are collected on a filter. Second, collected live bacteria are labeled with specific fluorescent dye. Finally, labeled live bacterial numbers are measured by counting bright points of labeled live bacteria on a photograph of the filter.

In this method, removing big food debris with a pre-filter or a centrifugal, and labeling bacteria with fluorescent dyes are conducted. This is a method to measure numbers of live bacteria on the filter one by one using the scan method. Thereby, this is high-sensitivity and less affected by types and states of bacteria. However, this method could identify food debris as live bacteria if food debris emit fluorescence as with live bacteria.

(4) Fluorescent flow cytometory

This is a method to measure numbers of live bacteria in a stream in the following procedure (Fig. 3-2). First, bacteria labeled with fluorescent dye are flowed through a narrow stream of a sample solution. Second, fluorescence from a bacterium flowing through the area on the stream eradiated by the excitation light is detected by fluorescence detectors. Finally, labeled live bacterial numbers are measured by counting pulse signals outputted from detectors [10].

In this method, removing big food debris with a pre-filter or a centrifugal, and labeling bacteria with fluorescent dye are conducted

This is a method to measure live bacterial numbers one by one using the flow method. Thereby, this is high-sensitivity and not susceptible to types and states of bacteria. Additionally, counts per time in the flow cytometry are more than counts per time in the imaging cytometry. However, this method could identify food debris as live bacteria if food debris emit fluorescence as with live bacteria.

Table 3-1 Easy and rapid measurement of bacteria

		(1) ATP method	(2) Impedance method	(3) Fluorescent image cytometory	(4) Fluorescent flow cytometory
(a) Principle of measurement		Measuring bioluminescence caused by lusiferin and luciferase reaction	Measuring impedance variation by composition change of liquid culture medium	Labeling bacteria caught on a filter with fluorescent dye, and counting	Counting bacteria labeled with fluorescent dye in flow
(b) Method to measure particles in chapter 2		-	-	(I)Scan method	(II)Flow method
(c) Preparation		Removing large food debris and clearing ATPs from food	Removing large food debris	Removing large food debris and labeling bacteria with fluorescent dye	Removing large food debris and labeling bacteria with fluorescent dye
(d) Performances ○:Good, Δ: ×: Bad	Ease	○	○	○	○
	Rapidness	○	×	○	○
	Sensitivity	○	Δ	Δ	○
	Stability of measurement	×	×	×	×
(f) Remarks		High sensitivity to measure ATP equivalent to a bacterium but instability to be affected by ATP from food, bacterial strain and state	Easy method without effort but Instability to be affected by bacterial strain and state	High sensitivity and stability not to be affected by bacterial strain and state but wrong count of food debris as bacteria	High sensitivity and stability not to be affected by bacterial strain and state but wrong count of food debris as bacteria
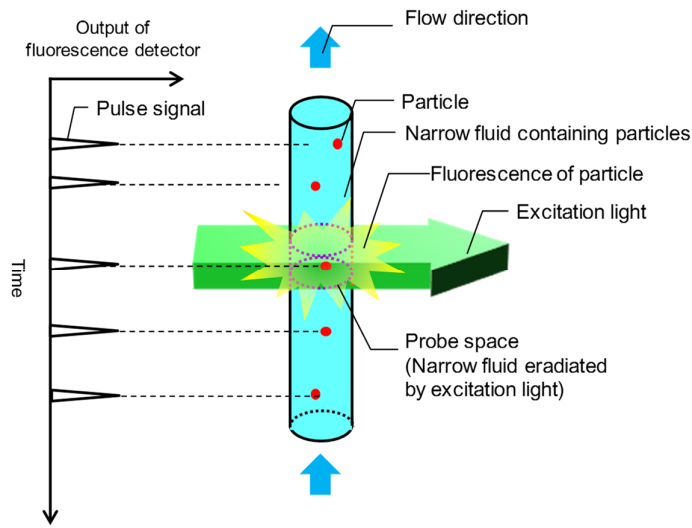
Fig. 3-2 Conceptual diagram of fluorescence flow cytometry

However, the above simple rapid measurements aren't the main measurement of bacteria in foods under the present circumstances for the following reasons: bad accuracy of a measurement, limited food of measurement targets, or long measurement time.

Thereby, advantages and disadvantages are considered to develop a new simple rapid measurement of live bacteria in foods. It is difficult to correct the demerits of the ATP method and the impedance method because these demerits derive from properties of bacteria.

On the other hand, fluorescent imaging cytometry and fluorescent flow cytometry require that food debris be removed from a sample solution containing bacteria. However, it is possible to measure live bacteria in a prepared sample simply, rapidly, and highly accurately. Thereby, we considered that it is possible to measure numbers of live bacteria in foods by suitably removing food debris by filtration or centrifugal force before a measurement.

Imaging cytometry is one of the scan methods and flow cytometry is one of the flow methods. Thereby, we select between imaging cytometry and flow cytometry using the methodology in chapter 2, section 3 (Fig. 3-3). Features of live bacteria in a homogenized food suspension are the following: (1) live bacteria moving in a sample solution, (2) a variety of shapes of bacteria such as spherical, oval, rod, or spiral, and (3) wide range of number concentration of bacteria from low to high.
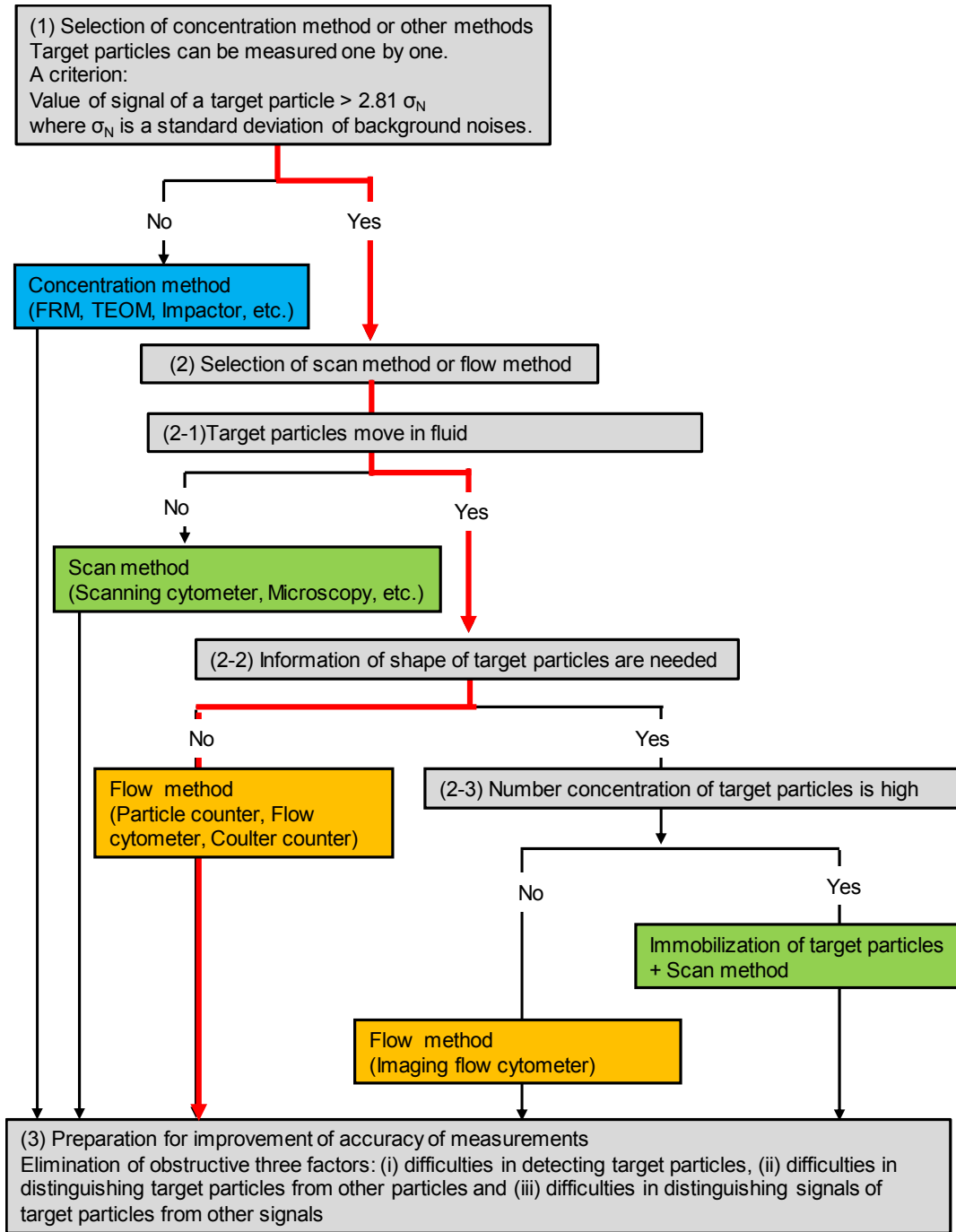
Fig. 3-3 Selection of flow method as a measurement method of live bacteria in food suspension using the methodology

(1) Selection of concentration method or other methods

We consider it is possible to measure bacteria one by one because there are precedent that bacteria were measured one by one by a flow cytometer[6]-[8]. Additionally, we selected other than concentration method on the assumption that a signal of a bacterium is larger than 2.81 σ_N where σ_N is a standard deviation of background noises. In evaluations of the system, we will check that the above assumption is true.

(2) Selection of scan method or flow method

We select a flow method which don't use image data of bacteria for the following reasons. First, live bacteria move in homogenized food suspension. Second, enormous database of shapes of bacteria are needed because shapes of bacteria are different depending on types of bacteria. Third, the flow cytometry measures numbers of bacteria in shorter time than the imaging cytometry.

(3) Preparation for improvement of accuracy of measurements

We took the following methods to improve a measurement accuracy of the system. Methods are shown in later sections.

(i)　To detect target live bacteria more easily, we labeled live bacteria with fluorescent dyes (Section 3) and made a flow cell emitting low back ground light from low autofluorescence materials (Section 5).

(ii) To distinguish live bacteria with other particles, we select most suitable combination of colors of fluorescent dyes (Section 3).

(iii) To distinguish signals of live bacteria with noise signals of detectors, we remove noise signals by a frequency-dependent filter (Section 9).

3.1.3 Specifications of system

The specifications of a system for measuring live bacterial numbers using fluorescence flow cytometry are considered. Targets of the specifications are shown in Table 3-2.

Table 3-2 Specifications of bacteria counter system using fluorescent flow cytometry

Items	Details
(1) Measuring samples	Homogenized food with distilled water
(2) Measuring range of bacteria	10^3 cell/mL – 10^6 cell/mL
(3) Measuring time	2 hours
(4) Automated measurement Process	Other than homogenizing food and injecting homogenized sample to the system

Reasons for determination of targets of specifications are shown in the following.

(1) Measuring sample

Homogenized food to be measured mixed with distilled water is selected for measuring samples used in the system as in the culture method, which is regarded as the official method.

(2) Measuring range of bacterial numbers

Standards of bacterial numbers in food, which differ depending on the kind of food, are specified as being from 10^3 cells/mL to 10^6 cells/mL (10^9 cell/m^3 - 10^{12} cell/m^3) by such standards as the Food Sanitation Act. Thereby, this range of bacterial numbers is set as a target of the measuring range of bacterial numbers of the system.

(3) Measuring time

It is considered that a permissible time to obtain measurement results is less than 2 hours because the system will be used in tests before the shipment of foods. Thereby, this time is set as a target of the measuring time of the system.

(4) Automated measurement process

It is proposed that anyone without specialized knowledge and techniques should be able to use the system. Thereby, every process to measure bacteria except homogenizing food and moving a homogenized sample to the system will be automated.

3.2 Measurement theory

3.2.1 Measurement using fluorescence

Fluorescence dyes for measurements of live bacteria are divided to following three types [11]: (a) dye increasing amount of fluorescence in binding to nucleic acid in cells (stated as fluorescent dye binding to nucleic acid), (b) dye mutated to fluorescent dye by

an esterase reaction in a live cell (stated as fluorescent dye using esterase reaction), and (c) dye mutated to fluorescent dye by a respiratory activity in a live cell (stated as fluorescent dye using respiratory activity).

(a) Fluorescent dyes binding to nucleic acid are divided to two types: fluorescence dyes specifically reacting with live/dead bacteria (stated as fluorescent dyes for live/dead bacteria), and fluorescence dyes specifically reacting with dead bacteria (stated as fluorescent dyes for dead bacteria). Difference of reactions in two types depends on a difference of membrane permeability stated as bellow. Fluorescence dyes for live/ dead bacteria pass through cellular membrane of live/dead bacteria and bind to nucleic acid in cells. By contrast, fluorescence dyes for dead bacteria can pass through only cellular membrane of dead bacteria. Fluorescence dyes for live/ dead bacteria (DAPI, SYTO®, etc) and fluorescence dyes for dead bacteria (PI, SYTOX®, etc) used in combination to measure live bacteria.

On the other hand, (b) fluorescent dye using esterase reaction and (c) fluorescent dye using respiratory activity are fluorescence dyes specifically reactive with live bacteria. These dyes passing through cellular membrane are mutated to fluorescent dyes by an esterase reaction in a live cell or a respiratory activity of a live cell.

In this chapter, (a) fluorescent dyes binding to nucleic acid are selected to use in the system. This type fluorescent dye emits stronger fluorescence by binding to nucleic acid. Thereby, it is easier to identify live bacteria from other particles [12].

3.2.2 Measuring process using flow cytometry

We considered the process of measuring the number of live bacteria in a homogenized food suspension using fluorescent flow cytometry. There is food debris other than live bacteria and dead bacteria in a homogenized food suspension. Food debris has the possibility to block a channel or to be identified as live bacteria. Thereby, food debris needs to be removed from homogenized food suspensions [6][7][8]. Additionally, live bacteria and dead bacteria need to be labeled in different colors with fluorescent dyes for live/dead bacteria and fluorescent dyes for dead bacteria only in measurements of live and dead bacteria using fluorescence.

Therefore, measurements of live bacteria using fluorescent flow cytometry require the preparations shown in Fig. 3-4: containing removing food debris from homogenized food suspensions and labeling live and dead bacteria with fluorescent dyes. Details of the preparation and measurement process are shown below.
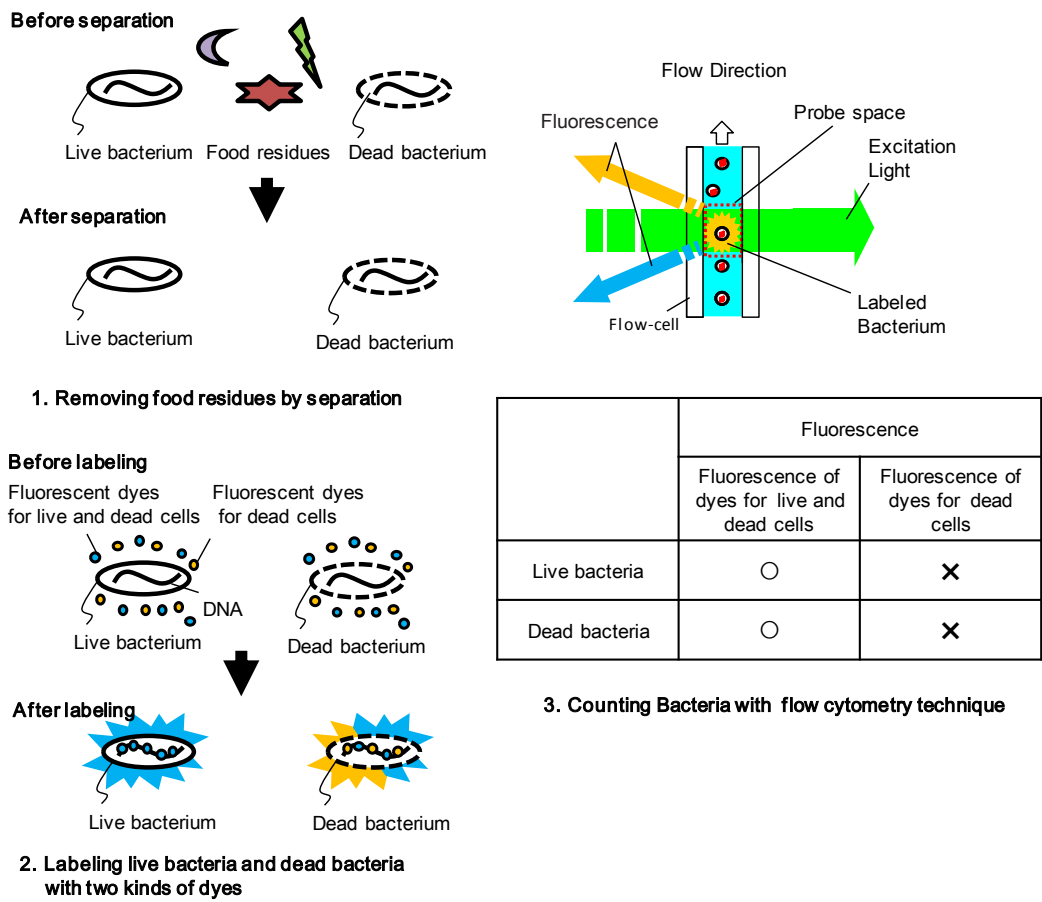
Before separation

Live bacterium　Food residues　Dead bacterium

After separation

Live bacterium

Dead bacterium

1. Removing food residues by separation

Before labeling

Fluorescent dyes
for live and dead cells

Fluorescent dyes
for dead cells

DNA
Live bacterium

Dead bacterium

After labeling

Live bacterium

Dead bacterium

2. Labeling live bacteria and dead bacteria with two kinds of dyes

Flow Direction

Fluorescence

Probe space

Excitation
Light

Labeled
Bacterium

Flow-cell

	Fluorescence	
	Fluorescence of dyes for live and dead cells	Fluorescence of dyes for dead cells
Live bacteria	○	✕
Dead bacteria	○	✕

3. Counting Bacteria with flow cytometry technique

Fig. 3-4 Detection process using fluorescence flow cytometry

(1) Food debris is removed from a homogenized food suspension.

(2) Fluorescent dyes for live/dead bacteria (blue color in Fig. 3-4) and fluorescent dyes for dead bacteria (yellow color in Fig. 3-4) are mixed with the sample solution to label live/dead bacteria with fluorescent dyes. Fluorescent dyes for live/dead bacteria pass through a cell membrane for live bacteria and one for dead bacteria. Thereby, fluorescent dyes for live/dead bacteria bind to nucleic acids in both bacteria. By contrast, fluorescent dyes for dead bacteria pass through only the cell membrane of dead bacteria. Thereby, fluorescent dyes for dead bacteria bind to only nucleic acids in dead bacteria.

(3) A sample solution is flowed through a flow cell to measure labeled bacteria one by one. Live bacteria emit only the fluorescence of the fluorescent dyes for live/dead bacteria (blue color) when they pass through the probe space in the flow cell. Dead

bacteria emit the fluorescence of the fluorescent dyes for live/dead bacteria (blue color) and the fluorescence of the fluorescent dyes for dead bacteria (yellow color). Thereby, it is possible to identify live and dead bacteria by color difference of fluorescence.

Next, we considered how to operate serially removing food debris, labeling bacteria with fluorescent dyes and measuring live bacteria using flow cytometry.

A typical method to operate serially multiple processes is a discrete type used in clinical chemistry analyzers, etc [13]. The discrete type, which automates hand methods in inspections, is very effective to inspect a large amount of samples. However, a system needs a complex mechanism. Then, to simplify system configuration as much as possible, we apply techniques used in Micro TAS (Micro Total Analysis Systems) [14][15][16] for measurements of live bacteria.

Micro TAS are devises, which contain micro channels and cells, analyze target substances by flowing sample solution inside and operating chemical and biochemical processes. A device in Micro TAS are called as a chip [17], a cassette [18] or a cartridge [19], etc. In particular, devices in this thesis are called as cartridges.

Fig. 3-5 shows a configuration diagram of a cartridge to measure numbers of live bacteria in a food suspension using fluorescence flow cytometry.
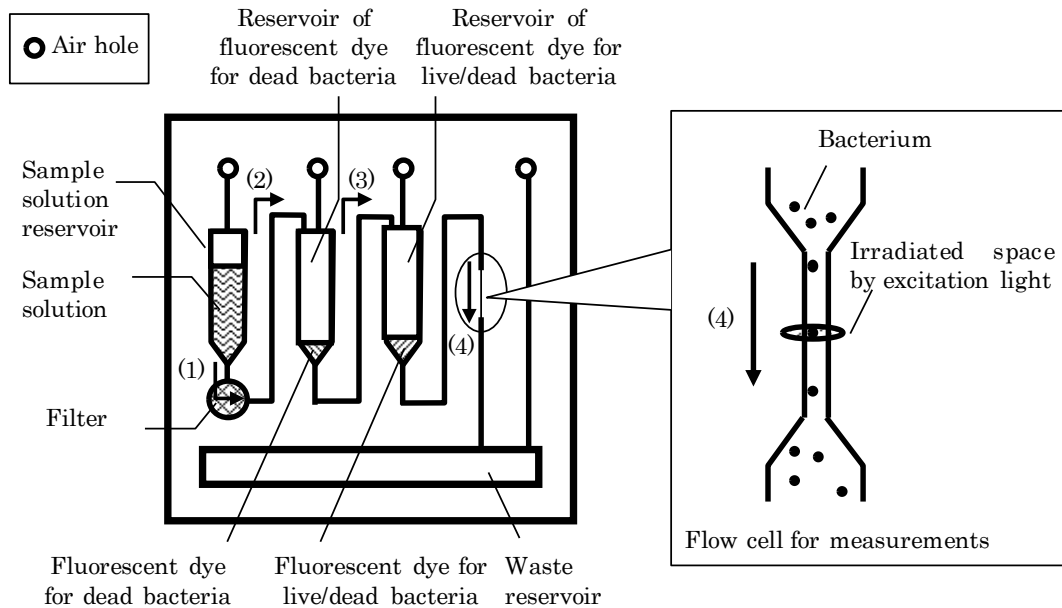
Fig. 3-5 Configuration diagram of the cartridge using fluorescence flow cytometry

The cartridge is integrated with a filter removing food debris, a reservoir of fluorescent dye solution for live/dead bacteria, a reservoir of fluorescent dye solution for dead bacteria, a flow cell for detecting bacteria, a waste reservoir, channels serially connecting reservoirs, the flow cell and the waste reservoir, and air holes on each reservoir for flow control of a solution. Processes in Fig. 3-4 (removing food debris, labeling bacteria with fluorescent dyes, and measuring live bacteria using flow cytometry) are carried out in the cartridge. This procedure is called a cartridge-type flow cytometry below.

In a device of Micro TAS, flows of a sample solution and reagent are often controlled by pumps and valves equipped on the outside of the device. Additionally, substances are often analyzed by a measuring part equipped on the outside of the device. In this concept, flows of a sample solution and reagent are controlled by changing pressure in the device by pumps and valves equipped on the outside of the device. Additionally, live bacteria in the sample solution are measured by an optical unit equipped on the outside of the device.

The process of a measurement of live bacteria in the cartridge is shown in the following.

(1) A sample solution of homogenized food suspension is flowed through the filter to remove food debris in the solution.

(2) Filtered sample solution is flowed to the reservoir of fluorescent dye solution for dead bacteria. The sample solution and fluorescent dye solution for dead bacteria are mixed to label dead bacteria.

45

(3) The mixed sample solution is flowed to the reservoir of fluorescent dye solution for live/dead bacteria. The sample solution and fluorescent dye solution for live/dead bacteria are mixed to label live and dead bacteria.

(4) After labeling, the mixed sample solution is flowed to the flow cell to measure live bacterial numbers using flow cytometry. Every time live and dead bacteria pass through a space irradiated by the excitation light, live and dead bacteria emit fluorescence. Fluorescence from a bacterium is detected by detectors. Finally, measured sample solution is flowed to the waste reservoir.

3.3 Multiple labeling for measurements of live bacteria in food suspension

3.3.1 Theory of distinguishing live bacteria by multiple labeling

Trash such as food debris needs to be removed from a sample solution before measuring live bacterial numbers using fluorescent flow cytometry [6][7]. Trash in measuring live bacterial numbers using fluorescent flow cytometry includes dead bacteria and particles of fluorescent dye other than food debris. This trash, which can emit autofluorescence or fluorescence of fluorescent dyes bound to the trash, can be measured as live bacteria [6]. Thereby, it is difficult to measure live bacterial numbers in a sample solution containing much trash using a system. In common fluorescent flow cytometry, trash is removed by some methods such as a centrifugation method and a column method from a sample solution separately before live bacterial numbers are measured [8][14].

The centrifugation method and the column method [20] can remove trash from a sample solution containing live bacteria highly efficiently. However, it is difficult to use the centrifugation method or the column method in view of the cartridge structure. This is because the centrifugal method needs a centrifugal force as much as a few thousand times gravitational force and the column method needs a few dozen MPa of pressure.

In the cartridge type flow cytometry, large-size trash which can block the flow cell (cross-section: 20 μm by 40 μm) is removed from the sample solution in passing through the filter (pore size: 20 μm) in the cartridge. However, it is difficult to remove trash smaller than a pore size of the filter. Thereby, we considered to distinguish live bacteria from trash using difference of color of fluorescence.

Trash derived from foods contain animal cells, plant cells, and component materials of cells, nuclei, plastids, and mitochondria, and substances produced by cells including agglomerations of starch, glycogen, or lipids. Additionally, there are particles of fluorescent dyes as trash derived from sources other than food.

Thereby, size, length of DNA, membrane damage, and autofluorescence are conditions

of trash that need to be considered to distinguish live bacteria from trashes. Details of the trash in these items are shown in the following [21][22][23].

(1) Particles of fluorescent dyes

It is difficult to remove particles of fluorescent dye with a filter because 0.1 μm - a few μm diameters of particles of fluorescent dyes pass through pores of the filter. Especially, it is difficult to distinguish live bacteria from particles of fluorescent dyes for live/dead cell which emit fluorescence at same wavelength of live bacteria.

(2) Animal cell, plant cell, and nucleus

Animal cells and plant cells can be removed with the filter because size of these is more than the pore size of the filter (20 μm).

Additionally, if these aren't removed, it is possible to distinguish live bacteria from these by the difference of fluorescent intensity. This is because fluorescent intensity of DNA binding fluorescent dyes is proportional to the length of DNA. Thereby, fluorescent intensity of these cells is larger than one of bacteria because the length of DNA in these cells is larger than thousand times of the length of DNA in bacteria.

(3) Plastids

Plastids, which are divided to chloroplast, chromoplast and leucoplast etc., are parts have functions of photosynthesis, storage of starch and lipid, and synthesis of various compounds [23].

Some plastids such as chloroplast emit autofluorescence. Thereby, it is considered that it is difficult to distinguish live bacteria and plastids which emit fluorescence at similar wavelength.

(4) Agglomeration of starch, glycogen or lipid

Agglomerations of starch, glycogen and lipid have possibility to emit fluorescence by absorbing fluorescent dyes although these agglomerations don't have DNA or cell membrane, or emit autofluorescence. However, it is possible to distinguish between live bacteria from these agglomerations because these absorb both fluorescent dyes for live/dead bacteria and fluorescent dyes for dead bacteria.

For the above-mentioned, we considered that it is difficult to distinguish live bacteria from particles of fluorescent dyes and plastids. Thereby, conditions to distinguish live bacteria from particles of fluorescent dyes and plastids are considered.

To distinguish live bacteria from dead bacteria by the difference in wavelength of fluorescence in particles of fluorescent dyes and plastids, we need to understand wavelengths of fluorescence from these particles. Moreover we need to find a labeling

condition under which live bacteria emit fluorescence whose wavelength is different from the wavelengths of fluorescence of other particles.

3.3.2 Fluorescent spectra of plastids

Unlike live bacteria, dead bacteria and particles of fluorescent dye, wavelengths of fluorescence of plastids are unknown. Thereby, fluorescence spectra of plastids are measured by a fluorescence spectrometer.

To measure fluorescence spectra of pure plastids, plastids need to be extracted from plants. However, fluorescence spectra of homogenized vegetable suspensions which contain a lot of plastids are measured because measurement targets of the system are live bacteria in a homogenized food suspension.

Table 3-3 shows vegetables as measurement targets and plastids in these vegetables [23]. Spinach containing chlorophyll, carrots containing carotene, red cabbage containing anthocyanin, and potatoes containing not pigments but leucoplast are selected.

Table 3-3 Vegetables used for fluorescence spectrum measurement

Vegetable	Spinach	Carrot	Red cabbage	Potato
Plastid	Chloroplast	Chromoplast	Chromoplast	Leucoplast
Pigment	Chlorophyll	Carotene	Anthocyanin	-

Procedures of measurement are shown.
(1) Homogenizing vegetable and distilled water in ten times mass of the vegetable in a homogenizing bag with a stomacher (Bagmixer 400, Interscience) for 1min.
(2) Homogenized suspension is filtered with a membrane filter (pore size: 20 μm, Isopore^{TM}, Millipore).
(3) Fluorescence spectrum of homogenized suspension is measured with the fluorescence spectrometer (RF-5300PC, Shimazu).

Fig. 3-6 shows measured fluorescent spectra of homogenized vegetable suspensions. In Fig. 3-6, Y-axis is relative intensity of fluorescence to maxima of intensity of fluorescence. X-axis is wavelength of fluorescence.
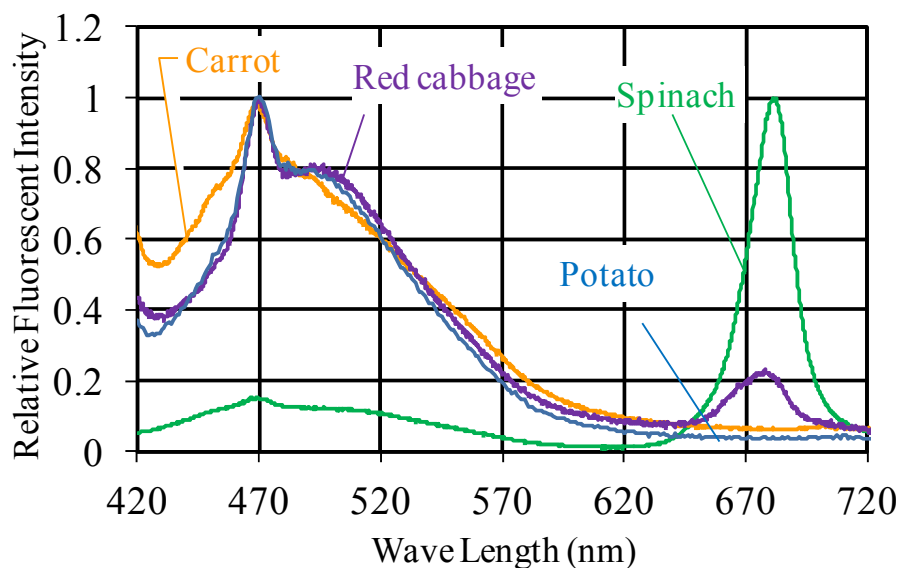
Fig. 3-6 Fluorescence spectra of homogenized vegetables

Fig. 3-6 shows that plastids of vegetable other than spinach emit fluorescence with emission maxima of 470nm, and chlorophyll of spinach emit fluorescence with emission maxima of 680nm.

3.3.3 Selection of fluorescent dyes

We considered that a combination of fluorescent dyes would distinguish live bacteria from other particles: dead bacteria, particles of fluorescent dyes, and plastids derived from foods.

First, a combination of fluorescent dyes to distinguish live bacteria from particles of fluorescent dyes are considered. If one kind of fluorescent dye for live/dead bacteria is used, it is difficult to distinguish live bacteria from particles of fluorescent dyes for live/dead bacteria because these emit fluorescence of the same fluorescent spectrum.

Thereby, we considered to use two kinds of fluorescent dyes for live/dead bacteria and one kind of fluorescent dye for dead bacteria.

Fig. 3-7 shows the concept of distinguishing live bacteria from particles of fluorescent dyes using two kinds of fluorescent dyes for live/dead bacteria and one kind of fluorescent dye for dead bacteria.

Before labeling

Live bacterium — DNA

Dead bacterium

- Fluorescent dyes 1 for live and dead cells
- Fluorescent dyes 2 for live and dead cells
- Fluorescent dyes for dead cells

After labeling

Live bacterium   Dead bacterium   Particles of fluorescent dyes
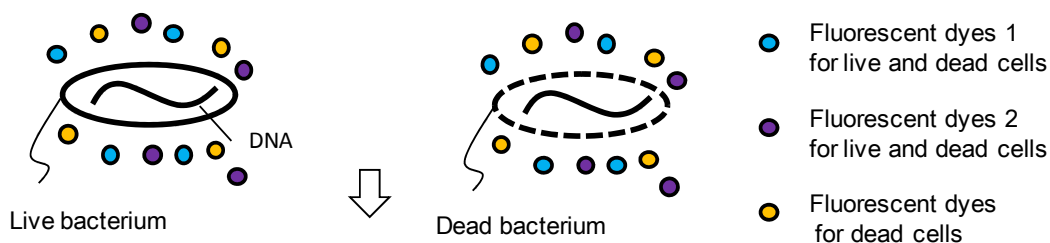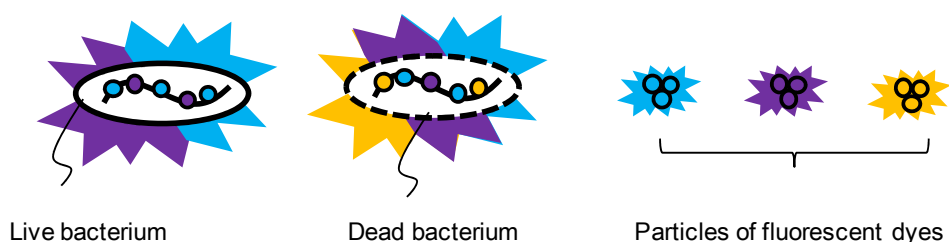
Fig. 3-7 Concept of determining live bacteria using three kinds of fluorescent dyes

In using two kinds of fluorescent dyes for live/dead bacteria and one kind of fluorescent dye for dead bacteria, live bacteria emit two kinds of fluorescence (blue and purple), while each of two kinds of particles of fluorescent dyes for live/dead bacteria emit one kind of fluorescence (blue or purple). Thereby, it is possible to distinguish live bacteria from the two kinds of particles of fluorescent dyes for live/dead bacteria.

Next, we considered a combination of fluorescent dyes to distinguish live bacteria from plastids derived from foods. It is difficult to distinguish live bacteria from plastids if the wavelength range of autofluorescence of plastids and the wavelength range of fluorescence of the two kinds of fluorescent dyes for live/dead bacteria overlap each other.

Thereby, we need to select two kinds of fluorescent dyes on the condition that the wavelength ranges of fluorescence of plastids don't overlap the wavelength ranges of fluorescence of either of the two kinds of fluorescent dyes.

Table 3-4 shows commercially supplied fluorescent dyes for live/dead bacteria and fluorescent dyes for dead bacteria [24]. On the other hand, Fig. 3-6 shows that intensity of fluorescence of a carrot and a red cabbage is high at 470 nm but low at 680 nm. By contrast, intensity of fluorescence of spinach is high at 680 nm but low at 470 nm.

With consideration for features of these fluorescence spectra, we considered that there are few vegetables which emit blue fluorescence (450 nm to 480 nm) and near-infrared

radiation (680 nm to 720 nm). Thereby, SYTO 41® emitting blue fluorescence and LDS751 emitting near-infrared fluorescence are selected as fluorescent dyes for live/dead bacteria to distinguish live bacteria from plastids of vegetables.

Additionally, SYTOX ORANGE® emitting orange fluorescence (550 nm to 650 nm) was selected as a fluorescent dye for dead bacteria.

Table 3-4 Typical fluorescent dyes

	Fluorescent dye	Abs (nm)*	Em (nm)*	Color of fluorescence
Fluorescent dyes for live and dead cells	SYTO®41	430	454	Blue
	SYTO®82	541	560	Orange
	SYTO®62	652	676	Red
	LDS751	532	720	Infrared red
	DAPI	350	470	Blue
	EB	520−525	615	Orange
Fluorescent dyes for dead cells	SYTOX Blue®	470	480	Blue
	SYTOX GREEN®	504	523	Green
	SYTOX ORANGE®	547	570	Orange
	POPO1®	434	456	Blue
	POPO3®	534	570	Orange
	PI	532	617	Red

*Wavelength in maximum absorption and fluorescence emission

A Venn diagram in Fig. 3-8 shows each complex of fluorescence from live bacteria, dead bacteria, plastids of vegetables, and particles of fluorescent dyes in using SYTO41®, LDS751, and SYTOX ORANGE®. We considered that live bacteria can be distinguished from other particles because there is no other particle emitting fluorescence of SYTO41® and LDS751 than live bacteria.
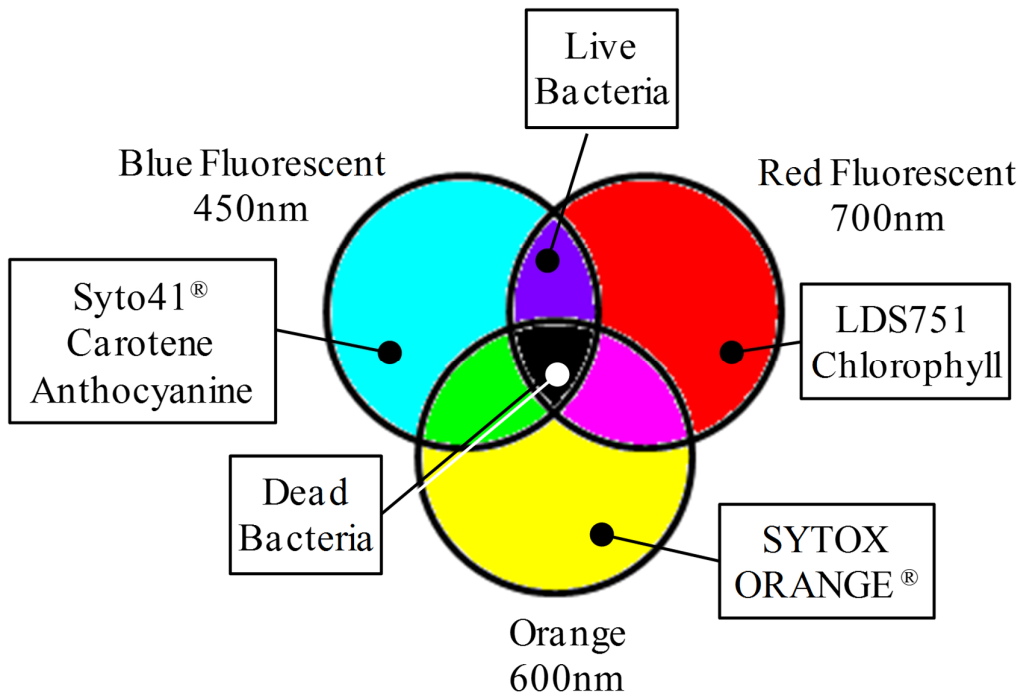
Fig. 3-8 Diagram to determine live bacteria from other particles

3.4 Design of the system by using statistical methods

3.4.1 Volume of target sample space

In this section, the needed volume of a sample solution for measurements and the dimensions of a flow cell for measurements in the cartridge are considered using the design methodology based on the statistical theory in Chapter 2. First, a minimum volume of a sample solution, which is mentioned as a minimum volume target sample space in Chapter 2, is considered in this subsection. Second, the dimension of the flow cell for measurements, which relates to the probe space mentioned in Chapter 2, is considered in next subsection.

The minimum live bacterial numbers needed in measurements using flow cytometry (n_{min} (cell)) is presumed as 50 (cell) and the probability of a sample solution containing more than n_{min} (cell) ($P(x > n_{min})$) is presumed as 0.999. Additionally, target specifications in Table 3-2 show the target of the minimum number concentration of the sample solution (ρ) as 10^3 (cell/mL) (=10^9 cell/m^3).

Thereby, these conditions and results of discussion in Chapter 2, section 4 give

$$P(x \geq n_{min} = 50) = \sum_{i=n_{min}}^{\infty} p(i) = 1 - \sum_{i=50}^{\infty} p(i) \geq 0.999 \quad \text{3-1}$$

where

$$p(x) = \frac{v^x e^{-v}}{x!},$$

$$v = \rho v = 10^9 v,$$

and v is the volume of a sample solution called a target sample space.

Moreover, calculation of equation 3-1 using Excel gives the minimum volume of a sample solution (v_{min}) as

$$v_{min} \geq 0.075 \quad \text{(mL)}.$$

Thereby, we decided the sample volume of the sample solution is 0.10 mL. Additionally, 0.10 ml prepared sample solution is divided from a total 1 mL of prepared sample in a measurement of this system to make handling the sample solution easy.

3.4.2 Design of probe space

Next, a probe space in the flow cell for measurements is considered. Flow cytometry, which is a measurement method for particles called the flow method in Chapter 2, is a method to measure particles by making particles pass through the probe space with a certain drive force.

In the flow method, a larger volume of the probe space increases the probability that bacteria enter the probe space simultaneously. Thereby, counting loss, which is counting a few live bacteria as bacterium, occurs more easily. Additionally, as equation 2-15 shows in the previous chapter, the counting loss is given by

$$P = 1 - p(0) = 1 - e^{(-\rho Q t_m)} \quad \text{3-2}$$

where Q is volume of flow of the sample solution, ρ is number concentration of target particles in the sample solution, and t_m is measurement time.

The probe space in the flow cell for measurements which is shown in Fig. 3-2 is the space where the excitation light irradiates a flow cell. Thereby, in the case that the cross-section area of the flow cell is s [m^2] and the length of the flow direction of the space where the excitation light irradiates a flow cell is l [m], equation 3-2 can be converted to

$$P = 1 - p(0) = 1 - e^{(-\rho sl)} \quad 3\text{-}3$$

where sl is equal to Qt_m.

By deforming equation 3-3, the volume of the probe space (sl) is given by

$$sl = \frac{1}{\rho}\log(1 - P) \qquad 3\text{-}4$$

3.4.3 Condition of flow cell for measurements

Equation 3-3 shows that the counting loss is smaller at the smaller cross-section area of the flow cell for measurements. However, the pressure loss in the flow cell for measurements is higher at the smaller cross-section area of the flow cell for measurements. Thereby, the counting loss and the pressure loss in the flow cell for measurements have to be considered in the dimension of the cross-section area of the flow cell for measurements.

The pressure loss of the flow cell for measurements whose length is L [m] is given by

$$\Delta P_L = \frac{32\mu LU}{D_e{}^2} \quad 3\text{-}5$$

where μ [Pa·s] is a viscosity of the sample solution, U [m/s] is the average flow rate of the sample solution, and D_e [m] is the equilibrium diameter of the flow cell for measurements.

Additionally, D_e [m] is given by

$$De = \frac{4s}{W} \quad 3\text{-}6$$

where s [m^2] is the cross-section area of the flow cell for measurements, and W is a perimeter of the flow cell for measurements.

Moreover, equations 3-5 and 3-6 give

$$s^2 = \frac{2\mu LUW^2}{\Delta P_L} \quad 3\text{-}7$$

Therefore, the dimension of the flow cell for measurements needs consideration of equations 3-4 and 3-7. Parameters in equation 3-4 and 3-7 were decided based on values

shown in Table 3-3. These parameters are decided in view of the measurement accuracy, the pressure tightness of the device, the ease of the fabrication of the flow cell, etc.

Fig. 3-8 shows the range of the cross-section areas of the flow cell for measurements meeting the conditions shown in Table 3-5 and equations 3-4 and 3-7.

Table 3-5 Parameters used for design of micro channel

Symbol	Meaning	Numerical value	Reason of numerical value	Equation
P	Counting loss	$\leqq 0.05$	Considering measurement accuracy	3-3
ρ	Number concentration	10^6 [cell/ml] (10^{12} [cell/m^3])	Maximum of measurement range of bacteria	3-3
l	Length of micro channel eradiated by excitation light in flow direction	30 [μm] (3.0×10^{-5} [m])	Three times of long side of a bacterium (Long side of a common bacterium falls between 1.0×10^{-6} and 1.0×10^{-5} [m] [19])	3-3
μ	Viscosity	1.2×10^{-4} [Pa·s]	Viscosity of 10 % glycerol aqueous solution	3-6
L	Length of micro channel	2.0 [m]		3-6
U	Mean flow rate	1.0×10^{-4} [mL/s] (1.0×10^{-10} [m^3/s])	Mean flow rate required to measure 0.1 mL sample in 1,000 s	3-6
W	Perimeter of cross-section surface of micro channel	6a [m]	Aspect ratio of the micro channel is 2 and short side of micro channel is a.	3-6
ΔP_L	Pressure loss of micro channel	$\leqq 1.0 \times 10^5$ [Pa]	Pressure resistance of a device with the micro channel	3-6
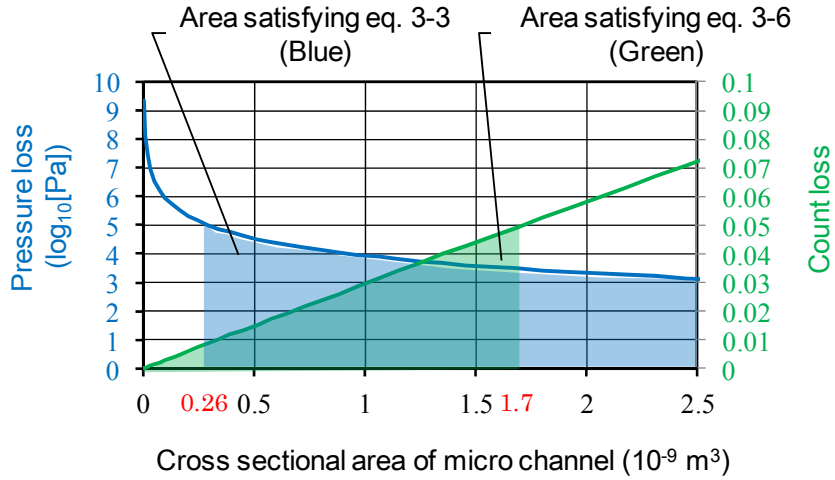
Fig. 3-9 Design of flow cell by theoretical calculations

Thereby, the range of the cross-section area of the flow cell for measurements is between 0.26×10^{-9} m² and 1.7×10^{-9} m² under the above condition.

Next, the length of the short side of the flow cell for measurements is decided to meet this condition. The measurement accuracy is improved by the decrease of the counting loss at the shorter length of the short side of the flow cell for measurements. However, considering that long diameter of normal bacteria is 1×10^{-6} m $- 10 \times 10^{-6}$ m [25], the length of the short side of the flow cell for measurements is set to be larger than double the long diameter of normal bacteria (20×10^{-6} m).

For these reasons, the length of the short side of the flow cell for measurements is set as 20×10^{-6} m (20 μm), and the length of the long side of the flow cell for measurements is set as 40×10^{-6} m (40 μm). Under these conditions, the cross-section area of the flow cell for measurements is 0.8×10^{-9} m².

3.4.4 Measuring range of number concentration of bacteria

In the previous section, the target value of the measuring range of number concentration of bacteria is decided between 10^3 and 10^6 cell/mL in the development of this system. Moreover, in this range, the flow cell for measurements is designed to meet the condition that the counting loss be less than 0.05.

In this subsection, we calculate theoretical bacterial numbers in using the designed flow cell for measurements. As previously discussed, the counting loss is given by

$$P = 1 - p(0) = 1 - e^{(-\rho sl)} \qquad \text{3-8}$$

56

where s is the cross-section area of the flow cell for measurements, and l is the length of the flow direction of the area irradiated by the excitation light. In this thesis, s is 20×40 μm^2 and l is 30 μm.

Under these conditions, counts of bacteria output by the system (N_c) in measuring a sample solution (number concentration of bacteria: N_r) are given by

$$N_c = N_r(1 - P) \qquad\qquad 3\text{-}9$$

Fig. 3-10 shows counts of bacteria output by the system (N_c) in case that the range of the number concentration of bacteria in the sample solution is from 10^1 cell/mL to 10^7 cell/mL.
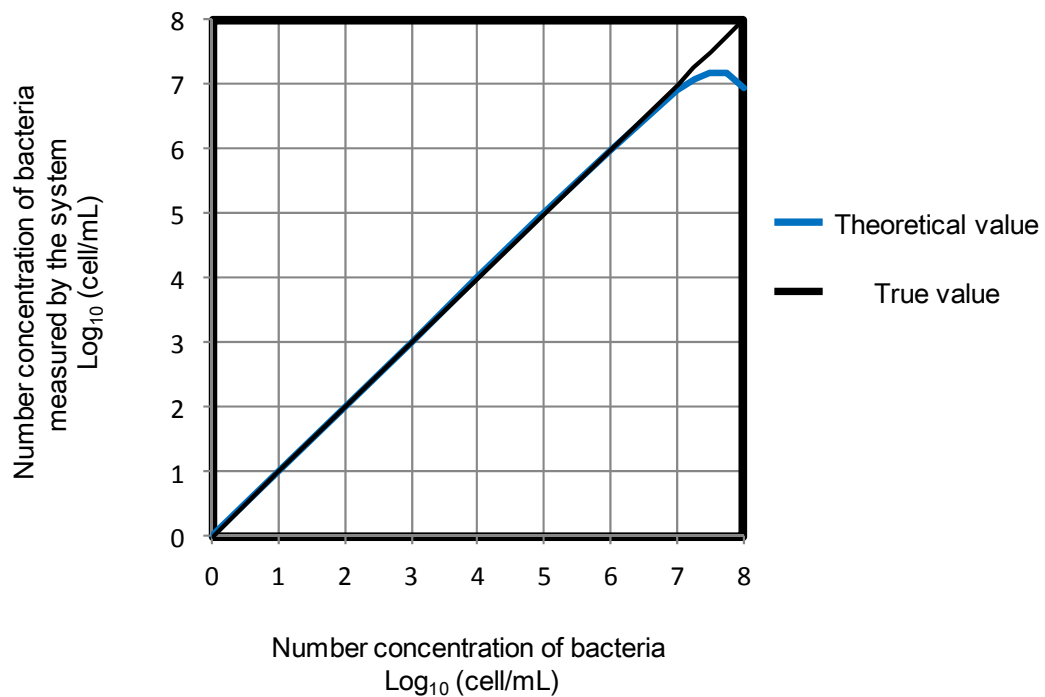
Fig. 3-10 Theoretical value of number concentration measured by the system

Fig. 3-10 shows that there is little difference between theoretical measured number of bacteria and true number of bacteria when the number concentration of bacteria in a sample solution is the target specific of the system: 10^3 - 10^6 cell/mL.

3.5 Fabrication of flow cell for measurements

3.5.1 Selection of fabrication process

The flow cell for measurements is designed in the previous section. However, fabrication processes of the flow cell are limited because the cross section area (20×40 μm^2) of the flow cell is very fine. Methods to fabricate the flow cell include the following: (a) method to use a glass capillary [26], (b) method to fabricate a micro groove on a glass surface by etching [27], and (c) method to fabricate a micro groove on a silicon resin having excellent optical property by casting [28]. Table 3-6 shows that results of consideration of these methods in (i) easiness of making a flow cell, (ii) easiness of attaching flow cell on a cartridge, (iii) autofluorescence from a flow cell, (iv) optical effect of a flow cell.

Table 3-6 Fabrication methods of micro channel

	(1) Using a glass capillary	(2) Microfabricating glass plate	(3) Casting resin on microfabricated molding die
(i) Easiness of making micro channel	○	×	○
(ii) Easiness of attaching micro channel on a cartridge	×	○	○
(iii) Autofluorescence from a micro channel	○	○	△
(iv) Optical effect of a micro channel	×	○	○

(a) Method to use a glass capillary

    It is possible to select a best suited capillary in length or diameter because glass capillaries are general-purpose products. Additionally, it is a merit that a glass capillary emits little autofluorescnece inhibiting measurements of fluorescence. However, it is difficult to attach a glass capillary on a cartridge. Additionally, a lens effect of a round surface of the glass capillary makes it difficult to focus the excitation light on inside of the glass capillary.

(b) Method to fabricate a micro groove on a surface of glass plate by etching

    There is little autofluorescence from a glass flow cell. Additionally, a tabular shape of a flow cell don't have lens effect making it difficult to focus the excitation

light on inside of the flow cell and make it easy to be attached the flow cell on the cartridge. However, microfabrication on a glass surface using wet etching need high cost.

(c) Method to fabricate a micro groove on a silicon resin with excellent optical property by casting.

As with glass plate, a tabular shape of a flow cell don't have lens effect making it difficult to focus excitation light on inside of the flow cell and make it easy to be attached the flow cell on the cartridge. Additionally, it is possible to fabricate the flow cell in low cost because casting resin is an excellent method in mass production. By contrast, a flow cell made by this method has possibility to emit autofluorescence depending on the property of resin material. However, if a resin material emitting little autofluorescence are found, the problem can be resolved. Thereby, in this thesis, casting method is selected to fabricate a flow cell.

3.5.2   Selecting material of flow cell

A material emitting weak autofluorescence is selected for the flow cell. When a certain material is irradiated by the excitation light, the intensity of autofluorescence emitted from a certain material (I_m) is given by

$$I_m \propto \rho S d i_e \qquad\qquad 3\text{-}10$$

where ρ is intensity of autofluorescence emitted from the material per unit volume irradiated by excitation light, S is the area irradiated by the excitation light, d is the thickness of the material to the direction of excitation light, and i_e is intensity of excitation light per area [29].

Therefore, to weaken intensity of autofluorescence of the flow cell, we need to select a material which emits weaker autofluorescence and to make the flow cell thinner in the direction of excitation light.

First, intensities of autofluorescence per unit thickness of materials are measured to select a material emitting weak autofluorescence. Measured materials, which are known as optical materials, are Polymethylmethacrylate (PMMA), Cyclo Olefin Polymer (COP), Poly Dimethyl Siloxane (PDMS) and glass. Measured COP materials are two types: ZEONOR® and ZEONEX®.

Autofluorescence of these materials are measured with an optical unit in Fig. 3-11. Additionally, specifics of the optical unit in Fig. 3-11 are shown in Table 3-7. An output

59

value of a photomultiplier measuring autfluorescence from a certain material is considered as relative intensity of autofluorescence from the material. A measured material is set on a focus position of the optical unit. Additionally, the excitation light of the green laser in the optical unit enters the measured material vertically.
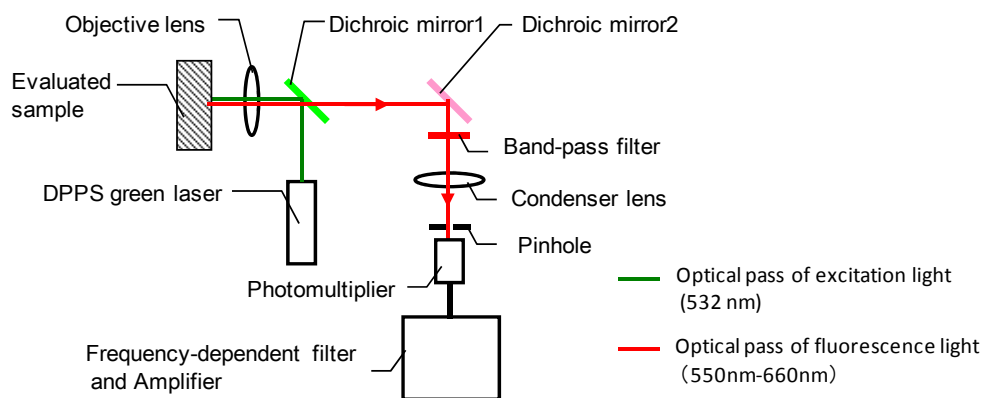
Fig. 3-11 Optical unit to measure autofluorescence intensity of material of flow cell

Table 3-7 Specifications of optical parts

Item	Part number	Specification	Maker
Objective lens	UPLFLN 10X2	Magnification: ×10 , N.A: 0.30 , W.D: 10 mm	Olympus
Dichroic mirror1	BI0036	Wavelength of 50% transmittance: 550 nm	Asahi spectra
Dichroic mirror2	XF2023	Wavelength of 50% transmittance: 660 nm	Omega optics
Band-pass filter	BP600-60	CWL: 600 nm, FWHM: 60 nm	Asahi spectra
Condenser lens	SLB-19-15P	WD: 15 mm	Sigma optics
Pinhole	39730-H	Pinhole size: 1mm	Sigma optics
Photomultiplier	H6780-02	Detection wavelength band: 450nm ～ 650nm	Hamamatsu photonics
DPSS green laser	DPGL-3020	Laser maximum power: 100 mW	CNI
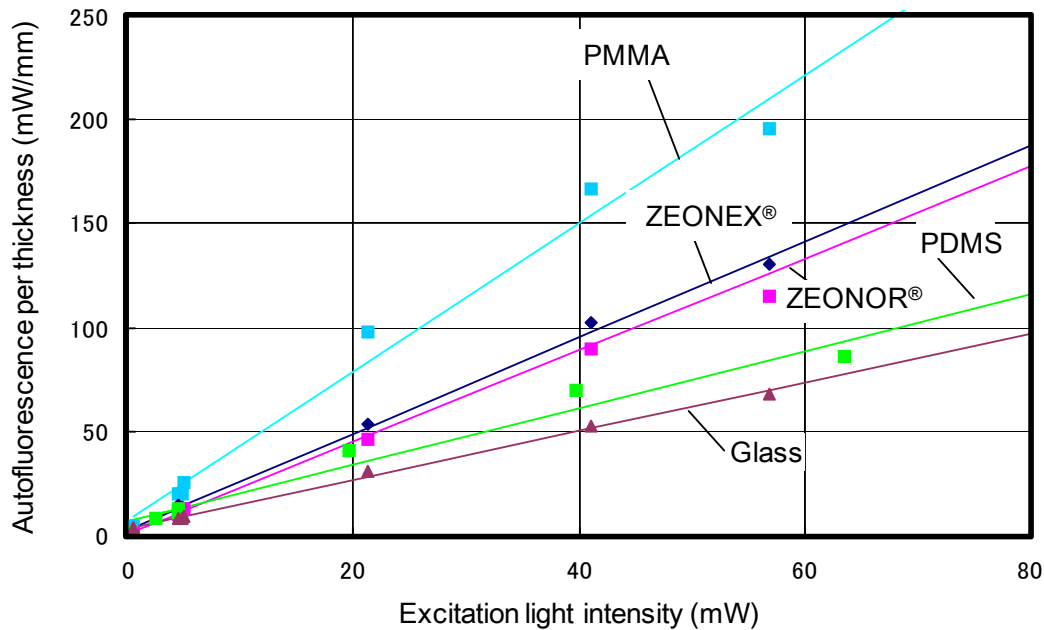
Fig. 3-12 Autofluorescence intensity of material of flow cell

Fig. 3-12 shows relative intensities of autofluorescence of materials depending on intensities of excitation lights. Fig. 3-12 shows that an order of material which emit stronger intensity of autofluorescence are PMMA, ZEONEX®, ZEONOR®, PDMS and glass. However, as mentioned previously, it needs high cost to make grooves on a surface of a glass. Thereby, PDMS which emits weakest fluorescence other than glass is selected for a material of a part with grooves. Additionally, glass is selected for a material of a laminar part. A flow cell is made by pasting the PDMS part with grooves and the laminar glass part.

Second, intensities of autofluorescence of PDMS and glass depending on thickness are measured by the optical unit in Fig. 3-11. In these experiments, intensity of excitation light is 40 mW. Experimental results are shown in Fig. 3-13.
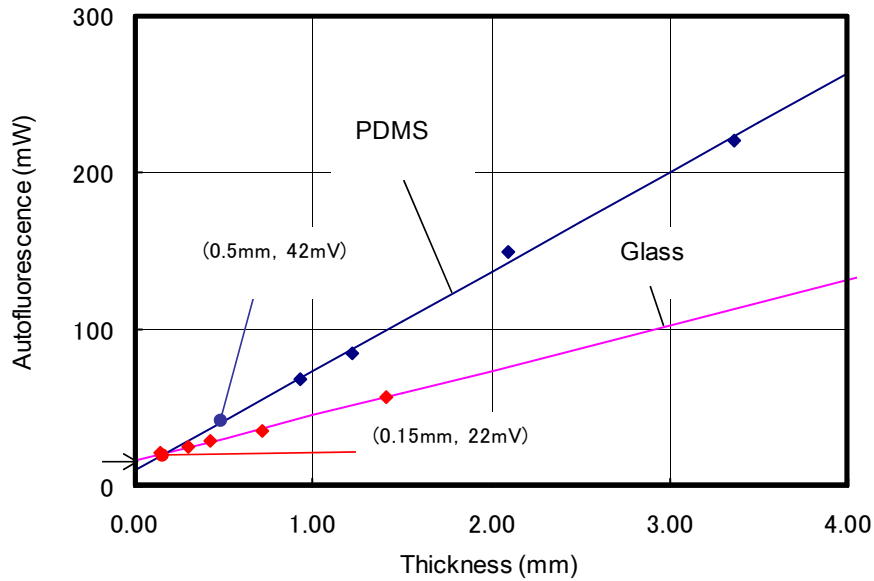
Fig. 3-13 Autofluorescence intensity of material of flow cell

Fig. 3-13 shows that intensity of autofluorescence of a certain material is proportional to the thickness of the material. Thereby, weakening autofluorescence needs to make a part as this as possible in consideration of a strength of the part and a fabrication possibility.

In this thesis, thickness of the PDMS part with groove is decided to 0.5 mm which is a fabricable minimum thickness. Additionally, 0.15 mm cover glass for a microscope (Matsunami) is selected for the laminar glass part.

3.5.3 Fabrication process of flow cell

hardener

PDMS base

(2) Mixing PDMS base and the hardener with a volume ratio of 10:1

Silicon wafer

(1) Making a shaping die by photolithography process using SU-8 resist

SU-8 resist (height: 20 μm)

(3) Casting PDMS mixture on the shaping die

(4) Keeping PDMS mixture on the shaping die at room temperature in Overnight to hardening the mixture

(5) Removing hardened PDMS mixture from the shaping die

(6) Separating micro-channel parts

Through holes

Micro-groove
Width: 40 μm,
Depth: 20 μm

(7) Making through holes at both end of a micro-groove and pasting a micro-channel parts with a cover glass

Fig. 3-14 Fabrication process of flow cell

Fig. 3-14 shows fabrication process of a flow cell.

(1) Making a shaping die by photolithography process using SU-8 resist

(2) Mixing PDMS base and a hardener with a volume ratio of 10:1

(3) Casting PDMS mixture on the shaping die

(4) Keeping PDMS mixture on the shaping die at room temperature in overnight to hardening the mixture.

(5) Removing hardened PDMS mixture from the shaping die

(6) Sepalating PDMS parts with a groove

(7) Making a thorough holes at both end of a groove and pasting the PDMS part on a cover glass

Fig. 3-15 shows SEM photomicrograph of the shaping die and photograph of the flow cell.

Width: 40 mm
Height: 20 mm
Length: 2 mm
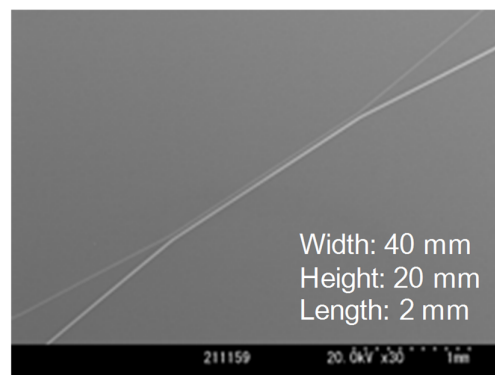
(a) Photograph of the shaping die by a SEM

Flow cell

Through holes
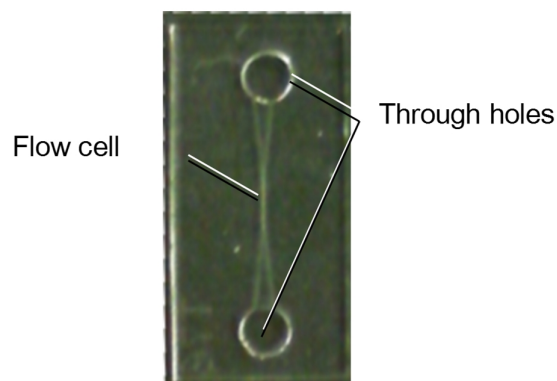
(b) Photograph of the flow cell by a microscope

Fig. 3-15 Photographs of shaping dye and flow cell

3.6 Design of cartridge

Next, a cartridge for measurement of live bacterial numbers is designed. Fig. 3-16 and 3-17 shows a drawing of the cartridge, Fig. 3-18 shows assembly drawing of the cartridge, and Fig. 3-19 shows a photograph of the cartridge.
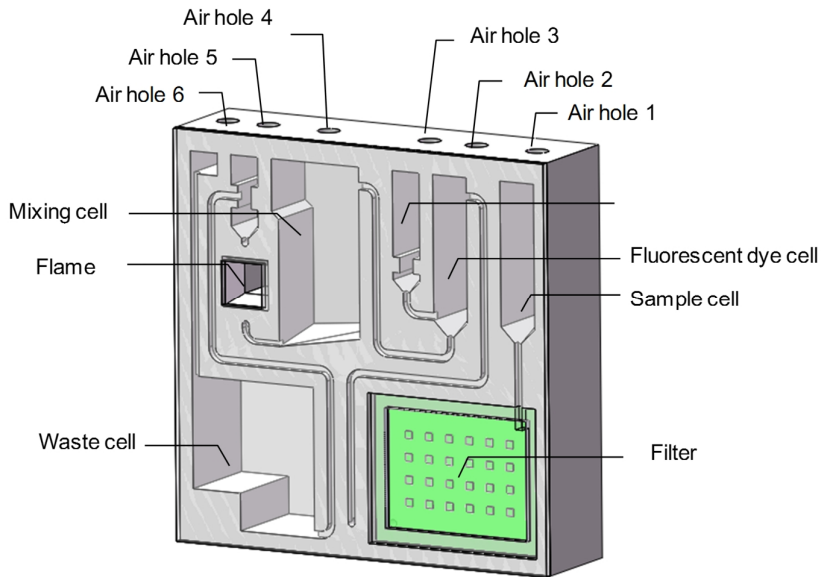
Fig. 3-16 Figures of cartridge (Front side)
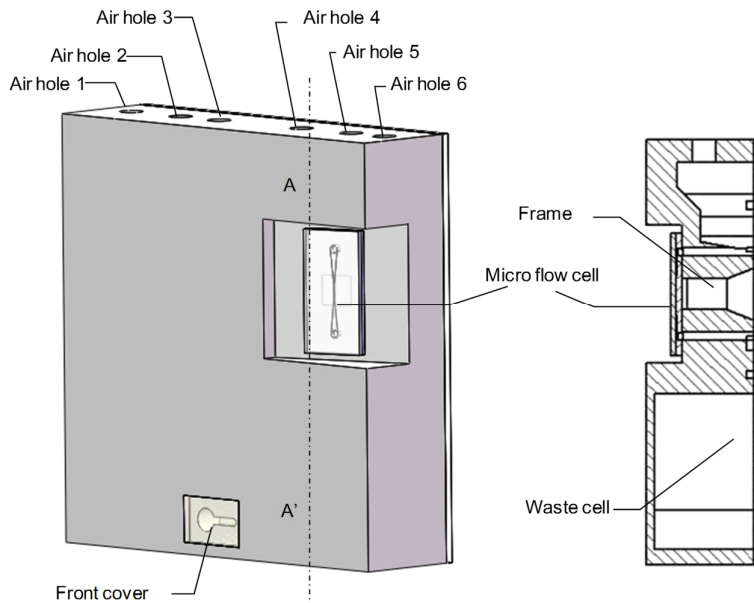
Fig. 3-17 Figures of cartridge (Back side)
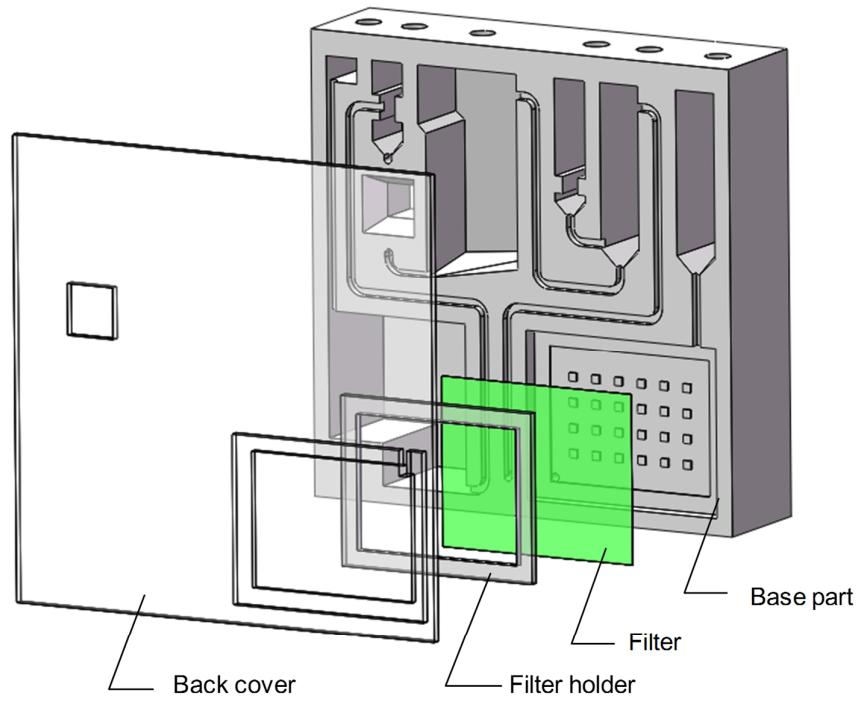
Fig. 3-18 Assembly drawing of cartridge
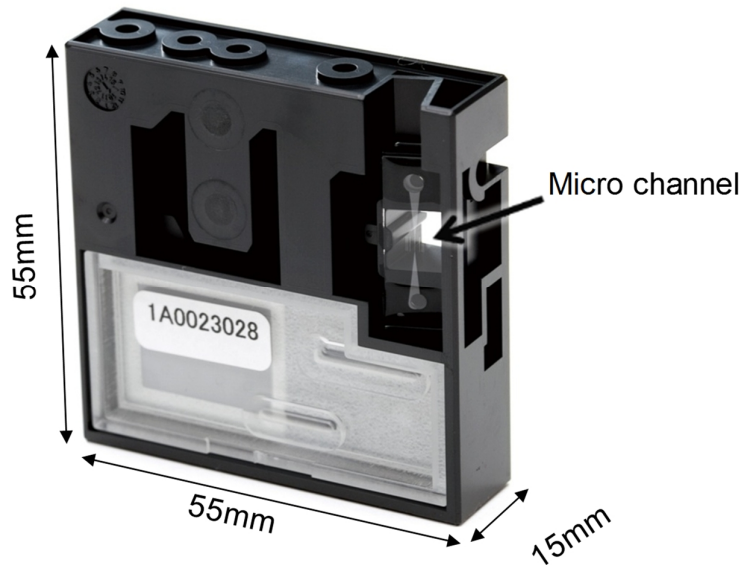
Fig. 3-19 Photograph of cartridge

Fabrication process of the cartridge (length 15 mm, width 55 mm, height 55 mm) is shown in the follow.

(1) A nylon net filter (NY2004700, pore size 20 μm, MERCK) is inserted into a base part with small and large grooves made by injection molding.

(2) An acrylic back cover is pasted on the base part with a double-stick tape.

(3) A flow cell made in other process is pasted on the base part. PDMS resin before hardening is used as an adhesive material.

(4) Fluorescent dye solution is injected in reservoirs in the cartridge before a measurement of live bacterial numbers.

The cartridge consists of a filter removing food debris, a sample solution reservoir, fluorescent dye solution reservoir, a mixing reservoir, a flow cell for measurements of live bacterial numbers, a waste reservoir, channels connecting these parts in series, and air holes to control of sending solutions.

Next, a way to send solutions in the cartridge is shown. The cartridge is set on the system with the air holes upward to utilize a gravity force for sending solutions because 1mL sample solution (1 mL) is large volume for a device in Micro TAS. When the cartridge is this position, the air is on the top of solution in a reservoir. Thereby, it is possible to send the solution through channels in the cartridge without residual solution by changing air pressure in reservoirs through air holes with sending solution control unit of the system.

Fig. 3-20 shows a mechanism to prevent fluorescent dye solution in a fluorescent dye reservoir from flowing out in sending sample solution to the reservoir. A valve connected to an air hole of the reservoir is opened in sending sample solution to a reservoir. Fluorescent dye solution are kept in the reservoir in sending sample solution because air on the top of fluorescent dye solution flows out through the air hole. Additionally, it is possible to mix the sample solution and the fluorescent dye solution by sending air through a channel connecting to the bottom of the reservoir.

(a) Sending sample solution   (b) Mixing by sending air
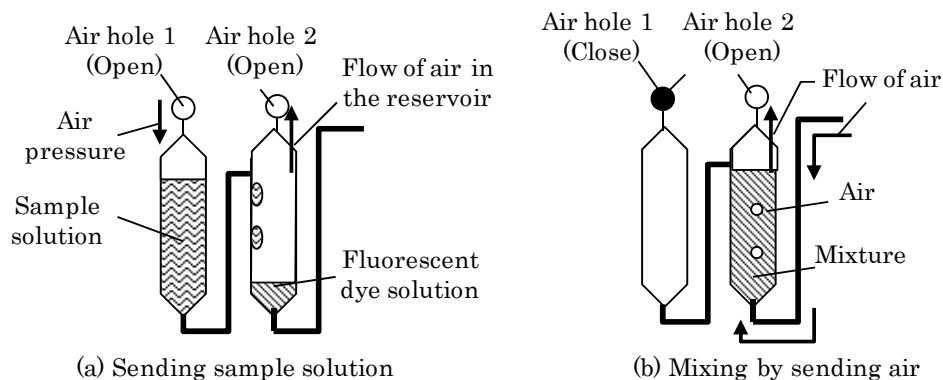
Fig. 3-20 Mechanism of preventing reagent from spilling out of cell

Next, measurement process in the system is shown according to flows of the sample solution in the cartridge.

(1) Removing residue

To remove big residue blocking the flow cell for measurements, the sample solution is send through a nylon net filter (pore size 20 μm).

(2) Labeling live and dead bacteria with fluorescent dyes

Sample solution sent to the fluorescent dye reservoir is mixed with fluorescent dye for live/dead bacteria by sending air through the channel connecting to the bottom of the fluorescent dye reservoir. The mixture is kept to labeled live and dead bacteria with fluorescent dyes for 1,800 s after mixing.

SYTO41$^®$ as fluorescent dye for live/dead bacteria (final concentration 2.0×10^{-3} mol/ml), LDS751 as fluorescent dye for live/dead bacteria (final concentration 3.3×10^{-3} mol/ml) and SYTOX ORANGE$^®$ as fluorescent dye for dead bacteria (final concentration 0.2×10^{-3} mol/ml) are used.

(3) Measurement of live bacterial numbers

The mixture is sent to the flow cell for measurements (length: 2.0 mm, width: 40 μm, height: 20 μm). Numbers of live bacteria in the mixture are measured by flow cytometry.

3.7 Configuration of system

Fig. 3-21 shows a photograph of the system (rapid live bacteria counter, length: 330 mm, width: 430 mm, height: 410 mm) and the cartridge. The system consists of a disposable cartridge, a flow control unit to control a flow of sample solution in the

cartridge, an optical unit to detect fluorescence of particles in the sample solution, and a data processing unit to count only signals originating from live bacteria among all signals output by the optical unit.

A user can measure live bacterial numbers in a sample solution by setting the cartridge injected with the sample solution in the system and providing a direction to start a measurement with a PC. In this section, details of the optical unit and the flow control unit are shown.
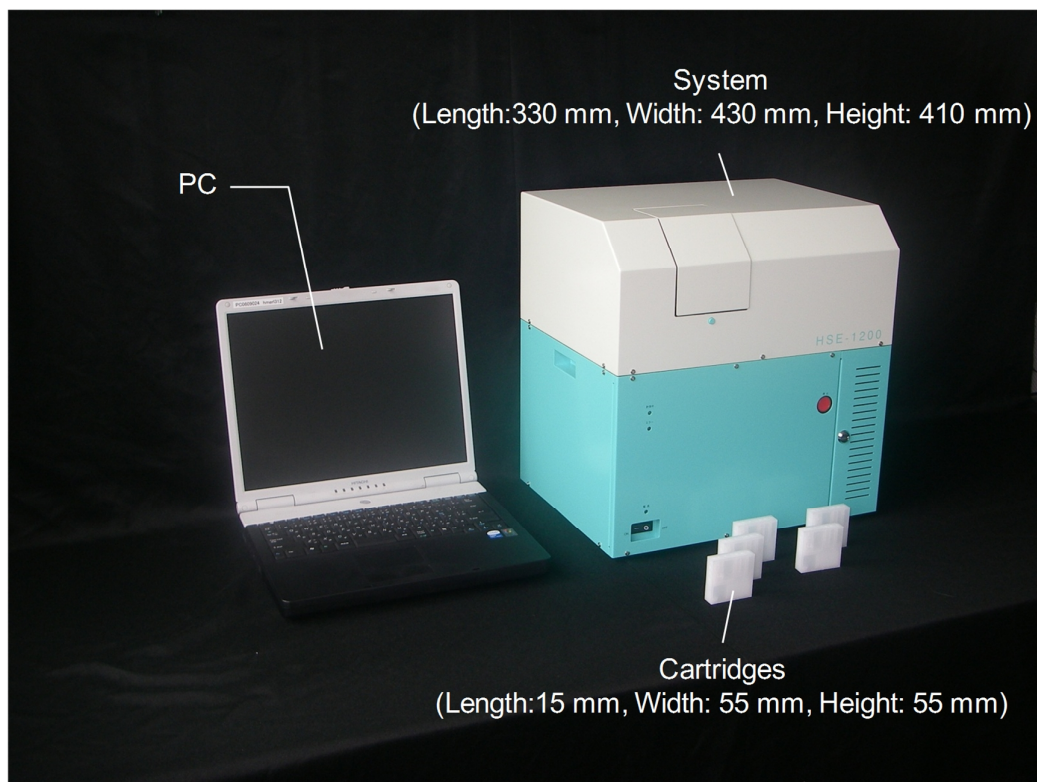
Fig. 3-21 Photograph of rapid live bacteria counter and cartridges

3.7.1 Optical unit

Fig. 3-22 shows the optical unit to measure fluorescence three kind of fluorescent dyes used in measurements: SYTO41®, LDS751 and SYTOX ORANGE®. A list of component parts of the optical unit is shown in Table 3-6.
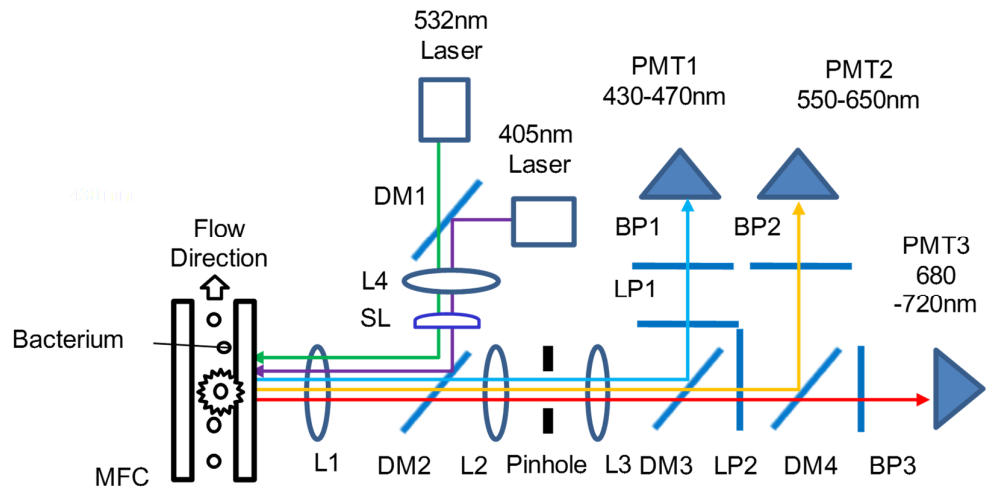
MFC: Micro Flow-Cell   L1, L2, L3, L4: Plano-convex lens, SL: Cylindrical lens
DM1, DM2, DM3, DM4: Dichroic mirror
LP1: Long-pass filter BP1, BP2, BP3: Band-pass filter   PMT1, PM2, PMT3: Photomultiplier

Fig. 3-22 Optical unit of rapid live bacteria counter

Table 3-8-1 Specifications of parts of the optical unit (1)

	Item	Part number	Necessary functions	Specification	Mfr.
Plano-convex lens	L1	-	(1) Irradiation of excitation lights of 405 nm laser and 532 nm laser to the detection area in the micro flow cell	W.D: 10 mm	Asahi spectra
	L2	-		W.D: 15 mm	Asahi spectra
	L3	-	(2) Concentration of fluorescent light from bacteria move along the micro flow cell	W.D: 15 mm	Asahi spectra
	L4	-	Expansion of excitation lights of 405 nm laser and 532 nm laser	-	Asahi spectra
Cylindric al lens	SL	-	Focus of excitation lights of 405 nm laser and 532 nm laser into a line crossing the micro flow cell	-	Asahi spectra

Table 3-8-2 Specifications of parts of the optical unit (2)

	Item	Part number	Necessary functions	Specification	Mfr.
Dichroic mirror	DM2	-	Reflection of excitation lights of 405 nm laser and excitation lights of 532 nm laser and transmission of fluorescence lights of SYTO41®, SYTOX ORANGE®, LDS751	Dual dichroic mirror Wavelength of 50% transmittance: 420 nm, 550nm	Asahi spectra
	DM3	DM500	Reflection of fluorescence light of SYTO41®, and transmission of fluorescence lights of SYTOX ORANGE®, LDS751	Single dichroic mirror Wavelength of 50% transmittance: 500 nm	Asahi spectra
	DM4	DM670	Reflection of fluorescence light of SYTOX ORANGE®, and transmission of fluorescence light of LDS751	Single dichroic mirror Wavelength of 50% transmittance: 670 nm	Asahi spectra
Long-pass filter	LP1	LP420	Blocking of stray light of 405 nm laser and transmission of fluorescence light of SYTO41®	Wavelength of 50% transmittance: 420 nm	Asahi spectra
Band-pass filter	BP1	BP460-60	Transmission of fluorescence light of SYTO41®	CWL: 460 nm, FWHM: 60 nm	Asahi spectra
	BP2	BP600-100	Transmission of fluorescence light of SYTOX ORANGE®	CWL: 600 nm, FWHM: 100 nm	Asahi spectra
	BP3	BP720-60	Transmission of fluorescence light of LDS751	CWL: 720 nm, FWHM: 60 nm	Asahi spectra
Pinhole	Pinhole	-	Blocking of stray light out of the detection area	Pinhole size: 1mm	Asahi spectra

Table 3-8-3 Specifications of parts of the optical unit (3)

	Item	Part number	Necessary functions	Specification	Mfr.
Photomultiplier	PMT1	H6780	Detection of fluorescence light of SYTO41®	Detection wavelength band: 300nm ～ 650nm Wavelength at maximum sensitivity: 420 nm	Hamamatsu photonics
	PMT2	H6780-02	Transmission of fluorescence light of SYTOX ORANGE®	Detection wavelength band: 300nm ～ 880nm Wavelength at maximum sensitivity: 500 nm	Hamamatsu photonics
	PMT3	H6780-20	Transmission of fluorescence light of LDS751	Detection wavelength band: 300nm ～ 920nm Wavelength at maximum sensitivity: 630 nm	Hamamatsu photonics
532 nm Laser	DPSS green laser	J050GS	Irradiation of excitation light of 405 nm	Laser maximum power: 50 mW Wavelength: 532 nm	Showa optronics
405 nm Laser	Blue laser	D405-C50	Irradiation of excitation light of 532 nm	Laser maximum power: 50 mW Wavelength: 405 nm	Showa optronics

The optical unit consists of a 405 nm Laser (D405-C50, Showa optronics) to excite SYTO41®, 532 nm Laser (J050GS, Showa optronics) to excite SYTOX ORANGE® and LDS751 lenses, optical filter to disperse fluorescence, and three photomultipliers to detect

dispersed fluorescence (H6780, H6780-02, and H6780-20 Hamamatsu photonics).

In popular flow cytometers, fluorescence is detected from the direction perpendicular to an optical axis of an excitation light to reduce influences of stray light [10]. However, the cartridge structure makes it difficult to detect fluorescence from the direction perpendicular to an optical axis of an excitation light. Thereby, an optical unit detects fluorescence from the coaxial direction of the excitation light. The reflected light of excitation light is prevented from entering photomultipliers with optical filters.

Fluorescent transmittance of optical unit from the flow cell to each photomultiplier are given by

$$T_{PMT1} = \frac{T_{DDM}}{100} \times \frac{(100 - T_{DM500})}{100} \times \frac{T_{LP420}}{100} \times \frac{T_{BP460}}{100} \quad 3\text{-}11\text{-}1$$

$$T_{PMT2} = \frac{T_{DDM}}{100} \times \frac{T_{DM500}}{100} \times \frac{T_{LP550}}{100} \times \frac{(100 - T_{DM670})}{100} \times \frac{T_{BP600}}{100} \quad 3\text{-}11\text{-}2$$

$$T_{PMT3} = \frac{T_{DDM}}{100} \times \frac{T_{DM500}}{100} \times \frac{T_{LP550}}{100} \times \frac{T_{DM670}}{100} \times \frac{T_{BP720}}{100} \quad 3\text{-}11\text{-}3$$

where T_{DMM} is a transmittance of a dual dichroic mirror, T_{DM500} is a transmittance of a dichroic mirror (500 nm), T_{LP420} is a transmittance of a long-pass filter (420 nm), T_{BP460} is a transmittance of a band-pass filter (460 nm), T_{LP550} is a transmittance of a long-pass filter (550 nm), T_{DM670} is a transmittance of a dichroic mirror (670 nm), T_{LP600} is a transmittance of a long-pass filter (600 nm), and T_{BP720} is a transmittance of a band-pass filter (720 nm).

Fig. 3-23 shows calculation results of fluorescent transmittance of optical unit. Each most of fluorescence of SYTO41®, SYTOX ORANGE® and LDS751 enter a target PMT and not enter other PMTs (Fig. 3-24).
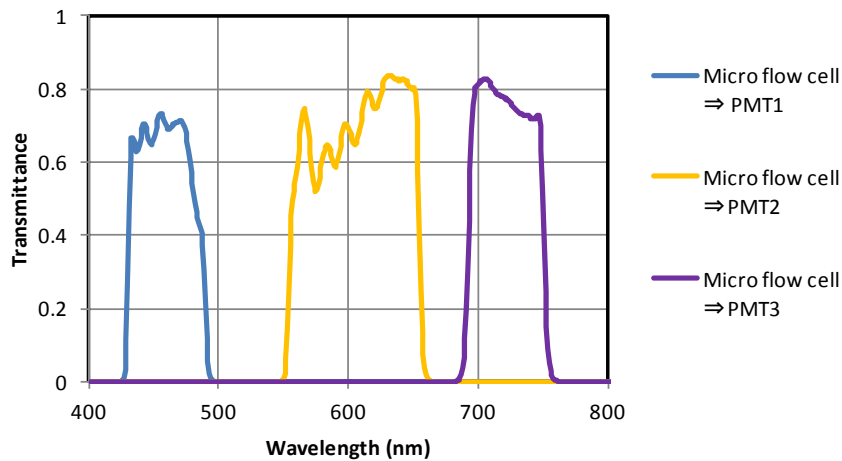
Fig. 3-23 Transmittance of optical unit for fluorescence
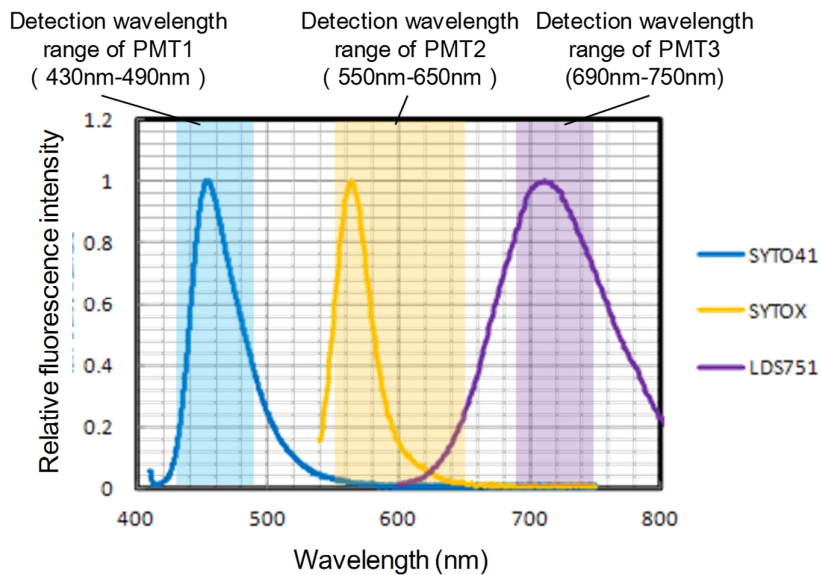
Fig. 3-24 fluorescence spectra of fluorescent dyes used in the system

Next, an intensity distribution of excitation light on the flow cell for measurements is considered. An intensity of fluorescence from a particle depends on the intensity of excitation light in flow cytometry. Thereby, the equalization of the intensity distribution of excitation light on the flow cell is needed for the equalization of the intensity of fluorescence from a particle of same type. Thereby, specifications of the intensity distribution of excitation light on the flow cell are decided as Table 3-9 in view of the

volume of the probe space (length 30 μm, depth 20 μm, width 40 μm) decided in 3.4.3.

Table3-9 Specification excitation light intensity eradiated on flow cell

	Width direction of flow cell	Flow direction of flow cell
Intensity of excitation light in detection area	> 80% maximum value	> 0

A large difference in the intensity of excitation light between the center and both sides of the flow cell causes large difference between the intensity of fluorescence from particles in the center of the flow cell and ones in both side of the flow cell. Thereby, an intensity of excitation light on the cross direction of the flow cell is stronger that 80 % of one on the center of the flow cell. On the other hand, an intensity of excitation light on the direction of the flow cell is more than 0 because irradiating out of the probe space increase the counting loss by increasing the volume of the probe space.

Fig. 3-25 which is the intensity distribution of excitation light (532 nm) on the flow cell measured with the camera-based beam profiler (OPHIR) shows that the designed optical unit meets the specific in Table 3-9.
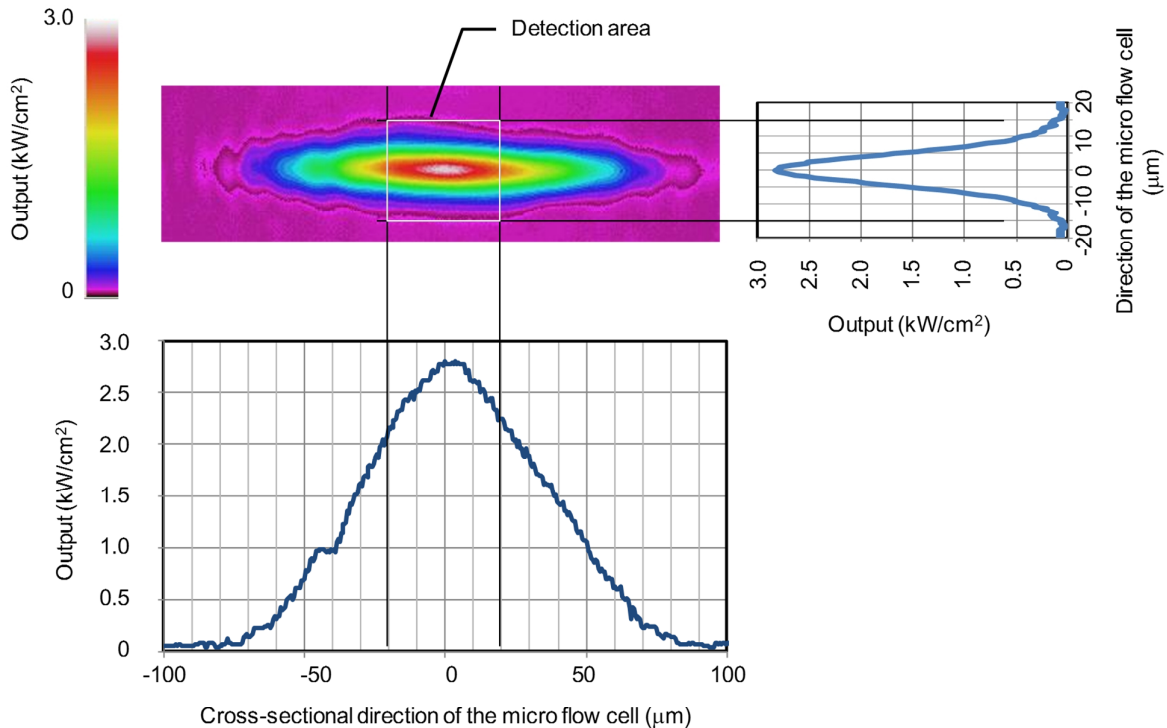
Fig. 3-25 Excitation light intensity eradiated on flow cell for measurements

3.7.2 Flow control unit

A flow control unit which consists of a pump and 10 valves adjusts pressure in reservoirs by controlling open and close of 10 valves for sending the sample solution and mixing the sample solution and fluorescent dye solutions. Fig. 3-26 shows a diagram of an air pressure circuit connecting a pump, valves and the cartridge in the system. Table 3-8 shows an operating procedure of the pump and valves in a measurement of live bacterial numbers.
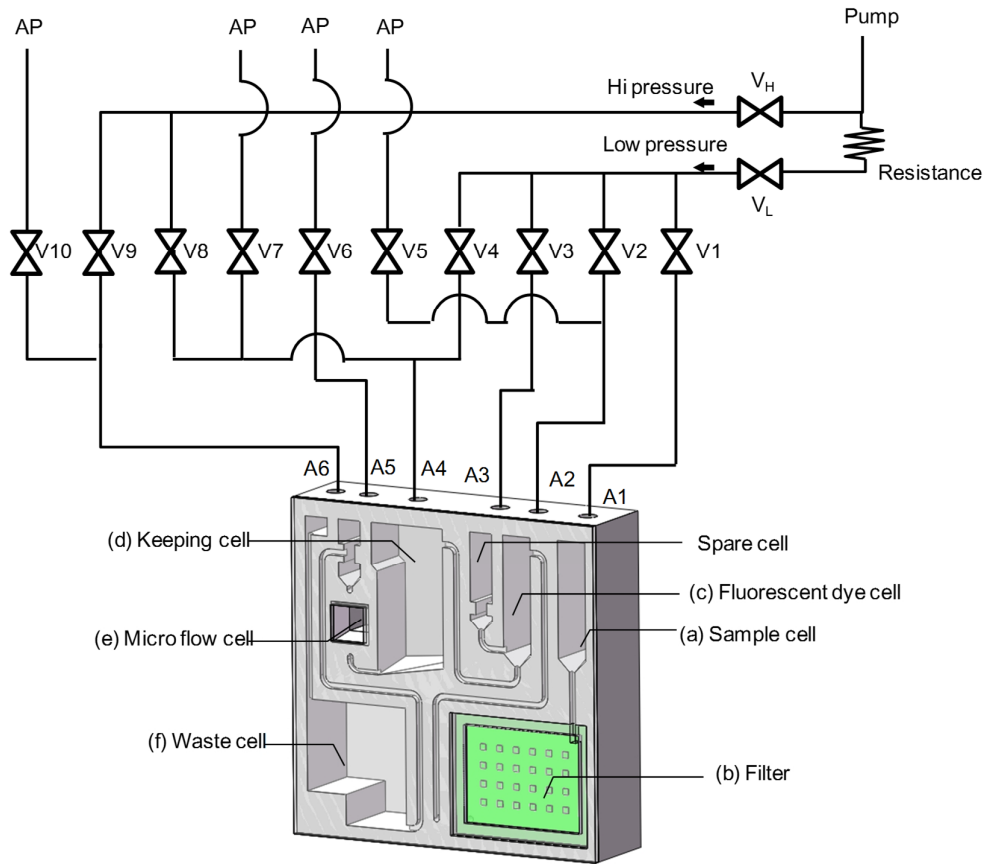
AP: Atmospheric pressure, A1~A6: Air hole1~Air hole6, V1~V10: Valve1~Valve10

Fig. 3-26 Diagram of an air pressure circuit of the system

Table3-10 Operating procedure of the pump and valves

Sample flow	Air flow	Process	Valve opening/closing											
			H	L	1	2	3	4	5	6	7	8	9	10
(a)→(b)→(c)	(a)→(b)→(c)	(1) Removing residues: filtering of a test sample by sending the test sample from the sample cell via the filterand to the fluorescent dye cell	C	O	O	C	C	C	O	C	C	C	C	C
(c)	(d)→(c)	(2) Staining viable and killed bacteria with fluorescent dyes: Mixing the sample, SYTO41$^®$, LDS751 and SYTOX ORANGE$^®$ with by sending air bubbles	C	O	C	O	C	C	O	C	C	O	C	C
(c)→(d)	(c)→(d)	Sending the mixture to the keeping cell	C	O	C	O	C	C	C	C	O	C	C	C
(d)→(e)	(d)→(e)	(3) Counting viable bacteria: counting viable bacteria by flow cytometry	O	C	C	C	C	C	C	C	C	O	C	O

O: Valve opening, C: Valve closing

The flow control unit needs to send the sample solution at high pressure through the fine flow cell in measuring process. However, this does at low pressure for handling the sample solution gently in other process. Thereby, the flow control unit has branched channel connecting to an output of the pump. One output of the branched channel, which is used to send the sample solution at low pressure, is connected to a fine and long channel serving as a flow resistance. This mechanism makes it possible to send the sample solution at high and low pressure with one pump.

3.7.3 Data processing unit

Details of a data processing unit are shown. When live or dead bacteria pass through the probe space in the flow cell, the optical unit outputs pulse signals such as those in Fig. 3-27.
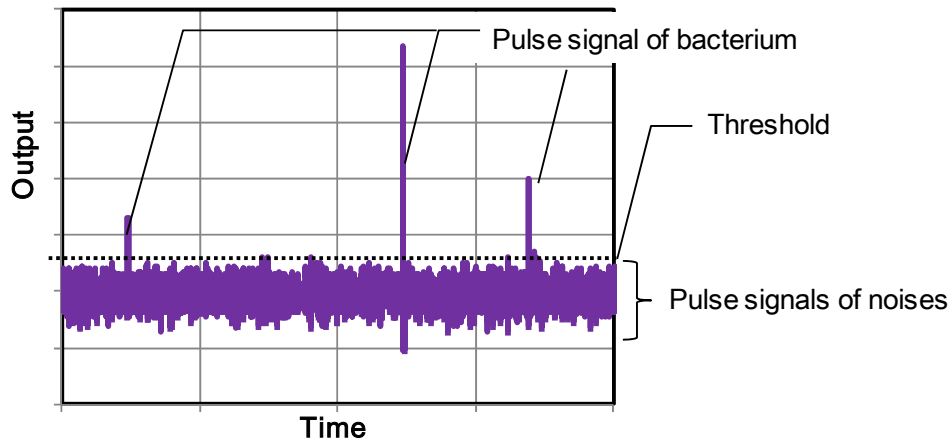
Fig. 3-27 Signals output by the optical unit in a measurement

The height of a pulse shows an intensity of fluorescence from a bacterium passing through the probe space and the width of a pulse shows the transit time of a bacterium passing through the probe space. The transit time of a bacterium passing through the probe space is very short. Thereby, the data processing unit needs to shorten sampling times. Additionally, all output signals of optical detectors bear a huge volume of data, which makes it difficult to be record. This is why the data processing unit reduces the volume of data by recording only data of signals meeting the condition of live bacteria and discarding data of signals not meeting the condition of live bacteria.

Next, details of a selection process with the data processing unit are shown. The selection process consists of a process to eliminate noise from all signals and a process to select signals meeting the condition of live bacteria.

(1) Noise reduction process

The data processing unit records the following three items about pulse signals output by three photomultipliers: duration time while a signal is above a threshold value (duration time of a pulse: t_p), difference between a vertex of a signal and a threshold (height of pulse), and time when a signal is at the vertex (appearance time), as shown in Fig. 3-28. The data processing unit records nothing about signals below a threshold value. Next, the data processing unit eliminates pulse signals whose duration is shorter than a certain value (threshold of duration) with a frequency-dependent filter.
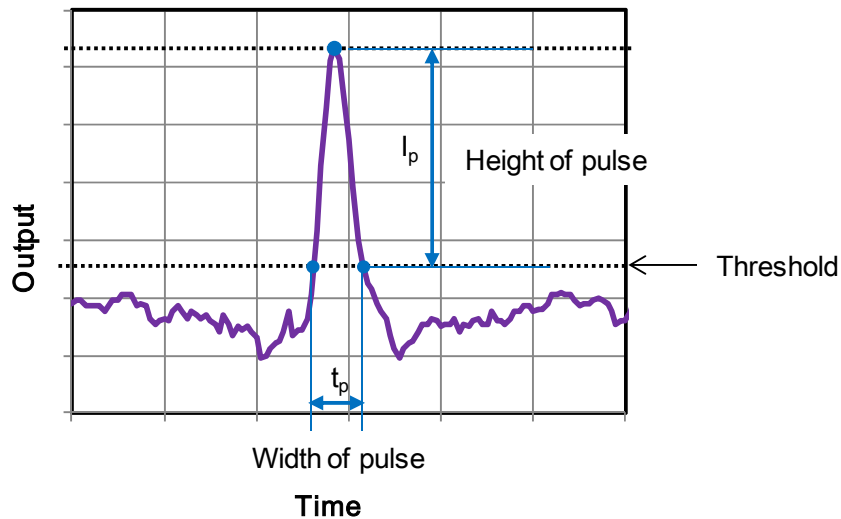
Fig. 3-28 Pulse signal outputted by the optical unit in a measurement

(2) Selection process of signals meeting the condition of live bacteria

The data processing unit regards pulse signals three photomultipliers output at same time as pulse signals from the same particle. Moreover, this unit outputs the number of the pulse signals meeting the condition of live bacteria shown in Chapter 3, section 5 as the number of live bacteria in the sample solution.

3.8 Experimental procedures

To evaluate the measurement performance of the system, we determine a correlation coefficient between live bacterial numbers in a sample solution measured by the system and live bacterial numbers in a same sample solution measured by the cultural method.

Fig. 3-29 shows evaluation process.

(1) Preparation of sample solution

    (a) Emulsion of E.Coli used as sample solution

        1. A dilution series of the emulsion of E Coli (10 fold, 100 fold, 1,000 fold, 10,000 fold) is prepared.

    (b) Homogenized food suspension used as sample solution

        1. 10 g of the target vegetable and 90 g the sterile dilute aqueous solution were put in a homogenizer bag.

        2. The mixture is homogenized by a food homogenizer (Interscience, BAGMIXER 400W).

3. A dilution series of the homogenized vegetable suspension (10 fold, 100 fold, 1,000fold, 10,000 fold) is prepared.

(2) Measurements of live bacterial numbers

(a) Measurements of live bacterial numbers using the system

1. One of a dilution series are injected to the sample solution reservoir in the cartridge. Additionally, three kind of fluorescent dye solution (1 μL 20 mM SYTO41®, 1 μL 2 mM SYTOX ORANGE®, and 1 μL 33 mM LDS751) are injected to the fluorescent dye reservoir in the cartridge before use.

2. The cartridge injected with the sample solution (volume: 1 ml) was set in the system. Next, the measurement process is started by the PC for controller. The system proceeds automatically the measurement process: removing residue, labeling live bacteria with fluorescent dyes and measuring live bacterial numbers using flow cytometry.

(b) Measurements of live bacterial numbers using the cultural method

1. 1 mL sample solution and agar medium just before solidification are poured on Petri dishes. Next, the sample solution and agar medium are mixed well and left until solidification. Petri dishes filled with solidified agar mediums are left in an incubator at constant temperature for 24 – 48 hours.

2. Colonies formed on an agar plate are counted. It is possible to count live bacteria in agar plate by counting number of colony because a colony is formed from a live bacterium.

(3) Comparing live bacterial numbers by both methods

Live bacterial numbers measured by the system and ones by the cultural method are compared in every dilution series.
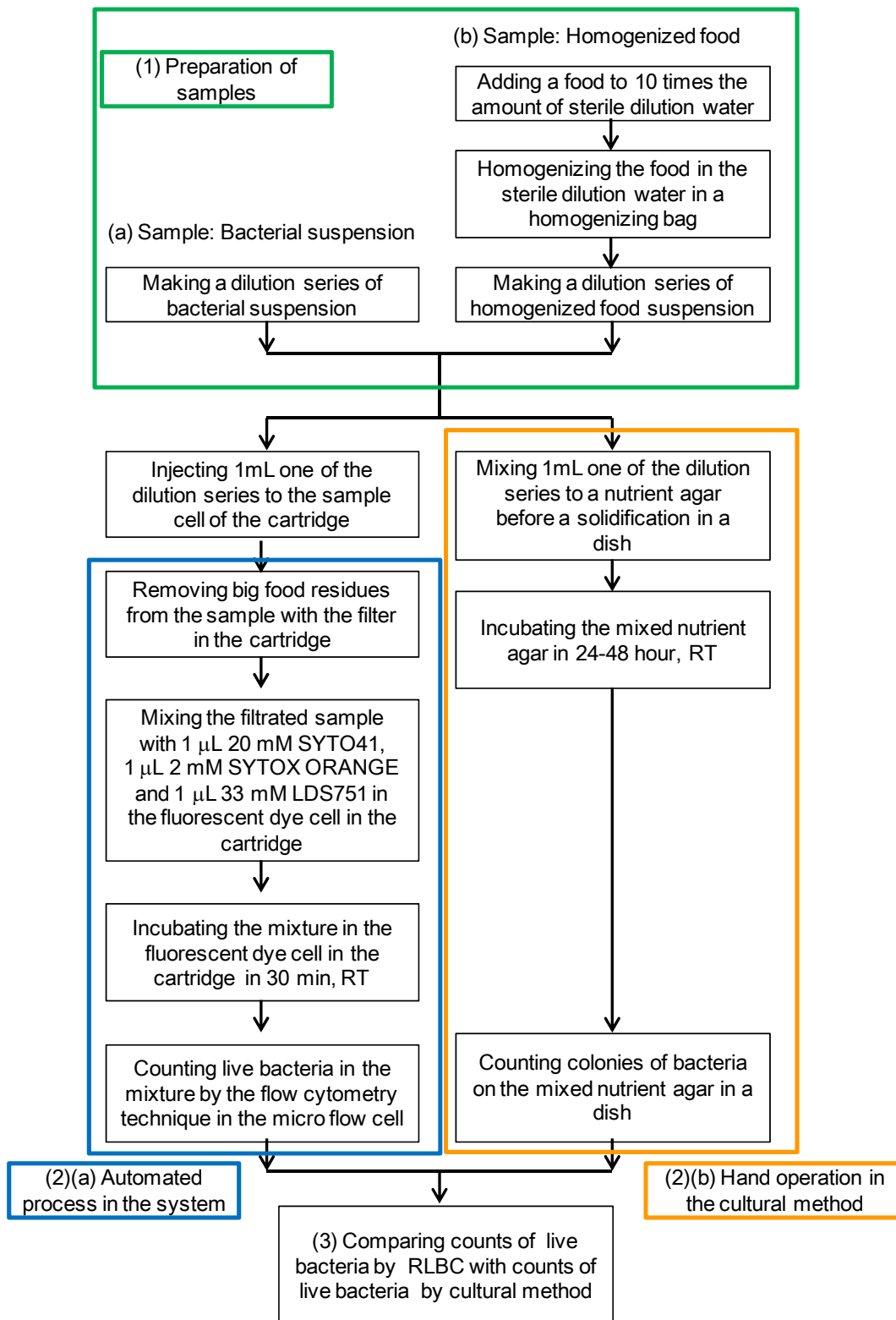
Fig. 3-29 Evaluation process of the system

3.9 Experimental results

3.9.1 Selection signals of particles from noises

Fig. 3-30 shows output signals of the photomultiplier for LDS 751 (PMT3 in Fig. 3-22) in a measurement of an E. coli solution. The PMT3 outputs pulse signals in detecting particles emitting near-infrared fluorescence, while it outputs signals of background noise.
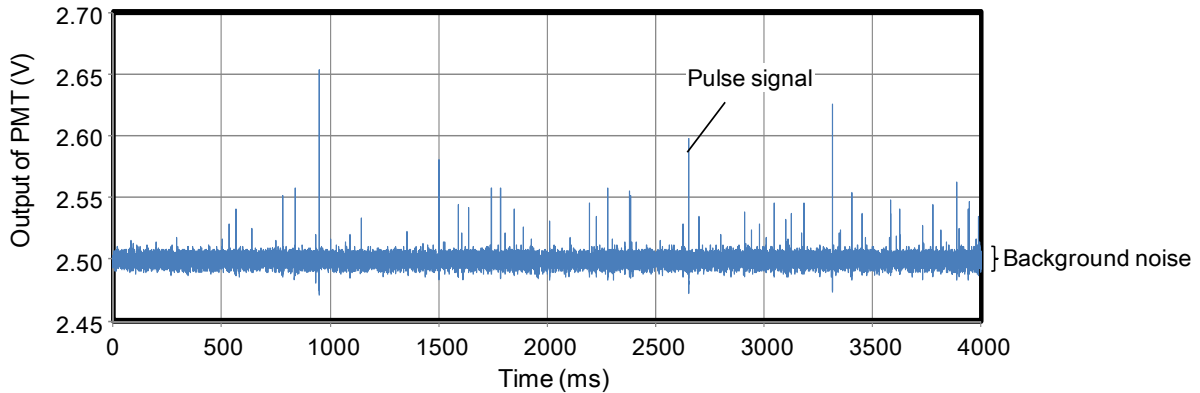
Fig. 3-30 Signals of PMT3 in a measurement of E.Coli solution

The threshold value to eliminate background noise is decided in the following manner. The average of background noise (I_b) is 2.499 V (=2,499 mV) and the standard deviation of background noise (σ_N) is 0.0037 V (=3.7 mV). It is shown in Chapter 2, section 4 that background noise bigger than $2.81\sigma_N$ is 0.5% of the total. Thereby, the threshold value of PMT3 is decided as 11 mV ($2.81\sigma_N$=10.4 mV ≈ 11 mV). Moreover, threshold values of the photomultiplier for SYTO41® (PMT1) and the photomultiplier for SYTOX ORANGE® (PMT2) are decided as 60 mV and 13 mV in the same way.

Fig. 3-31, Fig. 3-32, and Fig. 3-33 show histograms of output values of pulse signals of PMT1, PMT2, and PMT3 in a measurement of E. coli solution. Each histogram shows that the number of pulse signals which are 1.5 to 3 times bigger than the threshold values are biggest.

Validities of threshold values are evaluated in the following section by examining the correlation coefficient between the live bacterial numbers measured by the system and ones by the culture method. If threshold values are too high, live bacterial numbers measured by the system are smaller than ones by the culture method. By contrast, if threshold values are too low, live bacterial numbers measured by the system are bigger than one by the culture method.

Threshold of PMT1: 60 mV

Peak of histogram: 110 mV
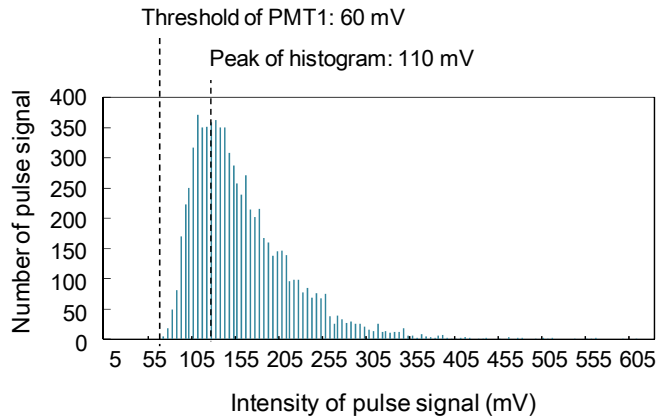
Fig. 3-31 Histogram of pulse signals of PMT1 in a measurement of E.Coli solution

Threshold of PMT1: 13 mV

Peak of histogram: 19 mV
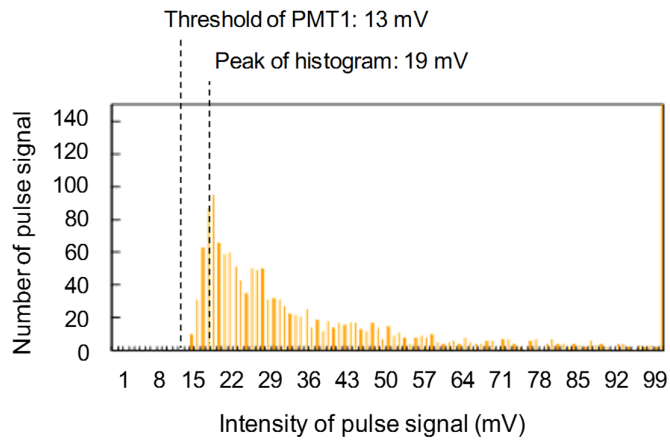
Fig. 3-32 Histogram of pulse signals of PMT2 in a measurement of E.Coli solution

Threshold of PMT1: 11 mV

Peak of histogram: 29 mV
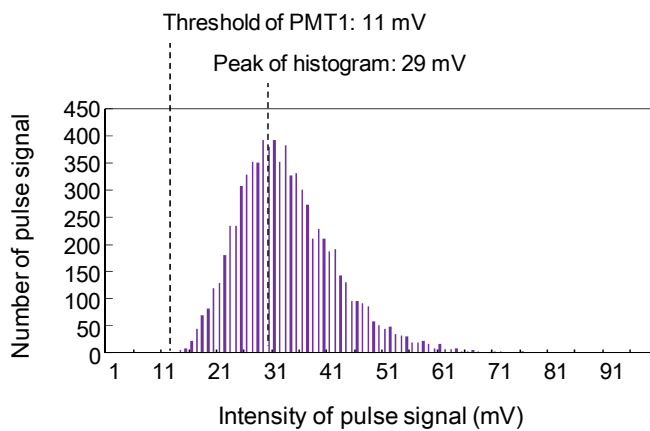
Fig. 3-33 Histogram of pulse signals of PMT3 in a measurement of E.Coli solution

3.9.2 Performance of optical unit to distinguish live bacteria

One of the features of this system is distinguishing live bacteria from other particles by measuring three types of fluorescence: two types of fluorescence of fluorescent dyes for live/dead bacteria (SYTO41®, LDS751) and one type of fluorescence of fluorescent dyes for dead bacteria (SYTOX ORANGE®). To evaluate this feature, we compared live bacterial numbers measured in the following three cases: the first case distinguishes live bacteria with signals of PMT1, PMT2 and PMT3, the second case distinguishes live bacteria with signals of PMT1 and PMT2, and the third case distinguishes live bacteria with signals of PMT3 and PMT2.

Fig. 3-34 shows live bacterial numbers measured by the system and by the culture method. The X-axis is live bacterial numbers measured by the culture method and the Y-axis is live bacterial numbers measured by the system. Comparing with the results in the first case, live bacterial numbers in the second or third case at low number concentration measured by the system have a poorer correlation with those measured by the culture method. Additionally, comparing results in the second case (using PMT1 and PMT2) with those in the third case (using PMT3 and PMT2), measurement results in the second case have a higher accuracy.
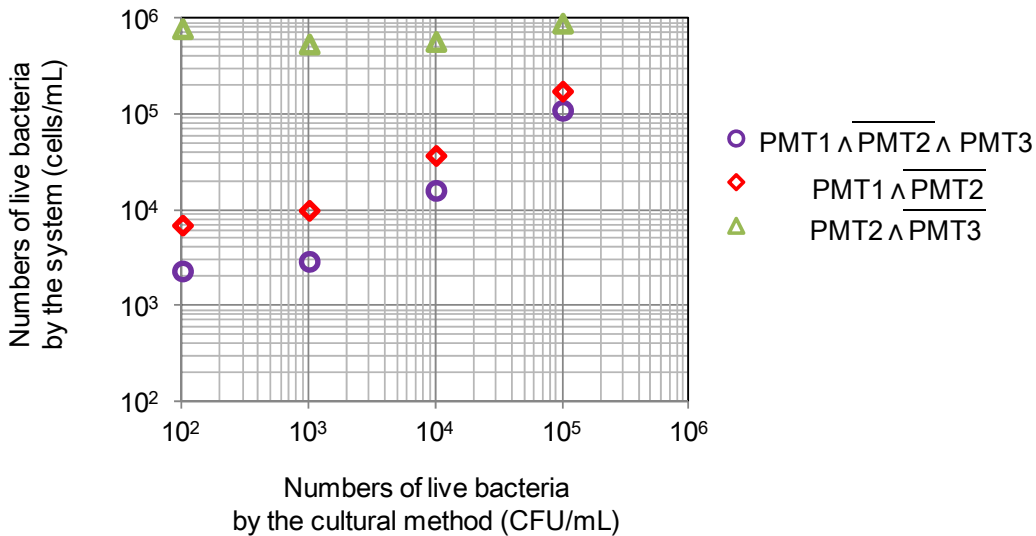
Fig. 3-34 Numbers of live bacteria in E. coli solution measured by the system and by the culture method

Next, a performance of the optical unit to eliminate signals of fluorescent dye particles is evaluated. Fig. 3-35 shows measurement results of live bacterial numbers in an E. coli

solution by the system. Plots in (PMT1 ∧ $\overline{\text{PMT2}}$ ∧ PMT3) show derived measurement results of live bacteria from signals of PMT1, PMT2, and PMT3.
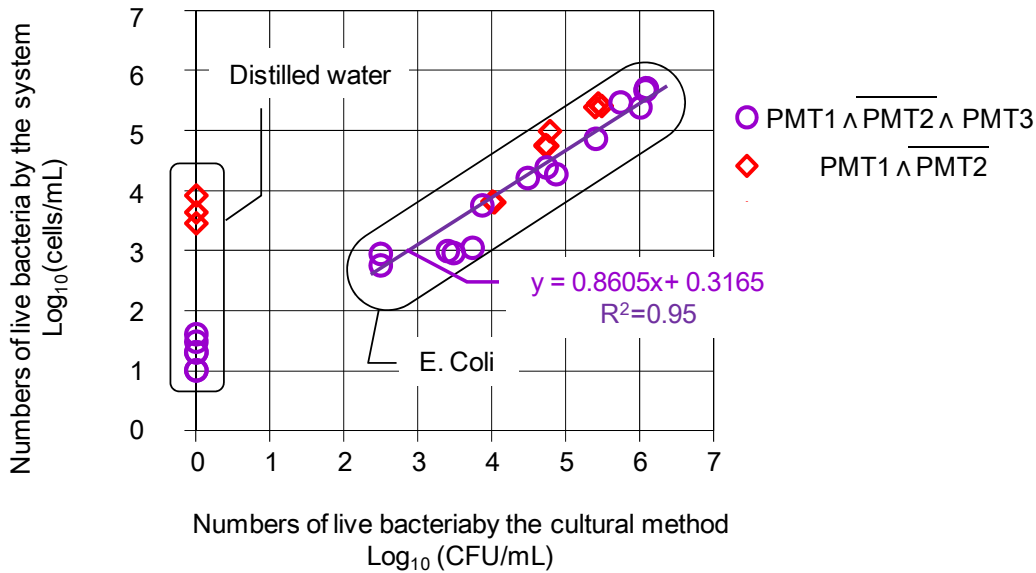
Fig. 3-35 Performance to eliminate signals of fluorescent dye particles

Plots in (PMT1 ∧ $\overline{\text{PMT2}}$) show derived measurement results of live bacteria from signals of PMT1 and PMT2. Additionally, live bacterial numbers in distilled water are measured by the system to evaluate the number of fluorescent dye particles counted as live bacteria. This number, which is an erroneous measurement number, has a great effect on the lower measurement limit of the system. The number of live bacteria in the distilled water measured by the culture method is 0 (particles/mL). However, this number is regarded as 10^0 (particles/mL) because the graph in Fig. 3-35 is a log-log graph.

Fig. 3-35 shows that the system measures live bacterial numbers in distilled water as 10^3 - 10^4 cell/mL deriving from signals of PMT1 and PMT2 while 10^1 -10^2 cells/mL deriving from signals of PMT1 and PMT2, while 10^1 - 10^2 cells/mL deriving from signals of PMT1, PMT2, and PMT3. It is possible to reduce the erroneous measurement number of live bacteria by using three types fluorescent dyes (two types are fluorescent dyes for live/dead bacteria and one type is a fluorescent dye for dead bacteria).

Moreover, the correlation coefficient between the live bacterial numbers measured by the system using the three types of fluorescent dyes and that by the culture method (R^2), which is 0.95, is confirmed to be very high. The high correlation coefficient shows that the threshold values determined in the previous section are considered reasonable and proper.

3.9.3 Measurements of general bacteria

To evaluate the measurement performance of the system for general bacteria other than E. coli, live bacterial numbers by the system and ones by the culture method are compared by measuring 24 kinds of typical bacteria as general bacteria.

Fig. 3-36 shows the measurement results. The measured 24 kinds of bacteria are classified as gram-negative bacillus, gram-positive coccus, and gram-positive bacillus.
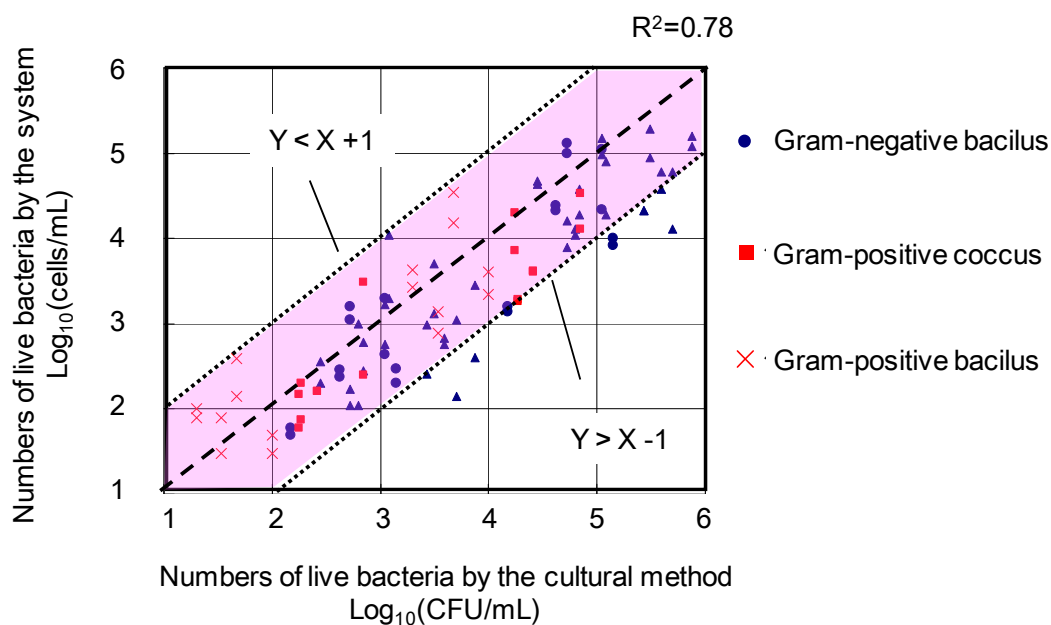
Fig. 3-36 Numbers of live bacteria in measuring 24 kinds of bacteria

Fig. 3-36 shows that the correlation coefficient between the live bacterial numbers measured by the system and those measured by the culture method (R^2), which is 0.78, is sufficiently high.

3.9.4   Measurements of live bacteria in vegetable suspensions

To evaluate the measurement performance of the system for live bacteria in vegetable suspensions, live bacterial numbers measured by the system and those measured by the culture method are compared by measuring live bacterial numbers in vegetable suspensions: spinach, carrots, red cabbage and potatoes. Measurement results are shown in Fig. 3-37.
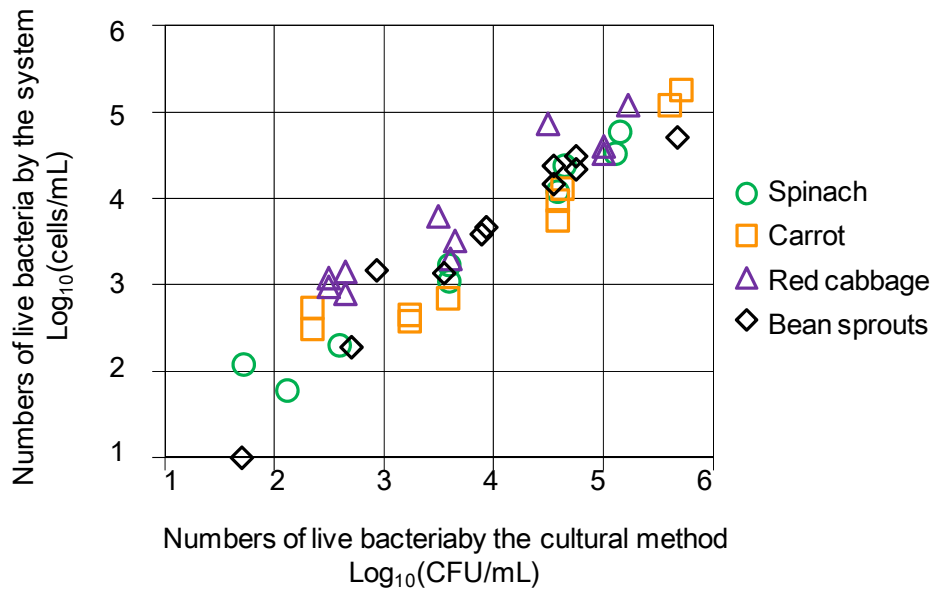
Fig. 3-37 Numbers of live bacteria in vegetable suspensions

Fig. 3-37 shows that the correlation coefficient between the live bacterial numbers measured by the system and ones by the culture method (i.e., R^2) is 0.96 for spinach, 0.91 for carrot, 0.90 for red cabbage, and 0.93 for potato in the range of a live-bacteria concentration of 10^2 to 10^6 cell/ml. We concluded the following: First, both methods had a high correlation of live bacterial numbers in vegetables that contain many fluorescent pigments. Second, the counting performance of the system and one of the culture method are equal.

3.10 Discussion

3.10.1 Measurement accuracy of the system for live bacterial numbers

We used the methodology to develop the system to measure live bacteria number in food suspensions. Measurement results shows that the system has the high correlation in measurements of live bacteria in vegetable suspensions with the cultural method. Thereby, we confirmed that the methodology can be applied to the development of the flow cytometer for live bacteria in vegetable suspensions.

3.10.2　Measurement accuracy of the system for live bacterial numbers

It is shown in Fig. 3-35 that the correlation coefficient between the live bacterial numbers measured by the system (X) and ones by the culture method (Y), which is 0.95 in E. coli solution, is very high. Additionally, a linear approximation of X and Y gives

$$Y = 0.8605X + 0.3165 \qquad 3\text{-}12$$

Next, we consider the counting loss of the systems from the results in Fig. 3-35. Fig. 3-35 shows that the counting loss in the range of number concentration of bacteria of 10^3 - 10^6 cell/mL is very small because the plots (X, Y) are not below the linear approximation (Equation 3-12) in Fig. 3-35. Therefore, the experimental results in Fig. 3-34 agree with the results of the study about design of the flow cell in Chapter 3, Section 4.

On the other hand, the slope of the linear approximation (Equation 3-12) is 0.8605, smaller than 1, which shows that the system can't measure all live bacteria in a sample solution. We presumed the reason to be that some live bacteria which emit weak fluorescence aren't measured as live bacteria. To measure these bacteria as live bacteria, the following three methods are considered to be effective: (1) improvement of the labeling condition of live bacteria, (2) improvement of the numerical aperture of the optical unit, and (3) intensification of the excitation light.

(1) Improvement of the labeling condition of live bacteria

Labeling bacteria with more fluorescent dyes has the potential to increase the intensity of fluorescence from bacteria. To label bacteria with more fluorescent dyes, we have to optimize the labeling condition such as types of fluorescent dyes, concentration of fluorescent dyes, and labeling time. The best labeling condition in this system is selected during development. However, labeling the condition needs to be further considered in the future.

(2) Improvement of the numerical aperture of the optical unit

It is possible to detect weak fluorescence by improving the numerical aperture of the optical unit. Improvement of the optical unit, which has effects on the structure of the cartridge, is a hard task. However, this is important in continual improvements of the system.

(3) Intensification of the excitation light

It is possible to intensify fluorescence bacteria emit using a stronger excitation light. However, introduction of a stronger excitation light needs close consideration because a larger housing is needed and the costs are higher.

3.10.3 Possibility to use for food sanitation

A possibility to use the system for examination of live bacteria in food is discussed from the evaluation results of the system. In this thesis, examinations of live bacteria in vegetable suspensions are performed by using the system. However, examinations of live bacteria in meats, seafood, or foods other than vegetables using the system have to be performed.

These examinations are evaluated in succeeding works, which show that the system has the performance to accurately measure live bacteria in meats, seafood, etc. [30]. Moreover, this system was commercialized by Hitachi Power Solutions Co., Ltd. from 2011 to 2017 [31].

3.11 Conclusion

In this chapter, a "rapid live bacteria counter" was developed to allow users to measure live bacterial numbers in a homogenized food suspension simply, rapidly, and accurately. With this system, discrimination of live bacteria by fluorescence staining and counting live bacteria by the flow cytometry are performed automatically in a disposable cartridge, in which numbers of live bacteria in sample solutions are measured. Consequently, the following conclusions based on our work are drawn.

(1)   The dimensions of a flow cell for the fluorescent flow cytometer and a volume of a sample solution were designed by a decision methodology based on statistical theory. The dimensions of the flow cell for measurements (height: 20 μm, width: 40 μm) are fixed on the basis of the conditions that the counting loss be less than 0.05 and the pressure loss be less than 1.0×10^5 Pa. Additionally, the volume of a sample solution was fixed as 100 μL on the basis of conditions on the minimum number of bacteria in the sample solution.

(2)   For an evaluation of the measurement performance of the system, live bacteria in an emulsion of Escherichia coli (E. coli) were counted by the system and a culture method. The measurement performance of the system and the culture method were judged to be equal in terms of measurement performance because the two methods had a high correlation, namely, a correlation coefficient of 0.97 in the range of a live bacteria concentration of 10^3 to 10^6 cell/ml. This result shows that the decision methodology based on statistical theory is effective for the design of this system.

(3)   To discriminate live bacteria in a homogenized food suspension which cannot be discriminated by common flow cytometry, the new discrimination method using three

89

kinds of fluorescent dyes (two kinds of fluorescent dyes for live/dead bacteria and one kind of fluorescent dye for dead bacteria) is developed. Live bacteria can be discriminated from other particles by difference in fluorescence wavelength.

(4)   To evaluate the measurement performance of the system, live bacterial numbers in homogenized vegetable suspensions were measured by the system and the culture method. The measurement performance of the system and the culture method are equal because both methods have a high correlation; namely, the correlation coefficient is 0.96 for spinach, 0.91 for carrot, 0.90 for red cabbage, and 0.93 for potato in the range of a live bacteria concentration of 10^2 to 10^6 cell/ml. These results show the new discrimination method using three kinds of fluorescent dyes is effective for sensitivity improvement of the system.

(5)   Using this methodology to develop a measurement method for target particles, flow cytometry, which is one of the flow methods, is selected to measure the number of live bacteria in a homogenized food suspension in consideration of the features of live bacteria. Measurement results using this system show that the methodology is effective in the development of a system which measures the number of live bacteria in a homogenized food suspension.

Reference

[1] Ministry of Health, Labour and Welfare, ed. *Standard methods of analysis in food safety regulation*, (2004), pp. 567-589 (in Japanese), ISBN: 978-4-889-25002-2.

[2] Mise, K., and Inoue, F. ed. *Practical guide of Bacteriological testing of food*, (1996), pp. 52-53, Kodansha scientific (in Japanese), ISBN: 978-4-06-153712-5.

[3] Trudil. D., Loomis, L., Pabon, R., Hasan, J. A. K., and Trudil, C. L. "Rapid ATP Method for the Screening and Identification of Bacteria in Food and Water Samples," *BIOCATALYSIS-2000: FUNDAMENTALS & APPLICATIONS.*, Supplement, Vol. 41(6), (2000), pp. 27-29.

[4] Foster, A. "Evaluation of Impedance Method for Monitoring Microbiological Quality of Cleaning Systems," *J. Am. Soc. Brew. Chem.*, Vol. 54 (2), (1996), pp. 76-77.

[5] Shimakita, T., Tashiro, Y., Katsuya, A., Saito, M., and Matsuoka, H. "Rapid Separation and Counting of Viable Microbial Cells in Food by Nonculture Method with Bioplorer, a Focusing-Free Microscopic Apparatus with a Novel Cell Separation Unit," *J. Food Prot.*, Vol. 69 (1), (2006), pp. 170-176.

[6] Patchetta, R. A., Back, J. P., Pinder, A. C., and Kroll, R. G. "Enumeration of Bacteria in Pure Cultures and in Foods Using a Commercial Flow Cytometer," *Food Microbiology*, Vol. 8, (1991), pp. 119-125.

[7] Laplace-Builhé, C., Hahne, K., Hunger, W., Tirilly, Y., and Drocourt, J. L. "Application of Flow Cytometry to Rapid Microbial Analysis in Food and Drinks Industries," *Biol. Cell*, Vol. 78, (1993), pp. 123-128.

[8] Gunasekera, T. S., Attfield, P. V., and Veal, D. A. "A Flow Cytometry Method for Rapid Detection and Enumeration of Total Bacteria in Milk," *Appl. Environ. Microbiol.,* Vol. 66(2), (2000), pp. 1228-1232.

[9] Stryer, L. *Biochemistry (4th edition)*, (1998), W. H. Freeman, ISBN: 978-0-716-72009-6.

[10] Shapiro, H. M. "Practical Flow Cytometry," (2003), pp. 1-6, John Wiley & Sons, Inc., ISBN: 978-0-471-62228-4.

[11] Dojindo Homepage, Method and specifications of fluorescent dyes for bacteria (In Japanese), http://www.dojindo.co.jp/download/bacdye/bacdye1.pdf?_ga=1.73481114.90127447.1488116869 [Accessed 1 April 2017].

[12] Thermofisher Scientific Homepage, Method to labeling cells with fluorescent dyes, https://www.thermofisher.com/jp/ja/home/life-science/cell-analysis/cell-analysis-learning-center/molecular-probes-school-of-fluorescence/labeling-your-

samples/different-ways-to-add-fluorescent-labels.html [Accessed 1 April 2017].

[13] Japan Analytical Instruments Manufactures' Association Homepage,
http://www.jaima.or.jp/jp/pdf/05.pdf [Accessed 1 April 2017].

[14] Manz, A. Graber, N., and Widmer, M. "Miniaturized total chemical analysis systems: a novel concept for chemical sensing," *Sensors and Actuator B: Chemical*, Vol. 1, (1990), pp. 244-248.

[15] Society for Chemistry and Micro-Nano Systems. ed. *Techniques and Applications of Micro Chemical Chip*, (2004), Maruzen (in Japanese),
ISBN: 978-4-621-07471-8.

[16] Kitamori, T. *Micro Chemical Chip*, (2006), Maruzen (in Japanese),
ISBN: 978-4-621-07761-0.

[17] Kitamori, T "Micro and Nano Chemical System on Chip," *Transducers & Eurosensors '07*, (2007), pp. 11-16.

[18] Chen, D., Mauk, M., Qui, X., Liu, C., Kim, J., Ramprasad, S., Ongagna, S., Abrams, W. R., Malamud, D., Corstjen, P. L., and Bau, H. H. "Finger-actuated, self-contained immunoassay cassettes," *Biomed. Microdevices*, Vol. 12(4), (2010), pp. 705-719.

[19] Cambridge Consultants Homepage, Disposable microfluidic cartridge,
https://www.cambridgeconsultants.com/projects/disposable-microfluidic-cartridge-diagnostics [Accessed 1 April 2017].

[20] Holm, C., and Jespersen, L. "A Flow-Cytometric Gram-Staining Technique for Milk-Associated Bacteria," *Appl. Environ. Microbiol.*, Vol. 69(5), (2000), pp. 2857-2863.

[21] Alberts, B. *Molecular Biology of the Cell 4th*, (2001), Garland Pub.,
ISBN: 978-0-815-33218-3.

[22] OECD Homepage,
https://www.oecd.org/science/biotrack/34525610.pdf [Accessed 1 April 2017]

[23] Chunxian, C., ed. *Pigments in Fruits and Vegetables*, (2015), Springer,
ISBN: 978-1-4939-2356-4.

[24] Thermofisher Scientific Homepage, Selection guide of fluorescent dyes,
https://www.thermofisher.com/jp/ja/home/life-science/cell-analysis/fluorophores.html [Accessed 1 April 2017].

[25] Water Quality Association Homepage, Bacteria & Virus Issues
https://www.wqa.org/Learn-About-Water/Common-Contaminants/Bacteria-Viruses [Accessed 1 April 2017].

[26] Bio surface technologies corporation Homepage, Capillary Flow Cells,
http://biofilms.biz/products/microscopy-flow-cells/capillary-flow-cells/

[Accessed 1 April 2017].

[27] Micronit Homepage, Flow cells http://www.micronit.com/products/flow-cells/ [Accessed 1 April 2017].

[28] Hongbin, Y., Guangya, Z., Siong, C. F., Shouhua,W., and Feiwen, L. "Novel polydimethylsiloxane (PDMS) based microchannel fabrication method for lab-on-a-chip application," *Sensor and Actuators B: Chemical*, Vol. 137(2), (2009), pp. 754-761.

[29]Chemistry Libretext[TM] Homepage, Fluorescence, https://chem.libretexts.org/Core/Physical_and_Theoretical_Chemistry/Spectroscopy/Electronic_Spectroscopy/Radiative_Decay/Fluorescence [Accessed 1 April 2017].

[30] Sasaki, Y., Watanabe, Y., and Takei, K. "Features and practical use of cassette type rapid live bacteria counter "Cassette labo One" ," *Japan food science*, Vol. 53(4), (2014), pp. 36-44 (In Japanese).

[31] Hitachi engineering and service News Release, Cassette labo One: Rapid live bacteria counter for food safety (In Japanese), http://www.hitachi-power-solutions.com/news/data/news20110905.pdf [Accessed 1 April 2017].

Chapter 4. Excitation-fluorescence spectral flow cytometer

4.1 Background and purpose

There are many different kinds of particles in liquids such as those in water in nature, drinks, and body fluids [1]-[7]. Such particles may strongly or weakly affect human life. For example, the number of fungi or bacteria in drinks is a hygiene indicator [6], [7]. Therefore, it is important to carry out tests to determine the number or types of particles in liquids for a healthy and hygienic life. Table 4-1 shows kinds of particles in liquid and these influences on human life.

Table 4-1 Particles in liquid and these influences on human life

Particles in liquid	Kinds of liquid	Influences by particles
Bacteria and fungi	Beverage, Medicine, etc.	Quality loss, Food poisoning, etc.
Plankton, bacteria	Sea, Lake, River, etc.	Water pollution, etc.
Cells	Body fluid (Blood, sweat, Urine, etc.)	Test objects of health diagnosis, etc.

Additionally, many different kinds of methods are available for measuring particles in liquids. Among them, fluorescence methods are well-known methods used to measure the number of particles in liquid and investigate the type or condition of particles by measuring the fluorescence produced from particles. The typical fluorescence methods of particle measurement are fluorescence microscopy [8], [9], fluorescence spectroscopy [10], [11], and fluorescence flow cytometry [12]-[14]. Fig. 4-1 shows concepts of these measurement methods and Table 4-2 shows features of these measurement methods.
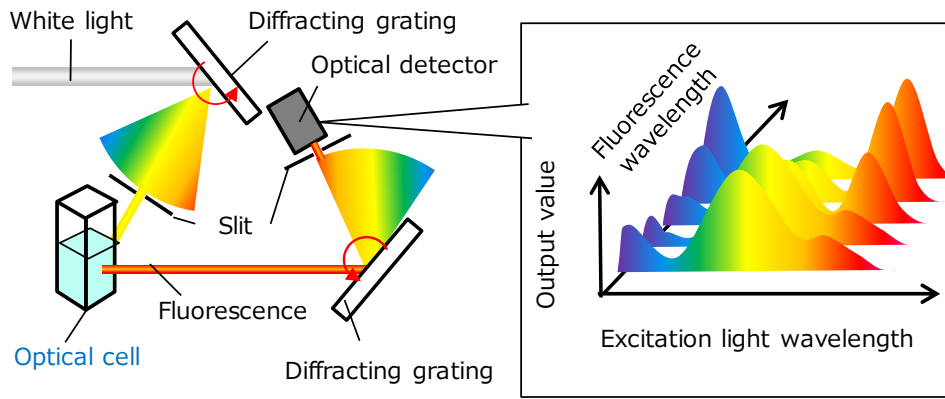
(a)　　　　Fluorescence spectrometer
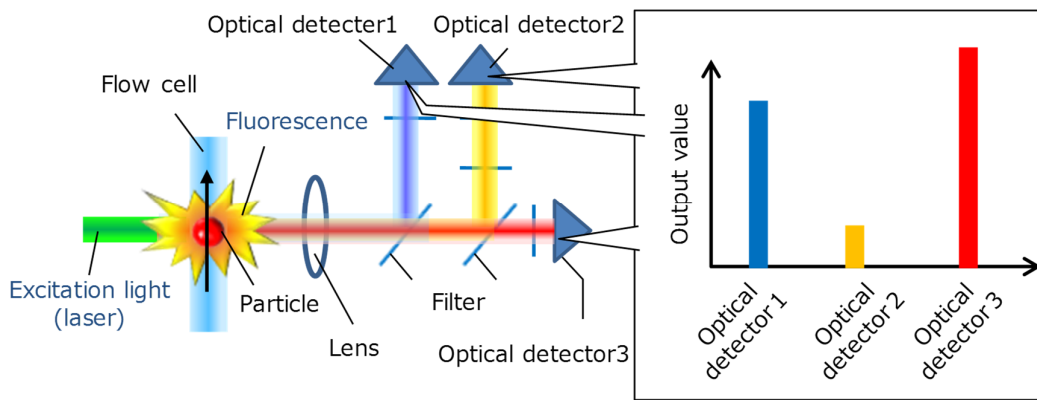
(b)　　　　Fluorescence flow cytometer
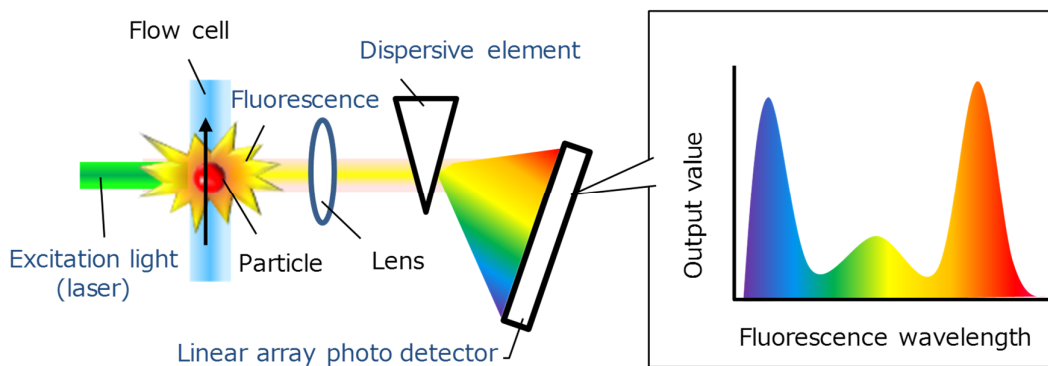
(c)　　　　Fluorescence spectral flow cytometer

Fig. 4-1 Concepts of fluorescence methods to measure particles in liquid

Table 4-2 Features of fluorescence methods to measure particles in liquid

Figure		(a)	(b)	(c)
Particle analysis method using fluorescence		Fluorescence spectrophotometer	Flow cytometer	Fluorescent spectral flow cytometer
Measurement items	Single particle analysis	-	✓	✓
	Excitation spectrum	✓	-	-
	Fluorescent spectrum	✓	-	✓

Fluorescence spectroscopy and fluorescence flow cytometry are used to rapidly analyze a large number of particles. In fluorescence spectroscopy, a fluorescence spectroscope is used to analyze the fluorescence spectra of targeted particles by irradiating the targeted particles in a liquid solution dispensed in an optical glass cuvette with excitation lights in a specific wavelength region followed by the measurement of the spectra of fluorescence emitted from the particle [10]. Using this method, one can easily obtain a large amount of information on the targeted particles and measure not only the fluorescence spectra but also the excitation spectra of targeted particles by using excitation lights of different wavelengths. However, it is difficult to analyze a single targeted particle on the basis of the fluorescence spectra of all particles in an optical glass cuvette.

In contrast, in fluorescence flow cytometry which is selected as a method to measure number of live bacteria in Chapter 3, a flow cytometer is used to analyze each particle on the basis of the fluorescence spectrum of a targeted particle by irradiating the particle in a stream of liquid solution with excitation lights in a specific wavelength region followed by the measurement of the fluorescence of the particle [12]. This method enables the rapid analysis of a large number of particles individually. However, the amount of information obtained from a single particle by fluorescence flow cytometry is smaller than that obtained by fluorescence spectroscopy because this method measures fluorescence intensities in several wavelength regions instead of the spectrum of fluorescence. Additionally, it is laborious; for example, the appropriate wavelengths of lasers of excitation light and optical filters depend on the objects of samples to be measured.

Fluorescence spectral flow cytometry, which has the combined features of fluorescence spectroscopy and fluorescence flow cytometry, has been reported recently [15], [16]. In this method, the fluorescence spectrum of a particle is measured by determining

the dispersed fluorescence of the particle with a spectroscopic photodetector array. This method can obtain a larger amount of information on the particle than conventional fluorescence flow cytometry. However, it is difficult to measure the excitation spectrum of a targeted particle compared with fluorescence spectroscopy, because it is hard to change the wavelengths of excitation lights serially in an extremely short time as the particle passes the area irradiated by excitation lights.

The methodology in chapter 2, section 6 shows that the flow method is most suitable to a measurement method for dispersed particles in liquid which can be measured one by one (Fig. 4-2). Additionally, the methodology shows that it is important to compare more features in target particles and other particles for an improvement of a measurement accuracy. Thereby, in this chapter, we worked on a feasibility study of an excitation-fluorescence spectral flow cytometer (EFSFCM) by applying the fluorescent flow cytometry developed in chapter 2 to increase amount of information of target particles.

The EFSFCM is a system that measures the excitation-fluorescence spectrum of a single targeted particle by irradiating the particle in a stream of liquid solution with dispersed white light used as excitation light and by measuring the dispersed fluorescence of the particle with a spectroscopic photodetector array. Using the EFSFCM, the excitation-fluorescence spectra (excitation wavelength range, $400 - 650$ nm; fluorescence wavelength range, $400 - 700$ nm) of a fluorescent particle were measured. Additionally, a homogenized tomato suspension and a homogenized spinach suspension were measured using the EFSFCM. Measurement results showed that it is possible to determine the components of vegetables.
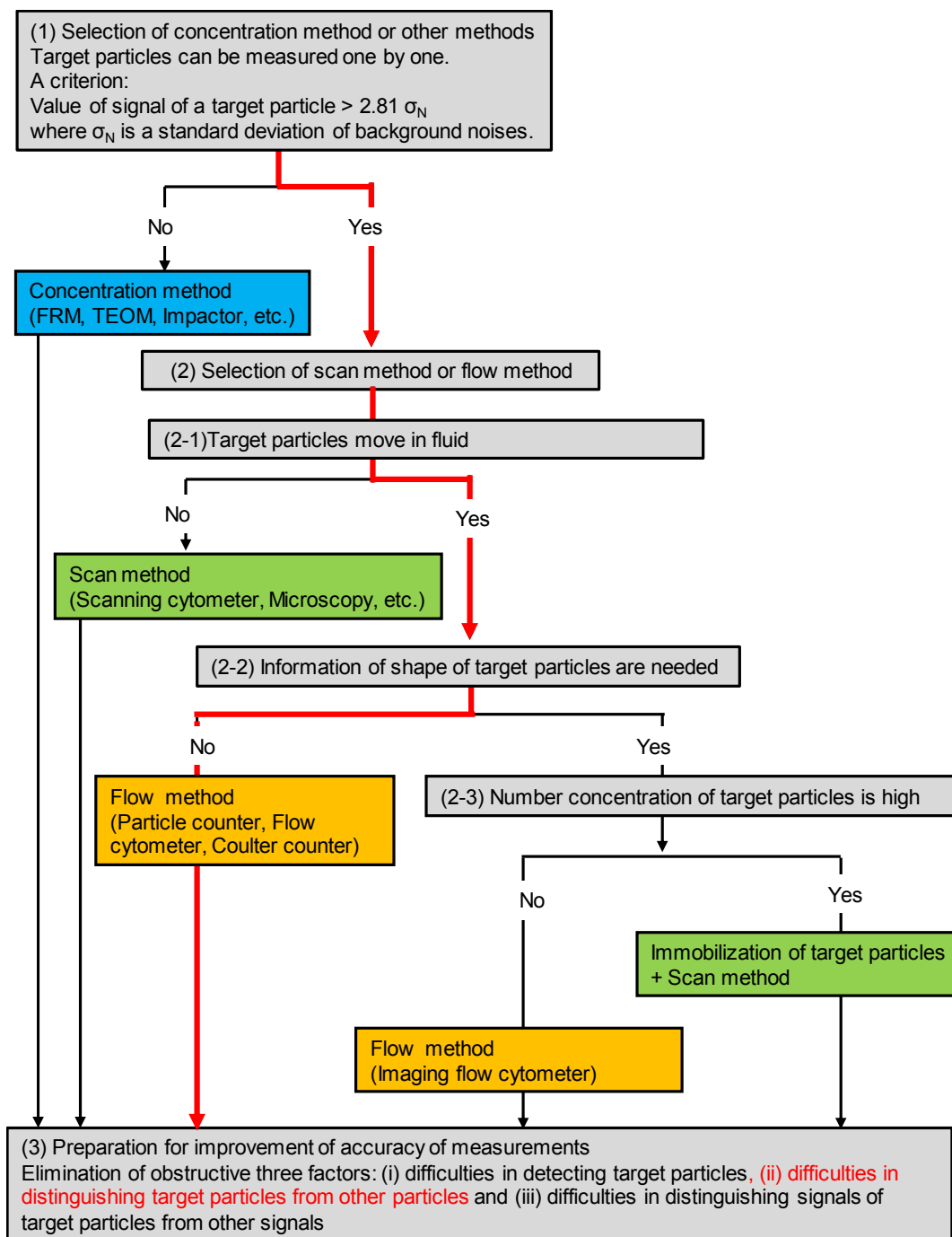
Fig. 4-2 Selection of flow method as an analysis of particles in liquid using the methodology

4.2 Concept of Excitation fluorescent spectral flow cytometer

Fig. 4-3 shows a configuration diagram of the EFSFCM. It consists of a solution-transmitting unit and an optical unit. The solution-transmitting unit allows a sample containing particles to flow through the center of a flow cell by hydrodynamic focusing on coaxial sheath flows. By the sheath flow method, particles can pass at a constant velocity through the center of the flow cell. Additionally, this has the advantage of keeping the inner surfaces of the flow cell clean because the sample solution does not come in contact with the inner surfaces [12].
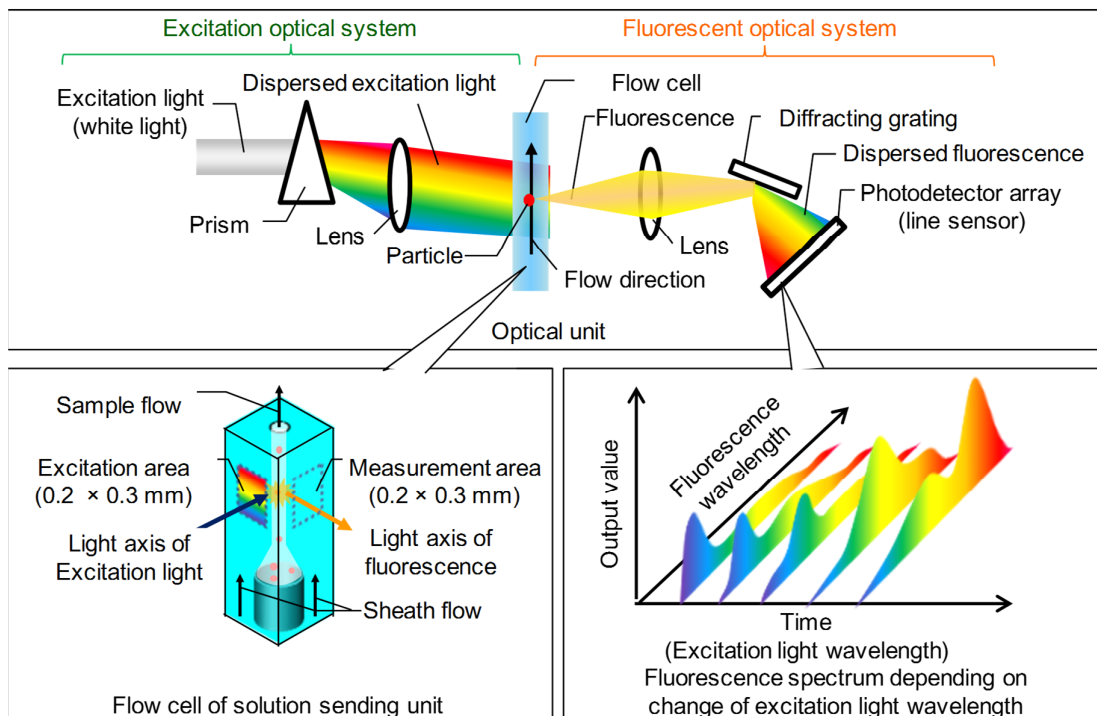
Fig. 4-3 Configuration diagram of the excitation-fluorescent spectral flow cytometer

The optical unit consists of an excitation optical system and a fluorescence optical system. The excitation optical system irradiates an excitation area (0.2×0.3 mm^2) of the flow cell with white light as an excitation light dispersed with a prism. The wavelength of the excitation light shifts from a short wavelength to a long wavelength along the flow direction of the sample. In the excitation optical system, the excitation light has to be dispersed along the flow direction. However, the wavelength of the excitation light has to be constant along the vertical direction of the flow direction. Thereby, the excitation optical system has to irradiate a long thin rectangular area, not an elliptical area, vertical to the flow direction with an excitation light of the same wavelength. Next, the

fluorescence optical system measures the dispersed fluorescence of particles using a diffracting grating with a spectroscopic photodetector array. The optical axis of excitation light and the optical axis of fluorescence bisect each other at right angles as is the case with a conventional fluorescence flow cytometer [12]. When a single particle passes through the excitation area in the upstream flow cell, the wavelength of the excitation light shifts from a short wavelength to a long wavelength depending on the particle's position. Additionally, the fluorescence spectrum of the particle changes depending on the shift of the wavelength of the excitation light.

Table 4-3 shows the specifications of the EFSFCM. We adopted these specifications of the EFSFCM for the following reasons. First, the measurement range of target particle sizes is fixed at a value lower than 10 μm because the sizes of the targets to be measured such as cells and bacteria are between 1 and 10 μm. Second, the wavelength range of excitation light is fixed between 400 and 650 nm, and the wavelength range of fluorescence is fixed between 400 and 700 nm because these wavelength ranges of excitation light and fluorescence are commonly used in cell analyses. Finally, the volume measured per unit of time is fixed at 1 μL/min. This is much smaller than those commonly used in conventional flow cytometers [17]. At a higher volume measured per unit of time, it is more difficult to discriminate signals of the fluorescence of a particle from noise signals when no high-performance frequency filter is used. The frequency filter is required in practical applications. However, the purpose of this study is to determine the feasibility of the EFSFCM. Thereby, we used a very low volume measured per unit of time to easily discriminate signals of the fluorescence of a particle from noise signals without using the frequency filter.

Table 4-3 Specifications of excitation-fluorescent spectral flow cytometer.

Items	Specifications	Reasons
Transmission method for sample solution in flow cell	Sheath flow method	To flow sample solution through the center of the flow cell To prevent the inner surface of the flow cell from stain of sample solution
Range of target particle size	< 10 μm	Size of target particles such as cell is less than 10 μm
Wave length band of excitation light	400 to 650 nm	General wave length band used in cell analysis
Wave length band of fluorescence	400 to 700 nm	General wave length band used in cell analysis
Volume measured per unit time	1.0 μL/min	To simplify discrimination of signals of target particles from electrical noise signal
Dimensions of flow cell	1.0×1.0 mm^2	-
Excitation area in flow cell	0.2×0.3 mm^2	To increase wave length of excitation light by 10 nm every time a particle moves 10 μM in flow direction
Measurement area of flow cell	0.2×0.3 mm^2	-
Measurement range of particle number concentration	$< 10^4$ particles/mL	Probability of more than two particles entering the excitation area at the same time is less than 0.05

4.3 Number concentration of sample solution

The volume of the probe area and the range of number concentration are considered in this section. The volume of the probe area in the flow cytometer is equal to the volume of the sample solution irradiated with the excitation light. Thereby, the volume of the probe area is expressed as a product of the cross-section area of the sample solution through the flow cell (s) and the flow direction length of the area irradiated by the excitation light (l) (Fig. 4-4).
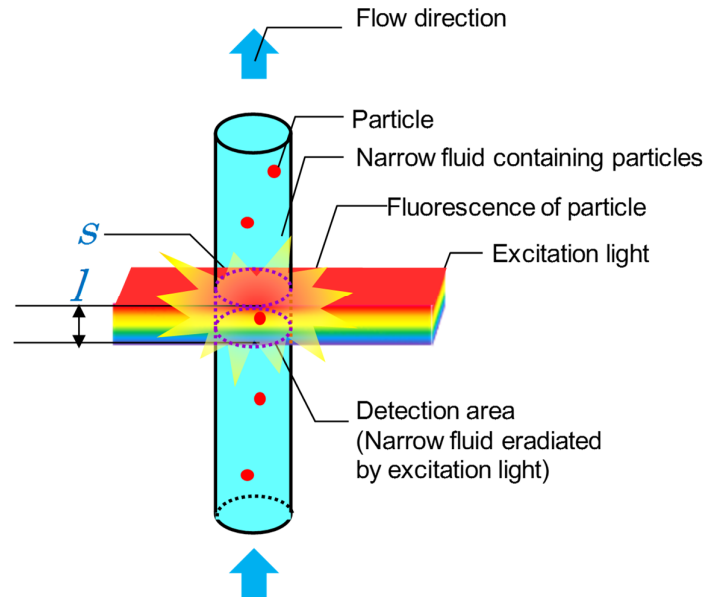
Fig. 4-4 Probe area in the flow cytometer

The cross-section area of the sample solution through the flow cell is one-tenth of the cross-section area of the flow cell (0.1 mm²) because the ratio of the sample solution and the sheath liquid is 1:10. Next, the flow direction length of the area irradiated by the excitation light is considered as follows. The flow direction length of the area irradiated by the excitation light (l) meets the condition that the wavelength of the excitation light irradiating an Φ 10 μm particle increase about 10 nm for every 10 μm of movement of the particle. The range of wavelengths of the excitation light entering the irradiated area is from 400 nm to 650 nm. Thereby, we decided that l is 0.3 mm (300 mm). For these reasons, the volume of the probe area is 0.03 mm³.

Finally, we considered the range of the number concentration of particles. The EFSFCM can't measure correct excitation-fluorescence spectra if more than two particles enter the probe area at the same time. The volume of the probe area is fixed earlier. Thereby, we have to consider the range of the number concentration of particles to prevent more than two particles from entering the probe area at the same time. We fixed the volume of the probe area and the range of number concentration of bacteria in Chapter 3 to meet the strict condition that the probability of more than one particle entering the probe area be less than 5%. This is because the purpose of the bacteria counter is to count live bacteria.

However, we consider that the condition for the EFSFCM in this chapter isn't stricter than this condition because it is possible to omit data of more than two particles entering

the probe area at the same time for the purposes of measuring an excitation-fluorescence spectrum of a particle. Thereby, we consider the range of the number concentration required to meet the condition that more than two particles entering the probe area is less than 5%.

As mentioned in Chapter 2, the probability of x particles entering the probe area at the same time p (x) is given by

$$p(x) = \frac{(\rho v_p)^x e^{-\rho v_p}}{x!} \qquad 4\text{-}1$$

where the volume of the probe area is v_p and the number concentration of particles is ρ.

The probability of more than x particles entering the probe area is given from Equation 4-1 by

$$P(x) = \sum_{i=0}^{\infty} p(i) \qquad 4\text{-}2$$

Thereby, the probability of two particles entering the probe area is given by

$$P(x \geq 2) = 1 - p(0) - p(1)$$
$$= 1 - e^{-\rho v_p} - \rho v_p e^{-\rho v_p} \qquad 4\text{-}3$$

Under the condition that $P(x \geqq 2) < 0.05$, equation 4-2 gives $\rho < 1.2 \times 10^4$ particles/mL.

Then we fixed the range of the number concentration of particles to be less than or equal to 1×10^4 particles/mL.

4.4 Design of the optical unit of the EFSFCM

We designed an optical unit to meet the above optical performance and the specifics with the optical design software (OpticStudio^{TM}, Zemax). The layout of the excitation optical system is shown in Fig. 4-5, the layout of the fluorescent optical system is shown in Fig. 4-6 and the cross-sectional view of the flow cell in the optical unit is shown in Fig. 4-7. Additionally, Table 4-4 shows specifics of optical parts in the optical elements.
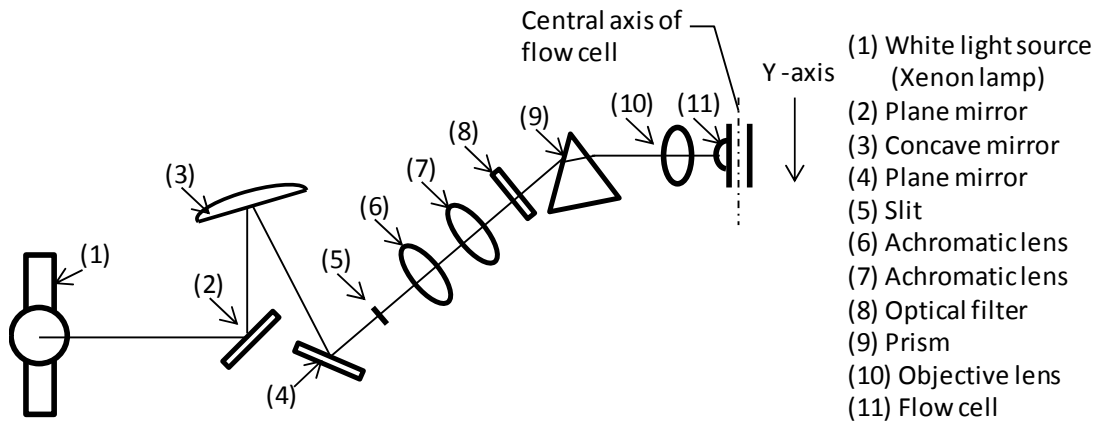
Fig.4-5 Layout of the excitation optical system

(1) White light source (Xenon lamp)
(2) Plane mirror
(3) Concave mirror
(4) Plane mirror
(5) Slit
(6) Achromatic lens
(7) Achromatic lens
(8) Optical filter
(9) Prism
(10) Objective lens
(11) Flow cell

Fig.4-6 Layout of the fluorescent optical system

(1) Flow cell
(2) Achromatic lens
(3) Optical filter
(4) Achromatic lens
(5) Slit
(6) Plane mirror
(7) Concave mirror
(8) Diffraction grating
(9) Concave mirror
(10) Plane- convex cylindrical lens
(11) 8-channel linear array multianode photomultiplier
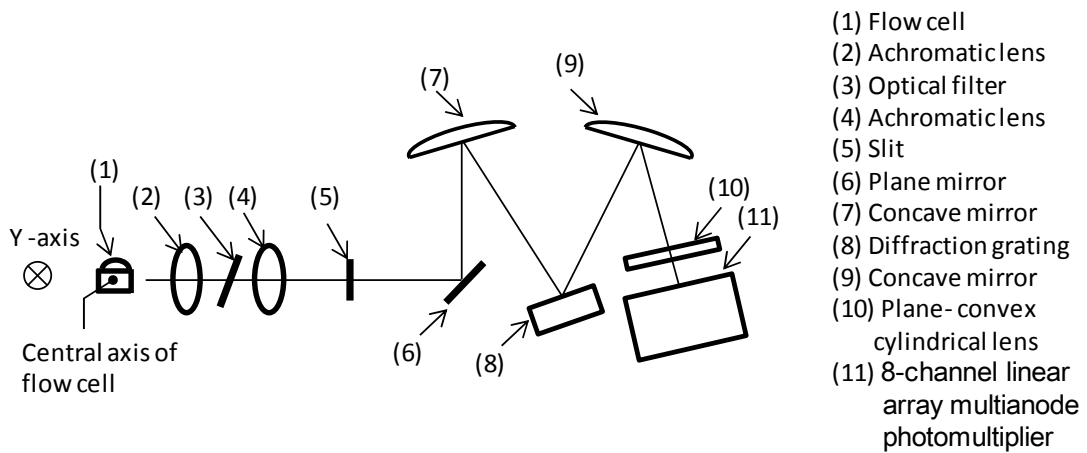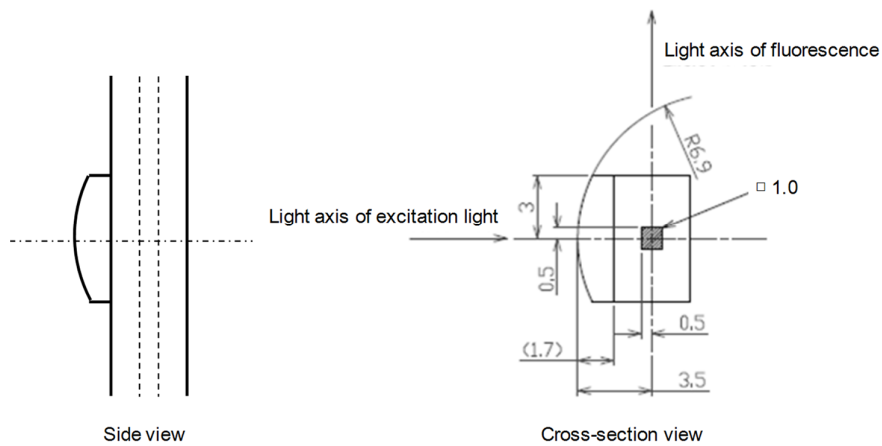
Fig.4-7 Cross-sectional view of flow cell

104
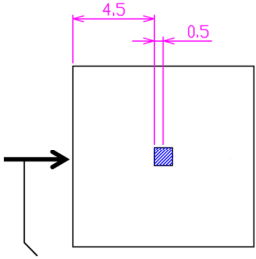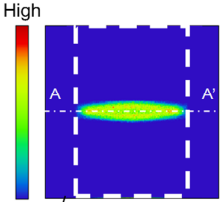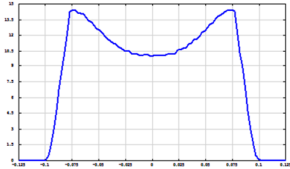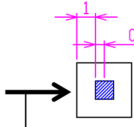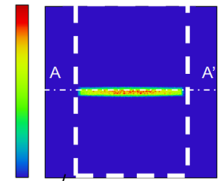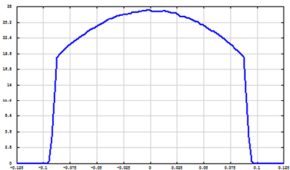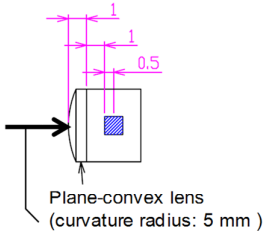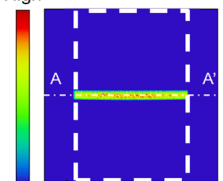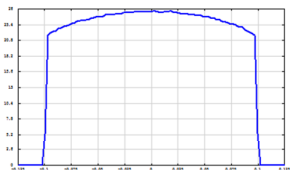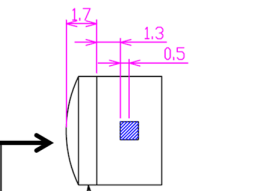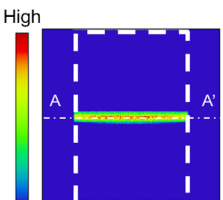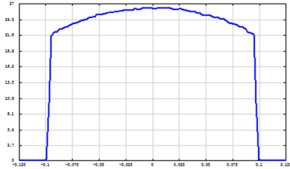
Table 4-4 Specifications of optical elements

Optical elements	Trade name (mfr.)	Specifications	
White light source	LAX-103 (Asahi spectra)	Wavelength range	240 to1000 nm
		Lump type	100W Xenon lump
Objective lens	LMPLFLN 20X (Olympus)	N.A	0.4
		Working distance	12.0 (mm)
		F.N.	26.5
Linear array multianode PMT	H11451-20 (Hamamatsu Photonics K.K.)	Spectra response	300 to 920 nm
		Cathode characteristics	Luminous (Min): 350 (mA/lm) Radiant: 78 (mA/W)
		Anode type	8-Channel linear array (2.0 mm x 2.5 mm, 2.8 pitch)

The flow cell has a rectangular cross-section channel (1×1 mm^2) on the inside and a lens on the surface irradiated with the excitation light. The lens structure needs to irradiate the irradiated area on the flow cell uniformly with excitation light. We selected the best lens structure of the following four flow cells. Table 4-5 shows cross sectional views of four flow cells and intensity distributions of the excitation light. Details of four flow cells are shown. Model A is a 10×10 mm^2 rectangular flow cell, Model B is a 3×3 mm^2 rectangular flow cell, Model C is a Model B with a lens structure on a side surface and Model D is a 3.6×6.9 mm^2 rectangular flow cell with a commercial lens structure on a side surface.

We selected a Model D because a variation in the intensity distribution of the excitation light on Model D is small and it is possible to make Model D by attaching a commercial lens on a rectangular flow cell.

Table 4-5 Light intensity distribution on irradiated area of flow cell

	Cross-section view of microchannel	435nm excitation light intensity distribution on irradiated area	
		2D intensity distribution	A-A' cross-section view
Model A	Light axis of excitation light	Irradiated area (0.2 mm x 0.3 mm)	
Model B	Light axis of excitation light	Irradiated area (0.2 mm x 0.3 mm)	
Model C	Plane-convex lens (curvature radius: 5 mm) Light axis of excitation light	Irradiated area (0.2 mm x 0.3 mm)	
Model D	Plane-convex lens (curvature radius: 6.9 mm) Light axis of excitation light	Irradiated area (0.2 mm x 0.3 mm)	

The excitation optical system consists of a xenon lamp as the white light source (LAX-103, Asahi Spectra), mirrors, a concave mirror, a slit, a prism, an objective lens, and a lens on the surface of the flow cell. The white light from the white light source is focused

on the slit by the concave mirror. The white light passing through the slit is dispersed by the prism and irradiated on the excitation area in the flow cell via the objective lens and the lens on the surface of the flow cell. The area on which dispersed excitation lights are irradiated is shifted from the lower to upper position along downstream to upstream of the flow cell by increasing the wavelength of the excitation light.

A xenon lamp was selected as the white light source rather than a mercury lamp. A mercury lamp has the advantage of having a sufficiently high intensity of light for use in a fluorescence microscope. However, it is unsuitable as the light source of the EFSFCM because its light intensity varies significantly in several bright-line spectra from 400 to 650 nm. In contrast, a xenon lamp has no bright-line spectrum and its light intensity is constant. Thus, we selected the xenon lamp as the light source of the EFSFCM for the above reason.

The fluorescence optical system consists of the flow cell, lenses, mirrors, a concave mirror, a slit, a diffraction grating, a cylindrical lens, and an 8-channel linear array multianode photomultiplier (H11451-20, Hamamatsu). The fluorescence of particles passing through the measurement area is focused on the slit by lenses. The fluorescence passing through the slit is dispersed by the diffraction grating and irradiated on different sensors of the 8-channel linear array multianode photomultiplier depending on the wavelength of the fluorescence. The 8-channel linear array multianode photomultiplier transduces the intensity of the fluorescence irradiated on each sensor to an electrical voltage. It is possible to measure the fluorescence spectrum of a particle by recording the electrical voltage with a data logger (Keyence NR500).

The 8-channel linear array multianode photomultiplier, which has eight optical sensors (2.0 mm × 2.5 mm) arrayed at intervals of 2.8 mm in alignment, was selected as a fluorescence detector of the EFSFCM. Each optical sensor of it measures intensities of fluorescence in the wavelength band from 400 nm to 700 nm with segmented eight wavelength bands.

The flow cell has a cuboid optical cell with a rectangular channel (□1.0 mm) inside and lens structure on the side surface where the excitation light enters. It is possible to fabricate the designed flow cell by binding a rectangular channel and a commercial spherical lens using the optical contact bonding method [18].

Fig. 4-8 shows a photograph of the optical unit and Fig. 4-9 shows a photograph and cross-section view of the flow cell. The flow cell has a structure to send the sample solution upward thorough a center of the flow cell by hydrodynamic focusing on coaxial sheath flows. By the sheath flow method, particles can pass at a constant velocity through the center of the flow cell. Additionally, this has the advantage of keeping the inner

surfaces of the flow cell clean because the sample solution does not come in contact with the inner surfaces [12]. Wavelength of dispersed excitation light increase at upper position in the irradiated area. Thereby wavelength of excitation light irradiating a particle shifts from a short wavelength to a long wavelength as the particle moving upward through the flow cell.
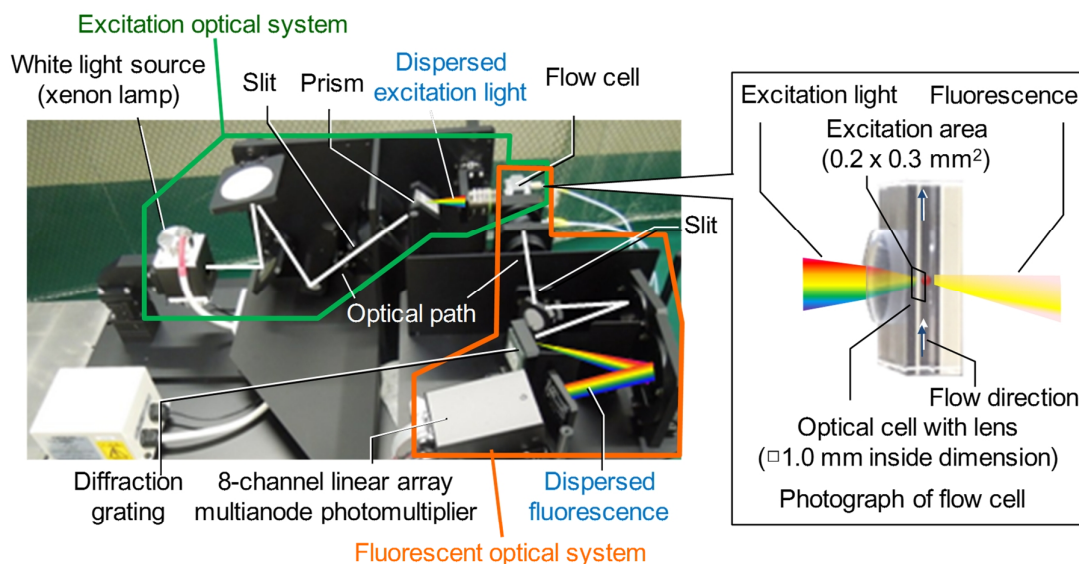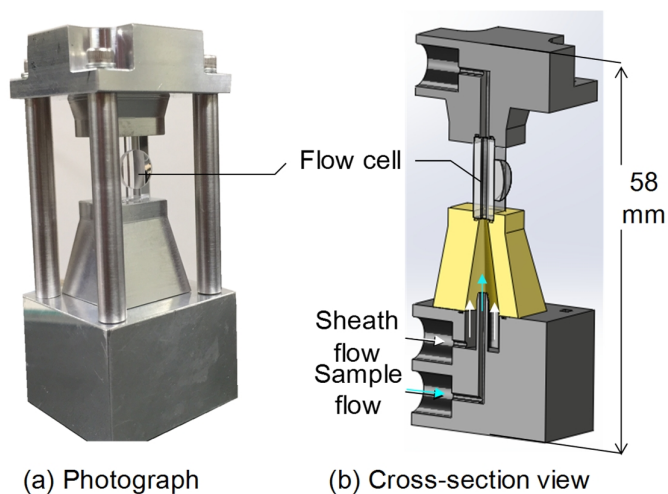

Fig.4-8 Photograph of optical unit of EFSFCM

(a) Photograph (b) Cross-section view

Fig. 4-9 Photograph and cross-section view of the flow cell

4.5 Evaluation of the optical unit by optical analysis and experiments

4.5.1 Evaluation of the excitation optical system

The excitation optical system was evaluated by checking that dispersed excitation light was irradiated the excitation area in the flow cell as same as optical analysis results. Fig. 4-10 shows the optical system for evaluations of the excitation optical system, which is modified from the excitation optical system (Fig. 4-5) by adding an optical filter, a diffuser plate and a CCD camera (Charge-Coupled Device camera). In above-mentioned optical system, (1) the excitation light in a specific wavelength passes through the bandpass filter set in the rear of the white light source, (2) the excitation light passing through the filter is scattered by the diffuser on the slit set on the position which is conjugated optically with the excitation area on the flow cell, (3) the scattered excitation light are dispersed and irradiated the excitation area via the prism and lenses. Moreover, observations of the excitation area were made with the CCD camera set on the rearward position of the flow cell.
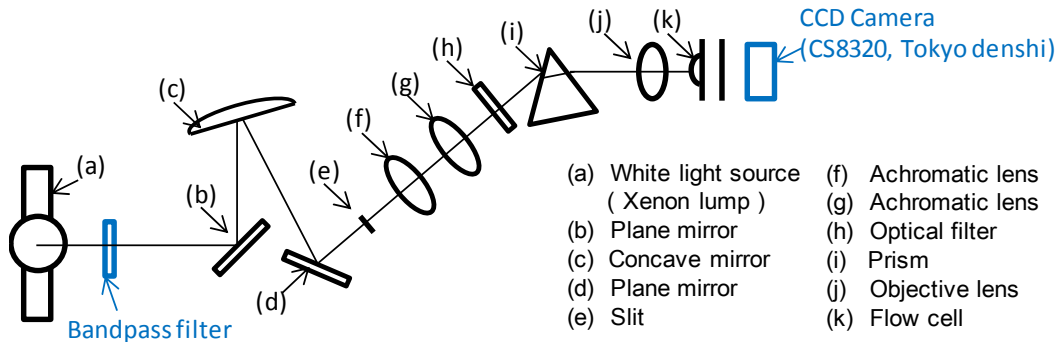
Fig.4-10 Optical system for evaluations of the excitation optical system

Fig. 4-11 shows the results of the optical analyses and experiments at the excitation area on which excitation lights with specific wavelengths are irradiated. Additionally, Fig. 4-12 shows that a position where excitation light in specific wavelength is irradiated moves upward by increases in wavelength of excitation light as same as optical analysis results.
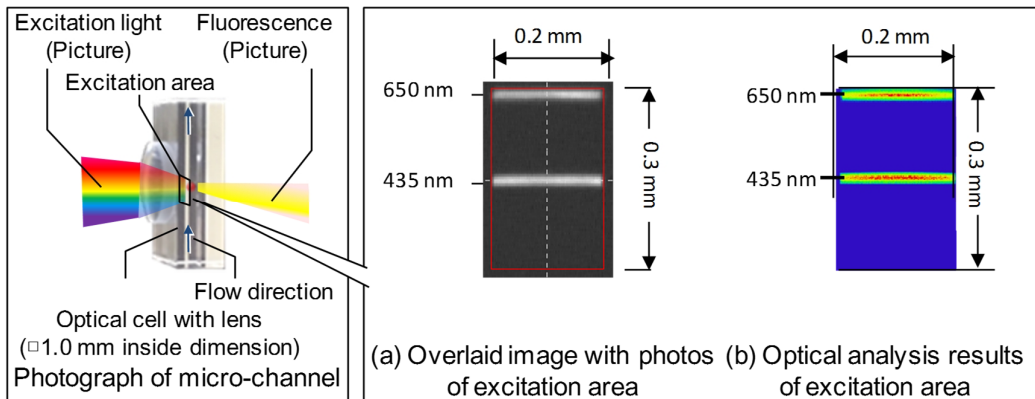
Fig. 4-11 Results of optical analyses and experiments of excitation area where excitation lights in specific wavelength are irradiated
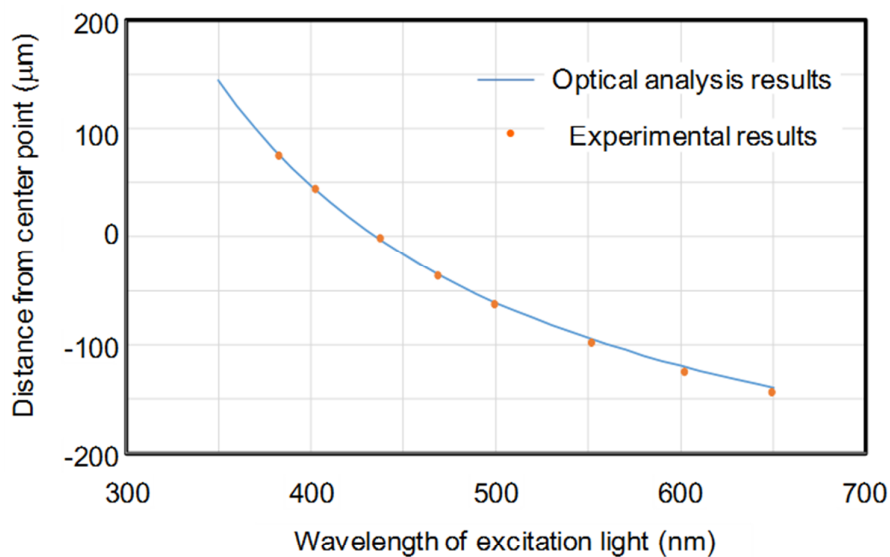
Fig. 4-12 Distance from center point of irradiated area

4.5.2 Evaluation of the fluorescence optical system

The fluorescence optical system was evaluated by checking that the fluorescence from the measurement area in the flow cell was detected dispersedly as same as results of optical analysis. Fig. 4-13 shows the optical system for evaluations of the fluorescence optical system, which is modified from the fluorescence optical system (Fig. 4-6) by adding the white light source, bandpass filters, the optical fiber, the 0.2 mm × 0.3 mm slit and the line sensor instead of the 8-channel linear array multianode photomultiplier.
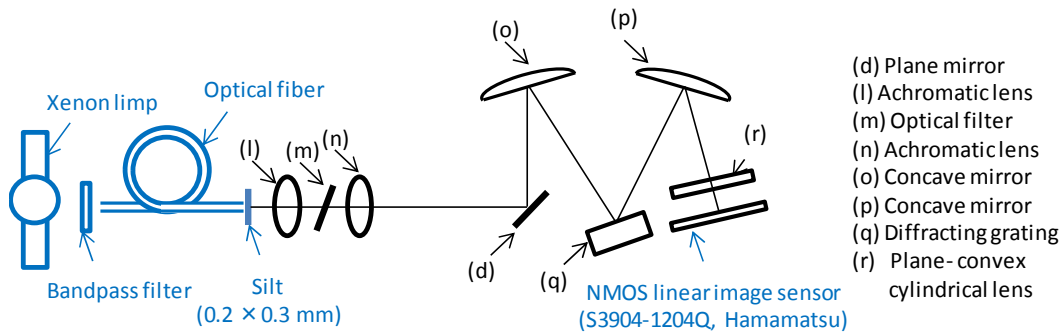
Fig. 4-13 Optical system for evaluations of the fluorescent optical system

In above-mentioned optical system, the light in the specific wavelength passing through the bandpass filter are emitted from the tip of optical fiber attached with the slit. The slit are set on the optically same position of the measurement area. The light passing through the slit are dispersed by the diffracting grating and irradiated to the line sensor (S3904-1024Q, Hamamatsu). The line sensor with 1024 pixels enables to measure accurate positions where lights in different wavelengths are irradiated.

Fig. 4-14 shows positions of sensors on the 8-channel linear array multianode photomultiplier. Fig. 4-15 shows experimental and analytical results about positions on the line sensor where the light in the specific wavelength are irradiated. Positions on the line sensor in the graph are relative from the center point of the line sensor. The graph in Fig. 4-15 shows fluorescence in the specific wavelength from the measurement area is irradiated on positions as designed.
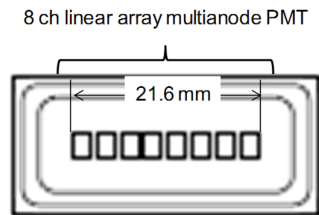
Fig. 4-14 Distance from center points of line sensor
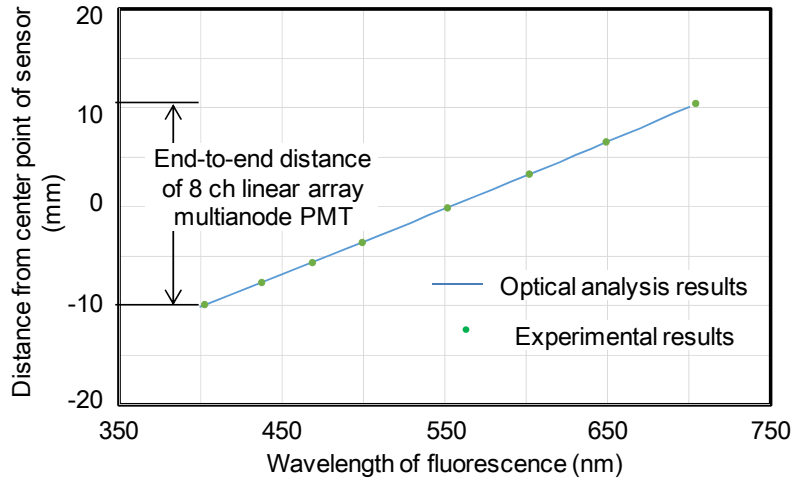
Fig. 4-15 Distance from center points of line sensor

4.6 Excitation-fluorescence spectrum of fluorescent particles

4.6.1 Experimental procedure

We measured the excitation-fluorescence spectra of fluorescent particles (Polyscience Fluoresbrite® YG microspheres) diluted with extrapure water using the EFSFCM to evaluate its performance. The measurement procedure is shown in Fig. 4-16. Fluorescent particles were used in experiments at 1×10^4 particles/mL number concentration diluted with extrapure water. Next, a sample solution is transmitted at 1 μL/min and sheath liquid is transmitted at 10 μL/min. Additionally, the specificatins of Fluoresbrite® YG microspheres are shown in Table 4-6. A 2.0 μm particle has excitation and emission spectra with an excitation maximum of 441 nm and an emission maximum of 485 nm.

Fluorescent particles are suitable for evaluating the performance of the EFSFCM because they emit fluorescence in a specific wavelength band.
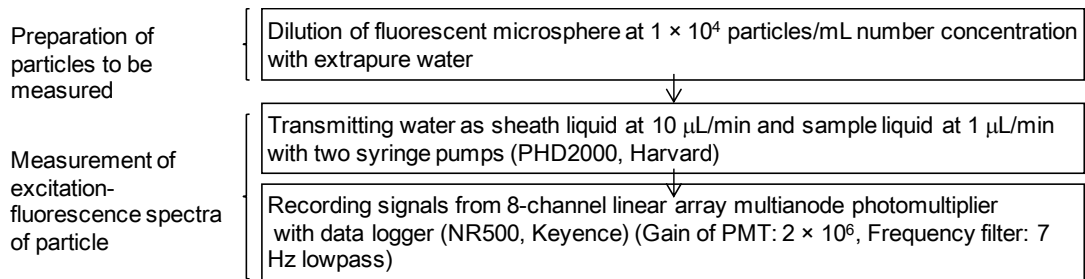
Fig. 4-16 Measurement procedure of excitation-fluorescent spectrum of fluorescent particles

Table 4-6 Specifications of fluorescent particles

	Trade name (Manufacture)	Size (μm)	Excitation max (nm)	Fluorescence max (nm)
Fluorescent microspheres	Fluoresbrite® YG Microspheres (Polyscience)	2.0	441	486

4.6.2 Experimental results

Fig. 4-17 shows the voltage signals of the 8-channel linear array multianode photomultiplier during the measurement of fluorescent particles with the EFSFCM. These particles characteristically emit strong green fluorescence. Few signals overlaps other pulse in Fig. 4-17. Thereby more than two particles enter rarely the probe space (irradiated area) at the same time according to the exception in the section 3. Fig. 4-18 shows a single-pulse signal near 42 s. This graph shows the time course of the fluorescence spectrum of a fluorescent particle according to the change in the wavelength of the excitation light irradiating the particle.

If the wavelength of the excitation light irradiating the fluorescent particle is fixed in Fig. 4-18, it is possible to convert this graph to an excitation-fluorescence spectrum. Therefore, we used information on the specifications of the fluorescent particles (Table 4-6) and the relative position on the flow cell irradiated by excitation light in different wavelength bands (Fig. 4-12). The peak excitation and fluorescence wavelengths of the Fluoresbrite® YG microspheres were 441 and 486 nm, respectively (Table 4-6). Therefore, the signal of channel 3, which is the most sensitive to 486 nm fluorescence, reached a peak when the Fluoresbrite® YG microspheres were irradiated with 441-nm-wavelength excitation light. Thus, the excitation-fluorescence spectrum of the Fluoresbrite® YG microspheres (Fig. 4-19) was converted from Fig. 4-18. The shape of an excitation fluorescence spectrum indicates features of a fluorescent particle; therefore, it is possible to identify particles precisely from the shapes of excitation fluorescence spectra.
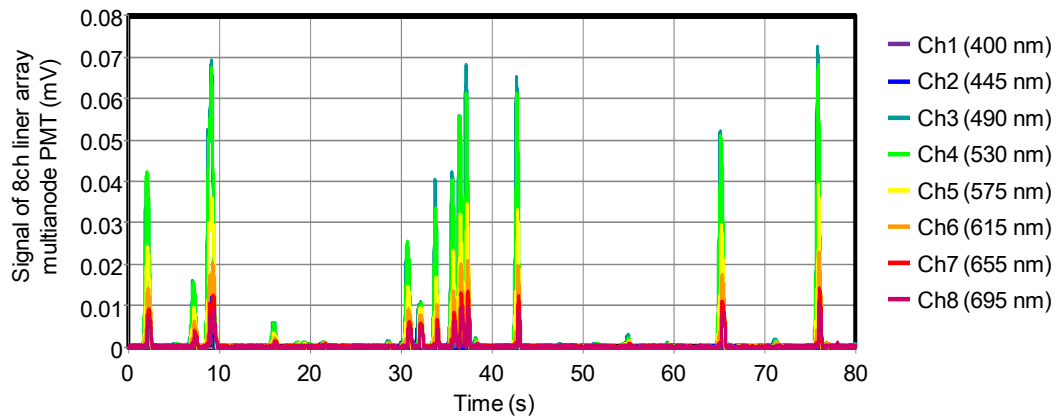
Fig. 4-17 Signal of fluorescent particle measured by 8ch liner array multianode PMT
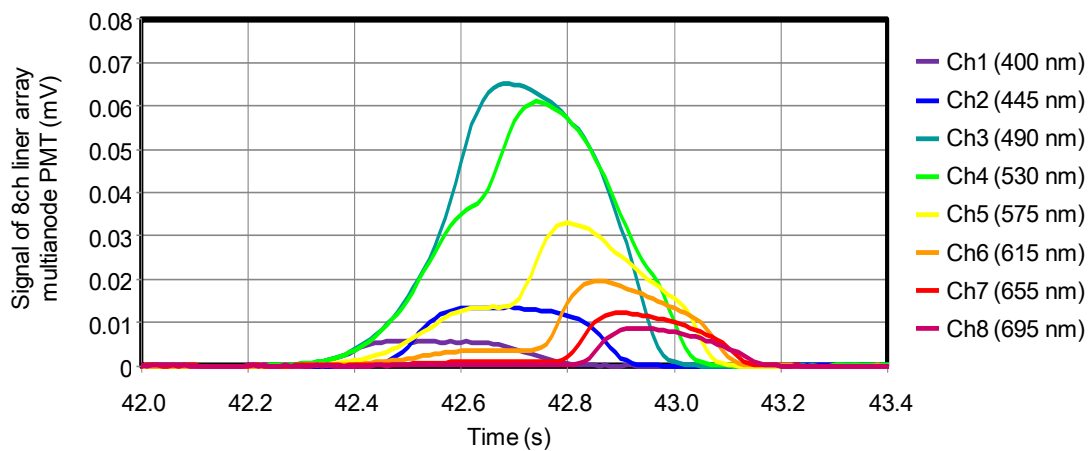

Fig. 4-18 Signal of fluorescent particle measured by 8ch liner array multianode PMT
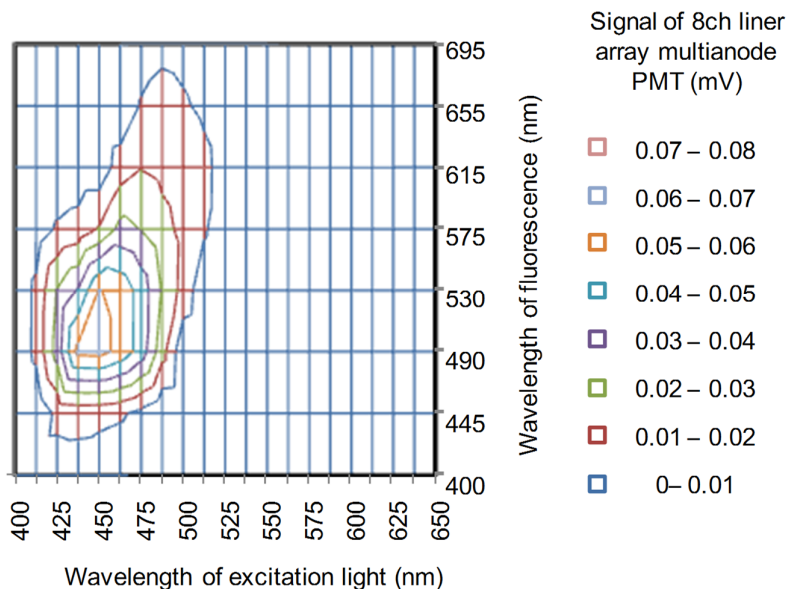
114

Fig. 4-19 Excitation-fluorescent spectrum of 2.0-µm Fluoresbrite® YG microspheres

4.7 Particle composition analysis in vegetable suspension

4.7.1 Experimental procedure

Substances in a homogenized vegetable suspension were determined from the results obtained using this system. All vegetables are known to contain many components materials that emit fluorescence such as NADH, whose wavelengths are shorter than 500 nm [19]. Additionally, green vegetables such as spinach contain chlorophyll, which emits near-infrared fluorescence [19]. T Therefore, it is considered that measurement results of a homogenized tomato or spinach suspension show the above features of vegetables. The experimental procedure is shown in Fig. 4-20. First, tomato or spinach is homogenized in distilled water. Second, the obtained homogenized vegetable suspension is centrifuged and the resulting supernatant is discarded. Third, the suspension diluted with distilled water is filtered to remove large particles. The filtrate is used in experiments at 1×10^4 particles/mL number concentration diluted with extrapure water. Finally, the suspension is transmitted at 1 µL/min and the sheath liquid at 10 µL/min.

```
┌─────────────────────────────────────────────────────────────────────────────┐
│ Homogenization of vegetable in distilled water                              │
└─────────────────────────────────────────────────────────────────────────────┘
                                    ↓
┌─────────────────────────────────────────────────────────────────────────────┐
│ Centrifugal separation of suspension and discard the supernatant            │
└─────────────────────────────────────────────────────────────────────────────┘
                                    ↓
┌─────────────────────────────────────────────────────────────────────────────┐
│ Filtration of the suspension mixed with distilled water (pore size: 5 μm)   │
└─────────────────────────────────────────────────────────────────────────────┘
                                    ↓
┌─────────────────────────────────────────────────────────────────────────────┐
│ Dilution of the suspension at 1.0 × 10⁴ particles/mL number concentration   │
│ with distilled water                                                        │
└─────────────────────────────────────────────────────────────────────────────┘
                                    ↓
┌─────────────────────────────────────────────────────────────────────────────┐
│ Transmitting water as sheath liquid at 10 μL/min and sample liquid at 1     │
│ μL/min with two syringe pumps (PHD2000, Harvard)                            │
└─────────────────────────────────────────────────────────────────────────────┘
                                    ↓
┌─────────────────────────────────────────────────────────────────────────────┐
│ Recording signals from 8-channel linear array multianode photomultiplier    │
│ with data logger (NR500, Keyence) (Gain of PMT: 2 × 10⁷, Frequency filter:  │
│ 7 Hz lowpass)                                                               │
└─────────────────────────────────────────────────────────────────────────────┘
```

Preparation of particles to be measured (first four boxes)

Measurement of excitation-fluorescence spectra of particle (last two boxes)

Fig. 4-20 Measurement procedure of particle composition analysis in vegetable suspension

4.7.2 Experimental results

Fig. 4-21 and 4-22 show the results of measurements of the homogenized spinach suspensions and tomato suspensions using the EFSFCM, respectively. Pulse signals at eight wavelengths show the changes in the fluorescence spectrum of a particle in the suspension with the change in the wavelength of excitation light. Fig. 4-22 shows that the homogenized tomato suspension contains many particles emitting blue-green fluorescence whose wavelengths are below 490 nm. In contrast, Fig. 4-21 shows that the homogenized spinach suspension contains two kinds of particles: one emits blue-green fluorescence and the other emits near-infrared fluorescence at 695 nm.
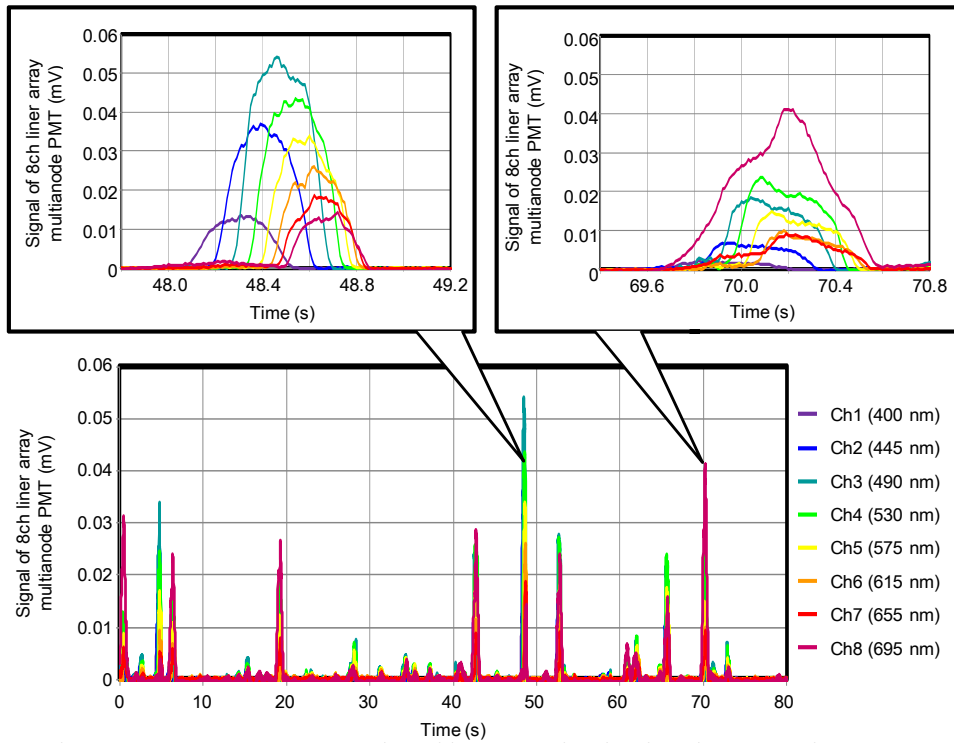
Fig. 4-21 Measurement results of homogenized spinach suspensions
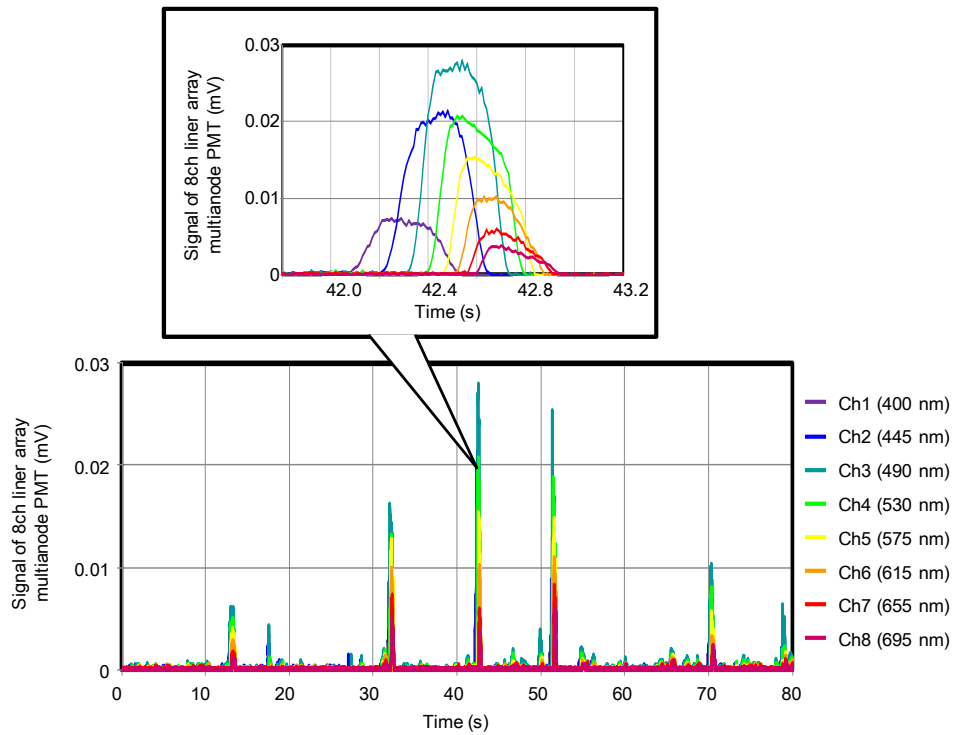
Fig. 4-22 Measurement results of homogenized tomato suspensions

117

Fig. 4-23 shows the distributions of ratios of fluorescence intensity at 695 nm to fluorescence intensity at 490 nm with respect to pulse signals in the tomato and spinach suspensions used for measurements. These results obtained using the EFSFCM agree with previously mentioned features of the components of tomato and spinach: vegetables contain many components that emit fluorescence such as NADH, whose wavelengths are below 500 nm [19]. Additionally, green vegetables such as spinach contain chlorophyll, which emits near-infrared fluorescence [19].
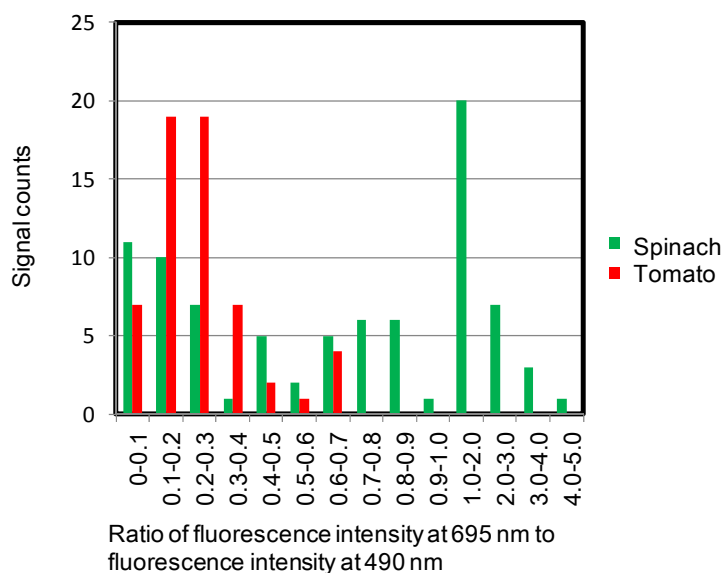
Fig. 4-23 Distributions of ratios of fluorescence intensity at 695 nm to fluorescence intensity at 490 nm in pulse signals

4.8 Discussion

This system is a kind of fluorescence flow cytometer for measuring the fluorescence spectrum of a particle. However, this system can measure the transition of the fluorescence spectrum according to the transition of the wavelength of excitation light, which is a unique feature of the EFSFCM compared with present systems. In this study, we measured the excitation-fluorescence spectra of fluorescent and targeted particles in homogenized vegetable suspensions using this system. Experimental results show that it is possible to measure the excitation-fluorescence spectra of a fluorescent particle and to determine the components of vegetables.

Moreover, a practical feature of this system is that the selection of the wavelengths of

excitation light and fluorescence according to target particles is not required as in conventional flow cytometers. Therefore, this system will be suitable for measurements of liquids that include unknown particles whose optimal wavelengths of excitation light and fluorescence are unknown. However, this system has the following problems to be solved for practical applications.

First, the volume measured per unit time is 1 μL/min, which is much smaller than those commonly used in flow cytometers [17], as mentioned above. For practical applications, improvement of frequency filters suitable for this system is required [12].

Second, to convert a transition of the fluorescence spectrum of an unknown particle to the excitation fluorescence spectrum of the particle, this system requires a step to determine the time when the particle passes across the detection area. It is possible to determine the time by detecting particles passing across the area located upstream of the detection area. Examples of detection methods are the Coulter counter technique [20] and detection of light scattering from the particle irradiated by laser [21].

4.9 Conclusion

In this chapter, we reported on the EFSFCM, which can measure the excitation-fluorescence spectra of single fluorescent particles. Consequently, we draw the following conclusions on the basis of the results of our work.

(1) The EFSFCM, which consists of a solution-sending unit and an optical unit, was designed by the decision methodology based on statistical theory. The solution-sending unit sends a sample containing particles through the center of a flow cell by hydrodynamic focusing on coaxial sheath flows. Next, the optical unit irradiates particles with dispersed white light (wavelength band: 400 - 650 nm) and measures their fluorescence spectra (wavelength band: 400 - 700 nm).

(2) The range of number concentration ($\leq 1.0 \times 10^4$ particle/mL) of particles is fixed from statistical theory. When fluorescent particles within the range of number concentration are measured with the EFSFCM, rarely is more than one fluorescent particle measured at the same time. Thereby, the decision methodology based on statistical theory is shown to be of benefit.

(3) The transition of the fluorescence spectrum of fluorescent particles (Fluoresbrite® YG microspheres) was measured by the EFSFCM. Measurement results show that particles characteristically emit strong green fluorescence. Additionally, an excitation-fluorescence spectrum (excitation wavelength range, 400 − 650 nm;

fluorescence wavelength range, 400 – 700 nm) of a fluorescent particle is converted from the transition of the fluorescence spectrum of a particle.

(4) Particles in homogenized tomato and spinach suspensions were measured using the EFSFCM. The homogenized tomato suspension contained many particles emitting blue-green fluorescence whose wavelengths are below 490 nm. Moreover, the homogenized spinach suspension contained two kinds of particles: one emitted blue-green fluorescence and the other emitted near-infrared fluorescence at 695 nm. These results agree with the features of the components of tomato and spinach.

(5) Results of analysis of particles in liquid using the EFSFCM show that it is possible to distinguish target particles from other particles more accurately by getting and comparing more information of particles as the methodology to develop a measurement method for target particles provides.

Reference

[1] Gilroy, D. J., Kauffman, K. W., Hall, R. A., Huang, X. and Chu, F. S. "Assessing potential health risks from microcystin toxins in blue-green algae dietary supplements," *Environ Health Perspect.*, Vol. 108(5), (2000), pp. 435-439.

[2] Hallegraeff, G. M. "Transport of toxic dinoflagellates via ships' ballast water: bioeconomic risk assessment and efficacy of possible ballast water management strategies," *Mar. Ecol. Prog. Ser.*, Vol. 168, (1998), pp. 297-309.

[3] Oliveira, H. M. B., Santos, C., Paterson, R. R. M., Gusmão, N. B. and Lima, N. "Fungi from a Groundwater-Fed Drinking Water Supply System in Brazil," *Int. J. Environ. Res. Public Health*, Vol. 13(3), (2016), p. 304, PMC4808967.

[4] Sandhaus, L. M. "Body fluid cell counts by automated methods," *Clin. Lab. Med.*, Vol. 35(1), (2015), pp. 93-103.

[5] Zhang, Y., Bai, J., Wu, H. and Ying, JY. "Trapping cells in paper for white blood cell count," *Biosens. Bioelectron.*, Vol. 69(15), (2015), pp. 121-127.

[6] Ministry of Health, Labour and Welfare, ed. *Standard methods of analysis in food safety regulation*, (2004), pp.567-589 (in Japanese), ISBN: 978-4-889-25002-2.

[7] Mise, K. and Inoue, F. ed. *Practical guide of Bacteriological testing of food*, (1996), pp. 52-53, Kodansha scientific (in Japanese), ISBN: 978-4-06-153712-5.

[8] Rost, F., and Oldfield, R. *Photography with a Microscope*, (2000), Cambridge University Press, Cambridge, United Kingdom, ISBN: 978-0-521-77096-5.

[9] Bjerling, P., Olsson, I. and Meng, X. "Quantitative Live Cell Fluorescence-microscopy Analysis of Fission Yeast," *J. Vis. Exp.*, Vol. 59, (2012), e3434.

[10] Sharma, A., and Schulman, S. G. *Introduction to Fluorescence Spectroscopy*, (1999), Wiley, New York, ISBN: 978-0-471-11098-9.

[11] Leeben, A., Mikomägi, A., Lepane, V. and Alliksaar, T. "Fluorescence spectroscopy of sedimentary pore-water humic substances: a simple tool for retrospective analysis of lake ecosystems," *T., J. Soils. Sediments*. Vol. 14(2), (2014), pp. 269-279.

[12] Shapiro, H. M. *Practical Flow Cytometry*, (2003), pp. 1-6, John Wiley & Sons, Inc., ISBN: 978-0-471-62228-4.

[13] Kalejta, R. F., Shenk, T. and Beavis, A. J. "Use of a membrane-localized green fluorescent protein allows simultaneous identification of transfected cells and cell cycle analysis by flow cytometry," *Cytometry*, Vol. 29(4), (1997), pp. 286-291.

[14] Schmid, I. and Sakamoto, K. M. "Analysis of DNA content and green fluorescent protein expression," *Curr. Protoc. Cytom*., Unit 7.16, (2001).

[15] Isailovic, D., Li, H-W., Phillips, G. J. and Yeung, E. S. "High-throughput single-cell

fluorescence spectroscopy," *Appl. Spectrosc.*, Vol. 59(2), (2005), pp. 221-216.

[16] Futamura, K., Sekino, M., Hata, A., Ikebuchi, R., Nakanishi, Y., Egawa, G., Kabashima, K., Watanabe, T., Furuki, M. and Tomura, M. "Novel full-spectral flow cytometry with multiple spectrally-adjacent fluorescent proteins and fluorochromes and visualization of in vivo cellular movement," *Cytometry part A*, Vol. 87(9), (2015), pp. 830-842.

[17] https://beckman.jp/products/flow-cytometers/gallios [Accessed 1 April 2017].

[18] Jia, Z-J., Fang, Q., and Fang, Z-L. "Bonding of Glass Microfluidic Chips at Room Temperatures," *Anal. Chem.*, Vol. 76, (2004), pp. 5597-5602.

[19] Sádecká, J. and Tóthová, J.,"Fluorescence Spectroscopy and Chemometrics in the Food Classification − a Review," *Czech J. Food Sci.*, Vol. 25(4), (2007), pp. 159-173.

[20] https://www.beckmancoulter.com/wsrportal/wsrportal.portal?_nfpb=true&_window Label=UCM_RENDERER&_urlType=render&wlpUCM_RENDERER_path=%25 2Fwsr%252Findustrial%252Fparticle-technologies%252Fcoulter-principle%252Findex.htm [Accessed 1 April 2017].

[21] https://www.bc-cytometry.com/FCM/fcmprinciple_3.html [Accessed 1 April 2017].

Chapter 5. Biological airborne particle detection system

5.1 Background

The 2009 influenza A (H1N1) epidemic is a well known example of a respiratory infection epidemic [1]. However, other respiratory infection epidemics often occur, such as the 2013 rubella epidemic and 2014 measles epidemic in Japan [2][3]. These epidemics caused many elementary, junior high, and high schools to temporarily close. Other many respiratory infections such as mycoplasma or tuberculosis also cause epidemics.

Causes of these respiratory infections are pathogens such as bacteria and viruses. These pathogens enter cells of a body of infected patient, which is infection. These pathogens grow in cells and bring on particular symptoms of pathogens such as cough, sneeze, algor, fever, headache, sore throat, etc. after infection [4]. Preventing infections of pathogens is a most effective method to keep out of deceases. Thereby, we consider that these respiratory infection epidemics can be effectively prevented by determining the presence or absence of infections in patients by frequent tests.

A common diagnosis method for respiratory infections such as influenza is an immnochromato test [5]. Fig. 5-1 shows an inspection procedure of using an immunochromato test.

(1) Inserting a cotton-tipped stick into a patient's cavitas nasi for sampling the nasal swabs

(2) Stirring a reagent with the cotton-tipped sampling the nasal swabs

(3) Dropping a mixture on a sample dropper area of immunochromato test. Positive mixture show a positive line in a detection area
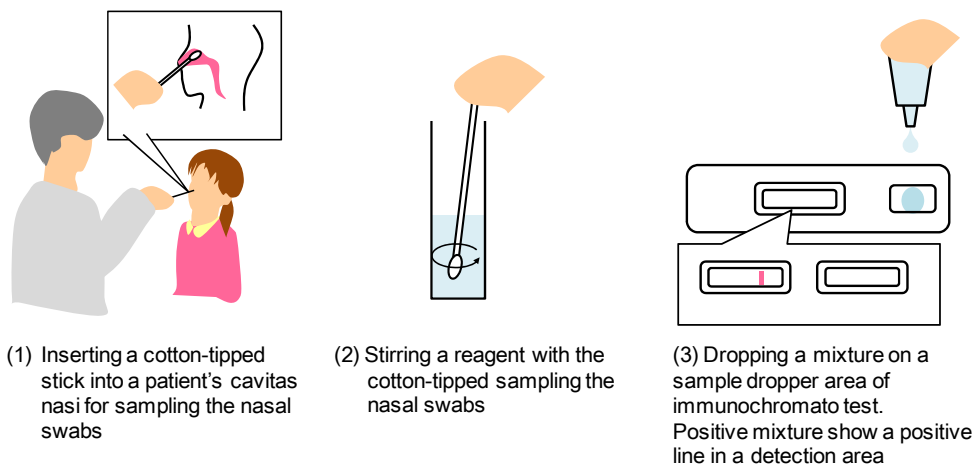
Fig. 5-1 Inspection procedure using an immunochromato test

This test enables the examiner to easily, rapidly, and inexpensively diagnose infected patients. However, self-diagnosis is difficult because it requires a medical professional to insert a cotton-tipped stick into a patient's cavitas nasi for sampling the nasal swabs including the pathogens of infections. Accordingly, patients have to go to clinics or hospitals and wait in a waiting room a certain time for the test.

Thereby, they may hesitate to have themselves tested frequently. For this reason, we thought that we can enable people to test themselves frequently without going to clinics or hospitals if we give them a method to self-diagnose respiratory infections rapidly and simply. Realizations of self-diagnoses of respiratory infections such as influenza need to sample pathogens without medical acts. Thereby, we focused breath of a patient.

When an influenza-infected patient breathes out, biological aerosol particles formed by the aggregation of pathogens and a patient's secretions are spread into the air. These biological aerosol particles are exhaled from 67 to 8,500 particles/L of air. Particle concentrations in the size selective bins ranged from 61 to 3,848 particles/L (particles between 0.3 μm and <0.5 μm), 5 to 2,756 particles/L (particles between 0.5 μm and <1 μm), 1 to 1,916 particles/L (particles between 1 μm and <5 μm), and 0 to 9 particles/L (>5 μm) [6]. Therefore, we thought that self-diagnosis may be possible using a system that can collect and detect more than just 0.3-μm biological aerosol particles in the patient's breathe because breath sampling is easy work requiring no examiner.

Fig. 5-2 shows a conceptual diagram of the diagnosis of a respiratory infection based on the detection of biological aerosol particles in a patient's breath using a sensing system of biological aerosol particles (SSBAP).
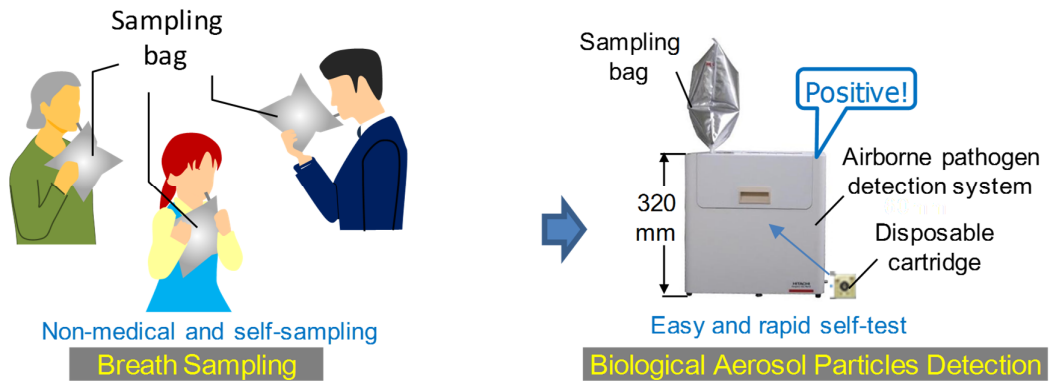
Fig. 5-2 Conceptual diagram of self-diagnosis of respiratory infections using sensing system of biological aerosol particles (SSBAP)

We assume that the SSBAP can be installed at schools, nursing homes, offices, drug stores, convenience stores, etc. because it does not need medical staff to administer it. Users blow into a sampling bag and set the SSBAP by themselves with the sampling bag filled with their breath and a disposable cartridge containing the biological aerosol particle detection function. The SSBAP set with the sampling bag and the cartridge

automatically detects any biological aerosol particles in the sampling bag and indicates whether or not the patient is positive for the infection.

Breath sampling and operating the SSBAP are easy work requiring no examiner, so anybody can use the SSBAP, not just medical staff. Furthermore, this kind of the system may be possible to use as an atmosphere monitoring system for biological aerosol particles. If biological particles in atmosphere can be monitored, the chance of infection may be able to be reduced without making everyone aware of the need for infection tests.

Only a few examples of the direct detection of biological aerosol particles from a patient's breath have previously been reported on, but the detection of airborne bacteria or fungi within biological aerosol particles has been commonly carried out in cleanliness evaluations of living spaces or medical facilities with a method that is a combination of the impaction and culture methods [7].

Fig. 5-3 shows inspection procedures using a combined method of an impaction and a culture method.

Collection of airborne bacteria on a culture medium using impactor

Formation of colonies of bacteria on the culture medium after 24-48 h cultivation
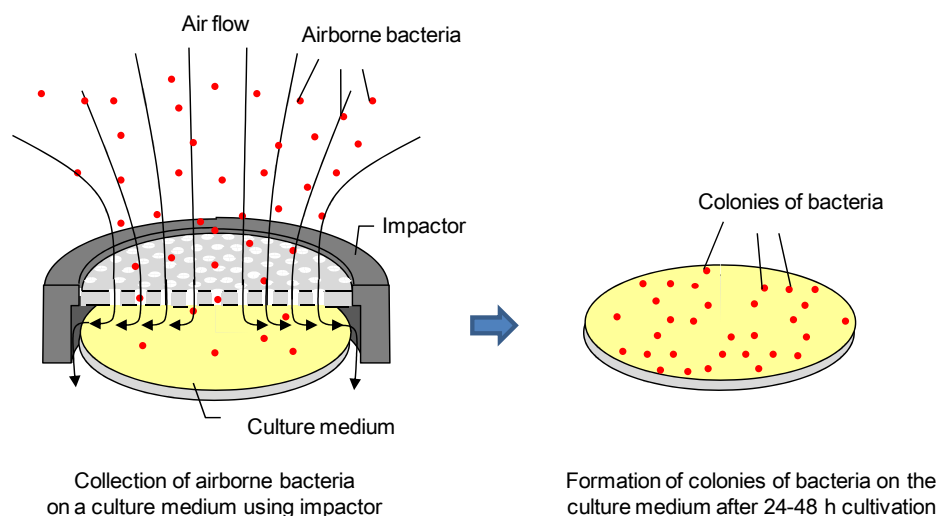
Fig. 5-3 Inspection procedures using a combined method of the impaction and culture methods

First, the impaction method is a commonly used method for sampling airborne particles that impacts the air onto a collection plate using volumetric air samplers such as Andersen [8]. In this method, the airborne bacteria or fungi are removed from an air stream by forcing the gasses to make a sharp bend and are then trapped on an agar media used as the collection plate. Second, the culture method is also a commonly used method for detecting bacteria. Bacteria collected on the agar media are cultured in an incubator for more than 48 hours, and microscopic bacteria grow together in visible colonies on the agar media [9]. An examiner counts the number of colonies as one of the bacteria through

visual examination or with an automated system. However, the bacteria culture requires more than 48 hours to obtain results of tests and the examiner requires special techniques.

On the other hand, bacteria or viruses are sometimes stained using special fluorescent dyes, which is known as a rapid detection method [10][11], but it is less common because it also requires the examiner to use special techniques.

Many studies have been reported regarding the rapid detection of biological particles such as fungi, bacteria, and viruses in water using devices of Micro TAS [12][13][14]. We even previously reported on a flow cytometry counter for viable bacteria in food suspension using a chip that included filtration and fluorescent labeling of bacteria functions [15]. However, very few devices in Micro TAS have been previously reported for biological aerosol particle detection that has collecting and labeling functions.

The final purpose of this research is to contribute to maintaining a healthy society by reducing the risk of respiratory infection epidemics. However, there are many technical and practical challenges to be resolved. In this chapter, we report a feasibility study of a system for sensing biological aerosol particles (SSBAP) using a disposable cartridge as a first step towards the final purpose.

5.2 Selection of a measurement method of biological airborne particles

First, we select the concentration method or other methods using the methodology in chapter 2, section 6 (Fig. 5-4). The selection condition of the concentration method is that it is possible to measure 0.3-μm biological aerosol particles labeled with fluorescent dyes one by one as was done with bacteria in chapter 3 and fluorescent particles in chapter 4. The range of diameter of a bacterium is from 1 to 10 μm. Thereby, this is 1.1×10^1 to 1.1×10^3 times larger than 0.3-μm biological aerosol particles in surface area and this is 3.7×10^1 to 3.7×10^4 times larger than 0.3-μm biological aerosol particles in volume. If intensity of fluorescence from a particle is proportional to a surface area or a volume of the particle, the intensity of fluorescence from a 0.3-μm biological aerosol particle is one-tenth times weaker than one from a bacterium.
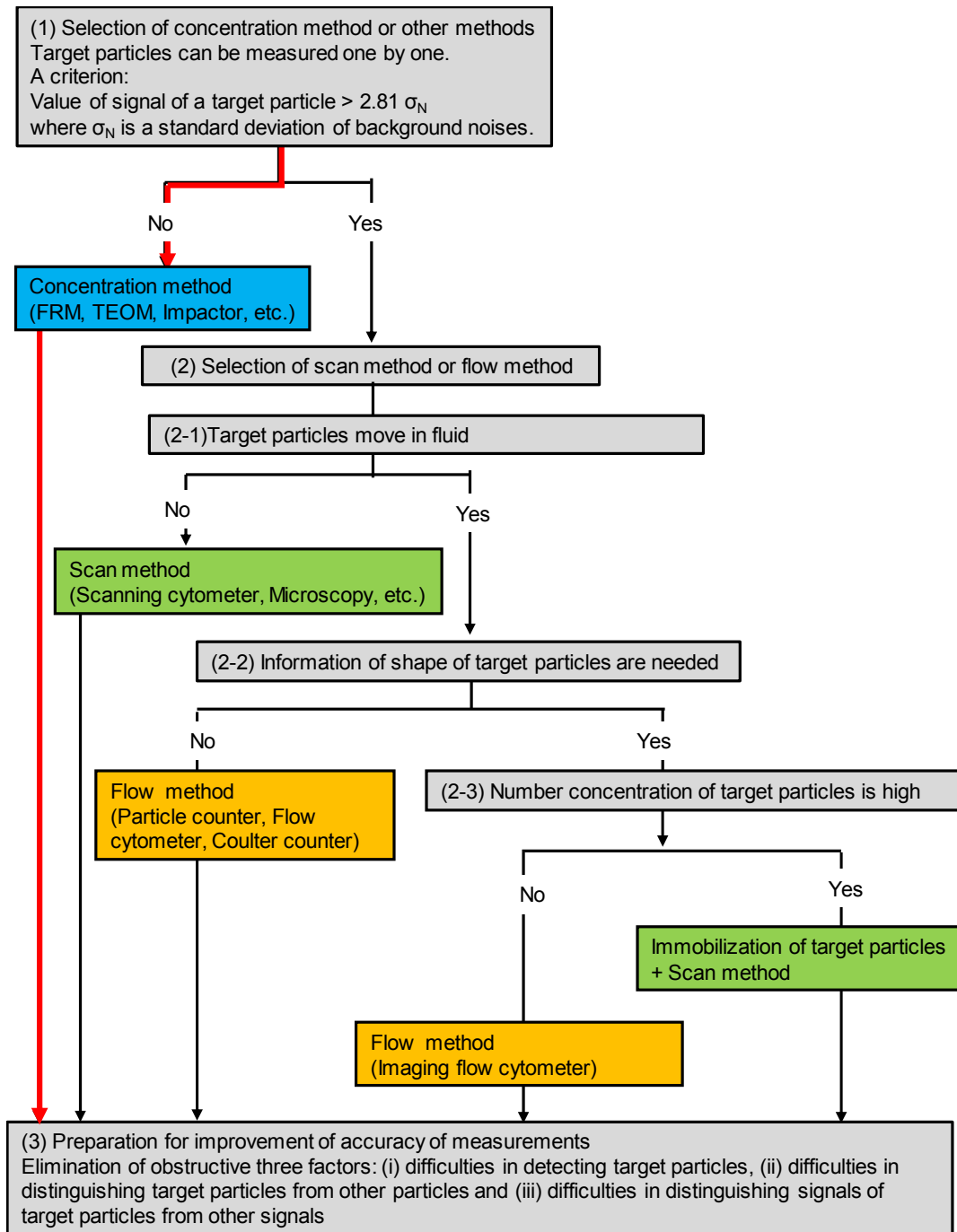
Fig. 5-4 Inspection procedures using a combination method of the impaction and culture methods

Furthermore, histograms of intensity of fluorescence emitted from a bacterium (Figs. 3-31, 3-32, and 3-33) show that intensity of fluorescence from a bacterium is often several times stronger than that of background light. Thereby, under a previous assumption, we presumed that a signal intensity of fluorescence from a 0.3-μm biological aerosol particle is similar to one of background noise. Consequently, we consider that it is difficult to measure 0.3-μm biological aerosol particles labeled with fluorescent dyes one by one. From the above presumption, we select the concentration method among measurements of target particles shown in chapter 2 to measure 0.3-μm biological aerosol particles. The concentration method measures particles in a measuring target sample space by collecting target particles in a probe area.

Next, we consider processes of measurements of 0.3-μm biological aerosol particles using the concentration method. A combined method of an impaction method and a culture method is used commonly to count airborne bacteria [16]. However, it is difficult to measure collected viruses using a culture method because viruses cannot grow by themselves. Otherwise, a plaque method is known as a method to count viruses using cells with the infective potential of the viruses [17]. However, we consider that it is difficult to measure collected viruses rapidly by the plaque method, which needs a long time for cultivation of cells.

For the above reasons, we select a method to measure 0.3-μm biological aerosol particles by a combined method of an impaction method and a fluorescence method whose processes consist of collecting these particles by the impaction method and labeling them with fluorescent dyes. Additionally, we develop a system (SSBAP: Sensing System of Biological Aerosol Particle) which can measure 0.3-μm biological aerosol particles using this combined method.

5.3 Concept of the sensing system of biological aerosol particle
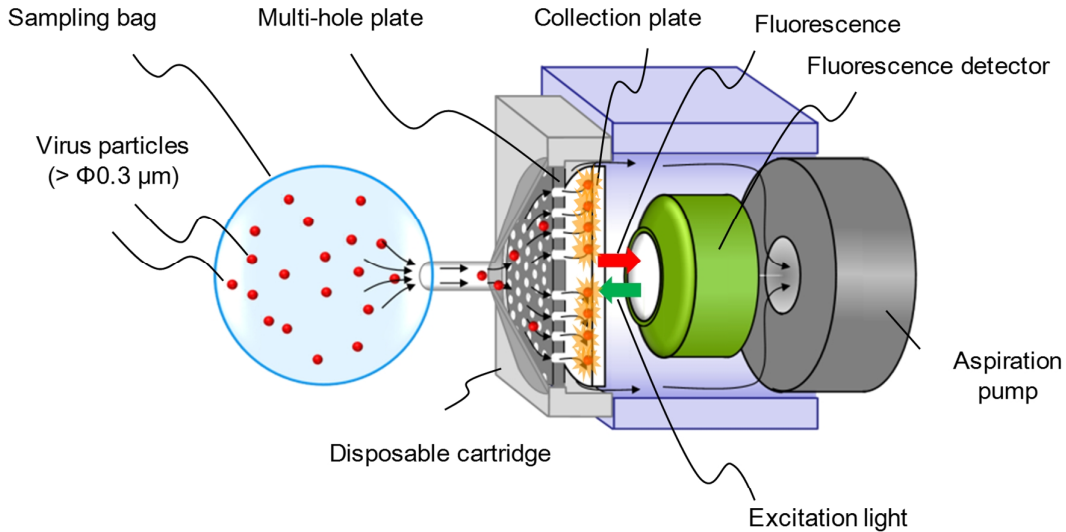
Fig. 5-5 Configuration diagram of SSBAP

Fig. 5-5 shows the configuration diagram of the SSBAP. The SSBAP consists of a sampling bag, disposable cartridge, fluorescence detector, and aspiration pump, and valves (not shown) for the flow control of the breath and reagents.

The SSBAP automates the following detection process in the cartridge (Fig. 5-6): (a) collecting biological aerosol particles on a collection plate in the disposable cartridge by using the impaction method, (b) labeling biological aerosol particles with fluorescent dyes, (c) removing the free dye from the collection plate, and (d) detecting the fluorescence of biological aerosol particles. The SSBAP detection process takes 10 min (collecting: 1 min, labeling: 7 min, washing: 1 min, detecting: < 1 s). The detection process details are as follows.

(a) Collecting biological aerosol particles:

A pump is used to aspirate the air containing biological aerosol particles from the sampling bag. Air flows through the nozzles on the multi-hole plate of the cartridge and impacts onto the surface of the collection plate. The direction of the airflow bends at an almost right angle, and thus the biological aerosol particles in the airflow are removed from it by the inertial force. Biological aerosol particles impact and are collected on the surface of the collection plate under the nozzles.

(b) Labeling biological aerosol particles with fluorescent dyes:

Fluorescent reagents stocked in the cartridge flow over the surface on which the biological aerosol particles are collected. The reagents are liquids containing

fluorescent antibodies, which are antibodies labeled with fluorescent dyes. The florescent antibodies bind to the antigens of the biological aerosol particles on the collection plate on the basis of the antigen-antibody reaction.

(c) Removing free dye from the collection plate:

Free fluorescent dyes attach non-specifically onto the surface of the collection plate in the previous step. The fluorescence of the free fluorescent dyes impedes the detection of the fluorescence of the fluorescent dyes bound to the biological aerosol particles, and thereby the free fluorescent dyes must be removed from the surface for detecting the collected biological aerosol particles on the collection plate. Washings stocked in the cartridge flow over the surface and remove all free fluorescent dyes.

(d) Detecting fluorescence of biological aerosol particles:

The fluorescent dyes binding with the biological aerosol particles emit fluorescence through the irradiation of the excitation light from the fluorescence detector, which irradiates excitation light and detects fluorescence. The SSBAP measures the amounts of the collected biological aerosol particles by focusing on the fluorescence intensity that the fluorescence detector measures.

| Collecting BAPs using impaction | Labeling fluorescent dyes to BAPs | Removing free fluorescent dyes | Detecting fluorescence from BAPs |
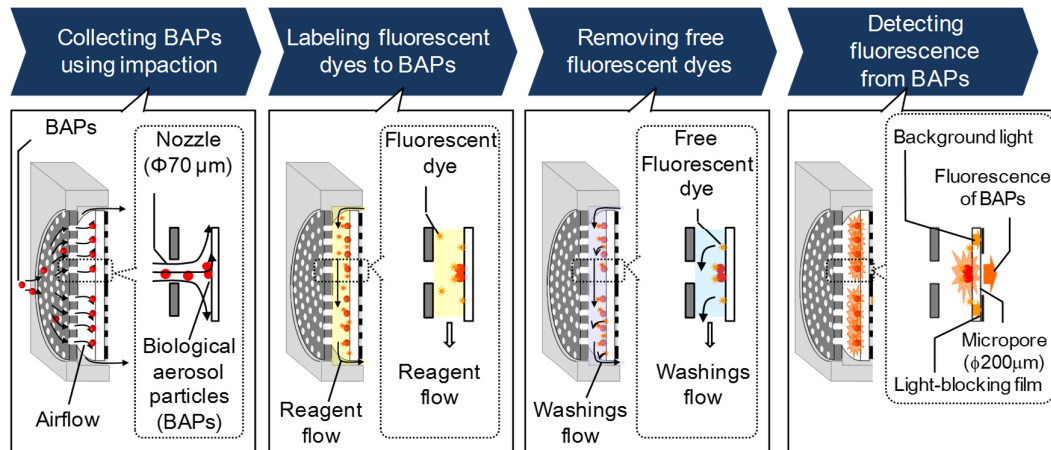
Fig. 5-6 SSBAP detection process of biological aerosol particles

Next, the effect of the light-blocking film covering the collection plate is explained. The fluorescence detector detects background light besides fluorescence from BAPs on the collection plate. Background light is fluorescence from the fluorescent dyes still attached to the surface of the collection plate or autofluorescence of the collection plate and the multi-hole plate. When the intensity of background light is comparable with that of the fluorescence of BAPs, it is difficult to determine whether no amount or only a very small amount of BAPs exists. Therefore, decreasing the amount of background light can improve the sensitivity of the SSBAP.

For this reason, the collection plate of the cartridge is covered with the light-blocking film having pores at biological aerosol particle impact positions. This film blocks background light from the outside of biological aerosol particle impact positions but does not block feeble fluorescence from biological aerosol particles. As a result, the light-blocking film improves the sensitivity of the SSBAP.

5.4 Design of the nozzle

5.4.1 Design procedure

This system uses the commonly used impaction method to collect the biological aerosol particles. However, the targets of the commercial impaction samplers for biological aerosol particles are bacteria which are bigger than 1 μm, and thus these samplers cannot collect the 0.3 – 1.0 μm biological particles targeted in this study [19]. Therefore, we designed a cartridge that has an impaction function to collect small particles larger than 0.3 μm.

Fig. 5-7 shows the concept of a collection part of the cartridge. Air containing airborne biological particles passes through each nozzle on a multi-hole plate. Then, the directions of air flow passing nozzles change on a collection plate. Finally, air flows from the center to an edge of the collection plate.
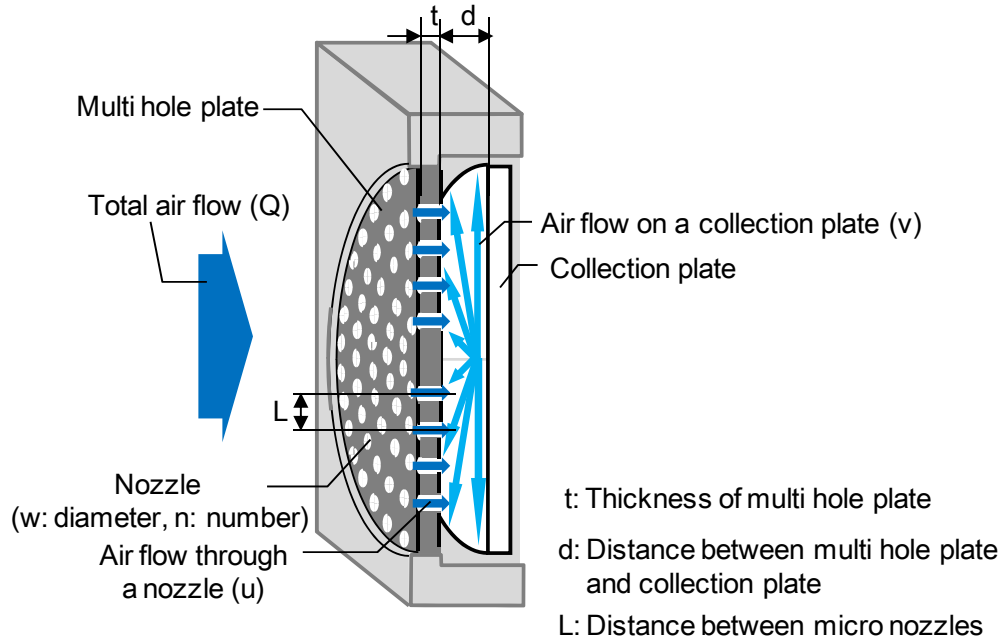
Fig. 5-7 Concept of collection part of cartridge

To design the cartridge, it is necessary to decide diameter of a nozzle (w (m)), distance between nozzles (L (m)), number of nozzles (n), thickness of a multi-hole plate (t (m)), and distance between the multi-hole plate and a collection plate (d(m)) by considering volumetric flow rate of total air flow (Q (m^3/s)), velocity of air flow through a nozzle (u(m/s)), and velocity of air flow on the collection plate (v(m/s)).

It is difficult to decide each parameter for all of the nozzles in the multi-hole plate at one time because it is necessary to consider the interactive effects of air flow through nozzles. Thereby, first, we decide parameters of a single nozzle to collect 0.3-μm biological aerosol particles, which are diameter of a nozzle, thickness of a plate, and velocity of air flow through a nozzle. Next, by considering parameters of a single nozzle, we decide conditions of a multi-hole plate, which are volumetric flow rate of total air flow, velocity of air flow on the collection plate, number of nozzles, and distance between nozzles.

5.4.2 Design of a single nozzle

The Stokes number, which is a dimensionless number corresponding to the behavior of the particles suspended in a fluid flow, is used as the indicator to collect the small aerosol particles by using the impaction method when the air containing particles flows through a small nozzle and impacts the surface of the collection plate.

This number is given as,

$$S_{tk} = C_c \frac{\rho_p d_p^2 u}{9 \mu w} \qquad 5\text{-}1$$

where S_{tk} is the Stokes number, w is the nozzle diameter, u is the velocity of the airflow passing through the nozzle, μ is the viscosity coefficient of the air, ρ_p is the particle density, d_p is the particle size, and C_c is the Cunningham corrective factor.

The particle collection efficiency is almost 100% when the square root of the Stokes number is more than 1.0 and the Reynolds number is more than 10 [20].

Equation 5-1 shows that the particle collection efficiency becomes higher depending on the increase of the particle size. Equation 5-1 shows that the particle collection efficiency becomes higher depending on the increase of the particle size.

In addition to the Stokes number, we had to design the cartridge under conditions that in which airflow through a nozzle is a laminar flow, the pressure loss of the airflow through a nozzle is minimized, and the velocity of the airflow is under a third of the sonic velocity.

The Reynolds number (Re) is used as the indicator of whether the flow is laminar or turbulent. This number is given as

$$Re = \frac{\rho_f u w}{\mu} \qquad 5\text{-}2$$

where Re is the Reynolds number and ρ_f is the fluid density.

The flow is laminar when the Reynolds number is under 2000 [21]. Additionally, the pressure loss of the airflow through a nozzle (ΔP) is given as

$$\Delta P = \frac{64}{Re} \frac{\rho_f l u^2}{2w} + \frac{\rho_f \varsigma_0 u^2}{2} \qquad 5\text{-}3$$

where the first term is the pressure loss in straight pipe, the second term is the pressure loss in sudden expansion and sudden contraction, ρ_f is the fluid density, l is the length of the nozzle, and ς_0 is the pressure loss coefficient [22].

We have to decide whether or not the condition of the pressure loss is less than 30 kPa

in order to use the small pump.

   Fig. 5-8 shows the design condition of the cartridge based on the above conditions: S_{tk} > 1.0, 10 < Re < 2000, ΔP < 30000 Pa, and u < 117 m/s when μ is 1.81 × 10^{-5} Pa·s, ρ_p is 1185 kg/m^3 (which refers to the density of the influenza virus [3]), d_p is 0.3 μm, C_c is for a 0.3 μm particle, a normal atmosphere of 1.55, a ρ_f that is 1.21 kg/m^3 when the temperature is 20ºC, l is 0.5×10^{-3} m, and ζ_0 is 3 [22].
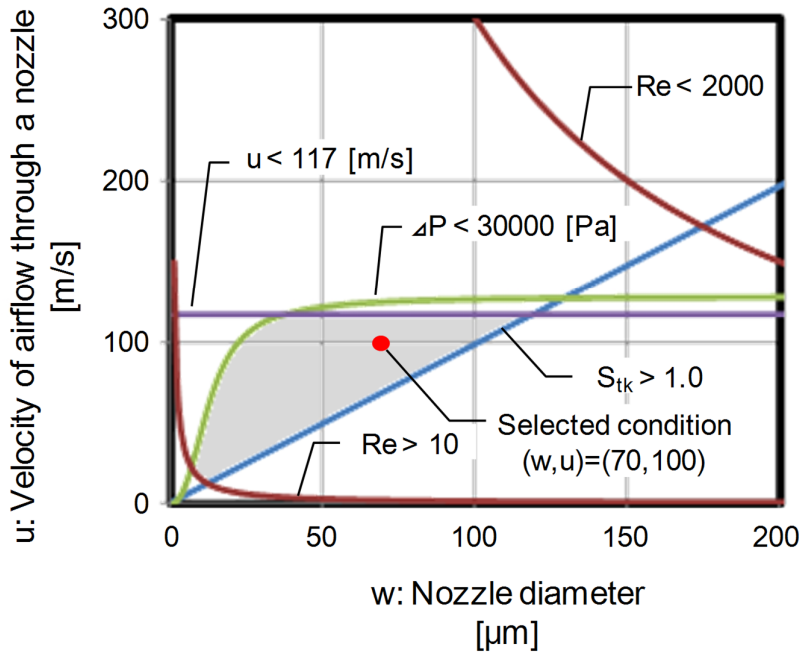
Fig. 5-8 Graph reflecting design condition of the cartridge for collecting aerosolized particles (> φ 0.3 μm)

   The nozzle diameter (w) and velocity of the airflow through a nozzle (u) were selected to be within the shaded area in the graph. We select 100 m/s as u and 70 μm as w in consideration of the workability of the nozzles and the pressure loss of the airflow through the nozzles. Particles larger than 0.3 μm are almost all collected in the selected nozzle diameter (w) and velocity of the airflow thorough a nozzle (u).

5.5 Design of the multi-hole plate

5.5.1 Array of nozzles on the multi-hole plate

   A collection efficiency for particles passing through a multi-hole plate is an average

of collection efficiencies for particles passing through each nozzle on the multi-hole plate. Thereby, the collection efficiency for particles passing through a multi-hole plate is given by

$$I = \frac{\sum_j^N i_j}{N} \qquad 5\text{-}4$$

where i_j is collection efficiency of a certain nozzle and N is total number of nozzle

In this subsection, to calculate the collection efficiency for particles passing through a multi-hole plate, we decide (1) number of nozzles, (2) distance between nozzles, and (3) distance between a multi-hole plate and a collection plate by considering the collection efficiency of each nozzle.

(1) Number of nozzles

First, we consider the number of nozzles. When the flow rate of the air through all nozzles is Q, velocity of air flow through a nozzle is u, and number of nozzles is N, Q, u, and N satisfy the following equation:

$$Q = N\pi \left(\frac{w}{2}\right)^2 u \qquad\qquad 5\text{-}5$$

Q is set to 2.5 L/min to aspirate 3 L of air from the sampling bag in 1 to 2 min, and therefore, N is decided as 109.

(2) Distance between the multi-hole plate and the collection plate

Next, we consider the distance between the multi-hole plate and the collection plate. Biswas showed that a condition for satisfying equation 5-1 is

$$0.5 \leq \frac{d}{w} \leq 5 \qquad\qquad 5\text{-}6$$

where d is distance between a multi-hole plate and a collection plate and w is diameter of a nozzle [23].

Equation 5-6 shows the range of the distance between a multi-hole plate and a collection plate is from 35 to 350 μm when nozzle diameter is 70 μm. However, decrease of the distance between the multi-hole plate and the collection plate increases the velocity of air flow on the collection plate. Consequently, the collection efficiency for particles is decreased. Thereby, we decide that d is 300 μm.

(3) Distance between nozzles

Finally, we decide the distance between nozzles. The distance between nozzles has an effect on the collection efficiency of a multi-hole plate. A shorter distance between nozzles makes it easier to measure particles because particles are collected on a smaller area on the collection plate. However, a shorter distance between nozzles makes the collection efficiency decrease because a higher-speed air flow on the surface of the collection plate prevents particles from impacting on the surface of the collection plate.

Thereby, we conducted track analyses of particles passing through every nozzle of the multi-hole plate. Additionally, by considering analysis results, we defined minimum distance between nozzles for meeting a specification of the collection efficiency of the cartridge.

However, we need an enormous analysis to calculate all tracks of particles passing through the 109 nozzles of the multi-hole plate. Thereby, we conducted track analyses of particles by using the following simplifying model.

Fig. 5-9 shows a simplified model for particle track analysis. Each nozzle on the multi-hole plate has the same shape. However, each velocity of air flow on the collection plate under each nozzle is different. Thereby, by considering a model where some air flows through a nozzle and other air flows onto the collection plate, we calculate a collection efficiency of the simplified model for particles flowing through the nozzle by analyzing tracks of particles. In this case, we considered that the collection efficiency (i) is expressed as a function of a velocity of an air flow on the collection plate (v).
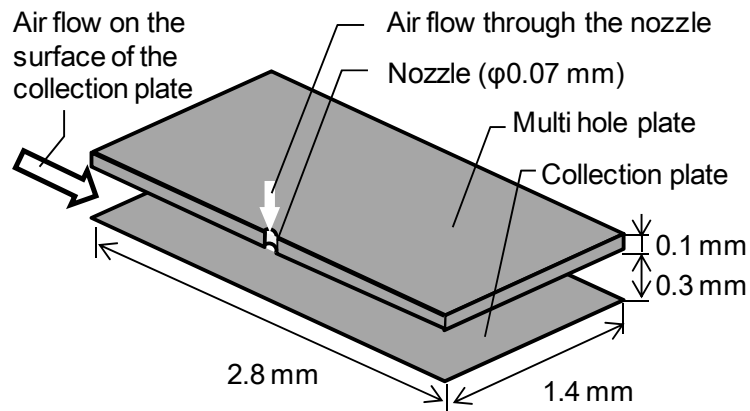
Fig. 5-9 Simplified model of particle track analysis

Particle track analyses are conducted by STAR-CD® (CD-adapco) used widely for fluid analysis. Fig. 5-10 shows a grid model for the particle track analysis. For shortening

calculation time, analyses are conducted on a model axisymmetric about the line passing through the center of the nozzle in the direction of air flow onto the collection plate.
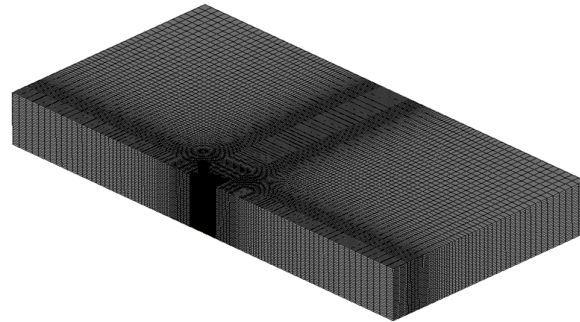
Node number: 328,727
Element number: 311,040

Fig. 5-10 Grid model of particle track analysis

Additionally, Fig. 5-11 shows boundary conditions of the simplified model. Entrance boundaries (red and yellow areas) are set as the following. Velocity of air flow at the inlet port of the nozzle (v_n) is 75, 100, or 125 m/s and velocity of air flow on the collection plate (v_c) is 0, 5.0, 7.5, or 10.0 m/s. Exit conditions (blue) are set as atmospheric pressure.

Entrance boundary (Yellow): v_c (0, 5, 10, 15, 25 m/s)

Wall boundary (Colorless)

Exit boundary (Blue): Atmosphere pressure

Entrance boundary (Red): v_n (75, 100, 125 m/s)

Symmetric boundary (Purple)
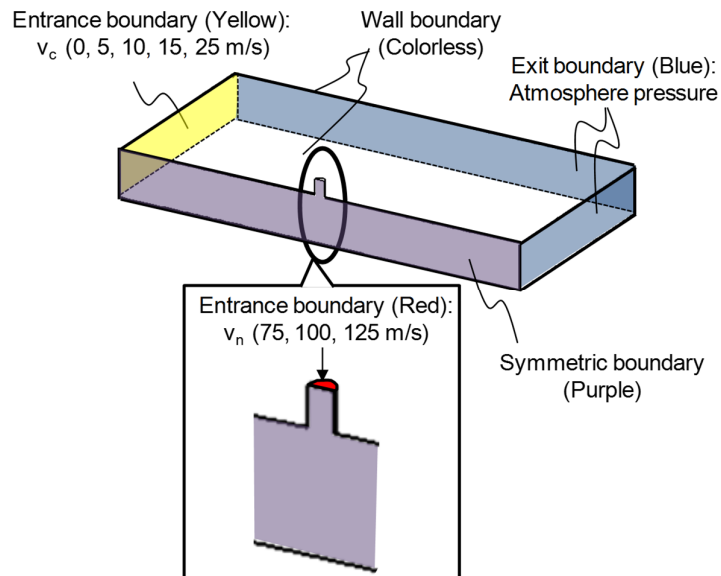
Fig. 5-11 Boundary condition of the simplified model

A particle track analysis is conducted in two steps. The first step is a steady flow analysis and the second step is a Lagrange particle track analysis under the conditions in Table 5-1. A particle track analysis is based on the equation of motion with a drag force and a pressure gradient force (equations 5-7, 5-8, and 5-9) [24]. In the analysis, particles entering cells at the bottom wall at a negative vertical velocity are considered to be collected on the collection plate.

Table 5-1-1 Condition of fluid analysis

Fluid	Ordinary temperature air
Density (kg/m³)	1.205
Coefficient of viscosity (Pa·s)	1.8×10^{-5}

Table 5-1-2 Condition of particle trajectory analysis

Number of particles	480
Initial position of particles	Entrance boundary of air flow through the nozzle
Diameter of particle (μm)	0.3
Density of particle (kg/m³)	1185

$$m_d \frac{du_d}{dt} = \mathbf{F}_{dr} + \mathbf{F}_p \qquad 5\text{-}7$$

where m_d is mass of a particle, $\mathbf{u}_d$ is velocity of a particle, $\mathbf{F}_{dr}$ is drag force, and $\mathbf{F}_p$ is pressure gradient force.

Moreover, drag force is given by

$$\mathbf{F}_{dr} = \frac{1}{2} C_d \rho A_d |\mathbf{u} - \mathbf{u}_d| (\mathbf{u} - \mathbf{u}_d) \qquad 5\text{-}8$$

where C_d is the coefficient of drag, ρ is density of the fluid, A_d is projective cross-section area of a particle, and **u** is velocity of the fluid.

Pressure gradient force is given by

$$\mathbf{F_p} = -V_d \nabla p \qquad \text{5-9}$$

where V_d is volume of a particle and ∇p is the pressure gradient.

Fig. 5-12 (a) and (b) show flow vectors of air flows and particle tracks in the case that velocity of air flow at the inlet port of the nozzle (v_n) is 100 m/s and velocity of air flow on the collection plate (v_c) is 0 m/s.

Next, Fig. 5-13 (a) and (b) show flow vectors of air flow and particle tracks for the case that velocity of air flow at the inlet port of the nozzle (v_n) is 100 m/s and velocity of air flow on the collection plate (v_c) is 25 m/s.

Finally, Fig. 5-14 shows collection efficiency in combinations of v_n and v_c.

(a) Flow vectors　　　　　　　　(b) Particle track analysis
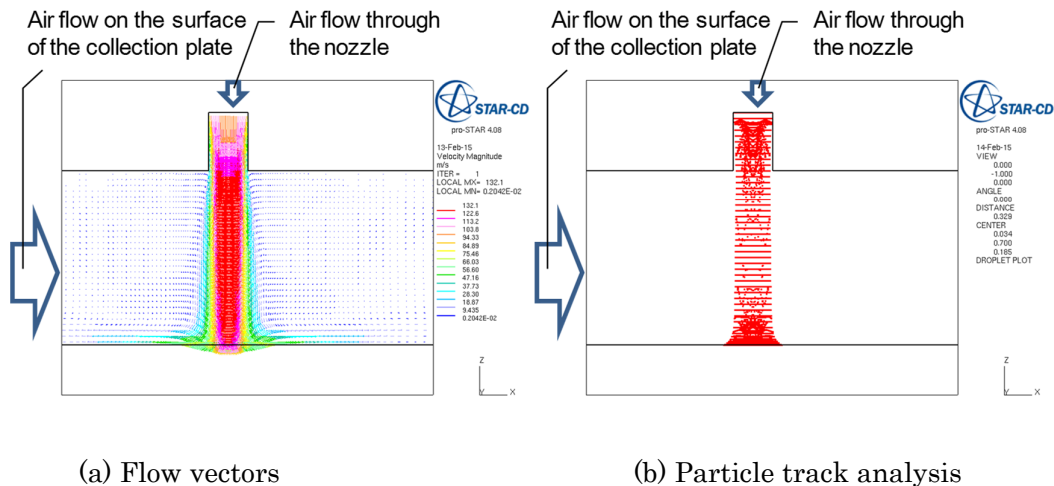
Fig. 5-12 Result of particle track analysis

Air flow on the surface of the collection plate — Air flow through the nozzle

(a) Flow vectors

Air flow on the surface of the collection plate — Air flow through the nozzle

(b) Particle track analysis
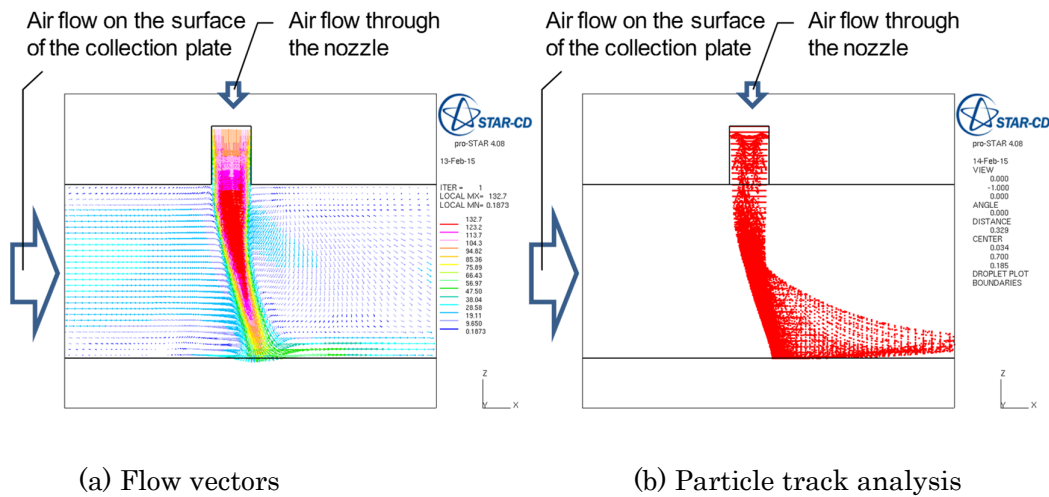
Fig. 5-13 Result of particle track analysis
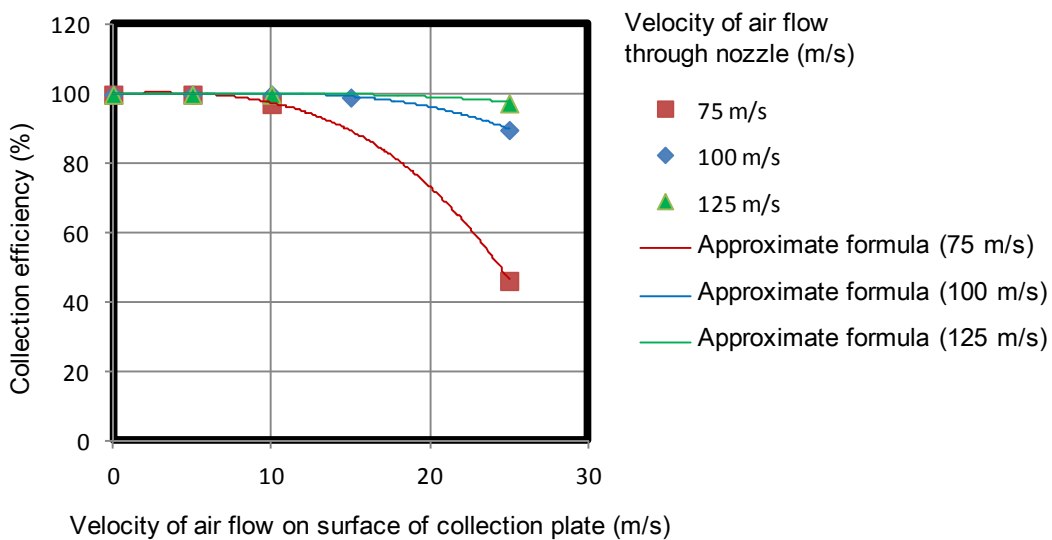
Fig. 5-14 Increasing velocity of air flow on surface of collection plate decreases collection efficiency

The results of particle track analysis in Fig. 5-14 are applied to a design array of nozzles on the multi-hole plate. First, a staggered 60° pattern is selected as an array of nozzles on the multi-hole plate because this pattern has a feature that distances between adjacent nozzles are equal. Fig. 5-15 shows the staggered 60° pattern of the 109 nozzles on the multi-hole plate.

140
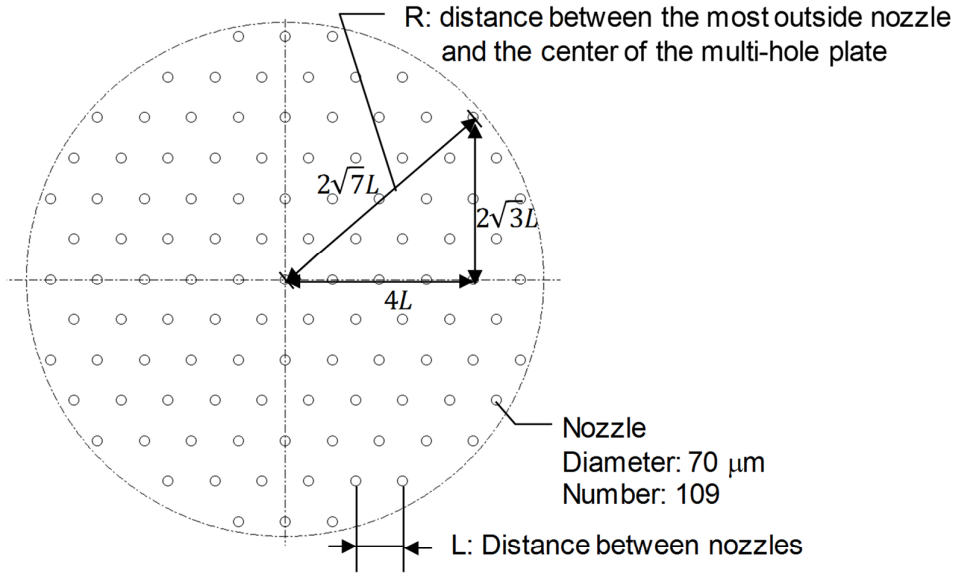
Fig. 5-15 Staggered 60° pattern of 109 nozzles on the multi-hole plate

Next, the distance between nozzles on the multi-hole plate (L) is decided by considering the velocity of air flow on the collection plate. In the case of a staggered 60° pattern of nozzles, number of nozzles per unit area of the multi-hole plate is given by

$$n = \frac{2\sqrt{3}}{3L^2} \qquad\qquad 5\text{-}10$$

where L is distance between nozzles.

The staggered 60° pattern has central symmetry. Thereby, a velocity of air flow on the collection plate under a certain nozzle (v_c) depends on the distance between the center of the nozzle and the center of the multi-hole plate. Moreover, the flow rate of airflows from nozzles inside of a radius r concentric circle of the multi-hole plate is approximated by

$$Q(r) = \pi \left(\frac{w}{2}\right)^2 u \times \pi r^2 \times \frac{2\sqrt{3}}{3L^2} \qquad 5\text{-}11$$

141

where u is velocity of air flow passing through a nozzle, $\pi\left(\frac{w}{2}\right)^2 u$ is flow rate of airflow from a nozzle, and $\pi r^2 \times \frac{2\sqrt{3}}{3L^2}$ is number of nozzles inside of a radius r concentric circle of the multi-hole plate.

Similarly, (Q(r)) is given by

$$Q(r) = 2\pi r \times d \times v(r) \qquad 5\text{-}12$$

where d is distance between the collection plate and the multi-hole plate, and v(r) is velocity of air flow across the circumference of a radius r concentric circle of the multi-hole plate.

Equations 5-11 and 5-12 give v(r) as

$$v(r) = \frac{\sqrt{3}w^2 u r^2}{12L^3 d} \qquad\qquad 5\text{-}13$$

Equation 5-13 shows that the velocity of the airflow under a more outer nozzle is higher. Additionally, equation 5-13 and Fig. 5-14 show that the collection efficiency of the outermost nozzle is lowest. Thereby, the collection efficiencies of all of the nozzles are higher than the target value if one of outermost nozzles is higher than the target value. For these reasons, the distance between nozzles (L) is selected to meet this condition. The distance between the outermost nozzles and the center of the multi-hole plate (R) in Fig. 5-15 is given by

$$R = 2\sqrt{7}L \qquad\qquad 5\text{-}14$$

Fig. 5-16 shows the range of the distance between nozzles (L) suitable to the condition that collection efficiencies of all nozzles be almost 100%. We selected 0.5 mm as L. In the case that L is 0.5 mm, the distance between the outermost nozzle and the center of the multi-hole plate (R) is 2.65 mm. Additionally, velocity of air flow under the outermost nozzle is 8 m/s from equation 5-13.
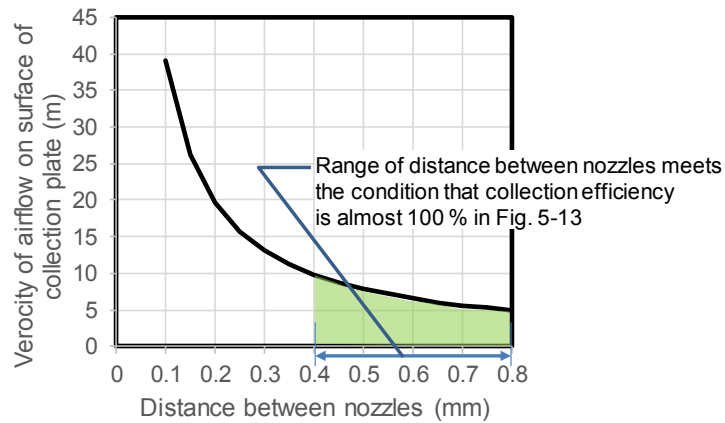
Fig. 5-16 Selection of distance between nozzles on the multi-hole plate

5.5.2 Design of light-blocking film

As mentioned above, areas where particles are collected under nozzles (called collection areas) move just a little from areas just below nozzles by an effect of air flow on the collection plate. Thereby, it is necessary to design a light-blocking film with consideration of the range of sizes of collection areas.

Fig. 5-17 shows a circumscribed circle diameter of a collection area at 0, 5, 10, or 15 m/s velocity of air flow on the collection plate using similar particle track analyses to those in the previous subsection. In Fig. 5-17, the x-axis is a radius of a circumscribed circle of a collection area and the y-axis is a proportion of particles collected on the area to all particles.

Additionally, Fig. 5-17 shows that almost all particles are collected inside a circle of radius 75 μm circle at a velocity of air flow on the collection plate of 0 - 10 m/s. Thereby, we decide the diameter of a pore of the light-blocking film as 150 μm because velocity of airflow on the collection plate under an outermost nozzle was 8 m/s in the above subsection.
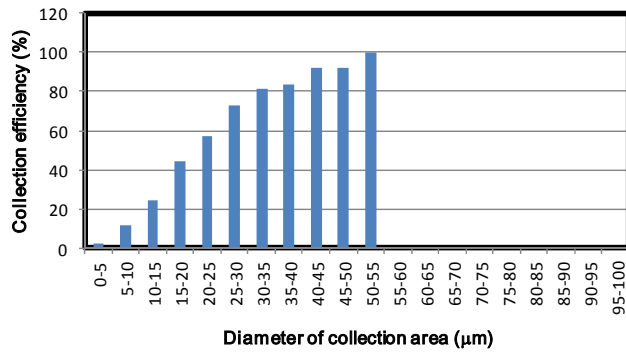
(a) 0 m/s velocity of air flow on the collection plate
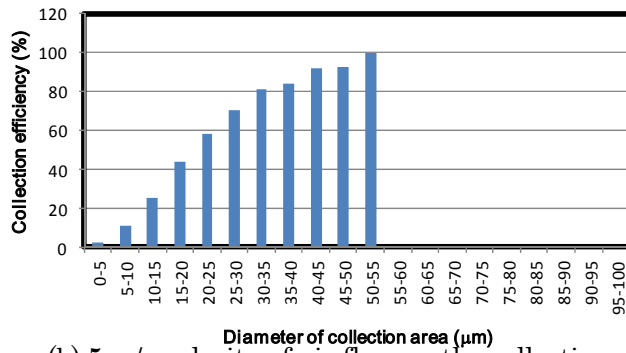
(b) 5 m/s velocity of air flow on the collection plate
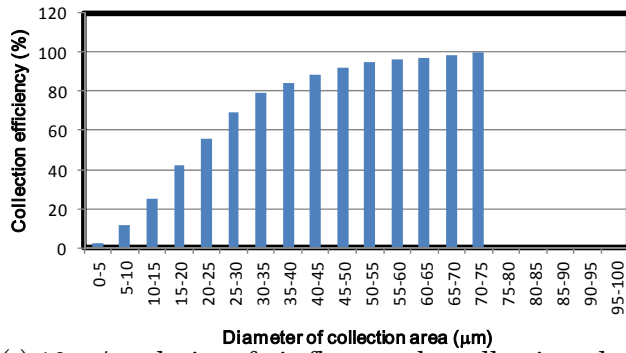
(c) 10 m/s velocity of air flow on the collection plate
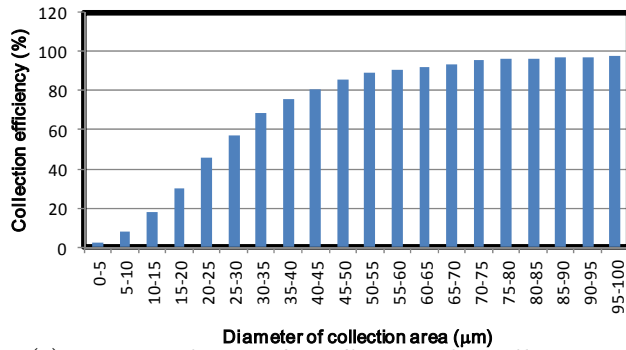
(d) 15 m/s velocity of air flow on the collection plate

Fig.5-17 Diameter of areas where particles are collected under nozzles

5.5.3 Material of multi-hole plate

Next, we select a material for the multi-hole plate by considering material properties: optical property, ease of fabrication and deflection by pressure difference in aspirating air. Table 5-2 shows material properties (optical property, ease of fabrication and physical property) of materials (PET, glass and SUS) [25][26].

Table 5-2 Optical properties, young's modulus and machining easiness of material of multi-hole plate

Properties		PET	Glass	SUS
Optical properties	Transmittance (%)	80-90	90	0
	Relative fluorescence intensity for glass	3	1	0
Physical properties	Young's modulus (MPa)	2×10^3	7×10^4	2×10^5
	Poisson's ratio	0.2	0.27	0.3
Ease of fabrication	Maximum length of φ 70 μm pore (μm)	100	100	500
	Cost of 100 pores (φ 70 μm) (¥)	100	100k-300k	30k-60k

First, glass is an excellent material in the optical property, however unsuitable to disposable use because it needs high-cost wet etching for fabrications of φ 70 μm nozzles on a glass.

Next, SUS is an inflexible material, however needs high-cost fabrication as with a glass. Additionally, SUS is unsuitable to fluorescence detection because SUS reflect almost 100 % the excitation light.

On the other hand, PET film is suitable to disposable use because this is easier in fabrication than SUS and glass. φ 70 μm nozzles on PET film can be made by punching with a laser or pins. Costs to make 109 nozzles by both methods in mass production are smaller than ¥ 100/sheet.

However, PET film is more flexible than SUS and glass. Thereby, it is necessary to check if a deflection of the PET multi-hole plate is within acceptable range by structural analyses of the PET multi-hole plate. The acceptable range is decided as 3 μm which is smaller than 1/100 times distance between the collection plate and the multi-hole plate

(300 μm).

Figs. 5-18 and 5-19 show a conceptual diagram of a multi-hole plate and a model of a structural analysis of the multi-hole plate.
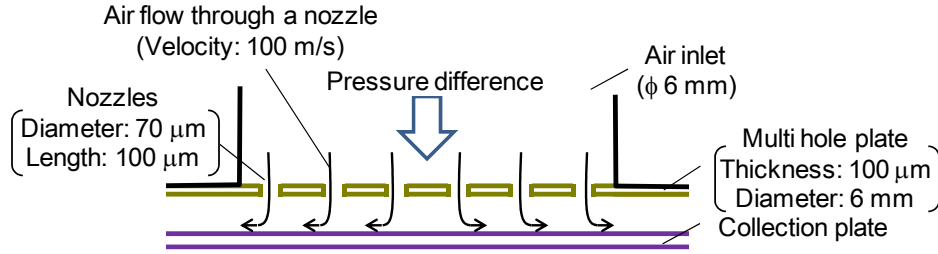
Fig.5-18 Conceptual diagram of a multi-hole plate
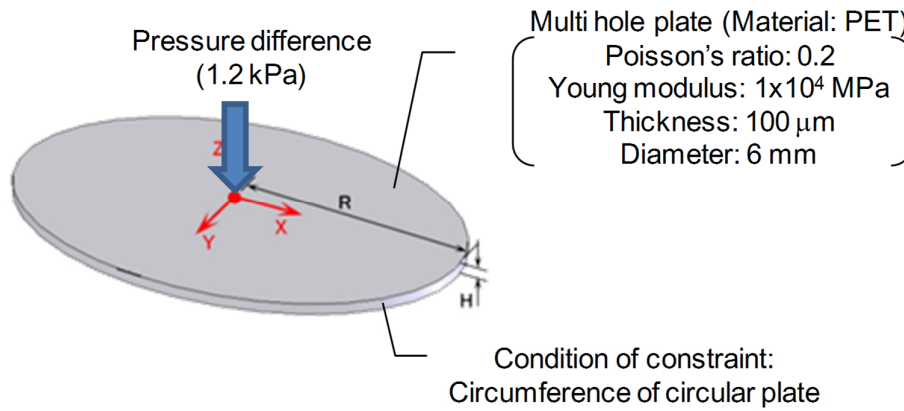
Fig.5-19 Model of a structural analysis of the multi-hole plate

A model of the structural analysis of the multi-hole plate is a circular disk (radius: 6 mm, thickness: 0.1 mm, material: PET) with a fixed circumference because the multi-hole plate is fixed on the ϕ 6 mm inlet. Additionally, the pressure difference in aspirating air is equal to pressure loss of the airflow through a nozzle (ϕ 70 μm). Thereby, the pressure difference in aspirating air is given by equation 5-14.

$$\Delta P = \frac{64}{Re} \frac{\rho_f l u^2}{2w} + \frac{\rho_f \varsigma_0 u^2}{2} \qquad 5\text{-}14$$

Then, equation 5-14 shows that the pressure difference (ΔP) is 1.2 kPa under the conditions shown in Fig. 5-18.

Finally, using the above conditions, the deflection of the PET multi-hole plate (Δy) in

Fig. 5-19 is calculated by FEXSOLVER. The structural analysis in Fig. 5-19 shows the deflection of the PET multi-hole plate (Δy) at the center is 1.8 μm and is smaller than the acceptable value (3 μm).

5.6 Counting loss in concentration method by impaction

We consider the measuring range of the SSBAP for the number of biological aerosol particles by using the theory of counting loss in the concentration method in Chapter 2, section 4.

Biological aerosol particles are collected on areas just below nozzles. Thereby, the volume of the target sample space (V_t) in the concentration method is equal to the product of the areas of the 109 nozzles and the diameter of a biological aerosol particle (d). Additionally, the volume of the probe space (v_p) is equal to the volume of biological aerosol particles ($\frac{4}{3}\pi\left(\frac{d}{2}\right)^3$).

Moreover, equation 2-16 gives the counting loss in the impaction method as

$$P = 1 - e^{-\left(\frac{N_r}{109sd} \times \frac{4}{3}\pi\left(\frac{d}{2}\right)^3\right)} \qquad 5\text{-}15$$

where N_r is the real number of collected biological aerosol particles

Thereby, equation 5-15 gives the number of biological aerosol particles in view of the counting loss (N_c) as

$$N_c = N_r(1 - P)$$
$$= N_r e^{-\left(\frac{N_r}{109sd} \times \frac{4}{3}\pi\left(\frac{d}{2}\right)^3\right)} \qquad 5\text{-}16$$

Then, equation 5-16 is applied to calculations of N_r in measurements of ϕ 0.3 μm aerosolized virus particles or ϕ 1.0 μm aerosolized bacteria.

First, we consider N_c under the condition that d is 0.3 μm, s is $\pi\left(\frac{70}{2}\right)^2$ μm^2, and N_r is from 0 to 4×10^5 particles. N_c and N_r are shown in Fig. 5-20.
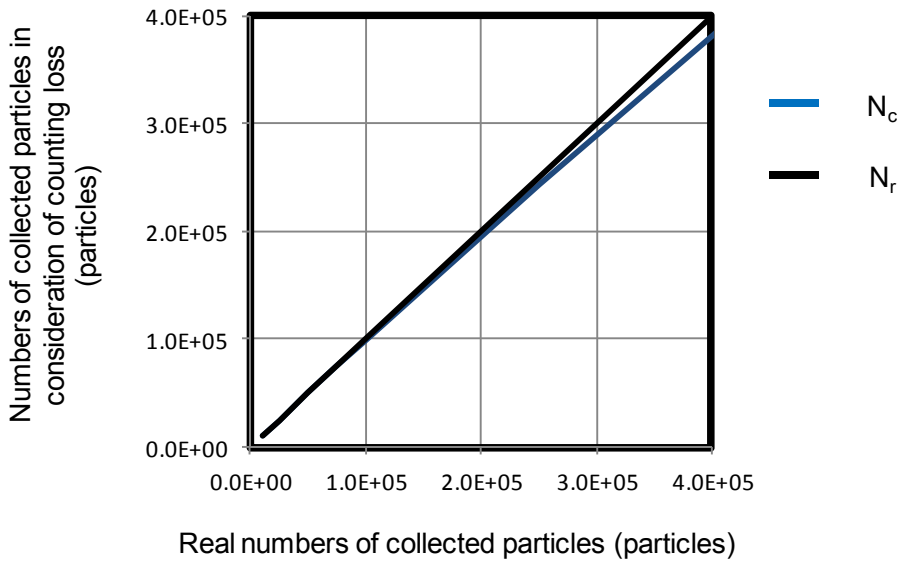
Fig.5-20 Theoretical value of number of 0.3 µm biological aerosol particles measured by the system

Fig. 5-20 shows that there is a very small difference between Nr and Nc in the range of the number of biological bacteria from 0 to 4×10^5 particles.

Next, we consider N_c under the conditions that d is 1.0 µm, s is $\pi\left(\frac{70}{2}\right)^2$ µm², and N_r is from 0 to 4×10^5 particles. N_c and N_r are shown in Fig. 5-21.
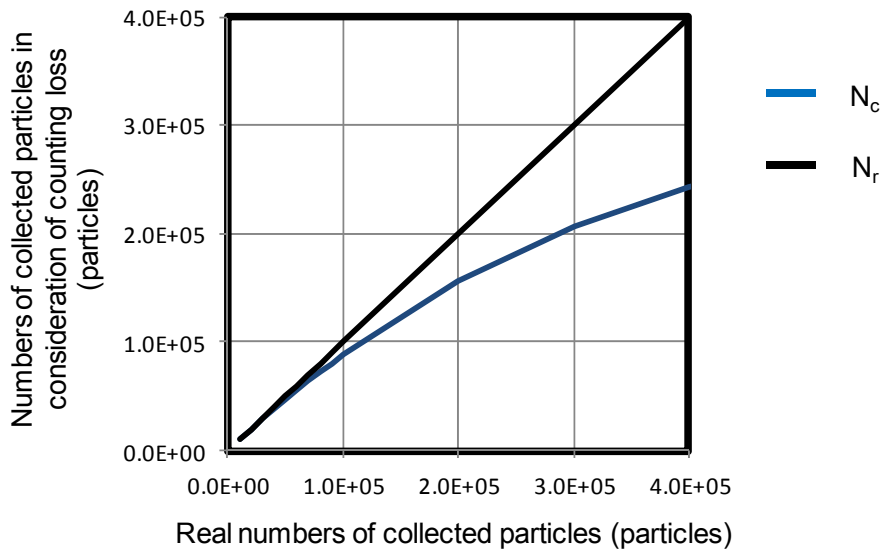
Fig.5-21 Theoretical value of number of ϕ 1.0 µm biological aerosol particles measured by the system

Fig. 5-21 shows that there is a large difference between N_r and N_c at more than 1×10^5 particles. We consider the reason to be as follows. Areas under nozzles are filled with fewer larger particles in the concentration method. Thereby, the counting loss of ϕ 1.0 µm particles becomes larger than that of ϕ 0.3 µm particles.

5.7 Fabrication process of the impaction cartridge

Fig. 5-22 shows a photograph of the disposable cartridge. This cartridge has a multifunctional part, reservoirs, and channels. The reagent reservoir, washings reservoir, waste reservoir, and the multifunctional part are connected with the channels. The reagent or washings flow from the reservoirs into the waste reservoir via the multifunctional part.

Fig. 5-23 and Fig. 5-24 show the A-A' cross-section view of the multifunctional part and assembly drawing of the disposable cartridge. The cartridge consists of a bottom part (acrylonitrile-butadiene-styrene resin, 60 mm × 60 mm × 10 mm) with reservoirs and channels, a multi-hole plate (light-permeable polyethylene terephthalate, 100 µm thick) with nozzles (ϕ 70 µm), a glass collection plate covered with a light-blocking film (light-blocking polyethylene terephthalate, 20 µm thick) with micropores (ϕ 200 µm), and a spacer (double-stick water-resistant tape, 300 µm thick). The multi-hole plate and the bottom part are adhered using double-stick tape (100 µm thick).
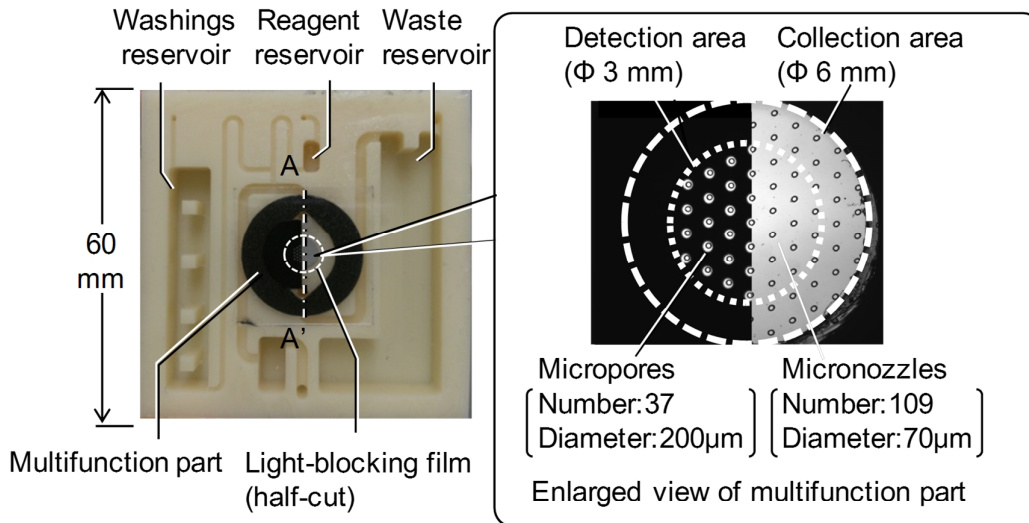
Fig.5-22 Photograph of impaction cartridge
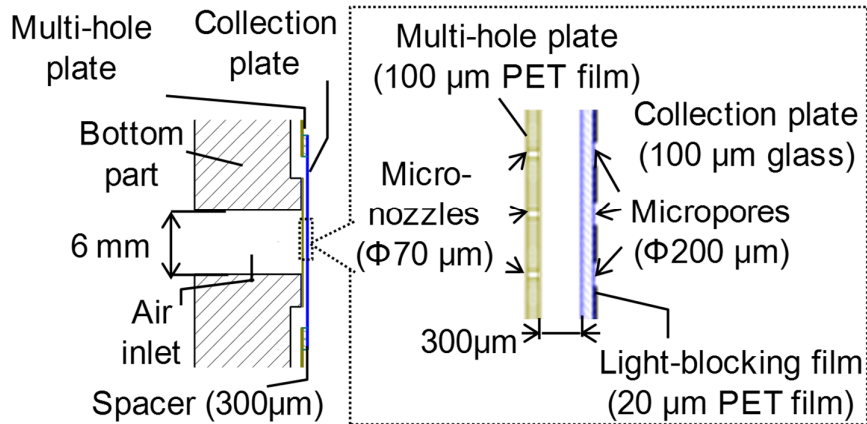
Fig.5-23 Sectional view of impaction cartridge
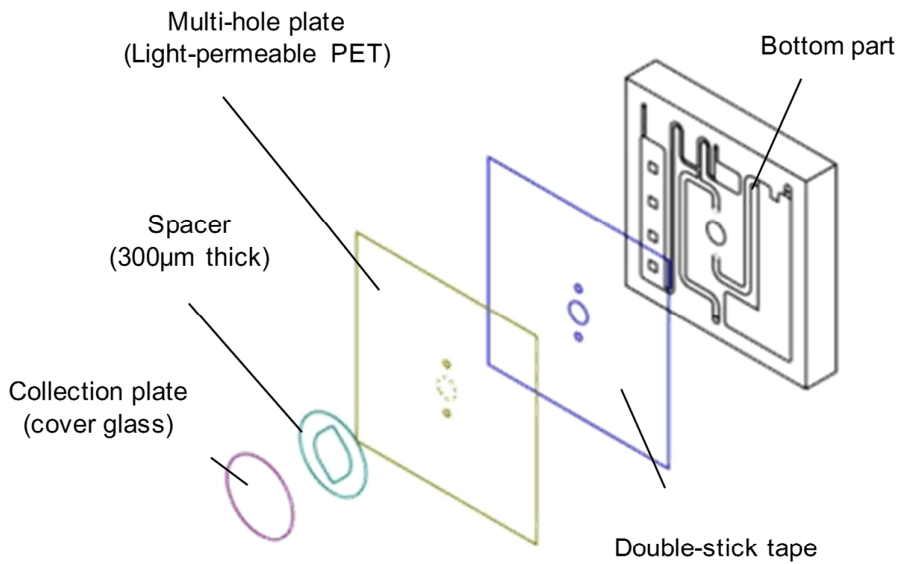
Fig.5-24 Assembly drawing of impaction cartridge

Aspirated air flows from the air inlet into the channels through the nozzles and the gap between the multi-hole plate and the collection plate. On the other hand, the reagent and washings flow from the upper channel to the lower one through the gap.

The 109 nozzles on the multi-hole plate are arranged in a staggered, 60° pattern at a 0.5 mm pitch. Nozzles of the multi-hole plate and pores of the light-blocking film are made by punching the original film with a Tea-CO$_2$ laser and placed so as to overlap. Pores were made only near the center (ϕ 3 mm) because outer impact positions of

biological aerosol particles are moved from positions under nozzles by air flows.

One of the functional features of the cartridge is that the multifunctional part consists of the multi-hole plate, the glass collection plate, and a spacer, which work as an impactor for the collection of biological aerosol particles, a flow-cell for the reagents or washings flows, and an optical window for the fluorescence detection. Additionally, a light-permeable PET, which is a material of a multi-hole plate, is less deformed and produces little autofluorescence and reflected light that disturbs the fluorescence detection of the biological aerosol particles [27].

The detection process in the cartridge is as follows. Air containing biological aerosol particles flows through the air inlet into the nozzles and impacts onto the surface of the collection plate at 100 m/s. The biological aerosol particles removed from the airflow are collected on the surface of the collection plate.

After that, the stocked reagents in the reservoir flow through the gap between the multi-hole plate and the collection plate in order to label the biological aerosol particles with fluorescent dyes and remove any free fluorescent dyes from the surface of the collection plate. The reagents passing through the surface of the collection plate are stocked in the waste reservoir.

Finally, the fluorescence detector detects the fluorescence of the biological aerosol particles on the collection plate, and thus, the amounts of the biological aerosol particles are measured on the basis of the light intensity of the fluorescence of the biological aerosol particles.

5.8 System configuration

5.8.1 Optical unit

Fig. 5-25 shows a diagram of the optical system in the fluorescence detector of the SSBAP. The optical unit for a coaxial epi-illumination is designed using optical illumination design software to uniformly irradiate the detection area (ϕ 6 mm) where the biological aerosol particles are collected. Table 5-3 shows specifics of the optical unit and Table 5-4 shows parts of the optical unit.

DA: Detection area,
 L1, L2: Lense
LED: Light emitting diode
M: Mirror
BPF1, BPF2: Band-pass filter
DM: Dichronic mirror
PMT: Photomultiplier tube
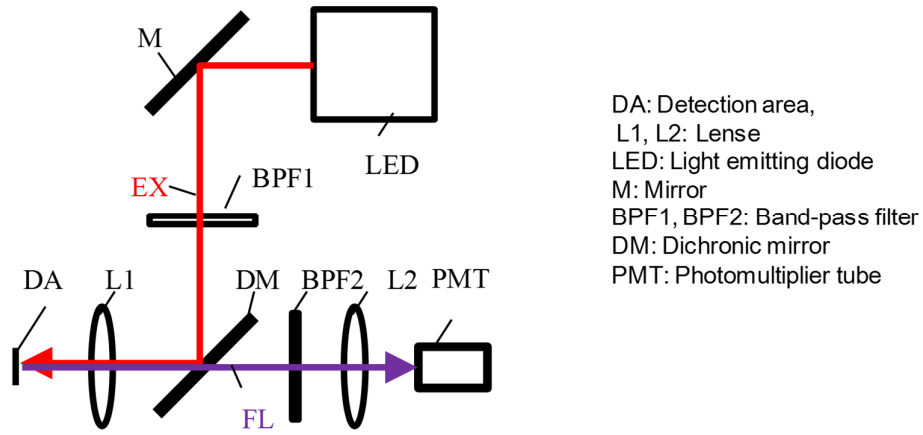
Fig.5-25 Optical unit of fluorescence detector

Table 5-3 Specification of optical unit

	Specification
Detection area	Size: ϕ 6 mm, Intensity of excitation light: > 75% of maximum
Wavelength of excitation light	CWL: 625 nm, FWHM: 40 nm
Wavelength of fluorescent light	CWL: 700 nm, FWHM: 40 nm

Table 5-4 Parts of optical unit

	Item	Part number	Necessary functions	Specification	Mfr.
Plano-convex lens	L1	-			Asahi spectra
	L2	-			Asahi spectra
Mirror	M	-	Reflection of excitation lights of 625 nm LED		Asahi spectra
Dichroic mirror	DM1	DM660	Reflection of excitation lights of 625 nm LED and transmission of fluorescence lights of Hilite Fluore™647	Single dichroic mirror Wavelength of 50% transmittance: 660 nm	Asahi spectra
Band-pass filter	BP1	BP625-20	Transmission of excitation lights of 625 nm LED	CWL: 625 nm, FWHM: 40 nm	Asahi spectra
	BP2	BP700-20	Transmission of fluorescence light of Hilite Fluore™647	CWL: 700 nm, FWHM: 40 nm	Asahi spectra
LED		M625L2	Red light emitting diodes	Wavelength:625 nm	Thorlabs
PMT	PMT	H10722-20	Transmission of fluorescence light of Hilite Fluore™647	Detection wavelength band: 300nm～920nm Wavelength at maximum sensitivity: 630 nm	Hamamatsu photonics

The optical unit irradiates the collection area with red excitation light (wavelength band 625 ± 20 nm) and detects near-infrared fluorescence by the PMT because the PET film, which is the material of the multihole plate of the disposable cartridge, emits autofluorescence that is weaker in the longer wavelength [28].

Fig. 5-26 shows the analysis results of the intensity distribution of the excitation light

on the detection area of the collection plate.
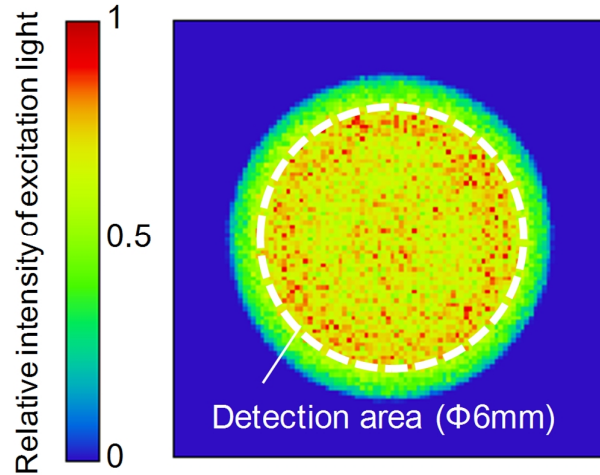
Fig.5-26 Relative intensity of excitation light on detection area

The analysis results show that 75% of the excitation light from the light source is irradiated onto the collection area and the optical unit meets specifications. Additionally, the analysis results show that 85% of the fluorescence from the detection area enters the acceptance surface of the photomultiplier tube (PMT)

5.8.2 Appearance of the SSBAP

Fig. 5-27 shows a photograph of the SSBAP. The SSBAP is 310 mm × 350 mm × 320 mm. It is composed of the fluorescence detector for the fluorescence detection and the control unit for the flow of the patient's breath, the reagents, or the washings in the cartridge. An examiner sets up the SSBAP with the sampling bag filled with patient's breath and the disposable cartridge. Next, they start the detection process of the SSBAP. Then, the SSBAP indicates a result on the basis of the number of biological aerosol particles in the sampling bag.
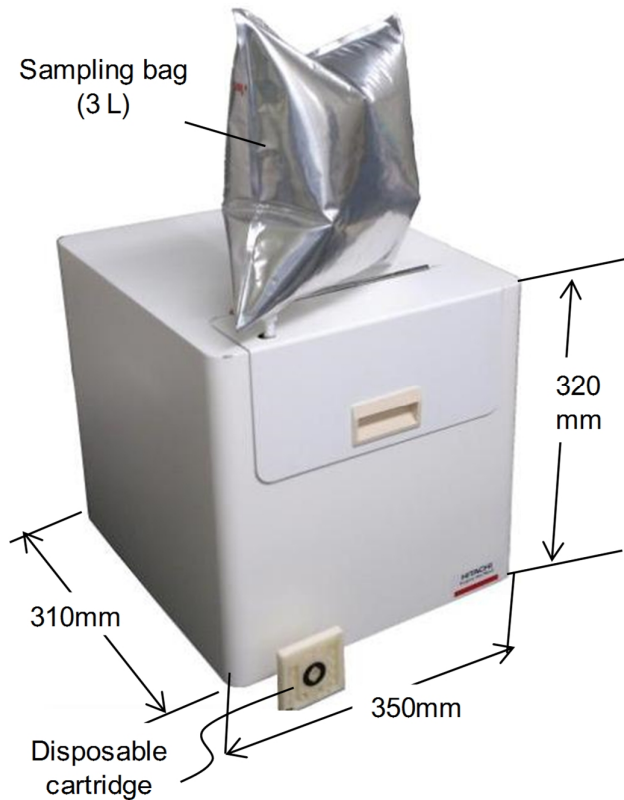
Fig.5-27 Photograph of the SSBAP

5.9 Collection efficiency of cartridge

5.9.1 Evaluation of collection efficiency of cartridge

We evaluated the collection efficiency of the disposable cartridge for aerosol particles in the sampling bag. It is important to use particles of uniform size in evaluations of the collection efficiency of the cartridge.

Thereby, we used polystyrene microspheres (Nanobead NIST Traceable Particle Size Standard 300 nm, Polysciences Inc.), which are used as standard reference materials, as substitutes for the smallest biological aerosol particles. Table 5-5 shows the specifications of these particles.

Table 5-5 Specifications of Nanobead NIST Traceable Particle

	Specifications
Particle size	$0.3 \pm 0.05 \ \mu m$
CV	3.2%
Density	1.05

Additionally, the collection efficiency for the aerosolized particles in the cartridge was evaluated as follows. Since the number of particles collected in the cartridge is difficult to measure, we focus on the difference between the number of aerosolized particles in the sampling bag and the number of particles passing through the cartridge. The collection efficiency of the cartridge (C) was given as

$$, \qquad C = \frac{N_{in} - N_{out}}{N_{in}} \qquad 5\text{-}17$$

where N_{in} is the concentration of particles in the sampling bag and N_{out} is the concentration of particles in the air passing through the cartridge. Both concentrations were measured by using the particle counter.

The following helps to better explain the standard experimental procedure.

(1) Spreading particles in a sampling bag

We spread microspheres in the sampling bag (3L) using an ultrasonic nebulizer (NE-U07, OMRON), filled this bag with dry gas, and then left it for 5 minutes to evaporate any micro water droplets because the sampling bag contains many water droplets of several micrometers shortly after aerosolization, but most droplets evaporate and vanish after 5 min of aerosolization [28].

(2) Measuring numbers of particles in the sampling bag

We measured the concentration of microspheres in the sampling bag using a particle counter (237B, Hach Ultra). The sampling bag, a flow meter, an aspiration pump (DP0110, Nitto koki) and a particle counter (237B, Hach Ultra) are connected in series (Fig. 5-28). We checked separately that the flow meter and the aspiration pump make little decrease of numbers of particles. A channel between the aspiration pump and the particle counter is branched off to be opened because an aspiration volume of the particle counter is larger than one of the aspiration pump.

We measured numbers of particles with the particle counter in 10 s after driving the aspiration pump.
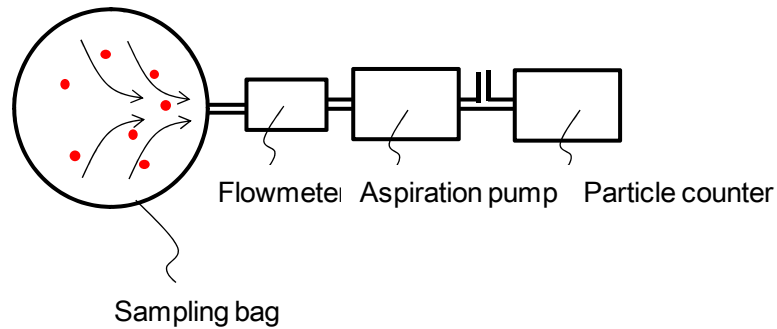
Fig.5-28 Experiment system for evaluation of collection efficiency

(3) Measuring numbers of particles passing through the cartridge

We measured the number of particles in the air passing through the cartridge using the experimental system containing the sampling bag, the disposable cartridge, a vacuum pump (DP0110, Nitto koki), and the particle counter (237B, Hach Ultra), which are connected in series (Fig. 5-29).

We measured numbers of particles passing through the cartridge with the particle counter in 10 s after driving the aspiration pump.
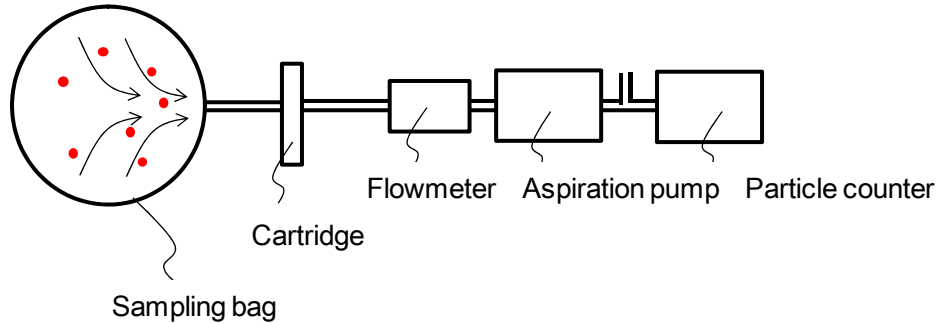
Fig.5-29 Experiment system for evaluation of collection efficiency

Fig. 5-30 shows the measured collection efficiency of the disposable cartridge for the aerosolized microspheres in the sampling bag. This disposable cartridge can collect most aerosolized microspheres (ϕ 0.3 μm) as substitutes for the smallest biological aerosol particles because the collection efficiency results were more than 97%.
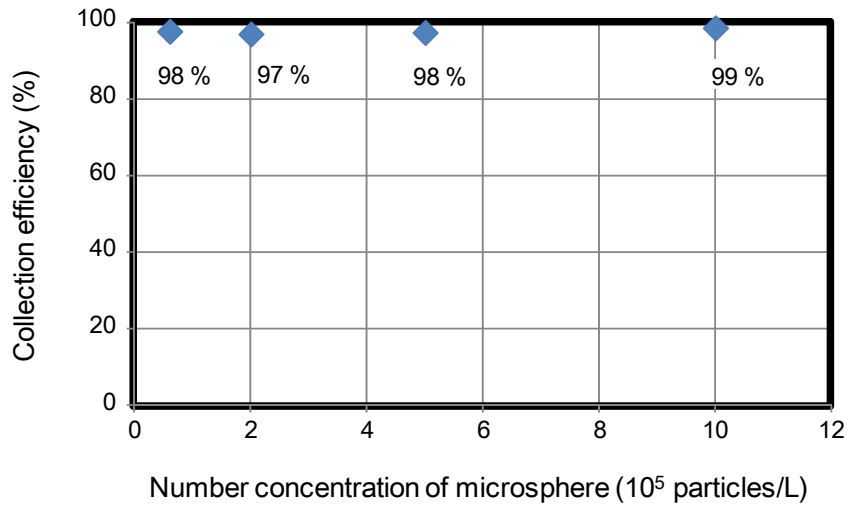
Fig.5-30 Collection efficiency of cartridge for 0.3 μm particles

5.9.2 Impaction position of particles

The collection plate of the cartridge is covered with a light-blocking film having pores at biological aerosol particle impact positions under nozzles. This film blocks background light from the outside of biological aerosol particle impact positions but does not block weak fluorescence from biological aerosol particles.

Thereby, the light-blocking film has the possibility of blocking fluorescence from biological aerosol particles if the impact positions of particles move from predicted impaction positions.

In this subsection, we evaluated impaction positions of particles by experiments. Experimental procedure is shown in the follows.

(1) Spreading particles in a sampling bag

As with the previous subsection, we spread particles in the sampling bag (3L) using an ultrasonic nebulizer (NE-U07, OMRON), filled this bag with dry gas, and then left it for 5 minutes to evaporate any micro water droplets.

(2) Measuring particles in the sampling bag

The sampling bag, the cartridge and the aspiration pump are connected in series. Particles in the sampling bag are collected on the collection plate of the cartridge in the aspiration of air in the sampling bag by the aspiration pump.

(3) Measurement of impaction area of particles

We measured every impaction areas of particles on the collection plate under nozzles with a digital micro scope (VHX-700F, Keyence).

Fig. 5-31 shows a measurement method of impaction positions. We set a minimum circle including an impaction area. This circle is called the circle of the impaction area. Additionally, we measured diameter of the circle of the impaction area, distance between the center of a nozzle and the center of the circle of the impaction area, and angle between the horizontal line and the line connecting the center of the circle of the impaction area and the center of the nozzle.
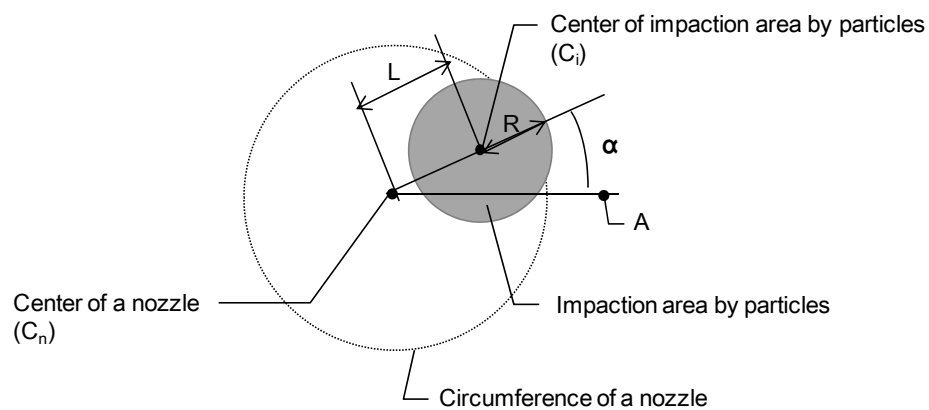
L: Distance between center of a nozzle and center of impaction area
R: Radius of impaction area
α: angle of $C_i C_n A$

Fig.5-31 Measurement of impaction points

Fig. 5-32 shows experimental results for four times. In Fig. 5-32, black circles show positions of nozzles and blue circles show circles of impaction areas.
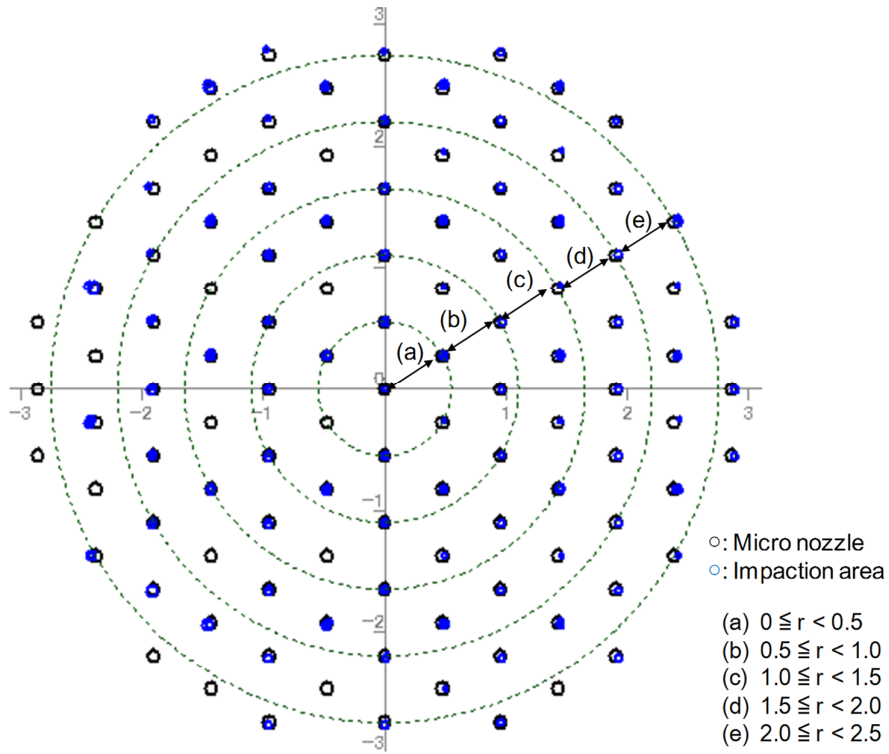
Fig.5-32 Impaction positions of particles

Next, we divided the nozzles shown in Fig. 5-32 into the following five groups: (a) nozzles inside a circle of radius 0.50 mm, (b) nozzles outside a circle of radius 0.50 mm and inside a circle of radius 1.0 mm, (c) nozzles outside a circle of radius 1.0 mm and inside a circle of radius 1.5 mm, (d) nozzles outside a circle of radius 1.5 mm and inside a circle of radius 2.0 mm, and (e) nozzles outside a circle of radius 2.0 mm and inside a circle of radius 2.5 mm. Additionally, we measured average diameter of circles of the impaction areas shown in Fig. 5-33 and average distance between the center of a nozzle and the center of the circle of the impaction area under the nozzle shown in Fig. 5-34.
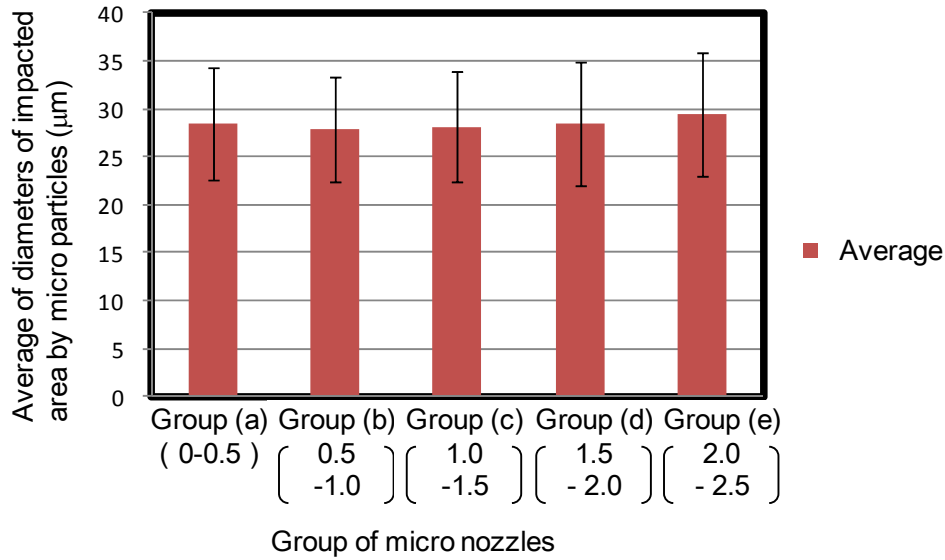
Fig.5-33 Average of circles of the impaction areas
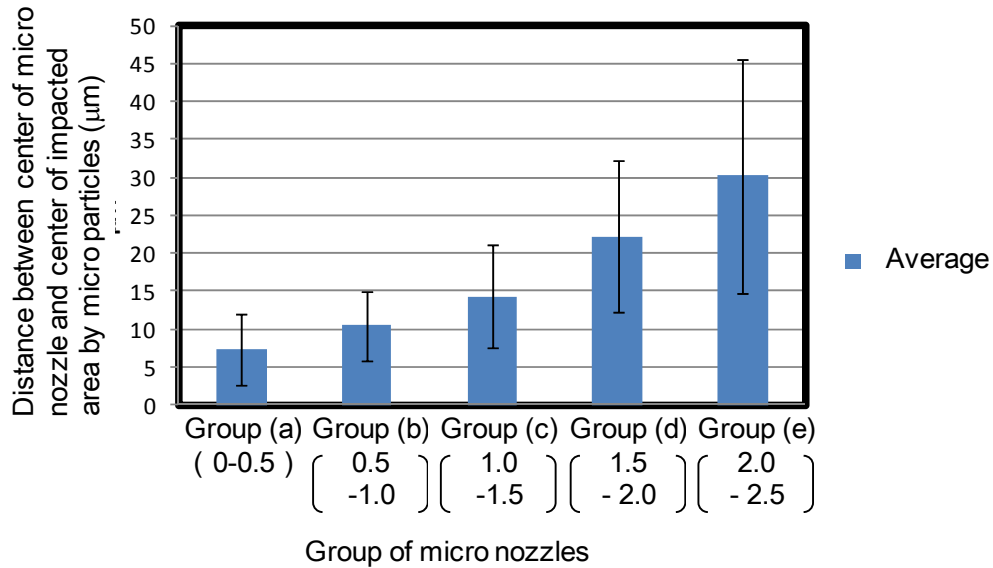
Fig.5-34 Distance between center of a nozzle and center of the circle of the impaction area

   Fig. 5-33 shows that the averages of diameters of circles of impaction areas are from 25 to 30 μm regardless of the position of the circle of the impaction area. However, Fig. 5-33 shows that the averages of distances between centers of nozzles and centers of circles

of impaction areas become larger at positions further outward from the center of the multi-hole plate. The distances between the centers of the outermost nozzles and the centers of the impaction area circles are from 15 to 45 μm.

Therefore, impaction areas are included inside pores of light-blocking film (150 μm) by considering the averages of the diameters of circles of impaction areas, and the distances between centers of nozzles and centers of circles of impaction areas.

5.10 Measuring biological aerosol particles

5.10.1 Measuring aerosolized Escherichia coli

We evaluated the detection performance of the SSBAP and the disposable cartridge without the light-blocking film for biological aerosol particles in the sampling bag. We used *E.coli* bacteria (BacTrace *Escherichia* O157:H7 positive control, KPL) as the substitute aerosolized bacteria and Hilite Fluore^{TM}647 (Anaspec) conjugated anti-E.coli antibodies (Anti-E.coli O157:H7, Goat-Poly, KPL) as the fluorescent dyes.

The experimental procedure was as follows.

(1) Spreading E. coli in a sampling bag

First, we spread biological aerosol particles in the sampling bag (3L) using an ultrasonic nebulizer (NE-U07, OMRON), filled this bag with dry gas, and left it for 5 minutes to evaporate any micro water droplets.

(2) Measuring E. coli in the sampling bag

Second, we measured the concentration of E.coli using the particle counter (237B, Hach Ultra).

(3) Measurement of aerosolized E. coli in the sampling bag by the SSBAP

Finally, we set this sampling bag and the cartridge in the SSBAP and started the detection process using the SSBAP. Table 5-6 lists the experimental conditions for the detection process in the SSBAP.

Table 5-5 Experimental procedure for detection performance of SSBAP

Step	Reagent (volume μl)	Time
Collecting biological aerosol particles	-	1 min
Labeling fluorescent dyes to biological aerosol particles	Hilite Fluore^{TM}647 conjugated anti-Ecoli antibodies (200 μl)	7 min
Removing free fluorescent dyes	Distilled water (2000 μl)	1 min
Detecting fluorescence from biological aerosol particles	-	<1 sec

Fig.5-35 shows measurement results of aerosolized E. coli in the sampling bag using the SSBAP. The intensity difference of the fluorescence is the difference between intensity of the fluorescence in a certain concentration of E.coli and that in zero particles/L concentration of E.coli.
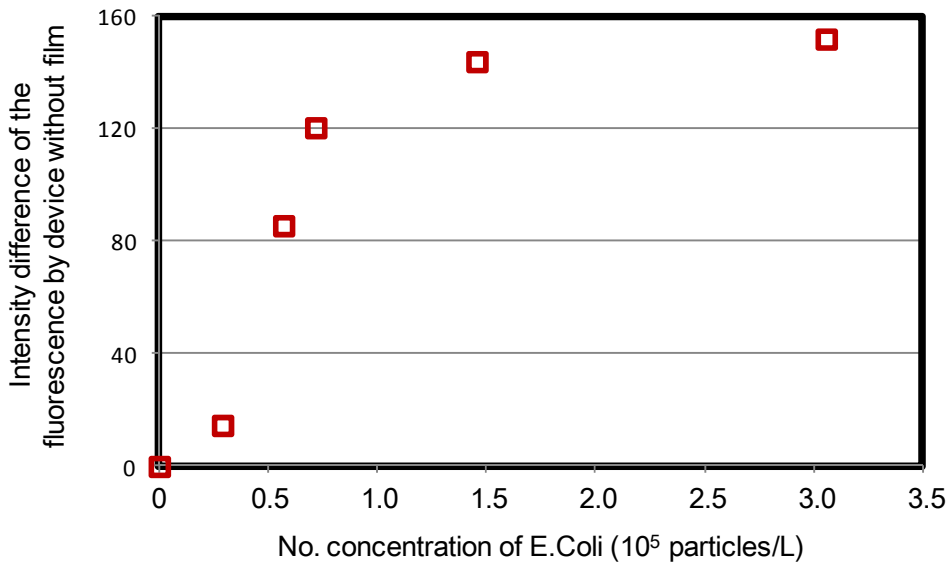
Fig.5-35 Measurement of aerosolized E.coli in sampling bag

The SSBAP using a cartridge not covered with the light-blocking film measures more than 3.0×10^4 to 7.0×10^4 particles/L aerosolized E.coli in the sampling bag. Nevertheless, the increments in the intensity difference of the fluorescence in the concentration from 0 to 3×10^4 particles /L or from 7.0×10^4 to 1.4×10^5 are smaller than the increments of the concentration from 3.0×10^4 to 7.0×10^4 of the aerosolized E.coli. Next, we discussed this reasons in the following.

(1) Low number concentration of E. coli

163

There are autofluorescnece emitted from the collection plate and the multi-hole plate, and fluorescence emitted from fluorescent dyes on the collection plate, which are comparable with intensity of fluorescence emitted from small numbers of E. coli.

Thereby, we presume that it is difficult to measure accurately small numbers of E.coli by using fluorescence of E. coli. For accurate measurements of low numbers of E. coli, we consider that the system needs improvements to decrease these autofluorescence and fluorescence.

(2) High number concentration of E. coli

Aerosolized E. coli are collected on small areas under nozzles in a staked condition. This condition prevents underlying E. coli from binding to fluorescent antibodies. Then, higher number concentration of E. coli decreases the correlation between intensity of fluorescence emitted from E. coli and number concentration of E. coli. As in section 5, the theory of counting loss in the concentration method such as impaction shows the correlation between measurement value and true numbers of ϕ 1.0 μm bacteria decreases in a greater than 1.0×10^5 particle/m^3 number concentration of bacteria (Fig. 5-21).

Fig. 5-36 shows a graph made by superimposing the graph in Fig. 5-21 on the graph in Fig. 5-35.
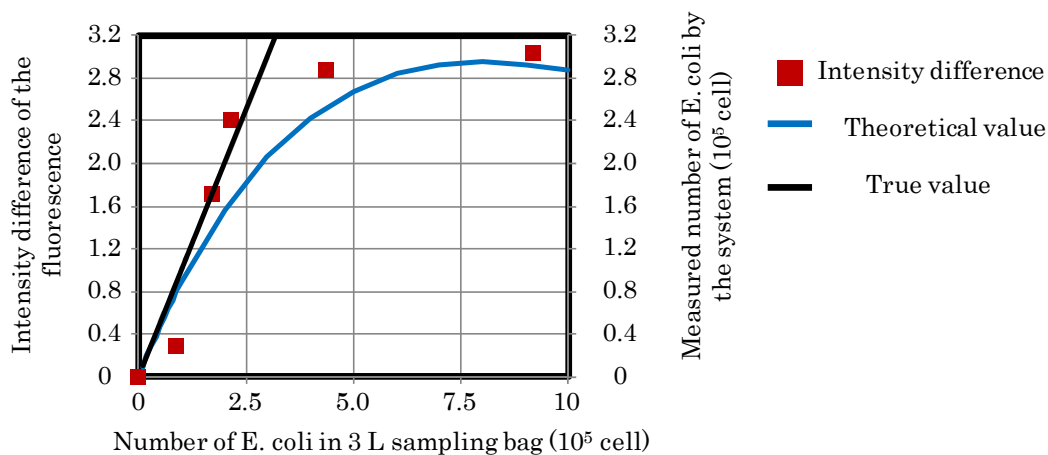
Fig.5-36 Comparison measurement value and theoretical value

Fig. 5-36 shows that the intensity difference of the fluorescence becomes closer to true number of E. coli under a low number of E. coli (0 – 2.5 $\times 10^5$ particles). However, Fig. 5-36 shows that the intensity difference of the fluorescence becomes closer to number of E. coli affected by the counting loss under a high number of E. coli (more than 2.5 $\times 10^5$

particles).

This reason is considered to be as follows. Collected bacteria are stacked in areas under nozzles; however, overlap of bacteria is thin under a low number of bacteria. Thereby, most collected bacteria are labeled with fluorescent dyes by spreading of fluorescent dye solution into the underlying E. coli. Consequently, the counting loss becomes small.

On the other hand, only bacteria near the top surface of overlaps are labeled with fluorescent dyes under a high number of bacteria in high number of bacteria because overlaps of bacteria thicken. Thereby, the counting loss of bacteria becomes large.

5.10.2 Improvement of sensitivity with light-blocking film

When the intensity of the fluorescence of biological aerosol particles is comparable with background light from the collection plate, it is difficult to determine whether no amount or only a very small amount of biological aerosol particles exists. Thus, decreasing the amount of background light with the light-blocking film can improve the sensitivity of the SSBAP.

To evaluate the improvement of the sensitivity with the light-blocking film, we measured aerosolized E. coli using cartridges covered with light-blocking film and cartridges not covered with light-blocking film. Additionally, we compared measurement results in both cases. Experimental procedure is skipped because this is same as procedures in previous subsection. Fig. 5-37 shows experimental results.
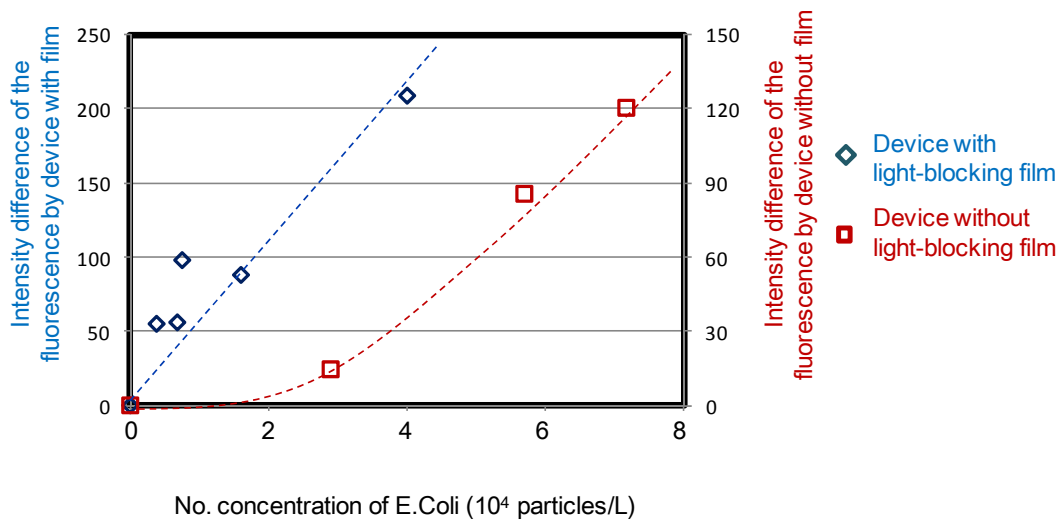
Fig.5-37 Sensitivity improvement using light blocking film

According to measurement results of the SSBAP using a disposable cartridge not covered with the light-blocking film, the increments in the intensity difference of the fluorescence in the concentration from 0 to 3×10^4 particles /L are smaller than the increments of the concentration from 3.0×10^4 to 7.0×10^4 of the aerosolized E.coli.

On the other hand, according to measurement results of the SSBAP using a disposable cartridge covered with the light-blocking film, the increments in the intensity difference of the fluorescence are proportional to the increments of the concentration of the aerosolized E.coli from 4×10^3 to 4×10^4 particles /L. This result shows that the sensitivity of this system using the disposable cartridge covered with the light-blocking film has been improved nearly tenfold on that of the present system.

5.10.3 Measurement of influenza virus

We evaluated the detection performance of the SSBAP and the disposable cartridge covered with the light-blocking film for influenza virus particles in the sampling bag. We used inactivated influenza A viruses [A/Udorn/72(H3N2)] as the substitute aerosolized virus and Hilite Fluore^{TM}647 (Anaspec) conjugated anti-influenza virus A antibodies (Abcam) as the fluorescent dyes. Experimental procedures other than biological aerosol particles and fluorescent dyes are same as procedures in previous subsection.

Fig. 5-38 shows the detection performance of the SSBAP using the disposable cartridge covered with the light-blocking film for aerosolized influenza viruses in the sampling bag. The three photos in this graph, which were taken for reference after the measurements, are fluorescent images of the collected and labeled influenza viruses on the area of the collection plate under a nozzle. The SSBAP can detect more than 8.3×10^3 particles/L aerosolized influenza viruses because the intensity difference of the fluorescence increases as the concentration of aerosolized influenza viruses increases from 8.3×10^3 to 1.0×10^4 particles/L.
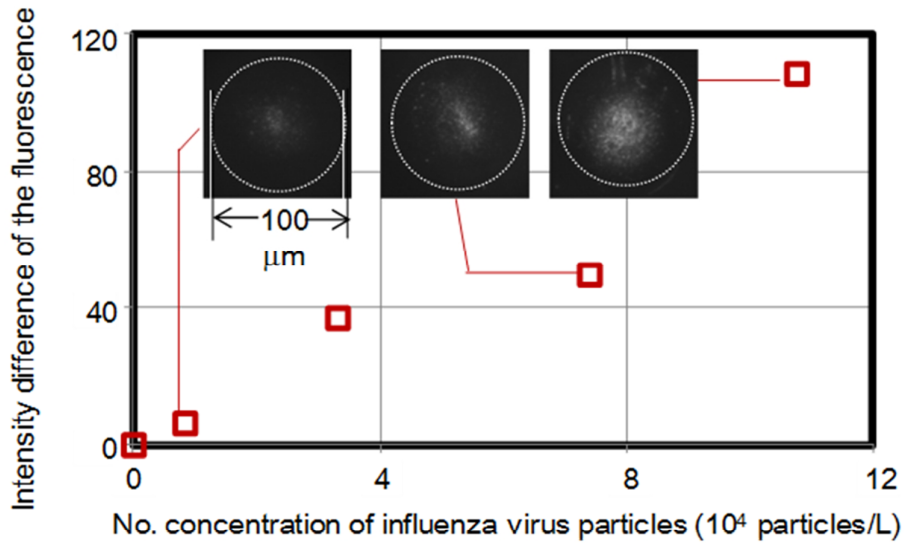
Fig.5-38 Measurement of aerosolized influenza viruses in sampling bag

5.11 Discussion

In this research, we have developed a sensing system of biological aerosol particles (SSBAP) using a disposable cartridge. The disposable cartridge can collect biological aerosolized particles with high efficiency and detect fluorescence of collected particles with high sensitivity. As a result, we could detect aerosolized influenza virus particles using this system. Three discussions about the system are shown in the following.

5.11.1 Advantage of the system

First, we will discuss advantages the SSBAP has over other systems used to collect and detect aerosol particles. Systems with a combination of the impaction and culture method are used for collecting and detecting airborne bacteria or fungi. These systems require more than 48 hours to obtain results of tests for culture of collected bacteria or fungi. Additionally, they cannot detect airborne viruses that cannot glow on the agar media.

In contrast, the SSBAP quickly detects collected airborne biological particles including viruses by labeling target particles with fluorescent antibodies that bind specifically with target particles. The proposed SSBAP can detect only one kind of biological particle. However, it will be able to detect several kinds of biological particles using several kinds

167

of fluorescent antibodies and an optical unit for fluorescence detection in several ranges of wavelength.

5.11.2   Sensitivity of the system

Second, we will discuss improving the sensitivity of the SSBAP to detect infected patients. The SSBAP may be able to detect only some infected patients at its present sensitivity because there are from 67 to 8,500 particles/L in a breath blown by an influenza-infected patient [6]. Therefore, the SSBAP needs its sensitivity further heightened.

In this paper, the SSBAP detected collected viruses using direct immunofluorescence. This has the potential to increase sensitivity by amplifying fluorescence using indirect immunofluorescence [29]. Moreover, it has the potential to increase sensitivity by improving the cartridge too. In this system, the light-blocking film covering the collection plate of the disposable cartridge has just 33 pores only near the center (ϕ 3 mm) of the collection plate, thereby this system can detect fluorescence of only 33 % of collected particles passing thorough 109 nozzles of a multi-hole plate. As mentioned above, we did not make pores at the outer area of the collection plate because outer impact positions of biological aerosol particles are moved from positions under nozzles by air flows. If we can understand impact positions of biological aerosol particles more precisely, we will be able to make pores at the outer area of the collection plate and detect fluorescence of more particles.

5.11.3   Practical challenges of the SSBAP

Third, we discuss practical challenges of the SSBAP. In this paper, aerosolized influenza viruses in a sampling bag were used to evaluate performance of the SSBAP. However, breaths of influenza-infected patients have to be used in clinical studies because the composition of a patient's breaths is different from that of the air in a sampling bag in this paper. Some substances other than virus particles in a patient's breath may decrease the sensitivity of the SSBAP.

Additionally, breaths of patients on clear elapsed days after infections have to be evaluated to know how soon after infection the SSBAP can detect virus particles in breath.

Moreover, to obtain regulatory approval, the SSBAP must be equipped with the function that excludes risk of infection to anyone else because it is used by many and unspecified patients. Additionally, for the SSBAP to be used widely, production costs of the system and disposable cartridge need to be lowered.

5.12 Conclusion

There are many respiratory infections such as influenza that cause epidemics. These respiratory infection epidemics can be effectively prevented by determining the presence or absence of infections in many patients by frequent tests. We think that self-diagnosis may be possible by using a system that can collect and detect biological aerosol particles in the patient's breathe because breath sampling is easy work requiring no examiner. Thereby, we made designs and experimental procedures, and conducted evaluations on a sensing system for biological aerosol particles (SSBAP) using a disposable cartridge and a sampling bag filled with a patient's breath. The cartridge works as an impactor for the collection of Φ 0.3 μm biological aerosol particles which cannot be collected by existing methods, a flow-cell for labeling collected particles with fluorescent dyes or washings away free fluorescent dyes, and an optical window for the fluorescence detection of collected biological aerosol particles. We draw the following conclusions on the basis of our findings.

We draw the following conclusions on the basis of our findings.

(1) We designed the disposable cartridge for an impaction use. The cartridge with 109 nozzles (ϕ 70 μm) are designed from theoretical consideration with combination of the Stokes number and the Reynolds number of the air flowing through a nozzle, and particle track analyses of particles flowing through a nozzle in addition to the decision methodology based on the statistic theory. A designed cartridge with the impaction function could collect more than 97% of the ϕ 0.3 μm aerosolized particles in the sampling bag, which cannot be collected by common existing impaction method.

(2) In the range of number concentration of E. Coli (less than 1.0×10^5 particles/L) decided by the statistic theory, we measured aerosolized E. Coli by the system. Measurement results show that there is a high correlation between outputs of the system and number concentration of E. Coli. Thereby the decision methodology based on the statistic theory is shown to be of benefit.

(3) We designed a light-blocking film covering the collection plate of the disposable cartridge. The light-blocking film has pores at biological aerosol particle impact positions. This film blocks background light from outside of the biological aerosol particle impact positions but does not block weak fluorescence from biological aerosol particles. Thereby, the lower detection limit of this system using the disposable cartridge covered with the light-blocking film was improved by one-tenth.

(4) We measured aerosolized influenza virus particles (number concentration: 8.3×10^3 - 1.0×10^4 particles/L) by the system. Measurement results show that there is a high

correlation between outputs of the system and number concentration of aerosolized influenza virus particles. Thereby, it is possible to measure small influenza particles by the SSBAP.

(5) Using the methodology to develop a measurement method of target particles, we selected an impaction method, one of the concentration methods, to collect airborne biological particles on the surface of a collection plate. Additionally, we invented a combined method of the impaction method and fluorescence detection to detect airborne biological particles. Measurement results using the system show that the methodology is effective in the development of the system which measures number of airborne biological particles.

We have done a feasibility study of the SSBAP so far. Improvements of the performance of the SSBAP and practical studies including clinical studies have to be done for the SSBAP to be widely used for tests of respiratory infections. Achieving these challenges will contribute to maintaining a healthy society by reducing the risk of respiratory infection epidemics.

Reference

[1] Centers for Disease Control and Prevention, The 2009 H1N1 Pandemic:
Summary Highlights, April 2009-April 2010, Available at:
http://www.cdc.gov/h1n1flu/cdcresponse.htm [Accessed 1 June 2016].

[2] Ujiie, M., Nabae, K., and Shobayashi, T. "Rubella outbreak in Japan," *The Lancet*,
Vol. 383, (2014), pp. 1460-1461.

[3] Takahashi, T., Arima, Y., Kinoshita, H., Kanou, K., Saitoh, T., Sunagawa, T., Ito, H.,
Kanayama, A., Tabuchi, A., Nakashima, K., Yahata, Y., Yamagishi, T., Sugawara, T.,
Ohkusa, Y., Matsui, T., Arai, S., Satoh, H., Tanaka-Taya, K., Komase, K., Takeda, M.
and Oishi, K. "Ongoing increase in measles cases following importations, Japan,
March 2014: times of challenge and opportunity," *WPSAR*, Vol. 5(2), (2014), pp. 1-3.

[4] Rensselaer Polytechnic Institute homepage,
https://www.rpi.edu/about/flu/SymptomDifferences.pdf
[Accessed 1 April 2017].

[5] Yamazaki, M., Mitamura, K., Kimura, K., Komiyama, O., Nirasawa, M., Yamamoto,
K., Ichikawa, M., Someya, K., Nakano, T., Hashimoto, Y., Hagiwara, N., Maezawa,
T., Watanabe, S., Shimizu, H., and Sugaya, N. "Clinical evaluation of an
immunochromatography test for rapid diagnosis of influenza," *Kansenshogaku Zasshi,*
Vol. 75(12), (2001), pp. 1047-1053 (in Japanese).

[6] Fabian, P., McDevitt, J. J., DeHaan, W. H., Fung, R. O. P., Cowling, B. J., Chan, K.
H., Leung, G. M., and Milton, D. K. "Influenza Virus in Human Exhaled Breath: An
Observational Study," *PLoS ONE*, Vol. 3(7), (2008), e2691.

[7] Yang, C. S. and Heinsohn, A. ed. *Sampling and Analysis of Indoor Microorganisms*
(2007), p.65, Wiley, ISBN: 978-0-470-11242-7.

[8] Jones, W., Morring, K., Morey, P. and Sorenson, W. "Evaluation of the Andersen
Viable Impactor for Single Stage Sampling," *Am. Ind. Hyg. Assoc. J.*, Vol. 46, Issue
5, (1985), pp. 294-298.

[9] Mise, K. and Inoue, F. ed. *Practical guide of Bacteriological testing of food*, (1996),
pp. 52-53, Kodansha scientific (in Japanese), ISBN: 978-4-06-153712-5.

[10] Kawai, M., Yamaguchi, N., and Nasu, N. "Rapid enumeration of physiologically
active bacteria in purified water used in the pharmaceutical manufacturing process,"
Journal of Applied Microbiology, Vol. 86, (2001), pp. 496-504.

[11] Ganzenmueller, T., Kluba, J., Hilfrich, B., Puppe, W., Verhagen, W., Heim, A.,
Schulz, T., and Henke-Gendo, C. "Comparison of the performance of direct
fluorescent antibody staining, a point-of-care rapid antigen test and virus isolation with

that of RT-PCR for the detection of novel 2009 influenza A (H1N1) virus in respiratory specimens," *Journal of Medical Microbiology*, Vol. 59, (2010), pp. 713-717.

[12] Manz, A. Graber, N., and Widmer, M. "Miniaturized total chemical analysis systems: a novel concept for chemical sensing," *Sensors and Actuator B: Chemical*, Vol. 1, (1990), pp. 244-248.

[13] Niimi, M., Masuda, T., Kaihatsu, K., Kato, N., and Arai, F. "Virus detection by on-chip hydroxyapatite chromatography," *Proceedings of the 16th International conference on Miniaturized Systems for Chemistry and Life Sciences (Micro TAS 2012)*, (2012), pp. 605-607, ISBN: 978-0-9798064-5-2

[14] Aritome, K., Takahata, Y., Sakamoto, K., Noda, K., Kuroda, A., Ishikawa, T., Miyake, R., and Murakami, Y. "Biochemical quantization by microfluidic droplets for the development of microbe counter," *Proceedings of the 14th International conference on Miniaturized Systems for Chemistry and Life Sciences (Micro TAS 2010)*, (2010), pp. 1136-1138, ISBN: 978-0-9798064-3-8.

[15] Takenaka, K., Sasaki, Y., Inami, H., Nakamoto, H., Watanabe, Y., Kurihara, M., Takei, K., Ishikawa, J. and Miyake, R. "Rapid Live Bacteria Counter Using Cassette-Type Flow Cytometry," *Trans. Jpn. Soc. Mech. Eng. Series C*, Vol. 77, (2011), pp401-410.

[16] Water Quality Association Homepage, Bacteria & Virus Issues
https://www.wqa.org/Learn-About-Water/Common-Contaminants/Bacteria-Viruses,
[Accessed 1 April 2017].

[17] Yang, C. S. and Heinsohn, A. ed. *Sampling and Analysis of Indoor Microorganisms*, (2007), p.65, Wiley, ISBN: 978-0-470-11242-7

[18] Jensen, M.M. "Bacteriophage Aerosol Challenge of Installed Air Contamination Control Systems," *Applied Microbiology*, Vol. 15(6), (1967), pp. 1447-1449,

[19] Li, C-S. "Sampling Performance of Impactors for Bacterial Bioaerosols," *Aerosol Sci. Tec.*, Vol. 30, (1999), pp. 280-287.

[20] Hind, W. C. ed. *Aerosol Technology: Properties, Behavior, and Measurement of Airborne Particles, 2nd Edition*, (1999), Wiley, ISBN: 978-0-471-19410-1.

[21] Ito, H. and Honda, M. *Fluid dynamics*, (1981), Maruzen (in Japanese), ISBN: 978-4621025277

[22] Japan Society of Mechanical engineers. ed. *Hydraulic losses in pipes and ducts*, (1979), Maruzen (in Japanese), ISBN: 978-4-88898-003-6.

[23] Biswas, P., and Flagan, R. C. "High-velocity inertial impactors," *Environ. Sci. Technol.*, Vol. 18(8), (1984), pp. 611-617.

[24] Star-CD Manual

[25] Misumi Homepage,
https://fawos.misumi.jp/fas/rp/data/view_property.php?page=tab2_cate2_all
[Accessed 1 April 2017].

[26] Japan stainless steel association Homepage,
http://www.jssa.gr.jp/contents/faq-article/q7/ [Accessed 1 April 2017].

[27] Sonnenschein, M. F. and Roland, C. M. "Absorption and Fluorescence Spectra of Poly (ethylene terephthalate) dimmers," *POLYMER*, Vol. 31, (1990), pp. 2023-2026.

[28] Takahashi, K. *Basis of Aerosol* (2003), Morikita Publishing Co., Ltd.,
ISBN: 978-4627672512.

[29] Fritschy, J‐M. and Härtig, W. *Immunofluorescence* (2001), Wiley, DOI: 10.1038/npg.els.0001174

Chapter 6. Conclusion

6.1 Summery of this work

There is a wide variety of biological particles on the Earth, such as bacteria and viruses. These biological particles have effects on human activities, more or less. It is essential for a comfortable and healthy life to understand the characteristics and dynamics of biological particles in the sphere of human habitation such as the foods, water, and air we ingest, and objects we contact directly. We predict that discoveries of new kinds of biological particles and basic knowledge of phenomena caused by the biological particles will increase at an accelerated pace. Thereby, we have to provide rapid measurement methods for biological particles in a timely manner to understand the characteristics and dynamics of target biological particles.

For this reason, a rapid measurement method for these particles are organized from a statistical perspective by understanding biological particles' characteristics and dynamics. Then, we advance a methodology to select a rapid measurement method and a system configuration using the method for particular purposes. Finally, we attempt to apply the methodology to three kinds of system development. This thesis consists of six chapters. Brief summaries of each chapter are shown in the following.

In chapter 1, first, we investigated biological particles in the sphere of human habitation from the perspective of particle type, particle size, and phenomena caused by these particles. Next, we investigated and classified existing measurement methods for these particles and preparations for measurements.

In chapter 2, we organized and discussed measurement methods for biological particles in the sphere of human habitation based on the above survey results from the perspective of statistics. The results of the discussion show it necessary to measure a lot of biological particles within a practical time to understand the characteristics and dynamics of these particles.

Additionally, we thought that measurement methods of particles in the sphere of human habitation can be divided into the following three methods from considering relative position between a space where sample containing target biological particles (called a target sample space in the following) and a space to measure target biological particles (called a probe space in the following).

The first method is to measure every particle directly in the target sample space by scanning through the target sample space with the probe space at high speed (called the scan method). The second method is to measure every particle one by one serially in the target sample space by transmitting the target sample space into the probe space (called

174

the flow method). The third method is to measure target biological particles collected in the probe space all at once by concentrating the target sample space to approximately the same volume as the probe space (called the concentration method). The scan method and flow method are effective to measure one by one detectable biological particles which are relatively large or bright, for example. Additionally, the concentration method is effective to measure one by one non-detectable particles which are very small such as virus particles.

Increase of undiscovered particles having large effect on our life makes the growing demands for new measurement methods for these particles. However, large cost and long time are needed. Thereby, a methodology to develop suitable measurement methods is required to develop a new measurement method for certain particles.

Thereby, we invented a method to select a suitable measurement method of target particles from the above three methods. The selection of a measurement method is done in the following order: (1) selection of the concentration method or other methods depending on signal value of a target particle, (2) selection of the scan method or flow method depending on mobility of particles or significance of information of the shape of a particle, and (3) improvement of measurement accuracy of target particles using the features of target biological particles maximally.

Furthermore, we found that the number distribution of biological particles in space follows the Poisson distribution on the premise that biological particles in space have no mutual interference and keep independence. Thereby, we invented a method as a unified concept to decide important specifications of a measurement method such as volume of a target sample space and dimensions of a probe space (a field of view of a measurement instrument) using a statistical theory based on Poisson's distribution.

Then, we applied these methodologies to the development of a rapid counting system for live bacteria in foods, an excitation-fluorescent spectral flow cytometer for particles in liquids, and a sensing system for airborne biological particles. The research and results are shown in chapter 3 to chapter 5.

We showed the development of the counting system for live bacteria in foods in chapter 3. The culture method, which is an accurate method, is used commonly for exhaustive measurements of live bacterial numbers in foods. However, it is difficult to measure live bacterial numbers simply and rapidly with this method.

Thereby, in this thesis, we applied the flow method selected among the above measurement methods to the measurement of live bacterial numbers in foods. Additionally, we developed a rapid counting system using flow cytometry technique as one of the flow method. This system carries out live bacteria counting processes in a

disposable cartridge; these processes consist of removing of food debris process, a labeling of live bacteria with fluorescent dyes process, and a measurement process of live bacterial numbers by flow cytometry.

We evaluated the performance of this system by measuring numbers of live bacteria in sample solutions. Consequently, the following conclusions based on our work are drawn.

(a) Using a decision methodology based on statistical theory, we designed a flow cell (20 × 40 μm^2) in the disposable cartridge for fluorescence flow cytometry. Additionally, we calculated the needed volume of sample solution (number concentration of live bacteria: 10^3 particles/mL). As a result, we decided that the volume of the sample solution was 100 μL.

(b) Live bacteria in an emulsion of Escherichia coli (E. coli) were counted by the system and a culture method. The measurement performances of the system and the culture method were judged to be equal because the methods had a high correlation, namely, a correlation coefficient of 0.97 in the range of a live bacteria concentration of 10^3 to 10^6 cell/ml. This result shows that the decision methodology based on statistical theory is effective for the design of this system.

(c) To improve the sensitivity of the system, we developed a new discrimination method for live bacteria in homogenized food suspension using three kinds of fluorescent dyes (two kinds of fluorescent dyes for live/dead bacteria and one kind of fluorescent dye for dead bacteria). By clarifying difference in wavelength of fluorescence from particles, live bacteria can be discriminated from other particles which cannot be discriminated by common flow cytometry.

(d) Live bacterial numbers in homogenized vegetable suspensions were measured by the system and the culture method. The measurement performance of the system and the culture method are equal because the methods give a high correlation; namely, the correlation coefficient is 0.96 in spinach, 0.91 in carrot, 0.90 in red cabbage, and 0.93 in potato in a range of live bacteria concentration of 10^2 to 10^6 cell/ml. These results show that the new discrimination method is effective for discriminating live bacteria from vegetable particles, which is difficult to discriminate from live bacteria by existing methods.

We showed the development of the system for detailed measurements of particles in liquids by developing the flow method further in chapter 4.

Fluorescence spectroscopy has enabled us to broadly understand the amounts and types

of particles in a liquid by measuring excitation-fluorescence spectra (fluorescence fingerprint) of a liquid containing particles. However, it is hard to measures particles in small amounts because it is impossible to analyze an individual targeted particle. An excitation-fluorescence spectra of a particle, which cannot measured by existing methods, is useful to analyze a character of a particle particularly. Therefore, we developed an excitation-fluorescent spectral flow cytometer (EFSFCM) which can measure an excitation-fluorescence spectra of a particle. Additionally, we determined the types of particles from the excitation-fluorescence spectra of a particle by the EFSFCM. Consequently, the following conclusions based on our work are drawn.

(a) We designed an optical unit of the EFSFCM by a decision methodology based on statistical theory. The optical unit irradiates a designed measurement area (probe space, 200 μm × 350 μm) with dispersed white light and measures a excitation-fluorescence spectra of a particle (excitation wavelength band, 400 - 650 nm; fluorescence wavelength band: 400 - 700 nm).

(b) Fluorescent particles (particle size: 2 μm; maximum wavelength of excitation light: 441 nm; maximum wavelength of fluorescence: 486 nm) in a range of number concentration ($\leq 1.0 \times 104$ particle/mL) fixed from statistical theory are measured by the EFSFCM. Excitation-fluorescence spectra of a fluorescent particle was measured in the case that more than one fluorescent particle are rarely measured at the same time. Thereby, the decision methodology based on statistical theory is shown to be of benefit.

(c) Particles in homogenized tomato suspensions and spinach suspensions were measured by the EFSFCM. These results agree with features of components of tomato and spinach. A homogenized tomato suspension contains many particles emitting blue-green fluorescence derived from a cell. Also, a homogenized spinach suspension contains two kinds of particles that emit blue-green fluorescence and emit near-infrared fluorescence derived from chloroplast.

We showed the development of the system for measurements of airborne biological particles such as virus particles in chapter 5.

Detecting airborne biological particles such as virus particles in breath can enable people to do self-diagnoses of respiratory infections such as influenza. However, it is difficult to detect airborne virus particles because these particles are small (minimum size: 0.3 μm). Thereby, we applied the concentration method selected among the above measurement methods to measurements of airborne biological particles. In particular, we

developed and evaluated a sensing system of biological aerosolized particles (SSBAP) which can collect biological aerosolized particles and detect the fluorescence of these particles using a disposable cartridge. Consequently, the following conclusions based on our work are drawn.

(a) We selected an impaction method, one of the concentration methods, to collect airborne biological particles on a surface of a collection plate. Additionally, we invented a combined method of the impaction method and fluorescence detection to detect airborne biological particles.

(b) We designed a disposable cartridge with 109 micro nozzles (Φ 70 μm) for impaction use. Diameter, number and array of nozzles, which is important factor to collect small particles in the air, was designed from theories of a fluid mechanics of the air flowing through a nozzle and particle track analyses of particles flowing through a nozzle. A designed cartridge was able to collect more than 97% of the ϕ 0.3 μm airborne biological particles in the air which can be collected rarely by the existing methods.

(c) Aerosolized E. coli in the range of number concentration (less than 1.0×10^5 particles/L) decided by statistical theory were measured by the system. Measurement results show that there is a high correlation between outputs of the system and number concentration of E. coli. Thereby, the decision methodology based on statistical theory is shown to be of benefit.

(d) Aerosolized influenza virus particles (number concentration: 8.3×10^3 - 1.0×10^4 particles/L) by the system. Measurement results show that there is a high correlation between outputs of the system and the number concentration of aerosolized influenza virus particles. Thereby, the SSBAP can measure small airborne influenza particles which cannot measured by the existing methods.

Conclusions in chapters 3 – 5 show that the decision methodology based on statistical theory is beneficial for designs of new measurement systems for biological particles in the sphere of human habitation.

6.2 Future outlook of measurements of particle in space

We showed the development of rapid measurement methods for microbiological particles in the sphere of human habitation in this thesis. In particular, we invented a methodology of developing a system based on statistical theory and proved the validity of the methodology by applying the methodology to developing the above three kinds of

particle measurement systems.

First, we show the future outlook for this work. Particles in the space of human habitation exert a large influence on human activities, as mentioned in chapter 1. We have to deal with these biological particles properly for a comfortable and healthy life because new infectious diseases or water pollutants caused by microorganisms have been increasing recently. Thereby, results in this work help us to know detailed features of these particles and to develop the most suitable method for measuring these particles.

Next, we show our understanding of users' expectations for measurement systems for biological particles. We interviewed target users in developing the above systems. Their opinions showed not only the requirement of rapid and accurate measurement but also other factors for specific systems such as usability and cost (initial cost and running cost). Their opinions showed us the importance of developing systems from the users' viewpoints.

I am a researcher belonging to a company. Thereby, I would like to contribute to society by inventing and offering required systems and services from users' viewpoints using the knowledge acquired and experiments developed in this work.

Publication

1. Thesis

Development of Rapid Measurement Methods of Micro Biological Particles in Sphere of Human Habitation

2. Published papers

(1) Rapid Live Bacteria Counter Using Cassette-type Flow Cytometry

K. Takenaka, Y. Sasaki, H. Inami, H. Nakamoto, Y. Watanabe,

M. Kurihara, K. Takei, J. Ishikawa and R. Miyake

Transactions of the Japan society of Mechanical Engineers Series C, **77** (2011), pp.401–10.

No.2010-JCR-0124.

(2) Airborne Virus Detection by a Sensing System Using a Disposable Integrated Impaction Device

K. Takenaka, S. Togashi, R. Miyake, T. Sakaguchi and M. Hide

Journal of Breath Research, **10** (2016), 036009 (11 pages)

DOI: 10.1088/1752-7155/10/3/036009

(3) Analysis of Particle in Liquid using Excitation-Fluorescence Spectral Flow Cytometer

K. Takenaka and S. Togashi

Japanese Journal of Applied Physics, **57** (1) (2018), 017001 (7 pages)

DOI: 10.7567/JJAP.57.017001

3. Reference papers

(1) Rapid Live Bacteria Counter with Disposable Flow Cytometry Cassette,

K. Takenaka, Y. Sasaki, H. Inami, H. Nakamoto, Y. Watanabe, M. Kurihara, K. Takei, J. Ishikawa and R. Miyake

Chemical and Biological Microsystems Society, 13th International Conference on Miniaturized Systems for Chemistry and Life Sciences (μTAS2009), Jeju, South Korea, (2009), pp.484-486

ISBN: 978-0-9798064-2-1

(2) Integrated Cassette for Counting Low-concentration Live Bacteria in Foods Using 3D Staining Technology,

K. Takenaka, Y. Sasaki, H. Inami, H. Nakamoto, Y. Watanabe, M. Kurihara, K. Takei, J. Ishikawa and R. Miyake

Chemical and Biological Microsystems Society, 14th International Conference on

Miniaturized Systems for Chemistry and Life Sciences (μTAS2010), Groningen, Netherlands, (2010), pp.1043-1045
ISBN: 978-0-9798064-3-8

(3) Rapid Airborne Virus Detection Using Mist-Labeling Based on Micro Reaction Effect,
K. Takenaka, S. Togashi and R. Miyake
Chemical and Biological Microsystems Society, 16th International Conference on Miniaturized Systems for Chemistry and Life Sciences (μTAS2012), Okinawa, Japan, (2012), pp.1885-1887
ISBN: 978-0-9798064-5-2

(4) Rapid Airborne Pathogens Detection System Using Disposable Impaction Cartridge,
K. Takenaka, S. Togashi and R. Miyake,
Chemical and Biological Microsystems Society, 17th International Conference on Miniaturized Systems for Chemistry and Life Sciences (μTAS2013), Freiburg, Germany, (2013), pp.877-879
ISBN: 978-0-9798064-6-9

(5) Integrated Micro-Impaction Cartridge Covered With Microporus Light-blocking Film for Low-Concentration Airborne Virus Detection,
K. Takenaka, S. Togashi, R. Miyake, T. Sakaguchi and M. Hide Chemical and Biological Microsystems Society, 18th International Conference on Miniaturized Systems for Chemistry and Life Sciences (μTAS2014), San Antonio, Texas, USA, (2014), pp.2041-2043
ISBN: 978-0-9798064-7-6

(6) Excitation-Fluorescent 3D Spectral Flow Cytometer for Single-Cell Analysis,
K. Takenaka and S. Togashi
Chemical and Biological Microsystems Society, 19th International Conference on Miniaturized Systems for Chemistry and Life Sciences (μTAS2015), Gyeongju, South Korea, (2015), pp.1813-1815
ISBN: 978-0-9798064-8-3

(7) Analyses of Particle Composition in Vegetables Suspension Using Excitation-Fluorescent Spectral Flow Cytometer,
K. Takenaka and S. Togashi
Chemical and Biological Microsystems Society, 20th International Conference on Miniaturized Systems for Chemistry and Life Sciences (μTAS2016), Dublin, Ireland, (2016), pp.1360-1361

4. Other papers

(1) Checkered Electrostatic Actuator for Two-dimensional Manipulation of Liquid Droplets

K. Takenaka and Y. Goto

Chemical and Biological Microsystems Society, 10th International Conference on Miniaturized Systems for Chemistry and Life Sciences (μTAS2006), Tokyo, Japan, (2006), pp.594-596

ISBN: 4-9903269-0-3-C3043

(2) Fingertip-size pressure sensor for luer taper of three-way stopcock in liquid circuit

K. Takenaka, S. Togahi, A. Kazama, K. Miyajima and T. Nagano

Chemical and Biological Microsystems Society, 21th International Conference on Miniaturized Systems for Chemistry and Life Sciences (μTAS2017), Savannah, Georgia, USA, (2017), pp.627-628

ISBN: 978-0-692-94183-6

Presentations on conferences

Presentations on conferences other than μTAS are shown.

(1) Disposable Bacterial Counting Cassette integrated with Pretreatment System and Micro flow-cell based on Flow Cytometry Technique

K. Takenaka, Y. Sasaki, H. Inami, H. Nakamoto, Y. Watanabe, M. Kurihara, K. Takei, J. Ishikawa and R. Miyake

The Society for Chemistry and Micro-Nano Systems (CHEMINAS), International Symposium on Microchemistry and Microsystems (ISMM2008), Kyoto, Japan

(2) Rapid Live Bacteria Counter Using Cassette-Type Micro Flow Cytometry

K. Takenaka, Y. Sasaki, H. Inami, H. Nakamoto, Y. Watanabe, M. Kurihara, K. Takei, J. Ishikawa and R. Miyake

Fluid and Particle Processing Division, Japan, International Workshop on Process Intensification 2010 (IWPI2010), Fukuoka, Japan

Patents

Chapter 3.

(1) JP04842796 and US 8409850 B2

(2) JP 05197290 and US 8404480 B2

(3) US 8889349 B2

Chapter 4.

(1) JP05895064 and US 9291503 B2

Chapter 5.

(1) JP05860175 and US 9702805

(2) JP05700594 and US 9433883 B2

Acknowledgement

Kei Takenaka
Kashiwa, Chiba, Japan
March 2018

公表論文

(1) Rapid Live Bacteria Counter Using Cassette-type Flow Cytometry
<u>K. Takenaka</u>, Y. Sasaki, H. Inami, H. Nakamoto, Y. Watanabe,
M. Kurihara, K. Takei, J. Ishikawa and R. Miyake
Transactions of the Japan society of Mechanical Engineers Series C, **77**,
401-410, (2011),
No.2010-JCR-0124.

(2) Airborne Virus Detection by a Sensing System Using a Disposable
Integrated Impaction Device
<u>K. Takenaka</u>, S. Togashi, R. Miyake, T. Sakaguchi and M. Hide
Journal of Breath Research, **10**, 036009 (11 pages), (2016),
DOI: 10.1088/1752-7155/10/3/036009.

(3) Analysis of Particle in Liquid using Excitation-Fluorescence Spectral
Flow Cytometer
<u>K. Takenaka</u> and S. Togashi
Japanese Journal of Applied Physics, **57** (1), 017001 (7 pages), (2018),
DOI: 10.7567/JJAP.57.017001

参考論文

(1) Rapid Live Bacteria Counter with Disposable Flow Cytometry Cassette
K. Takenaka, Y. Sasaki, H. Inami, H. Nakamoto, Y. Watanabe, M. Kurihara, K. Takei, J. Ishikawa and R. Miyake
Chemical and Biological Microsystems Society, 13th International Conference on Miniaturized Systems for Chemistry and Life Sciences (μTAS2009), Jeju, South Korea, 484-486, (2009),
ISBN: 978-0-9798064-2-1

(2) Integrated Cassette for Counting Low-concentration Live Bacteria in Foods Using 3D Staining Technology
K. Takenaka, Y. Sasaki, H. Inami, H. Nakamoto, Y. Watanabe, M. Kurihara, K. Takei, J. Ishikawa and R. Miyake
Chemical and Biological Microsystems Society, 14th International Conference on Miniaturized Systems for Chemistry and Life Sciences (μTAS2010), Groningen, Netherlands, 1043-1045, (2010),
ISBN: 978-0-9798064-3-8

(3) Rapid Airborne Virus Detection Using Mist-Labeling Based on Micro Reaction Effect,
K. Takenaka, S. Togashi and R. Miyake
Chemical and Biological Microsystems Society, 16th International Conference on Miniaturized Systems for Chemistry and Life Sciences (μTAS2012), Okinawa, Japan, 1885-1887, (2012),
ISBN: 978-0-9798064-5-2

(4) Rapid Airborne Pathogens Detection System Using Disposable Impaction Cartridge,
K. Takenaka, S. Togashi and R. Miyake,
Chemical and Biological Microsystems Society, 17th International Conference on Miniaturized Systems for Chemistry and Life Sciences (μTAS2013), Freiburg, Germany, 877-879, (2013),
ISBN: 978-0-9798064-6-9

(5) Integrated Micro-Impaction Cartridge Covered With Microporus Light-blocking Film for Low-Concentration Airborne Virus Detection
K. Takenaka, S. Togashi, R. Miyake, T. Sakaguchi and M. Hide
Chemical and Biological Microsystems Society, 18th International Conference on Miniaturized Systems for Chemistry and Life Sciences (μTAS2014), San Antonio, Texas, USA, 2041-2043, (2014),
ISBN: 978-0-9798064-7-6

(6) Excitation-Fluorescent 3D Spectral Flow Cytometer for Single-Cell Analysis,
K. Takenaka and S. Togashi
Chemical and Biological Microsystems Society, 19th International Conference on Miniaturized Systems for Chemistry and Life Sciences (μTAS2015), Gyeongju, South Korea, 1813-1815, (2015),
ISBN: 978-0-9798064-8-3

(7) Analyses of Particle Composition in Vegetables Suspension Using Excitation-Fluorescent Spectral Flow Cytometer
K. Takenaka and S. Togashi
Chemical and Biological Microsystems Society, 20th International Conference on Miniaturized Systems for Chemistry and Life Sciences (μTAS2016), Dublin, Ireland, 1360-1361, (2016),
ISBN: 978-0-9798064-9-0